Analysis of channel quality reporting mechanisms and their impact into 4G and beyond technologies

Live LTE networks
LTE Band 7
Downlink LTE schedulers
Centralized RAN
Mobile edge computing

eman ta zabal zazu

Universidad del País Vasco

Euskal Herriko Unibertsitatea

Author: Jose Oscar Fajardo
(joseoscar.fajardo@ehu.eus)
Supervisor: Fidel Liberal

December 2015

Abstract

Modern broadband mobile networks such as 4G LTE are designed to cope with stringent performance levels, i.e. considerable peak data rates and low latencies. With the wide-spreading of LTE networks all over the world, the access to Internet services through mobile connections is increasing considerably, leading to a plethora of mobile services. However, the inherent characteristics of the radio interface results in variable service performance. First, radio resources are shared among the different mobile users and thus the eNB scheduling functions determine the assigned share of resources for each user in a dynamic way. Moreover, the channel quality of each individual user fluctuates over time due to propagation and fading effects. These aspects introduce new issues in the tasks of performance evaluation and adaptive traffic management at different layers of the protocol stack. Currently, there is a gap between advanced research proposals and the actual network and service performance experienced in commercial mobile networks. Although it is generally assumed that the radio channel may introduce considerable quality fluctuations, there is little evidence of the quality dynamics experienced in live LTE networks at different temporal scales. This PhD work aims at providing some insights of these quality variations by analyzing the Channel State Information generated by UEs. Specifically, the document focuses on the downlink direction and on the effects of using spatial multiplexing techniques. From field testing, the main characteristics of the channel quality are studied at the scale of one second. Besides, LTE emulation tests allow evaluating the characteristics of the reported channel quality at the scale of milliseconds. Therefore, valuable information is captured for different layers of the protocol stack. Finally, the impact of the dynamics of these Channel State Information values into different adaptive traffic management schemes is evaluated. For a comprehensive analysis, different mobile network architectures are considered including classical LTE systems and novel proposals such as centralized radio access networks and mobile edge computing.

Resumen

La nueva generación de redes móviles de banda ancha como 4G LTE han sido diseñadas para soportar unos niveles de rendimiento bastante exigente en cuanto a tasas pico de transferencia de datos y mínimas latencias. Con la proliferación de las redes LTE a nivel mundial, la proporción de accesos a Internet a través de redes móviles está en constante aumento. Esto lleva a un aumento de la oferta de servicios móviles disponibles a nivel comercial. Sin embargo, las características inherentes al medio radio resultan en niveles de rendimiento de servicio variables. En primer lugar, los recursos radio son finitos y están compartidos entre los diferentes usuarios móviles, por lo que es el propio planificador LTE el que decide en tiempo real la cantidad de recursos radio asignados a cada usuario. Además, la calidad del canal radio de cada usuario experimenta fluctuaciones a lo largo del tiempo debido a efectos de propagación y desvanecimientos. Estos aspectos introducen nuevas problemáticas en cuanto a la adecuada evaluación del rendimiento obtenido y en lo relativo a la gestión dinámica y adaptativa del tráfico a diferentes niveles de la pila de protocolos. Actualmente, existe una brecha a cubrir entre a las propuestas de investigación que podrían aplicarse a entornos de redes móviles y el conocimiento real de los niveles de calidad que pueden experimentarse en las redes móviles comercialmente disponibles. Si bien generalmente se asume que el canal radio introduce fluctuaciones de calidad considerables, no existe una gran cantidad de información que evidencie este comportamiento en entornos de uso reales y a diferentes escalas de tiempo. Este trabajo de tesis doctoral se centra en monitorizar y analizar los valores de información de estado del canal que los dispositivos móviles generan y reportan a las estaciones base LTE. En concreto, el estudio se focaliza en el análisis del canal descendente y en los efectos de usar técnicas de multiplexación espacial para mejorar el rendimiento de las transmisiones. En base a medidas de campo en redes LTE comerciales, se identifican una serie de características de la calidad del canal radio a una escala de tiempo de un segundo. Posteriormente, las características de los informes de calidad a nivel de milisegundos son analizados por medio de una serie de experimentos de emulación. Como resultado, se obtienen una serie de resultados valiosos de cara a evaluar el impacto de la evolución temporal del estado del canal en diferentes mecanismos de gestión de tráfico a diferentes niveles de la capa de protocolos. De cara a realizar un estudio pormenorizado, se han considerado diferentes arquitecturas de red móvil incluyendo los esquemas clásicos en LTE y diversas propuestas de evolución hacia nuevas arquitecturas en base a la centralización de la red de acceso radio y a la aplicación de instancias de procesamiento en el extremo de la red móvil.
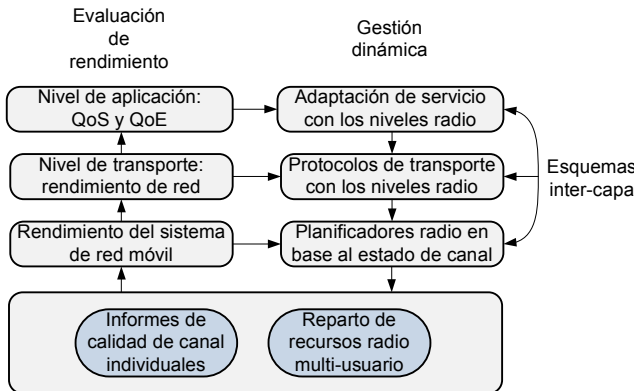
Laburpena

Gaur egungo banda zabaleko sare mugikorrak, hala nola 4G LTE, errendimendu eskakizun zorrotzei moldatzeko diseinatuta daude, hau da datu abiadura handiak eta atzerapen txikiak jasan behar dituzte. Mundu mailako LTE sareen hedapenaren ondorioz, konexio mugikorren bitartez egindako Internet zerbitzuen atzipena bereziki handiagotu da, eta honek zerbitzu mugikor gehiegi izatera eraman gaitu. Hala ere, irrati interfazeari zuzenki atxikirik dauden ezaugarriek zerbitzuaren errendimendu aldakor bat izatea eragiten dute. Alde batetik, irrati baliabideak erabiltze mugikor desberdinen artean partekatzen dira eta ondorioz, eNBaren esleitze funtzioek erabiltzaile bakoitzari esleitutako baliabideak modu dinamiko batean zehaztu behar dituzte. Bestetik, erabiltzaile bakoitzaren kanalaren kalitateak gorabeherak jasaten ditu denboran zehar hedapen eta itzaltze efektuen ondorioz. Ezaugarri hauek arazo berriak sortzen dituzte errendimenduaren ebaluazio eta trafikoaren kudeaketa moldagarriari lotutako lanetan protokolo pilaren geruza ezberdinetan. Gaur egun, ikerketa aurreratuek egindako proposamenen eta sare mugikor komertzialetan jasandako zerbitzuaren errendimenduaren artean alde handia dago. Orokorrean irrati kanalak kalitatearen gorabehera nabarmenak eragin ditzakeela onartzen bada ere, benetako LTE sare batean eta denbora eskala ezberdinetan jasaten den kalitatearen froga gutxi daude. Doktorego lan honen helburua kalitatearen gorabehera hauek argitzea da, erabiltzailearen ekipamenduak emandako kanalaren egoeraren informazioa (Channel State Information)aztertuz. Dokumentu honek beheranzko norabidean eta espazio-multiplexazio tekniken ondorioetan arreta jarriko du bereziki. Landa probetatik abiatuz, kanalaren kalitatearen funtsezko ezaugarriak aztertzen dira segundo bateko eskalan. Beste alde batetik, LTE emulazio frogek kanalaren kalitatearen ezaugarriak aztertzea ahalbidetzen dute milisegundoko eskalan. Beraz, informazio esanguratsua jaso daiteke protokolo pilako geruza ezberdinetatik. Azkenik, kanalaren egoeraren informazio balio hauen aldakortasunak trafiko kudeaketa estrategia moldakor ezberdinetan daukan eragina aztertu da. Ikerketa sakon bat egin ahal izateko, sare mugikor arkitektura ezberdinak kontuan hartu dira, LTE sistema klasikoetatik abiatuz sare arkitektura berriak eskaintzen duten proposamenetara helduz. Azken hauen artean, irrati sarbide sareen zentralizazioa proposatzen duten eta prozesamendua sare mugikorraren muturretan egiten duten arkitekturak aztertu dira.

Resumen Ejecutivo

La nueva generación de redes móviles de banda ancha como 4G LTE han sido diseñadas para soportar unos niveles de rendimiento bastante exigente en cuanto a tasas pico de transferencia de datos y mínimas latencias. Con la proliferación de las redes LTE a nivel mundial, la proporción de accesos a Internet a través de redes móviles está en constante aumento. Esto lleva a un aumento de la oferta de servicios móviles disponibles a nivel comercial.

Sin embargo, las características inherentes al medio radio resultan en niveles de rendimiento de servicio variables. En primer lugar, los recursos radio son finitos y están compartidos entre los diferentes usuarios móviles, por lo que es el propio planificador LTE el que decide en tiempo real la cantidad de recursos radio asignados a cada usuario. Además, la calidad del canal radio de cada usuario experimenta fluctuaciones a lo largo del tiempo debido a efectos de propagación y desvanecimientos.

Estos aspectos introducen nuevas problemáticas en cuanto a la adecuada evaluación del rendimiento obtenido y en lo relativo a la gestión dinámica y adaptativa del tráfico a diferentes niveles de la pila de protocolos, tal y como se muestra en la siguiente figura.

Actualmente, existe una brecha a cubrir entre a las propuestas de investigación que podrían aplicarse a entornos de redes móviles y el conocimiento real de los niveles de calidad que pueden experimentarse en las redes móviles comercialmente disponibles. Si bien generalmente se asume que el canal radio introduce fluctuaciones de calidad considerables, no existe una gran cantidad de información que evidencie este comportamiento en entornos de uso reales y a diferentes escalas de tiempo.

Este trabajo de tesis doctoral se centra en monitorizar y analizar los valores de información de estado del canal que los dispositivos móviles generan y reportan a las estaciones base LTE. En concreto, el estudio se focaliza en el análisis del canal descendente y en los efectos

de usar técnicas de multiplexación espacial para mejorar el rendimiento de las transmisiones.

En base a medidas de campo en redes LTE comerciales, se identifican una serie de características de la calidad del canal radio a una escala de tiempo de un segundo. Posteriormente, las características de los informes de calidad a nivel de milisegundos son analizados por medio de una serie de experimentos de emulación.

Como resultado, se obtienen una serie de resultados valiosos de cara a evaluar el impacto de la evolución temporal del estado del canal en diferentes mecanismos de gestión de tráfico a diferentes niveles de la capa de protocolos.

De cara a realizar un estudio pormenorizado, se han considerado diferentes arquitecturas de red móvil incluyendo los esquemas clásicos en LTE y diversas propuestas de evolución hacia nuevas arquitecturas en base a la centralización de la red de acceso radio y a la aplicación de instancias de procesamiento en el extremo de la red móvil.

El **Capítulo 1** (Introducción) plantea las motivaciones principales del trabajo de tesis e identifica una serie de cuestiones que deben ser cubiertas de cara a alcanzar los objetivos planteados.

El **Capítulo 2** (Revisión Tecnológica de LTE) se centra en analizar los estándares del 3GPP en relación a LTE y su evolución a LTE-A. Este conjunto de estándares incluyen a lo largo de las diferentes versiones numerosas opciones de configuración en lo relativo a frecuencias de uso, anchos de banda posibles, diferentes esquemas de transmisión agrupados en un conjunto de Modos de Transmisión, etc. Todas estas alternativas tienen un impacto diferente en los mecanismos de generación de los informes de estado del canal por parte de los dispositivos móviles, tanto en la cantidad y precisión de la información como en los modos de envío de la información al eNB.

De cara a centrar las actividades de investigación en las tecnologías realmente disponibles en las redes comerciales, se ha realizado un análisis pormenorizado de los despliegues actuales y planificados a nivel mundial. De acuerdo a los informes de la asociación GSA, únicamente las categorías marcadas en la tabla siguiente son soportadas actualmente.

UE Cat.	1	2	3	4	5	6	7	8	9	10	11	12
Tasa de pico DL (Mbps)	10	50	100	150	300	300	300	3,000	450	450	600	600
Tasa de pico UL (Mbps)	5	25	50	50	75	50	100	1,500	50	100	50	100

En resumen, las implicaciones tecnológicas puedes resumirse en los siguientes aspectos:

- Los despliegues comerciales se basan en tecnologías MIMO de 2x2 antenas, mientras que esquemas de antenas 4x4 no se plantean actualmente.
- Las modulaciones soportadas en sentido descendente se limitan a 64QAM, salvo para el único caso de red de categoría 11 que habilita 256QAM en entornos muy concretos. En el sentido ascendente, 16QAM es el máximo permitido.
- Las mayores evoluciones en cuanto a tasa de datos soportada se basan en la tecnología "Carrier Aggregation", que permite usar de forma simultánea dos bandas LTE de un mismo operador para alcanzar anchos de banda mayores a 20 MHz.
- Los esquemas de transmisión MIMO se basan en el modo de transmisión TM3, que permite la utilización alternativa de los esquemas de transmisión "Transmission Diversity" para mejorar la fiabilidad de las transmisiones y "Large delay CDD", que permite alcanzar mayores tasas de transferencia en condiciones de recepción adecuadas.

Por tanto, los posibles esquemas de información de estado del canal se centran en:

- Provisión de los parámetros "Channel Quality Indicator" (CQI) y "Rank Indicator" (RI) por parte de los dispositivos móviles.
- Utilización de informes en banda ancha o en bandas selectivas.
- Envío de informes periódicos o bajo demanda.

En base a este posicionamiento tecnológico, el **Capítulo 3** está orientado a analizar el estado del arte relativo a documentos científicos y de propósito general que ofrecen información relativa a la calidad experimentada en redes móviles operativas.

De estos estudios se puede extraer información interesante respecto a las diferentes metodologías de medida existentes, y respecto a las relaciones existentes entre los valores de CQI con diferentes parámetros de rendimiento radio (RSSI, RSRP, RSRQ, SNR) o con los resultados de los procesos de "Adaptive Modulation and Coding" (en base al MCS).

Si bien se obtienen una serie de conclusiones interesantes de cara al análisis planteado, ninguno de los estudios ofrecen información de calidad del canal a las escalas temporales requeridas por un planificador LTE. Además, muchos de los estudios ofrecen resultados incompletos respecto a los esquemas MIMO utilizados en cada momento, o se basan en métricas de rendimiento diferentes al CQI/RI para estimar los niveles de calidad alcanzables.

Por tanto, se fundamenta la necesidad real de acometer las tareas de investigación planteadas en este trabajo de cara a obtener un mayor nivel de entendimiento de las dinámicas de la evolución del estado del canal radio a diferentes escalas temporales.

El **Capítulo 4** describe las actividades de medidas de campo realizadas sobre redes LTE comercialmente operativas, y presenta los principales resultados obtenidos en relación a la calidad del medio radio experimentado en diferentes condiciones de movilidad.

Desde el punto de vista de configuración, los parámetros más relevantes se muestran a continuación:

Banda LTE	Ancho de banda LTE	Categoría de UE	Modo de Transmisión	Frecuencia de informes de CQI	Frecuencia de informes de RI	Frecuencia muestreo del SW
Band 7	20 MHz	UE Cat. 3	TM3	5 ms	80 ms	1 s

Por tanto, los valores de CQI disponibles en el eNB podrían cambiar cada 5 ms, mientras que los cambios de esquema de transmisión MIMO se podrían producir cada 80 ms.

Desde el punto de vista de las medidas, la primera conclusión de estas medidas de campo es que el equipamiento de medida es capaz únicamente de proporcionar muestras de medida en una escala temporal de un segundo. Por tanto, esta metodología de medidas resulta en la práctica insuficiente de cara a analizar las dinámicas de calidad del canal radio a los niveles de milisegundo requeridos por los elementos de planificación de tráfico LTE.

Desde un punto de vista macroscópico, el procesamiento de las muestras adquiridas ofrece resultados muy interesantes acerca del comportamiento real de las conexiones móviles. Aunque no se correspondan con valores instantáneos, los valores obtenidos permiten evaluar los valores predominantes en cada periodo de muestreo.

Por un lado, se analizan los resultados relacionados con el parámetro RI. Se comprueba que las tendencias a usar RI = 1 o RI = 2 son diferentes en función de las condiciones de recepción radio. Así mismo, las tendencias observadas difieren en cierta medida entre los diferentes patrones de movilidad considerados.


[x]
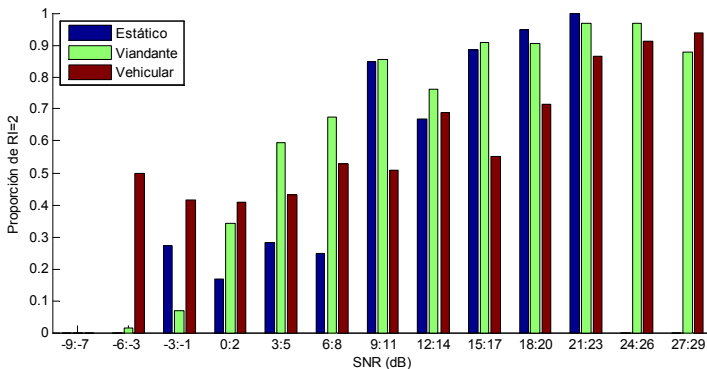
Se demuestra también que el uso dinámico del parámetro RI es muy importante de cara a analizar los valores de CQI proporcionados por el equipamiento de medias de campo.

Como puede observarse en la siguiente figura, los valores de CQI reportados experimentan grandes fluctuaciones al cambiar de valor de RI, es decir, al cambiar de esquema de transmisión MIMO.
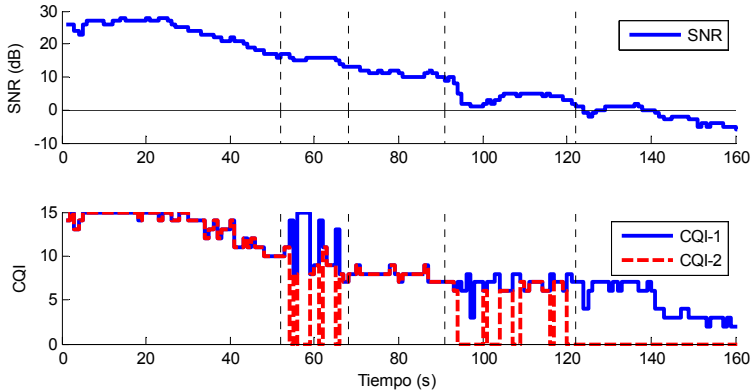
Sin embargo, estas variaciones de CQI no significan que la calidad del canal esté cambiando bruscamente ya que el resultado a efectos de transferencia de datos puede ser similar. Por tanto, se demuestra que este tipo de transmisiones MIMO de rango adaptativo requieren de un adecuado procesamiento de las muestras de CQI en base a los valores de RI asociados, lo cual no es acometido por la mayoría de estudios analizados en el Capítulo 3. En términos generales, la probabilidad de que el parámetro RI cambie entre dos muestras consecutivas varía entre un 30% y un 50%, en función del tipo de movilidad.

En cuanto a las muestras de CQI obtenidas, la variabilidad temporal observada se refleja en la siguiente figura.
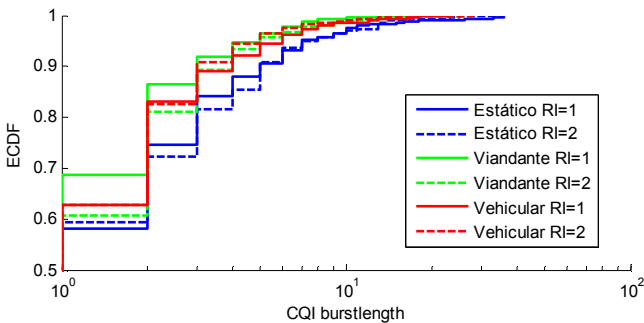
Como puede observarse, la probabilidad de cambiar de valor entre dos muestras consecutivas está entre el 55% y el 70% en función del tipo de movilidad y del esquema de transmisión MIMO. Por tanto, se observa que los valore de CQI son poco estables en general aún desde el punto de vista macroscópico. Sin embargo, analizando las amplitudes asociadas a estas variaciones, se observa que las fluctuaciones de calidad experimentadas no son tan bruscas como cabría esperar.

Otra de las conclusiones principales de las actividades de medidas de campo es que ninguno de los parámetros identificados en el Capítulo 3 ofrece realmente una buena estimación de los niveles de CQI generados por el dispositivo móvil. Únicamente en condiciones concretas de elevada carga de tráfico, el MCS puede asociarse a los niveles de CQI reportados ya que los eNB utilizan esquemas conservadores de asignación de modulación.

Como un paso más hacia entender lo que sucede a niveles microscópicos, en el **Capítulo 5** se describen una serie de experimentos de cara a reproducir las condiciones observadas en las medidas de campo en un emulador LTE. La siguiente figura muestra la metodología propuesta, que se basa en configurar de manera dinámica las condiciones de recepción de las medidas de campo y repetir las pruebas con diferentes patrones de desvanecimiento. El emulador LTE utilizado permite almacenar la traza completa de valores de CQI enviados por el dispositivo comercial para su posterior tratamiento y análisis.
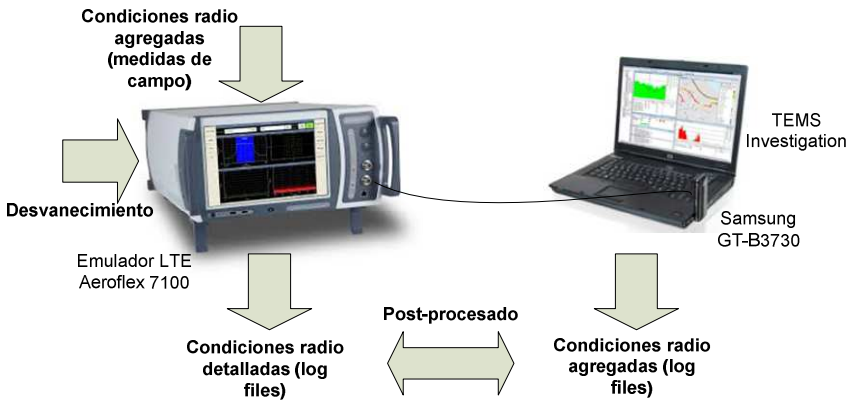

Los resultados obtenidos indican que los valores de CQI obtenidos a diferentes escalas temporales muestran una elevada correlación. Por tanto, puede decirse que los valores de CQI mostrados por el equipamiento de medidas de campo puede reflejar de manera fiel el comportamiento agregado de los valores reales.

Por otro lado, mediante la comparación de las características estadísticas de los valores de CQI y de su variación temporal, se puede establecer cierta relación entre los diferentes patrones de desvanecimiento y las muestras de CQI correspondientes a las muestras de los diferentes esquemas de transmisión MIMO (diferentes valores de RI).
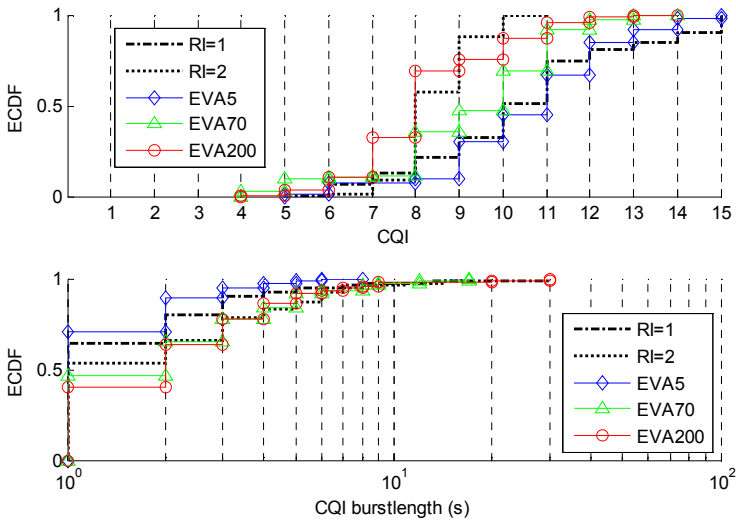
Como puede observarse, los valores de CQI asociados a RI = 1 (TxD) se asemejan más a patrones de desvanecimiento con frecuencias Doppler bajas, mientras que los valores de CQI asociados a RI = 2 (Large delay CDD) muestran una tendencia más similar a patrones de desvanecimiento con frecuencias Doppler altas.

Por otro lado, puede observarse que las dinámicas de variabilidad de los valores de CQI reales son mucho más altas que las observadas en las medidas de campo.
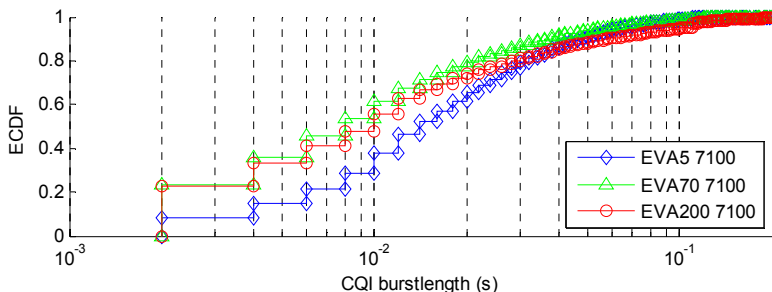
Analizando los periodos de tiempo sin que el valor de CQI cambie en los diferentes patrones de desvanecimiento considerados, se observa que los valores no permanecen en general constantes más allá de 100 ms. Más aún, aproximadamente la mitad de la veces el valor de CQI varía en menos de 10 ms.

En base a los resultados obtenidos en los Capítulos 4 y 5, el **Capítulo 6** se centra en analizar el impacto de las dinámicas de variabilidad de CQI observadas en diferentes elementos de gestión de tráfico.

El capítulo se organiza en torno a tres desafíos y cuatro casos de estudio que permiten analizar el rendimiento en diferentes casuísticas.

Los desafíos identificados son:

- Reto #1: Problema de tener información parcial de CQI en el eNB, debido a las periodicidades de envío configuradas por la red.
- Reto #2: Problema de añadir retardos adicionales a la transmisión de informes de CQI, teniendo en cuenta posibles arquitecturas de eNB con funciones de gestión de recursos centralizadas sobre enlaces no óptimos.
- Reto #3: Problema de utilizar valores de CQI de escala temporal macroscópica para la gestión de tráfico a nivel de servicio, por ejemplo en instancias de procesamiento en el eNB.

Los cuatro casos de estudio planteados son:

- Caso de Estudio #1: Estudio del impacto de las dinámicas de CQI en el eNB con tráfico de propósito general en diferentes valores de periodicidad y hasta 8 ms de retardo.
- Caso de Estudio #2: Estudio del impacto de las dinámicas de CQI en el eNB centralizado con tráfico multimedia, con diferentes valores de periodicidad y de retardo de CQI.
- Caso de Estudio #3: Estudio del impacto de las dinámicas de CQI a diferentes escalas temporales para la gestión de flujos de propósito general a nivel de servicio.
- Caso de Estudio #4: Estudio del impacto de las dinámicas de CQI a diferentes escalas temporales para la gestión de flujos multimedia a nivel de servicio.

Los resultados obtenidos en cada uno de los casos de estudio planteados ha llevado a la consecución de una publicación científica, tal y como se recoge a continuación.

Caso de Estudio	Reto relacionado	Publicación
#1	#1	Jose Oscar Fajardo, Ianire Taboada, Fidel Liberal, "Analysis of CQI traces from LTE MIMO deployments and impact on classical schedulers", 13th International Conference on Wired and Wireless Internet Communications (WWIC), Malaga, Spain, May 25-27, 2015.
#2	#2	Jose Oscar Fajardo, Ianire Taboada, Fidel Liberal, "Joint impact of CQI feedback delay and CQI reporting rate on channel-aware scheduling" XII edición de las Jornadas de Ingeniería Telemática (JITEL), Palma de Mallorca, Spain, October 14-16, 2015.

#3	#3	Jose Oscar Fajardo, Ianire Taboada, Fidel Liberal, "Radio-Aware Service-Level Scheduling to Minimize Downlink Traffic Delay Through Mobile Edge Computing", 7th EAI International Conference on Mobile Networks and Management (MONAMI 2015), Santander, Spain, September 16–18, 2015.
#4	#3	Jose Oscar Fajardo, Ianire Taboada, Fidel Liberal, "Improving Content Delivery Efficiency through Multi-Layer Mobile Edge Adaptation", IEEE Network Magazine, Feature topic Quality-of-Experience (QoE)-Aware Design in Next-Generation Wireless Networks, November 2015.

Finalmente, el **Capítulo 7** recoge las principales conclusiones del trabajo realizado, tanto a nivel de contribuciones como de méritos científicos alcanzados. Así mismo, se incluyen las principales limitaciones de aplicabilidad identificadas y se plantean una serie de posibles líneas futuras de actuación.

Document Conventions

References to figures included in the document follow the format "Figure #".

References to figures included in cited documents follow the format "figure #".

The same rule applies to tables and sections.

The document is made up of a series of chapters, referenced as "Chapter #".

Each chapter includes a series of sections, which are referred to as "Section #.#".

All the abbreviations used in the text are defined in their first appearance, within brackets.

Since many abbreviations are used and repeated all over the document, the meaning of already defined abbreviations is included within brackets in an arbitrary way.

Table of Contents

LIST OF FIGURES

LIST OF TABLES

LIST OF ABBREVIATIONS

Abbreviation	Meaning
3G	Third Generation (of mobile telecommunication systems)
3GPP	3rd Generation Partnership Project
4G	Fourth Generation (of mobile telecommunication systems)
AMC	Adaptive Modulation and Coding
API	Application Programming Interface
AWGN	Additive White Gaussian Noise
ASPI	Attained Service dependent Potential Improvement
BBU	BaseBand Unit
BC	Best CQI
BLER	Block Error Rate
BP	Bandwidth Part
CA	Carrier Aggregation
C-BBU	Centralized BaseBand Unit
CC	Component Carrier
CDD	Cyclic-delay-diversity (applies to Large-delay CDD transmission scheme)
CG-CQI	Coarse Grain - Channel Quality Indicator
CG-CSI	Coarse Grain - Channel State Information
CG-RI	Coarse Grain – Rank Indicator
CIF	Carrier indicator field
CLSM	Closed-Loop Spatial Multiplexing
CN	Core Network
C-RAN	Cloud Radio Access Network
C-RNTI	Cell Radio Network Temporary Identifier
CoMP	Coordinated Multi Point
CQI	Channel Quality Indicator
CRR	CQI Reporting Rate
CRS	Cell-specific reference signals
CSI	Channel State Information
CSI-IM	Channel State Information -interference measurement
CSI-RS	Channel State Information- Reference Signals

DASH	Dynamic Adaptive Streaming over HTTP
DCI	Downlink Control Information
DL	Downlink
ECDF	Empirical cumulative distribution function
eNB (or eNodeB)	Evolved Node B
EPA	Extended Pedestrian A
EPC	Evolved Packet Core
ETU	Extended Terrestrial Urban
E-UTRAN	Evolved Universal Terrestrial Radio Access Network
EVA	Extended Vehicular A
FG-CQI	Fine Grain - Channel Quality Indicator
FG-CSI	Fine Grain - Channel State Information
FG-RI	Fine Grain – Rank Indicator
FDD	Frequency Division Duplex
GOP	Group of Pictures
HARQ	Hybrid Automatic Repeat Request
HARQ-ACK	Hybrid Automatic Repeat Request – Acknowledgement
HSDPA	High-Speed Downlink Packet Access
HSS	Home Subscriber Server
HTTP	Hypertext Transfer Protocol
IMT-Advanced	International Mobile Telecommunications-Advanced
IP	Internet Protocol
ITU-R	International Telecommunication Union - Radiocommunication Sector
LTE	Long-Term Evolution
LTE-A	Long-Term Evolution - Advanced
MASPI	Multi-user Attained Service Potential Improvement
MBSFN	Multicast Broadcast Single Frequency Network
MCS	Modulation and Coding Scheme
MEC	Mobile Edge Computing
ME-DAF	Mobile Edge-DASH Adaptation Function
MESch	Mobile Edge Scheduler
MI	Mutual Information

MIMO	Multiple-Input and Multiple-Output
MME	Mobility Management Entity
MOS	Mean Opinion Score
MU-MIMO	Multi User - Multiple-Input and Multiple-Output
NDI	New data indicator
NFV	Network Function Virtualization
OLLA	Outer Loop Link Adaptation
OLSM	Open-Loop Spatial Multiplexing
PCC	Primary Component Carrier
PCell	Primary Cell
PF	Proportional Fair
P-GW (or PDN-GW)	Packet Data Network Gateway
PM	Precoding matrix
PMI	Precoding matrix indicator
PMF	Probability Mass Distribution
PRB	Physical Resource Block
PDCCH	Physical Downlink Control Channel
PDSCH	Physical Downlink Shared Channel
PTI	Precoding type indicator
PUCCH	Physical Uplink Control Channel
PUSCH	Physical Uplink Shared Channel
QPSK	Quadrature Phase Shift Keying
QAM	Quadrature amplitude modulation
QoE	Quality of Experience
QoS	Quality of Service
RAN	Radio Access Network
RE	Resource Element
RI	Rank Indicator
RNC	Radio Network Controller
RNIS	Radio Network Information Services
RR	Round Robin
RRC	Radio Resource Control
RRH	Remote Radio Header

RRM	Radio Resource Management
RS	Reference Signal
RSRP	Reference Signal Received Power
RSRQ	Reference Signal Receive Quality
RSSI	Received Signal Strength Indicator
SB	Sub-band
SCC	Secondary Component Carrier
SCell	Secondary Cell
SDN	Software Defined Networking
SDR	Software Defined Radio
S-GW (or Serving-GW)	Serving Gateway
SIMO	Single-Input Multiple-Output
SISO	Single-Input Single-Output
SINR	Signal-to-Interference and Noise Ratio
SNR	Signal to Noise Ratio
SU-MIMO	Single User - Multiple-Input and Multiple-Output
SVC	Scalable Video Coding
TB	Transport Block
TBS	Transport Block Size
TCP	Transmission Control Protocol
TDD	Time Division Duplex
TM	Transmission Mode
TR	Technical Report (by 3GPP)
TS	Technical Specification (by 3GPP)
TTI	Transmission Time Interval
TxD	Transmission Diversity
UCI	Uplink control information
UE	User Equipment
UE Cat.	User Equipment Category
UL	Uplink
UMTS	Universal Mobile Telecommunications System
USRP	Universal Software Radio Peripheral

1 INTRODUCTION

1.1 CONTEXT AND MOTIVATION OF THE WORK

Broadband mobile networks have significantly evolved in the last decade, from the perspectives of both the underlying technology and the supported services.

The key performance indicators used for mobile network planning and management have been traditionally related to physical parameters such as the Signal to Noise Ratio (SNR). As broadband mobile networks evolved to digital communications, the relationship between those physical performance metrics and the resulting Quality of Service (QoS) became more and more blurry.

In basic digital wireless communications, some metrics such as the peak data rate and the bit error rate could be gauged from radio performance metrics. However, modern broadband mobile technologies introduce much more complex relationships.

The complexity of evaluating the service-level performance is aggravated by two key characteristics of modern mobile networks. First, wireless channels exhibit variable quality levels over time due to complex propagation and fast fading effects. Second, modern broadband networks are founded upon a scheme of shared radio resources, which are dynamically assigned to different users on demand.

Meanwhile, a plethora of types of mobile services have emerged in the last decade.

In fact, broadband mobile networks are becoming nowadays a common access not only to traditional data services such as web browsing and simple messaging, but also to multimedia content distribution, real-time communications, social networks, etc. In this sense, the concept of Quality of Experience (QoE) has replaced traditional service performance evaluation schemes based on network performance or QoS aspects.

Additionally, the wide-spreading of modern broadband mobile networks all over the world has triggered the possibility of incorporating new types of services beyond classical consumer communications, such as machine-type communications and mission critical communications. Therefore, specific QoS models will be required for these new services.

As a result, the performance evaluation and dynamic management of mobile services becomes a challenging issue that promotes addressing a series of research areas.

Figure 1.1 illustrates some of these hot research topics and their relationships.
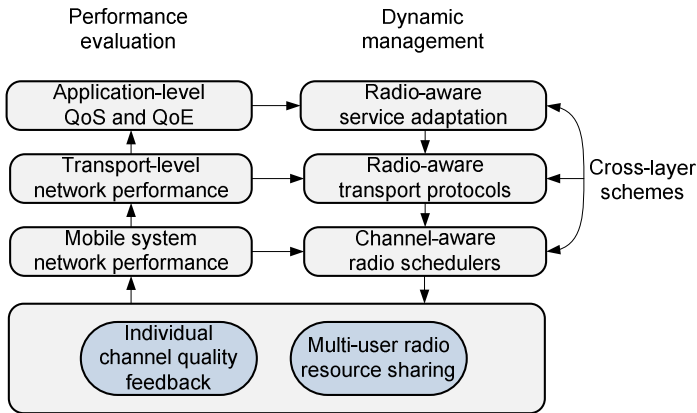
Figure 1.1 – Impact of radio channel quality on different layers.

The performance level achievable by an individual mobile user mainly depends on the radio channel quality that is experienced over time. In modern mobile networks, this information is reported to the radio base stations as an input for the management of radio resources. These radio base stations dynamically determine the best configuration for each mobile user, in terms of supported modulation scheme and coding efficiency.

Additionally, base stations need to determine the assignation of shared radio resources to multiple mobile users in real-time. This procedure is driven by the traffic scheduling functions, which may make use of the channel awareness to maximize the overall performance of the mobile network. More complex scheduling algorithms may aim at maximizing the QoE/QoS of specific services based on cross-layer designs.

Since modern broadband mobile networks are based on Internet Protocol (IP) principles, the impact of the radio performance on the service performance can be evaluated from a layered approach. In this sense, the overall service performance will be affected by the behaviour of the transport protocols. For instance, the Transmission Control Protocol (TCP) includes a series of mechanisms for rate adaptation and congestion control that are not always tailored to the variable mobile quality conditions.

Thus, different transport schemes are being proposed nowadays to better adapt the behaviour of different transport protocols to the specific context of use of different mobile services. These initiatives propose adding the required knowledge of the underlying mobile network in order to adapt the protocol configurations to radio channel quality fluctuations, either from a statistical perspective or by monitoring the actual quality levels.

Finally, the QoE and QoS experienced at application layer for different types of services will significantly depend on the individual channel quality status of the different mobile users and on how its effects are propagated to upper layers. Depending on the type of

communication, the evaluation mechanism will need to take into account different performance metrics inherent to the mobile system.

Finally, service-level adaptations can be driven based on the application-level performance or taking directly into consideration lower level performance metrics.

As a result, different actors involved in the mobile service provisioning chain demand new methods for an accurate performance evaluation and optimized planning and management of mobile networks and services. In this sense, an accurate characterization of the underlying channel quality levels will help on the proper design of the required solutions.

As a preliminary but necessary step in the whole process, this PhD work focuses on understanding the characteristics of the individual channel quality observed in live commercial networks, and on analyzing their implications into different dynamic management functions included in the mobile service provisioning.

1.2 CHALLENGES AND MAIN OBJECTIVES

The main challenge addressed in this PhD work deals with the problem of understanding the channel quality levels than can be expected in mobile services.

Currently, there is a gap between the scientific and commercial worlds that needs to be closed.

- Some research studies provide valuable information about the performance experienced by different mobile services in live mobile networks. However, the low level details are not usually provided and therefore it is difficult to understand the main causes of service degradation in multi-user environments. Additionally, although many research proposals deal with the optimal management of mobile traffic at different layers, these papers are usually based on simulation-driven channel quality models. Therefore, the suitability of these proposals for real-world implementations remains unclear.
- Many commercial products and services claim to maximize their performance over modern mobile network conditions. However, the underlying mechanisms are not fully described and it is difficult to compare the achieved performance against other research-focused proposals.

Therefore, a comprehensive study of the channel quality levels and fluctuations experienced in commercial deployments would benefit both worlds, and would contribute towards closing the identified gap.

Table 1.1 presents the main objectives of the PhD work, together with a set of secondary objectives that are required for the fulfillment of the primary objectives:

Table 1.1 – Primary and secondary objectives.

Primary objective	Secondary objectives
Objective 1 To characterize the performance metrics related to the radio channel quality experienced in live broadband mobile networks, with special focus on Fourth Generation (4G) Long-Term Evolution (LTE) networks.	• To identify the key LTE quality reporting procedures, with special focus in commercially available deployments. • To identify the different quality reporting parameters and the associated accuracy in the temporal and frequency domains. • To identify different alternatives to quantify the quality metrics, and to evaluate the suitability of each methodology. • To perform all the necessary field tests and laboratory experiments that allows collecting the required channel quality values at different time and frequency scales. • To perform all the necessary data analytics in order to extract the main characteristics of the observed channel quality metrics.

Objective 2 To evaluate the implications of the observed channel quality dynamics at system level, including different services and evolutionary mobile network architectures.	• To analyze the impact of the observed channel quality dynamics into the performance of classical LTE architectures based on Adaptive Modulation and Coding (AMC) procedures. • To analyze the impact of the observed channel quality dynamics into the performance achieved in multi-user scenarios with classical scheduling algorithms. • To analyze the impact of the observed channel quality dynamics into the performance of evolutionary LTE architectures with centralized radio resource management functions, from the standpoint of channel-aware AMC process. • To analyze the impact of the observed channel quality dynamics into the performance of evolutionary LTE architectures with centralized radio resource management functions, taking into account the effect of radio resource sharing multi-user contexts. • To analyze the impact of the observed channel quality dynamics into the performance of novel mobile edge computing architectures, which propose to make use of channel quality information for driving service-level adaptations. In order to avoid excessive control information, the effects of using aggregated channel quality reports at lower temporal scale need to be evaluated. • To analyze the impact of the observed channel quality dynamics into the performance of multi-user mobile edge computing, with special focus on mobile multimedia delivery.

The scope of this PhD is restricted to the channel quality reporting mechanisms observed in commercial LTE technologies and to the analysis of downlink transmissions.

1.3 STRUCTURE OF THE DOCUMENT

The document is structured in seven main sections, organized and related among them as depicted in Figure 1.2.

<div align="center">
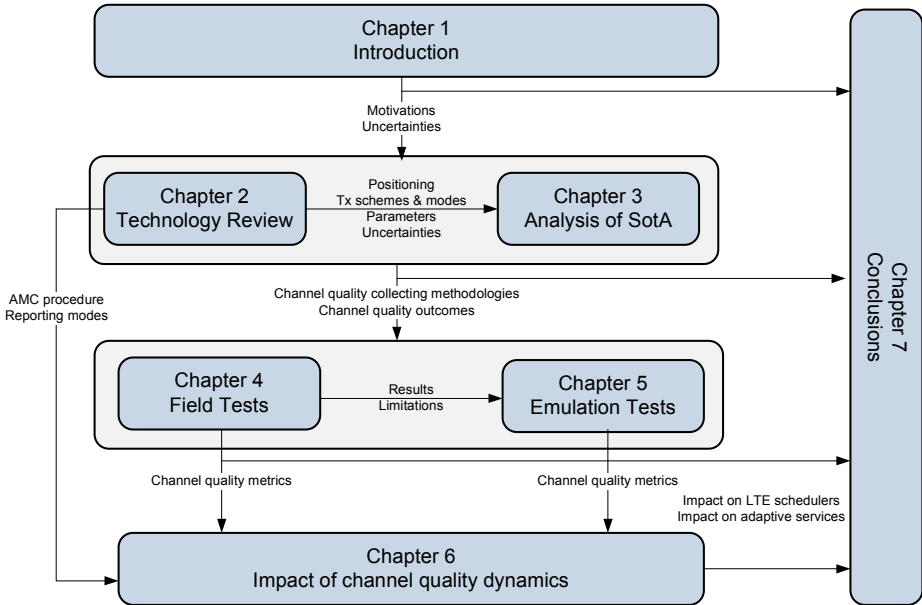
Figure 1.2 – Structure of the document.

</div>

- Chapter 1: Introduction

Chapter 1 states the main motivations of the PhD work and identifies a series of open issues that need to be addressed to fulfil the general objectives.

- Chapter 2: LTE Technology Review

LTE standards are very comprehensive and introduce many different possible configuration alternatives throughout the different releases. Chapter 2 is aimed at identifying the most relevant features related to channel quality reporting and its use in the adaptive modulation and coding process. For this aim, the chapter first analyzes the main LTE architectural aspects, the possible transmission schemes and transmission modes, and identifies the subset of standardized features that are currently in use in commercial deployments.

- Chapter 3: Analysis of the state of the Art

Chapter 3 provides the literature review concerning the publicly available research articles and electronic resources related to channel quality feedbacks in LTE networks. A series of valuable outcomes and some deficiencies are identified.

- Chapter 4: Field Testing in LTE

Chapter 4 describes the performed field testing activities and stresses the main outcomes regarding the key channel quality reporting parameters. Although field testing provides valuable information about the real-world performance, they do not provide the necessary level of detail when compared to the time scale used in LTE schedulers.

- Chapter 5: LTE emulation tests

Based on the previous results, Chapter 5 describes a series of experiments carried out to emulate the behaviour of monitored LTE networks. Although the validity of these results do not reach the reliability of the field tests, some main patterns and trends are inferred concerning the behaviour of the channel quality at very fine granularity.

- Chapter 6:Impact of CSI dynamics on LTE and beyond

Chapter 6 includes all the data analytics and simulation-driven experiments carried out to evaluate the impact of the observed channel quality dynamics at different time scales and taking into account classical and evolutionary LTE architectures.

- Chapter 7: Conclusions

Chapter 7 summarizes the main conclusions to the research activities and to the PhD work, and identifies the main limitations to the work and future research lines.

2 LTE TECHNOLOGY REVIEW

This chapter provides an overall review of modern broadband mobile technologies, commercially known as 4G networks, and the significance of channel quality awareness for the proper adaptation of the radio transmissions to the specific conditions of the mobile users.

Section 2.1 introduces the different versions of the technology and identifies the most relevant aspects such as the possible transmission schemes and the mechanisms standardized to dynamically switch to the most beneficial scheme.

In order to focus the research activities into real-world technologies, Section 2.2 overviews the evolution of LTE deployments since 2009 to the date.

Once identifies the precise LTE technologies nowadays used in live mobile networks, Section 2.3 provides a detailed analysis of the channel quality reporting mechanisms that allow the base station to implement the AMC (Adaptive Modulation and Coding) process.

Finally, Section 2.4 summarizes the main conclusions to the technology review.

2.1   EVOLUTION OF LTE TECHNOLOGIES

LTE (Long-Term Evolution) is the candidate technology specified by the 3rd Generation Partnership Project (3GPP) to move forward towards the 4G (Fourth Generation) of mobile telecommunications technology. Besides enhanced broadband radio transmission schemes, LTE introduces new flat network architecture based on all-IP packet switching.

LTE was originally introduced in 3GPP Release 8 (R8), frozen in December 2008.

Later, LTE-Advanced (LTE-A) was introduced in 3GPP R10 in December 2010 as the evolution of LTE. Taking the same network architecture as the basis, LTE-A introduces a series of enhancements to reach higher transmission bitrates and improve the efficiency of radio resources.

The latest frozen 3GPP release, R12 in March 2015, incorporates further enhancements related to small cells, device-to-device and machine-type communications, enhanced interference management, enhanced downlink multiplexing, etc [3GPP]

Figure 1.1 represents the main architectural elements in LTE networks.
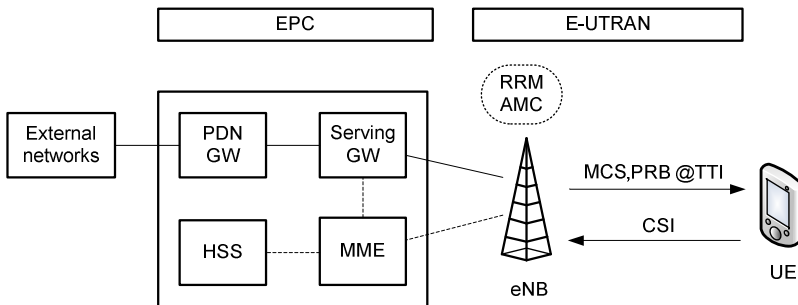
eNB (or eNodeB): Evolved NodeB
UE: User Equipment
PDN GW: PDN Gateway
Serving GW: Serving Gateway
MME: Mobility Management Entity
HSS: Home Subscriber Server

RRM: Radio Resource Management
AMC: Adaptive Modulation and Coding
MCS: Modulation and Coding Scheme
PRB: Physical Resource Block
TTI: Transmission Time Interval
CSI: Channel State Information

Figure 2.1 - LTE architecture.

The LTE network architecture is split into a Core Network (CN) and a Radio Access Network (RAN), interconnected through the mobile backhaul.

The Evolved Packet Core (EPC) implements all the required functionalities of the CN. In brief, the main elements of the EPC and their functionalities are:

- Home Subscriber Server (HSS): the database storing user- and subscription-related information.
- Serving Gateway (Serving GW or S-GW): the IP-level anchor concerning user mobility and intra-technology / inter-technology handovers.
- Packet Data Network Gateway (PDN GW or P-GW): the IP gateway between the LTE network and external IP networks.
- Mobility Management Entity (MME): the main control node for the LTE access, implementing several user- and topology-related functions.

The Evolved Universal Terrestrial Radio Access Network (E-UTRAN) is the network segment in charge of implementing the radio interface to the User Equipment (UE). In LTE, all the radio control functions within an LTE cell are implemented at a unique functional element denoted as Evolved Node B (eNodeB or eNB).

In order to foster the maximum adoption all over the world, the LTE radio segment is specified to support both Frequency Division Duplex (FDD) and Time Division Duplex technology (TDD).

Likewise, to support as many regulatory requirements as possible, the 3GPP specifies a number of possible frequency bands to develop LTE in section 5.5 of TS 36.101 [3GPP-TS36101].

- In the scope of LTE specifications, 3GPP R9 determines 29 different frequency bands: 21 frequency bands (LTE Band 1 to LTE Band 21) are defined for FDD in the range of 700 MHz (LTE Band 12) to 2600 MHz (LTE Band 7); 8 frequency bands (LTE Band 33 to LTE Band 40) are defined for TDD in the range of 1900 MHz (LTE Band 35) to 2620 MHz (LTE Band 38).
- For LTE-A specifications, 3GPP up to R12 determines 15 new LTE Bands: 11 new bands (LTE Band 22 to LTE Band 32) for FDD, in the range of 450 MHz (LTE Band 31) to 3500 MHz (LTE Band 22); 4 new bands (LTE Band 41 to LTE Band 44) for TDD, in the range of 700 MHz (LTE Band 44) to 3700 MHz (LTE Band 43).

Each LTE Band is associated to a set of supported channel bandwidths, according to 3GPP TS 36.101, section 5.6.1. The channel bandwidth is defined as the radiofrequency bandwidth supporting a single LTE carrier with the transmission bandwidth configured in the uplink or downlink of a cell. The set of channel bandwidths for a unique LTE carrier is measured in MHz, with the following possible values: 1.4 MHz, 3 MHz, 5 MHz, 10 MHz, 15 MHz, 20 MHz.

Additionally, according to the specifications of LTE-A, it is also possible to make up an aggregated channel bandwidth by making use of multiple contiguously aggregated carriers. Thus, the total channel bandwidth available would be the sum of the individual carrier bandwidths.

Historically, the Radio Resource Management (RRM) functions in cellular networks have evolved towards more user-centric schemes. RRM elements are nowadays able to perform enhanced channel-aware scheduling decisions based on real-time feedback provided by UEs. In this way, cellular networks can meet the objectives of maximizing the efficiency of radio resources while coping with multi-user resource sharing.

Taking 3GPP technologies as a reference, the evolution of RRM from 3rd Generation (3G) to 4G is mainly based on two aspects:

- First, the RRM logic is moved towards the radio interface. In 3G Universal Mobile Telecommunications System (UMTS) technology, the Radio Network Controller (RNC) is the element in charge of RRM and controls a series of Node Bs within the RAN. Meanwhile, in LTE the RRM and other functions are placed at the eNB with direct access to feedbacks provided by UEs in the form of Channel State Information (CSI). This way, the eNB is able to perform AMC (Adaptive Modulation and Coding) in order to dynamically adapt the radio transmissions to the actual channel quality experienced by UEs.
- Second, the Transmission Time Interval (TTI) is reduced to support a quicker reaction to instantaneous channel conditions in the multi-user context. In 3G UMTS the possible TTI values are between 10 ms and 80 ms. This value was reduced to 2 ms in the transitional High-Speed Downlink Packet Access (HSDPA) technology, and, finally, configured to 1 ms in LTE. As a result, the eNB must implement the scheduling functions at TTI scale. Every TTI, the eNB needs to determine the amount of data to transmit for each active user in the cell. This data budget is associated to the combination of assigned Physical Resource Blocks (PRB) and supported Modulation and Coding Scheme (MCS).

The transmissions in the downlink (DL) are scheduled by the eNB through the Physical Downlink Control Channel (PDCCH) and implemented through the Physical Downlink Shared Channel (PDSCH) using one of the QPSK, 16QAM, 64QAM or 256QAM modulation types. Meanwhile, the CSI feedbacks from UEs to eNB are sent over the Physical Uplink Control Channel (PUCCH), and are restricted to QPSK modulation.

The transmissions in the uplink (UL) are scheduled by the eNB providing resource grants to the UEs through the PDCCH. According to these assignments, UEs may transmit user data through the Physical Uplink Shared Channel (PUSCH) using one of the QPSK, 16QAM and 64QAM modulations.

For a better understanding of the multi-user scheduling problem, the overall downlink LTE Frame Structure for FDD is depicted in Figure 2.2. As can be observed, the length of an LTE frame is 10 ms and contains ten LTE subframes of 1 ms each. At the same time, each LTE subframe is made up of two slots of 0.5 ms. While LTE frames are useful to transmit system information, LTE subframes are the basic unit for radio resource allocation. Therefore, the duration of LTE subframes are defined as the system basic transmission unit or TTI. LTE slots are introduced for synchronization purposes.
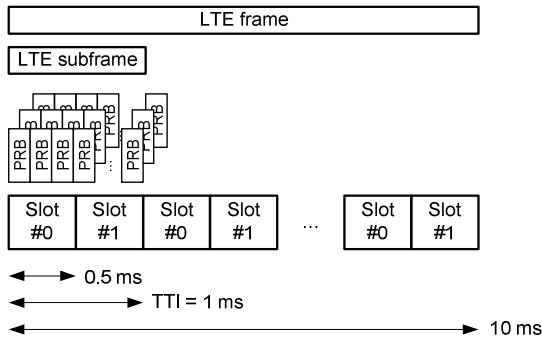
Figure 2.2 - Radio resources in LTE.

Within each TTI, the eNB needs to allocate data transmission demands to the set of available radio resources. These PRBs are multiplexed in time and frequency along the TTI and the channel bandwidth respectively. Table 1.1 gathers the total number of PRBs per TTI for the possible LTE channel bandwidths, according to 3GPP TS 36.101 (table 5.6-1).

Table 2.1 – LTE possible channel bandwidths and number of PRBs per TTI.

Channel bandwidth [MHz]	1.4	3	5	10	15	20
Transmission bandwidth [Number of PRBs]	6	15	25	50	75	100

In a general sense, the performance of the LTE cell may be gauged by means of the total throughput achieved in a multi-user scenario. To cope with this requirement, each UE needs to operate at the most efficient transmission scheme supported at every moment, which in turn translates to using the highest MCS possible. The MCS value determines the radio transmission efficiency in terms of number of data bits per modulation symbol.
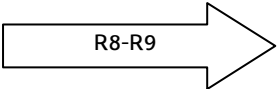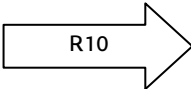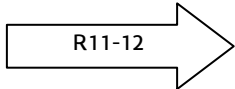
The mapping between the CSI information reported by UEs and the MCS to be used in the next transmission slot is specified in 3GPP TS 36.213 [3GPP-TS36213]. However, using perfect AMC with ideal CSI knowledge is unrealistic in real-world deployments, since this would entail a series of performance bottlenecks especially in the UL reporting channels. Moreover, the specific scheme used by eNBs to assign the available PRBs among different users is not specified by the 3GPP. Therefore, a number of scheduling algorithms have been designed and implemented to cope with different performance and fairness objectives beyond the total cell throughput.

In consequence, the final data rate achievable by each user and by the LTE cell in an aggregated way depends both on the scheduling function and the non-ideal AMC scheme deployed at the eNB. The combination of assigned PRBs and MCS determines the total amount of bits carried by a Transport Block (TB), denoted as Transport Block Size (TBS).

2.1.1   UE CATEGORIES

Concerning the target DL and UL data rates, Table 2.2 summarizes the maximum achievable peak bitrate taking into account the different UE Categories (UE Cat.) defined by the 3GPP in TS 36.306 [3GPP-TS36306]. These data rates are achieved for a single user in optimal conditions, with the whole set of PRBs in 20 MHz and the highest possible MCS.

Table 2.2 – Evolution of UE Categories and peak data rates.

UE Cat.	1	2	3	4	5	6	7	8	9	10	11	12
DL peak rate (Mbps)	10	50	100	150	300	300	300	3,000	450	450	600	600
UL peak rate (Mbps)	5	25	50	50	75	50	100	1,500	50	100	50	100

Taking into consideration the requirements established by ITU-R, LTE technology (3GPP R8-R9) may be considered as a forerunner technology towards 4G. However, the true 4G requirements are only met with the enhancements introduced by LTE-A (3GPP R10 and beyond) and specifically with UE Cat. 8. International Mobile Telecommunications-Advanced (IMT-Advanced) systems are mobile systems that include the new capabilities of IMT that go beyond those of IMT-2000. IMT-Advanced sets the requirements and specifications issued by the ITU-R for the 4G of mobile telecommunications technology. The main requirements imposed by ITU-R in Recommendation M.2012 include peak data rates of 1 Gbps for low mobility and 100 Mbps for high mobility [ITU-M2012].

Table 2.3 and Table 2.4 provide detailed information concerning how these data rates may be achieved. Specifically, Table 2.3 and Table 2.4 have been structured in order to clearly identify the number of simultaneous transmission layers that can be used in each case and the supported DL and UL modulation schemes respectively.

Table 2.4 – Evolution of UE Categories and UL physical layer parameter.

UE Cat.	1	2	3	4	5	6	7	8	9	10	11	12
Max. bits of an UL-SCH TB n a TTI	5,160	25,456	51,024	51,024	75,376	51,024	51,024	1,497,760	51,024	51,024	51,024	51,024
Max. num. of UL-SCH TB bits in a TTI	5,160	25,456	51,024	51,024	75,376	51,024	102,048	1,497,760	51,024	102,048	51,024	102,048
Support for 64QAM in UL	NO	NO	NO	NO	YES	NO	NO	YES	NO	NO	NO	NO

Table 2.3 – Evolution of UE Categories and DL physical layer parameter.

UE Cat.		1	2	3	4	5	6	7	8	9	10	11	12
	Layers												
Max. bits of a DL-SCH TB in a TTI	1	10,296											
	2		51,024	75,376	75,376		75,376	75,376		75,376	75,376	75,376 |64QAM 97,896 |256QAM	75,376 |64QAM 97,896 |256QAM
	4					149,776	149,776	149,776		149,776	149,776	75,376 |64QAM 97,896 |256QAM	75,376 |64QAM 97,896 |256QAM
	8								299,856				
Max. DL-SCH TB bits in a TTI		10,296	51,024	102,048	150,752	299,552	301,504	301,504	2,998,560	452,256	452,256	603,008	603,008

LTE devices (up to 3GPP R9) can be categorized in five different UE Categories.

- UE Cat. 1 only supports Single-Input Single-Output (SISO) transmissions.
- UE Cat. 2 – Cat. 4 devices support Multiple-Input and Multiple-Output (MIMO) 2x2, with up to two layers.
- UE Cat. 5 supports MIMO 4x4, with a maximum of four transmission layers in DL.

Actually, UE Cat. 4 is the first family of devices that benefits of the full additive characteristics of MIMO. When a Cat. 4 device uses SISO in the LTE DL channel, it is able to achieve around 75 Mbps in the optimal configuration (bandwidth of 20 MHz, 100 PRBs assigned to this device by the eNB and using the highest 64QAM modulation scheme with MCS 28). In the case of MIMO, this type of device is able to achieve around 150 Mbps through the simultaneous reception of two different layers with spatial multiplexing.

Although a UE Cat. 3 device supports the same efficiency in SISO configuration, the number of bits per layer is limited to 51,024 when using when using MIMO. As a result, UE Cat. 3 devices only reach around 100 Mbps of DL peak data rate (with cell bandwidth of 20 MHz, 100 PRBs assigned to this device by the eNB and using the highest allowed 64QAM modulation scheme in MIMO with MCS 23).

Finally, UE Cat. 5 is the first family of devices supporting MIMO 4x4 in DL and 64QAM in UL. Therefore, a UE Cat. 5 device should be able to exploit the spatial multiplexing capabilities of four different transmission layers to achieve 300 Mbps in DL. In the UL, the use of 64QAM should contribute to achieve up to 75 Mbps for a single user.

LTE-A (R10 and beyond) introduces a series of enhancements in the radio transmission techniques in order to cope with IMT-Advanced requirements and achieve actual 4G data rates. In R10, three new UE Categories are specified: UE Cat. 6 and UE Cat. 7 represent the evolution of LTE towards carrier aggregation, while UE Cat. 8 is the evolution towards MIMO 8x8.

- LTE-A Carrier Aggregation (CA) allows using different LTE carriers to increase the total available bandwidth through the addition of the bandwidths associated to different LTE carriers. In case of inter-band CA, the device is capable of receiving data from two different eNBs at different LTE Bands with a total of 2 x 20 MHz. Compared to a UE Cat. 4 device, a UE Cat. 6 (and 7) would achieve twice the peak DL data rate for a total of 300 Mbps in MIMO 2x2. Alternatively, UE Cat. 6 and 7 devices could make use of MIMO 4x4 to achieve 300 Mbps in DL within a single 20 MHz carrier, similarly to LTE UE Cat. 5. The main difference between Cat. 6 and Cat. 7 devices is the support in UL to achieve up to 100 Mbps.
- UE Cat. 8 can ideally combine both evolutions, supporting the aggregation of up to five carriers (100 MHz of bandwidth) and MIMO 8x8, to achieve a target DL bitrate of 3 Gbps. Similarly, these types of devices would achieve 1.5 Gbps in UL with the combination of CA and 64QAM.

3GPP R11 introduces four new UE Categories, from UE Cat. 9 to UE Cat. 12.

- UE Cat. 9 and UE Cat. 10 devices target 450 Mbps in DL, and 50 Mbps / 100 Mbps in UL respectively. Taking into account CA and MIMO 2x2, three different carriers are required to ideally achieve 450 Mbps in 3 x 20 MHz.
- Meanwhile, UE Cat. 11 and UE Cat. 12 devices target 600 Mbps in DL, and 50 Mbps / 100 Mbps in UL respectively. This goal can be theoretically achieved through different technologies, e.g. combining four 20 MHz LTE carriers with MIMO 2x2, combining two 20 MHz LTE carriers with MIMO 4x4, or adding 256QAM support to one or several of the involved carriers.

Since the different capabilities required for certain UE Categories may be reached through different radio technologies, the specific radio capability is established by means of UE DL Category and UE UL Category concepts introduced in R12 (section 4.1A of [3GPP-TS36306]). Eleven UE DL Categories are specified, denoted as "DL Category 0", "DL Category 6", "DL Category 7", "DL Category 9", "DL Category 10"- "DL Category 16". Six UE UL Categories are specified, denoted as "UL Category 0", "UL Category 3", "UL Category 5", "UL Category 7", "UL Category 8" and "UL Category 13". The combinations of UE DL Category and UE UL Category and the resulting UE Categories are specified in table 4.1A-6 of [3GPP-TS36306] (from R12).

2.1.2   LTE TRANSMISSION MODES

Considering the different alternative transmission methods supported in LTE, the mechanism to configure and dynamically switch between transmission schemes plays a key role in LTE systems. This mechanism is based on the concepts of transmission scheme, Transmission Mode (TM) and Downlink Control Indicator (DCI).

Before addressing this mechanism, some basic notions of the signal processing are highlighted. Figure 2.3 illustrates the process of generating the baseband signal representing a downlink physical channel such as the PDSCH. When taking into account MIMO systems, the key configuration parameters are:

- Codeword. In LTE, a codeword is associated to a TB (Transport Block) generated from upper layers. Each LTE subframe can transport one or two codewords.
- Layer. Each codeword is mapped into one or more layers, with the number of transmit antennas as upper threshold. The number of layers is also known as Rank in LTE. Depending on the transmission scheme used, there is a fixed mapping between codewords and layers.
- Antenna port. Each layer is mapped for transmission into one or more antennas using a precoding matrix (PM) in order to support spatial multiplexing. When different reception antennas experience significant difference in SNR, the precoding matrix may divide the layers between the transmit antennas to balance the SNR between the layers.
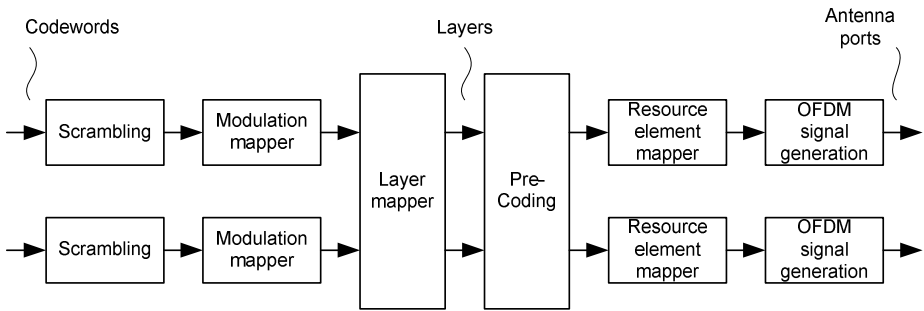
Figure 2.3 - Physical channel processing in LTE downlink.

The complete set of transmission schemes are detailed in 3GPP TS 36.213 (section 7.1). These schemes are designed to maximize the radio performance in different channel and multipath conditions, with different eNB antenna configurations, and taking into account different UE capabilities and mobility patterns. In summary, the transmission schemes supported by LTE in PDSCH are summarized in Table 2.5.

Therefore, a key issue is how eNB and UE are synchronized about the transmission scheme used at every moment.

In LTE, the eNB determines the specific transmission scheme based on the CSI provided by each UE. In order to let UEs know the transmission scheme used by the eNB at every moment, a combination of the Transmission Mode and the Downlink Control Indicator is used. The selected TM is assigned to the UE in the RRC_Connection_Setup Message. Moreover, the specific data format that will be used in the PDSCH is notified to each UE with the DCI message, which is sent over the PDCCH [3GPP-TS36212].

Table 2.6 gathers the complete set of Transmission Modes, as specified in 3GPP TS 36.213 up to R12. Additionally, the table shows the supported transmission schemes and allowed DCI formats for DL assignments at each TM.

The eNB may dynamically switch between different TMs through new RRC reconfiguration procedures, which is known as "adaptive mode selection". However, frequent switches would result on considerable signalling overhead and significant adaptation delays.

In order to introduce an enhanced adaptation capability, LTE supports "rank-adaptive transmission". While the UE maintains an active RRC connection, and based on the dynamic UE-provided CSI, the eNB may switch between any of the transmission schemes supported in the TM or even between different Ranks for a same transmission scheme. This information is announced to each UE within the content of the DCI messages in the PDCCH.

Table 2.5 – LTE transmission schemes.

Transmission scheme	Main characteristics
Single-antenna port	1 codeword, 1 layer, 1 antenna.
	Single-antenna port (port 0) is the most simple radio transmission scheme and represents SISO transmissions, when only one antenna is used both at the eNB and the UE. If the UE implements several antennas, Single-Input Multiple-Output (SIMO) is used.
	Single-antenna port (port 5).
	Alternatively, the eNB with a unique transmit antenna may implement beamforming techniques in order to enhance the reception of radio signals. With beamforming, the eNB antenna configuration is modified to address the wavefront towards a specific UE, obtaining increased effective SNR in cell edges. This is possible by using UE-specific reference signal for demodulation, thus properly weighting the amplitude and phase of individual antenna signals taking into account UE's reception conditions. In this case, single transmit antenna means that a unique UE-specific reference signal is used and it appears as a single transmit antenna to the UE ("virtual" antenna port 5).
Transmit diversity (TxD)	SU-MIMO, 1 codeword, 2-4 layers, 2-4 antennas. Number of layers equal to number of antennas.
	Multipath propagation may degrade the LTE signals associated to different paths with different fading characteristics. Transmit diversity is a spatial multiplexing technique based on transmitting the same information in different layers through different antennas. Thus, multiple layers may be combined at the receiver in order to compensate some fading patterns, obtaining an enhanced effective SNR. Therefore, TxD is designed to increase the robustness in low SNR conditions, such as at cell edge or severe fading scenarios.
Large delay CDD or Open-loop spatial multiplexing (OLSM)	SU-MIMO, 2 codewords, 2-4 layers, 2-4 antennas. Number of layers equal to or lower than number of antennas.
	Large delay CDD is designed to maximize the throughput achievable by a user in high SNR conditions. Spatial multiplexing requires rich multipath conditions to achieve rich scattering characteristics and high SNR at the same time. In this case, spatial multiplexing is used to transmit different information through different layers, resulting in additive outcomes. The effective SNR at the receiver is shared among the different layers. Therefore, the SNR associated to each layer is lower but still enough to decode the user data. Since Large delay CDD uses a fixed set of precoding matrices to implement MIMO for fast-moving UEs, both layers use the same modulation and coding format.

Table 2.5 – LTE transmission schemes (cont.).

Transmission scheme	Main characteristics
Closed-loop spatial multiplexing (CLSM)	SU-MIMO, 2 codewords, 2-4 layers, 2-4 antennas. Number of layers equal to or lower than number of antennas. Similarly to OLSM, CLSM is aimed at enhancing a user's throughout in good SNR conditions. Unlike OLSM, CLSM optimizes the precoding process taking into account the current channel conditions for each layer as reported by UEs through the precoding matrix indicator (PMI). This way, the SNR of each layer is increased over the OLSM approach in low mobility conditions. In high mobility scenarios, the quality of the PMI feedback may quickly deteriorate. By using tailored precoding matrices, the modulation and coding format of each layer may be different.
	SU-MIMO, 1 codeword, 2-4 layers, 2-4 antennas. CLSM can be forced to use a single codeword, resulting in CLSM Rank-1 scheme. Similarly to TxD, CLSM Rank-1 is aimed at enhancing the robustness in low SNR conditions. Beyond TxD, eNB is able to implement UE-selected precoding matrices in order to enhance the SNR and user throughput at cell edges.
Multi-user MIMO (MU-MIMO)	MU-MIMO, 2 codewords (addressed at 2 UEs), 2-4 layers, 2-4 antennas. MU-MIMO is targeted to increase the overall cell capacity rather than the throughput of a single user. Spatial multiplexing techniques are used in this case to transmit two codewords belonging to different users at the same time. Thanks to the rich scattering conditions, the two UEs are able to decode their data independently.
Dual layer [R9]	Combined beamforming and MIMO up to 2 antennas. Beyond single-antenna port beamforming, dual layer transmission utilizes two antenna ports (port 7 and 8) to combine 2x2 MIMO and beamforming techniques. This way, LTE signal is directed towards the addressed UE, supporting up to two layers. Additionally, MU-MIMO is supported by addressing each layer to a different UE. The combination of beamforming and spatial multiplexing is implemented by using different UE-specific Reference Signals in the precoding process. CLSM is assumed for spatial multiplexing.
Up to 8 layer transmission [R10]	Combined beamforming and MIMO up to 8 antennas. This transmission scheme is proposed as an evolution to dual layer scheme, adding support of MIMO 8x8 (antenna ports 7-14) in combination with beamforming. SU-MIMO and MU-MIMO are supported seamlessly, with up to two simultaneous codewords.

Table 2.6 – LTE Transmission Modes [3GPP TS 36.213, table 7.1-5].

Transmission mode	Supported transmission schemes and DCI formats for DL assignments
TM1	• Single antenna port (SISO, SIMO) with port 0. • DCI format 1A and 1.
TM2	• SU-MIMO with 2 or 4 antennas, with TxD. • DCI format 1A and 1.
TM3	• SU-MIMO with 2 or 4 antennas. • DCI format 1A supports TxD. • DCI format 2A allows dynamic switching between Large delay CDD (or OLSM) and TxD.
TM4	• SU-MIMO with 2 or 4 antennas. • DCI format 1A supports TxD. • DCI format 2 allows dynamic switching between CLSM and TxD.
TM5	• MU-MIMO. • DCI format 1A supports TxD. • DCI format 1D supports MU-MIMO.
TM6	• SU-MIMO with 2 or 4 antennas but 1 layer • DCI format 1A supports TxD. • DCI format 1B supports CLSM Rank-1.
TM7	• DCI format 1A supports single-antenna port (port 0) or TxD. • DCI format 1 supports beamforming with single antenna port (port 5).
TM8 [R9]	• DCI format 1A supports single-antenna port (port 0) or TxD. • DCI format 2B allows switching between dual-layer beamforming and beamforming with single antenna port (port 7 and 8). o Adds "scrambling identity" to DCI format 2.
TM9 [R10]	• DCI format 1A adds support for Multicast Broadcast Single Frequency Network (MBSFN). • DCI format 2C adds support for seamless switching between SU-MIMO and MU-MIMO with beamforming and MIMO up to Rank 8. o Adds "Antenna ports" and "Number of Layers" to DCI format 2B.
TM10 [R11]	• DCI format 1A similar to TM9. • DCI format 2D is similar to DCI format 2C, adding specific support for Coordinated Multi Point (CoMP) transmissions with port co-location and interference information.

2.2   COMMERCIAL LTE TECHNOLOGIES

The first commercial LTE network deployments started by the end of 2009 in Norway and Sweden [Merz-2014], and today they account for a total of 442 networks in 147 countries worldwide including both LTE and LTE-A [GSA-2015].
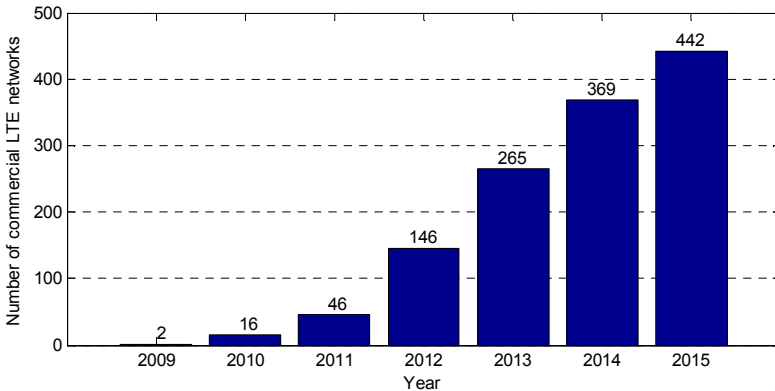
Figure 2.4 - Commercial LTE/LTE-A network deployments [GSA-2015].

From these networks, almost the 85% are deployed over FDD technology and 1800 MHz is the most popular spectrum for LTE deployments, used in over 43% of commercially launched LTE networks.

In general, R8-R9 LTE networks support UE Cat. 3 devices with SISO, and many of them also support UE Cat. 4 with MIMO. Moreover, it is significant that none of the deployed LTE networks support UE Cat. 5, since it requires a significant upgrade in all the eNBs. Alternatively, the evolution of commercial LTE networks has moved to LTE-A UE categories based on carrier aggregation. While this technology also requires upgrades in LTE network elements and UEs, the modifications required by current deployments are more related to the system and protocol architecture than to the problem of placing higher density of antennas within the eNB [ElNashar-2014].

Concerning LTE-A, the first commercial deployments started by mid-2013 and the y are mainly based in the introduction of Carrier Aggregation. By October 2015, 95 LTE-A networks are commercially available in 48 countries worldwide, while 142 mobile operators in 62 countries (third of operators) are investing on new LTE-A deployments [GSA-2015].

A complete list of commercial LTE networks and their characteristics is maintained in [Wikipedia-LTE1], including information of the deployment frequency, LTE Band, system

bandwidth, supported UE Categories and details on the supported LTE Band combinations for CA. According to [GSA-2015], the current status of LTE-A deployments is as follows:
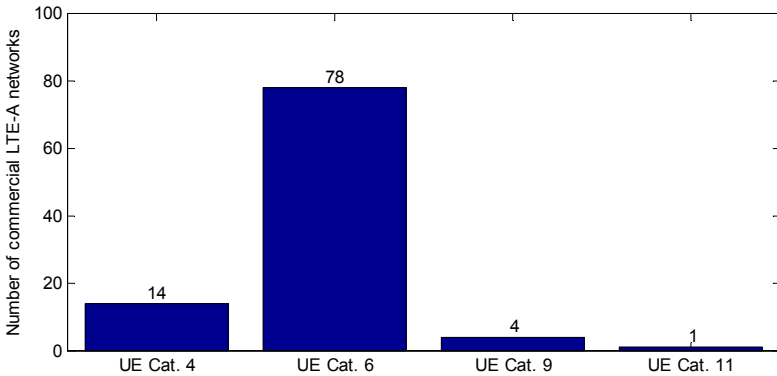
Figure 2.5 – Commercial LTE-A network deployments [GSA-2015].

As observed, most of the LTE-A networks support UE Cat. 6 by aggregating two LTE carriers. Almost half of networks support 2x20 MHz for a total of 40 MHz in DL, which provides the required peak 300 Mbps with MIMO. Some networks in Australia, Greece, Qatar and Singapore already support UE Cat. 9, by using the aggregation of three carriers. However, rather than the maximum 450 Mbps, the achievable peak DL rates range between 330 Mbps and 375 Mbps depending on the aggregated bandwidth combinations. As an example, the combination of LTE Bands 3, 7 and 20 (i.e., 1800 MHz, 2600 MHz and 800 MHz) has been deployed in Europe. Other 28 UE Cat. 9 and beyond systems are in deployment, trial, or test phase. Finally, one operator in Australia currently suuports UE Cat. 11 since September 2015, with tri-band carrier aggregation of 60 MHz and peak DL rates of 600 Mbps by adding 256QAM.

It must be noted that not all the UE Cat. 4 networks are really pure LTE networks. Several mobile network operators reach the requirements of UE Cat. 4 through LTE-A carrier aggrgation rather than using 20 MHz bandwidths with MIMO.

Although some field trials and pilot demonstrations claim for successful transmissions based on 4x4 MIMO and 256QAM, currently UE Cat. 8 is not in the roadmap of any commercial deployment.

With regard to the Transmission Modes, TM1-TM4 are the most commonly used in the deployed LTE networks with SISO or MIMO 2×2 [ElNashar-2014, Merz-2014]. In MIMO scenarios, TM3 is the most widely used TM leading to the use of Large delay CDD.

Finally, concerning the CSI reporting periodicity, no information is publicly available.

2.3   CHANNEL STATE INFORMATION

As stated along the review of LTE technologies, one the key aspects for an accurate system operation is the implementation of suitable Channel State Information at the eNB scheduling and AMC functions. The different UEs are required by the eNB to provide feedback information concerning the experienced radio channel conditions, and the eNB dynamically determines the most suitable transmission scheme at every TTI.

CSI reporting is a complex subject with multiple alternative configuration options. The whole set of procedures and data formats for CSI reporting are specified in 3GPP TS 36.213, section 7.2 [3GPP-TS36213].

- First, CSI reporting schemes have evolved along the different 3GPP releases, in accordance with the evolution of transmission schemes supported in LTE. Each transmission scheme requires a specific set of CSI data to perform AMC and scheduling of radio resources.
- Additionally, CSI reporting entails a significant signalling load in the UL channels, which could compromise the performance of the UL transmissions. Therefore, periodic and aperiodic CSI reporting are specified:
    - With periodic reporting, the eNB determines the type and periodicity of CSI data and this configuration is announced to each UE during the RRC Connection Setup or RRC Connection Reconfiguration procedures. UEs perform the required CSI reporting over the PUCCH (Physical Uplink Control Channel) or simultaneously to user data over the PUSCH (Physical Uplink Shared Channel) if allowed.
    - Aperiodic reporting allows an eNB to request instantaneous CSI to a specific UE, by issuing a DCI Format 0 message with the field CSI request field activated ([3GPP-36213], section 10.1.1). The addressed UE would send the required information in the next allocated UL transmission slot over the PUSCH.
- In addition to reporting periodicity, the amount and type of CSI information determines the trade-off between reporting granularity and overhead. Different types of CSI parameters are required in different transmission schemes, and CSI information may be provided as wideband or sub-band information. These parameters directly impact the expected Block Error Rate (BLER).
- In those Transmission Modes supporting "rank-adaptive transmission", the format of CSI feedbacks needs to be dynamically adapted to the instantaneous transmission scheme, taking also into account the current RRC configuration.
- Different types of CSI reference signals are defined for transmission modes TM1-TM8 and TM9-TM10. TM10 may require more than one CSI process per UE.
- Finally, each type of CSI reporting is associated to a specific CSI reporting mode over the PUCCH or PUSCH respectively for periodic and aperiodic reporting, according to tables 7.2.1-1 and 7.2.2-1 in 3GPP TS 36.213.

According to 3GPP R12, CSI is made up of the following parameters, which will be detailed later in this section:

- Channel Quality Indicator (CQI)
- Rank indication (RI)
- PMI (Precoding matrix indicator)
- Precoding type indicator (PTI)

CSI measurements are performed by LTE UEs based on a series of Reference Signals (RS) transmitted by the eNB in specific positions of the radio resource grid, including well-known symbols (section 10 of [3GPP-TS36211] and sections 7.2.5 and 7.2.6 of [3GPP-TS36213]).

In LTE (3GPP R8-R9), two main RS are especially relevant:

- Cell-specific reference signals (CRS) are transmitted with a set of known symbols over the PDSCH, and are used by UEs to estimate the channel quality and to generate CQI reports among other functions. CRS are defined since 3GPP R8 and their placement in the resource grid is detailed in 3GPP TS 36.211, section 6.10.1.
- UE-specific Reference Signals, as cited in Table 2.5, are used to leverage the specific demodulation process at each UE when beamforming is used.

CRS is designed to support up to MIMO 4x4, supporting CQI estimations of each layer by using separate CRS sequences for each antenna. With the introduction of MIMO 8x8 in LTE-A (R10 and beyond), using individual CRS sequences entails significant system overhead (section 8.3.1 in [ElNashar-2014]).

UE-specific Reference Signals are also used in LTE-A for TM9 and TM10 for tailored demodulation purposes. However, this type of RS cannot be used for CQI estimation since they use the same precoding matrix as other PDSCH transmissions [Tran-2012].

Therefore, LTE-A introduces in 3GPP R10 a new RS, aimed only at supporting CSI estimation.

- Channel State Information- Reference Signals (CSI-RS) are defined in 3GPP TS 36.213 section 7.2.5 and their placement in the resource grid is detailed in 3GPP TS 36.211, section 6.10.5. CSI-RS are transmitted over 1-2-4-8 antennas, which determine the number of CSI-RS ports.

CSI-RS are designed to be sparse in both the time and frequency domains to minimize the interference on R8-R9 devices. As a result, the reporting period is longer compared to CRS-based reports and consequently low mobility UEs are targeted.

It must be noted that in TM10, the UE can be configured with one or more CSI processes per serving cell. Each CSI process is associated with a CSI-RS resource and up to two CSI-interference measurement (CSI-IM) resources. Every CSI report transmitted by the UE is associated to one of the configured CSI processes. Each CSI process can be configured with or without PMI/RI reporting, and with different wideband and sub-band configurations.

The eNB needs to notify each UE about the desired CSI scheme, including the required CSI data, the configured CSI granularity in the frequency domain and the CSI periodicity. In order to support the different combinations, a set of CSI reporting Modes are specified as illustrated in Figure 2.6.
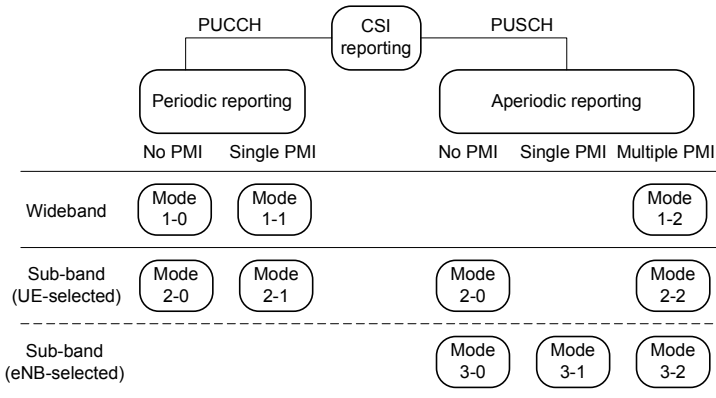
Figure 2.6 - CSI reporting modes.

Besides the temporal reporting granularity based on the configured reporting period, the frequency domain granularity is determined by splitting the total channel DL bandwidth into smaller bandwidth segments (sub-bands).

Considering the possible LTE system bandwidths gathered in Table 1.1, the possibility to exhibit different fading conditions over the different frequencies is not negligible. This issue is especially significant when wide bandwidths are used under high transmission frequencies.

Therefore, for CSI reporting purposes, the total bandwidth is divided in N sub-bands of size k PRBs each sub-band. Similarly, bandwidth parts are defined as higher-level segments of the total bandwidth covering more than one sub-band.

Figure 2.7 illustrates the concepts of sub-band (SB) and bandwidth part (BP) for an LTE DL channel, considering N_{RB} as the total amount of PRBs. The set of sub-bands (S) a UE shall evaluate for CSI reporting spans the entire downlink system bandwidth.
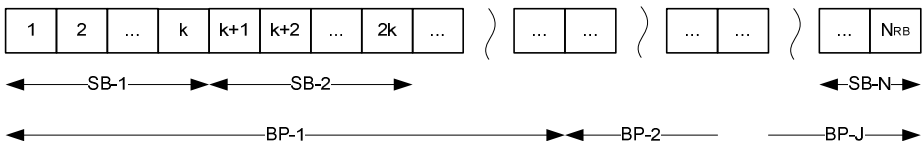
Figure 2.7 - LTE DL bandwidth split into sub-bands and bandwidth parts.

The specific splitting of the bandwidth is dependent on the channel bandwidth, and is also specific for the different types of CSI reporting:

- Periodic reporting
  - o Sub-band sizes (k) and number of bandwidth parts (J) are specified per system bandwidth in 3GPP TS 36.213, table 7.2.2-2.
- Aperiodic reporting
  - o For wideband and Higher Layer-configured sub-band reporting, the sub-band size is specified per system bandwidth in 3GPP TS 36.213, table 7.2.1-3. In these cases, the whole set S of sub-bands is used.
  - o For UE-selected sub-band reporting, only a subset of M sub-bands is used for CSI reporting. The number of sub-bands (M) and their size (k) are specified per system bandwidth in 3GPP TS 36.213, table 7.2.1-5.

For instance, a 20 MHz LTE cell with 100 PRBs would implement 13 sub-bands for periodic reporting, with 12 sub-bands of 8 PRBs and 1 sub-band of 4 PRB. The 100 PRBs would be split into 4 bandwidth parts of 25 PRBs each. For aperiodic reporting, the same sub-band configuration is used, except for UE-selected sub-band reporting where 6 sub-bands of 4 PRBs each are used.

The required CSI data is closely related to the configured transmission schemes and consequently to the LTE Transmission Mode. Accordingly, the CSI reporting Modes applicable to the different LTE TM are:

- TM1, TM2, TM3 and TM7 implement open loop spatial multiplexing with pre-defined precoding matrices, and therefore no PMI reporting is required.
  - o CSI reporting Mode 1-0 and 2-0 for periodic reporting, with wideband and sub-band CQI respectively,
  - o CSI reporting Mode 2-0 and 3-0 for aperiodic reporting including sub-band CQIs in UE-selected or eNB-configured sub-bands.
- TM4, TM5 and TM6 implement closed loop spatial multiplexing with UE-specific precoding matrices, and thus PMI reporting is required.
  - o CSI reporting Mode 1-1 and 2-1 for periodic reporting.
  - o CSI reporting Mode 1-2, 2-2, 3-1 and 3-2 for aperiodic reporting.
  - o TM5 mandates CSI reporting Mode 3-1 for aperiodic reporting.
- TM8 support two alternative operations:
  - o TM8 behaves as TM4 if PMI/RI reporting is enabled.
  - o TM8 behaves as TM3 if PMI/RI reporting is not enabled.
- TM9 and TM10 support two alternative operations:
  - o TM8 behaves as TM4 when PMI/RI reporting is enabled and the number of CSI-RS ports is higher than one.
  - o TM8 behaves as TM3 when PMI/RI reporting is not enabled or when the number of CSI-RS ports is one.

A more detailed analysis of each CSI parameter is provided hereafter:

- **CQI (Channel Quality Indicator)**

The CQI is a measure of the coding efficiency expected to be supported by an UE, based on actual channel quality measurements in the current TTI. In those measurement conditions, a PDSCH TB with the combination of MCS and TBS that best approximates the target coding efficiency is likely to be correctly transmitted with a BLER of 10%.

Table 2.7 gathers the set of valid CQI values and its interpretation in different 3GPP releases. As can be observed, higher CQI values indicate higher coding efficiencies assuming favourable radio channel conditions in the subsequent TTI. Lower CQI values entail less efficient but more resilient coding schemes.

Table 2.7 – CQI indexes and target coding efficiency.

CQI index	UE Cat. 1-10 and Cat. 11-12 ‹ R12		UE Cat. 11-12 in R12	
	modulation	efficiency	modulation	efficiency
1	QPSK	0.1523 (over 2 bits)	QPSK	0.1523 (over 2 bits)
2	QPSK	0.2344 (over 2 bits)	QPSK	0.3770 (over 2 bits)
3	QPSK	0.3770 (over 2 bits)	QPSK	0.8770 (over 2 bits)
4	QPSK	0.6016 (over 2 bits)	16QAM	1.4766 (over 4 bits)
5	QPSK	0.8770 (over 2 bits)	16QAM	1.9141 (over 4 bits)
6	QPSK	1.1758 (over 2 bits)	16QAM	2.4063 (over 4 bits)
7	16QAM	1.4766 (over 4 bits)	64QAM	2.7305 (over 6 bits)
8	16QAM	1.9141 (over 4 bits)	64QAM	3.3223 (over 6 bits)
9	16QAM	2.4063 (over 4 bits)	64QAM	3.9023 (over 6 bits)
10	64QAM	2.7305 (over 6 bits)	64QAM	4.5234(over 6 bits)
11	64QAM	3.3223 (over 6 bits)	64QAM	5.1152 (over 6 bits)
12	64QAM	3.9023 (over 6 bits)	256QAM	5.5547 (over 8 bits)
13	64QAM	4.5234 (over 6 bits)	256QAM	6.2266 (over 8 bits)
14	64QAM	5.1152 (over 6 bits)	256QAM	6.9141 (over 8 bits)
15	64QAM	5.5547 (over 6 bits)	256QAM	7.4063 (over 8 bits)

For devices up to 3GPP R11, the UE determines the CQI value according to table 7.2.3-1 in 3GPP TS 36.213 taking into consideration .QPSK, 16QAM and 64QAM modulation schemes. The maximum coding efficiency is 2, 4 and 6 bits per modulation symbol respectively. For

R12 devices supporting 256QAM modulation (UE Cat. 11 and 12), table 7.2.3-2 in 3GPP TS 36.213 shall be used with a maximum modulation order of 8 bits per symbol.

As cited before, CQI estimations are performed by LTE UEs based on a series of Reference Signals transmitted by the eNB in specific known positions of the radio resource grid. According to 3GPP TS 36.213, different TMs are associated to the use of different RS:

- For TM1-TM8, UE shall derive CQI from the measurement of CRS.
- For TM9:
    - When PMI/RI reporting is enabled, the UE shall alternatively use CSI-RS for computing CQI.
    - When PMI/RI reporting is not enabled, the UE shall use CRS for CQI estimation.
- For TM10:
    - UE may be requested to implement more than one CSI process per serving cell with possibly different reporting types for each CSI process.
    - For each CSI process configured, UEs are required to use the CSI-RS associated to the CSI process for CQI computation.
    - For each CSI process configured, reported CQI values include interference measurements based on only the configured CSI-IM resource(s) associated with the CSI process.

- **RI (Rank indication)**

The Rank Indication is used to report the most beneficial number of layers that should be used by the eNB in the subsequent TTI. Based on the DL channel quality measurements, the UE is able to estimate the throughput achievable with the different transmission schemes supported in the configured TM. RI determines the number of layers that can be used in the DL transmission.

- For TxD, RI is always one.
- For spatial multiplexing, RI is equal to the target number of transmit layers according to 3GPP TS 36.212, section 5.2.2.6.
    - For TM3, the UE sends the detected RI number in each RI report, to support the dynamic switching between TxD and OLSM.
    - For TM4, the UE shall determine a RI from the supported set of RI values and report the number in each RI report.
    - In case TM 8, 9 and 10 are configured with PMI/RI reporting, the same procedure as in TM4 applies.

According to 3GPP TS 36.211, if the UE is required to provide RI feedback for more than one serving cell, the RI report for each cell is concatenated prior to coding in increasing order of cell index. Additionally, if the UE is required to provide RI feedback for more than one CSI process, the RI reports are concatenated prior to coding first in increasing order of CSI process index for each DL cell and then in increasing order of cell index.

- **PMI (Precoding matrix indicator)**

As illustrated in Figure 2.3 for the general LTE DL channel processing, each layer is mapped for transmission into one or more antennas using a precoding matrix in order to support spatial multiplexing.

Additionally, as cited in Table 2.5, CLSM optimizes the precoding process taking into account the current channel conditions for each layer as reported by UEs through the PMI.
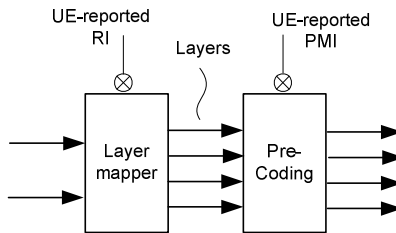
Figure 2.8 - CSI used in TM4.

Consequently, PMI needs to be reported for those transmission schemes using tailored precoding matrices.

- For TM4, TM5 and TM6, PMI feedback is used for channel dependent codebook-based precoding.
- For TM8, PMI is required if the UE is configured with PMI/RI reporting enabled.
- For TM9 and TM10, PMI is required if the is configured with PMI reporting enabled and the number of CSI-RS ports is larger than 1.

Only one or several PMIs can be reported by any UE.

- **PTI (Precoding type indicator)**

The precoding type indicator is a new CSI indicator added in R10 as part of the LTE-A specification, but applies to TM8, TM9 and to TM10 without a RI-reference CSI process. Although the parameter is not properly defined in 3GPP TS 36.213, it is included in the set of CSI parameters required in Type 6 reports together with RI and described for reporting Mode 2-1.

Its function is related to informing the eNB about the preferred precoder type, according to the current fading conditions, from slow to fast fading environments.

2.3.1   LTE SISO

According to Table 2.6, those UEs configured to use LTE TM1support only SISO/SIMO transmission schemes. In SISO, radio transmissions are based on the use of a single antenna at the eNB and a single antenna at the UE. The operation of LTE SISO is illustrated in Figure 2.9 for a single UE.
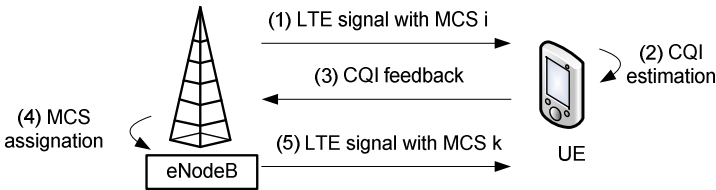
Figure 2.9 – AMC operation in LTE SISO.

Additionally, Figure 2.10 details the process of PDSCH signal generation taking into account a single UE, and depicts how the UE-reported CSI is used at the eNB.

Figure 2.10 - CSI and PDSCH signal generation for LTE SISO.

As can be observed, the transmissions in the PDSCH include a reference signal, which corresponds to CRS in this case. This information transmitted at one TTI is used by the UE to estimate the channel quality and the most suitable signal characteristics for the next TTI, in terms of modulation order and coding efficiency. As a result, the UE codifies the CQI value according to Table 2.7 and send the required report to the eNB.

It must be noted that the process of generating CQI values is not standardized by the 3GPP and is dependent on the specific implementations. The only standardized features are the result of the CQI generation process, which should address the target of BLER lower to 10%, and the different procedures for wideband/sub-band periodic/aperiodic CSI reporting.

In this sense, the 3GPP provides a series of recommendations and performance requirements that a UE should fulfil for accurate CSI reporting. Section 9 of [3GPP-TS36101] proposes a series of tests under Additive White Gaussian Noise (AWGN) and frequency-selective fading conditions, and provides guidance concerning the expected outcomes in terms of variance of CSI parameters, BLER performance and SNR levels.

- If the PDSCH BLER using the transport format indicated by median CQI is less than or equal to 0.1, the BLER using the transport format indicated by the (median CQI + 1) shall be greater than 0.1.
- If the PDSCH BLER using the transport format indicated by the median CQI is greater than 0.1, the BLER using transport format indicated by (median CQI − 1) shall be less than or equal to 0.1.

Taking into account the CQI reported by the UE, the eNB needs to determine the number of PRBs and the MCS to be used in the next transmission to that UE.

- The standard procedure provides the mapping from CQI to modulation order (i.e., QPSK, 16QAM, 64QAM or 256QAM).
    - 3GGP TS 36.21 table 7.2.3-1.
- The selected modulation order determines a set of allowed MCS values and the associated TBS index values.
    - 3GGP TS 36.21 table 7.1.7.1-1.
- The combination between possible MCS values and the number of PRBs assigned to the UE determines the TBS.
    - 3GGP TS 36.21 table 7.1.7.2.1-1.
- With the resulting TBS values, and taking into account the maximum bits allowed by the specific modulation in that bandwidth fraction, the coding efficiency can be obtained for the whole set of possible configurations.
- The selected configuration will be the combination of MCS and number of PRBs closer to the target efficiency set up by the CQI.

It must be noted that the number of PRBs assigned by the eNB to a specific UE is not specified. Therefore, all the possible combinations of MCS values and number of PRBs should be checked. Additionally, in multi user scenarios, the PRB allocation depends on the aggregated traffic demands and the scheduling policy implemented at the eNB. Thus, determining the MCS and TBS for each UE usually becomes a vendor-dependent iterative process.

For guidance, [3GPP-TR37901] provides the expected mappings between CQI and MCS for a UE that receives the full set of PRBs for different bandwidths and for different transmission schemes.

Figure 2.11 identifies the specific CSI reporting Modes supported in LTE SISO, which is limited to provide information about the CQI. Therefore, in the case of periodic reporting the CSI reporting periodicity is commonly denoted as CQI Reporting Rate (CRR).
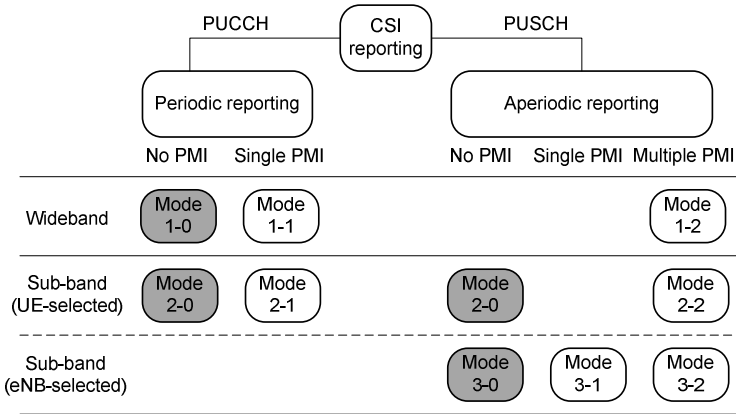
Figure 2.11 – Supported CSI reporting modes in LTE SISO.

Table 2.8 provides detailed information about the CQI data uploaded by UEs to the eNB either through the PDCCH or through the PDSCH for periodic and aperiodic reporting respectively.

Table 2.8 – CSI data in LTE SISO.

CSI Mode	CSI data
PERIODIC REPORTING OVER PDCCH	
Mode 1-0	Wideband CQI reporting: • Type 4 report 4-bit wideband CQI value, which is calculated assuming transmission on set S subbands.
Mode 2-0	In the subframe where wideband CQI is reported: • Type 4 report including: 4-bit wideband CQI value, which is calculated assuming transmission on set S sub-bands. In the subframe where CQI for the selected sub-bands is reported: • UE selects one preferred sub-band per bandwidth part. • One type 1 report per bandwidth part, including the CQI for the selected sub-band and the label identifying that sub-band.
APERIODIC REPORTING OVER PDSCH	
Mode 2-0	Sub-band CQI reporting: • UE selects a set of M preferred sub-bands. • Report one CQI value reflecting transmission only over the M selected subbands. • Report one wideband CQI value, which is calculated assuming transmission on set S sub-bands.
Mode 3-0	Sub-band CQI reporting: • Report one wideband CQI value, which is calculated assuming transmission on set S sub-bands. • Report one CQI value for each set S sub-band, assuming transmission only in that sub-band.

2.3.2   LTE MIMO

MIMO techniques are used in LTE since R8 for UE devices configured in TM2-TM10. As detailed in Table 2.5, different alternative MIMO schemes are supported in LTE, including open loop and closed loop spatial multiplexing techniques and from MIMO 2x2 to MIMO8x8.

As previously described, LTE implements an "adaptive mode selection" procedure, which allows switching between different Transmission Modes to adapt the transmissions to the service provisioning context. Additionally, MIMO-enabled TMs support the "rank-adaptive transmission", which enables quick reactions to the channel conditions by switching the transmission scheme or the number of MIMO layers within the same Transmission Mode.

Consequently, the MIMO configuration has a significant impact in the CSI process. Although alternative configurations are allowed in the standard, the assumed transmission schemes for the different MIMO-enabled TMs are the following:

Table 2.9 – PDSCH transmission scheme assumed for CSI reference resource [3GPP TS 36.213, table 7.2.3-0].

Transmission mode	Supported transmission schemes
TM2	Transmit diversity.
TM3	Transmit diversity if the associated rank indicator is 1. Otherwise large delay CDD.
TM4	Closed-loop spatial multiplexing.
TM5	Multi-user MIMO.
TM6	Closed-loop spatial multiplexing with a single transmission layer.
TM7	If the number of PBCH antenna ports is one, Single-antenna port, port 0. Otherwise Transmit diversity.
TM8 [R9]	If the UE is configured without PMI/RI reporting: if the number of PBCH antenna ports is one, single-antenna port, port 0; otherwise transmit diversity. If the UE is configured with PMI/RI reporting: closed-loop spatial multiplexing.
TM9 [R10]	If the UE is configured without PMI/RI reporting: if the number of PBCH antenna ports is one, single-antenna port, port 0; otherwise transmit diversity. If the UE is configured with PMI/RI reporting: if the number of CSI-RS ports is one, single-antenna port, port 7; otherwise up to 8 layer transmission, ports 7-14.
TM10 [R11]	If a CSI process of the UE is configured without PMI/RI reporting: if the number of CSI-RS ports is one, single-antenna port, port7; otherwise transmit diversity. If a CSI process of the UE is configured with PMI/RI reporting: if the number of CSI-RS ports is one, single-antenna port, port 7; otherwise up to 8 layer transmission, ports 7-14.

TM3, TM4 and TM8-TM10 with enabled PMI/RI reporting support the simultaneous transmission of more than one codewords for a UE. Regardless the number of antenna ports and layers, CQI is calculated assuming transmission of one codeword for RI=1 and two codewords for RI › 1. A detailed analysis of the operation in open loop and closed loop spatial multiplexing is provided, with special focus on the impact on CSI reporting.
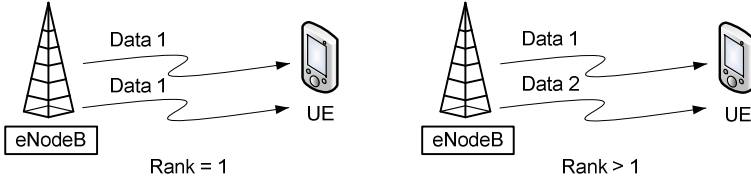
Figure 2.12 – Use of codewords in LTE MIMO.

Transmission Mode 3

In TM3, the transmission scheme is either configured in TxD if the reported RI is 1, or in large delay CDD if the reported RI is higher.

- With RI=1, MIMO is employed to obtain higher resiliency by exploiting the characteristics of spatial diversity in high Doppler and cell edge conditions.
- With RI›1, MIMO is used to achieve higher performance for a single user by transmitting two distinct codewords at the same time.

Open loop spatial multiplexing is targeted at scenarios with limited or inaccurate CSI, including mobile UEs, and high SNR conditions. For that reason, specific per-layer codification is not suitable in TM3 and both codewords share the same configuration parameters.

Figure 2.13 illustrates the operation of LTE MIMO in TM3 for a single UE. As can be observed, in this case the UE is required to provide feedback not only by means of the CQI but also with the most suitable RI value. It must be noted that the frequency for reporting RI values is configured as a multiple of the CQI reporting period during the RRC establishment.
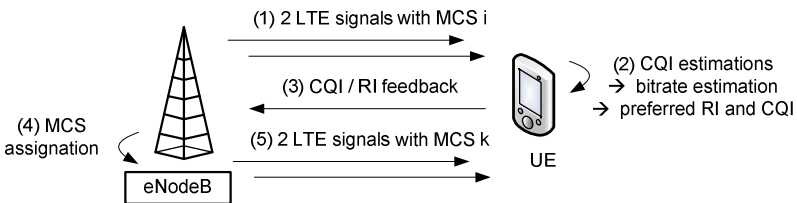
Figure 2.13 - AMC operation in LTE MIMO TM3.

At each RI reporting opportunity, the UE estimates the throughput achievable with the different alternatives:

- With TxD, the eNB transmits the same information through two antennas and the effective SNR is increased. Only one codeword with an MCS associated to a higher CQI is used. The achievable bitrate in this case can be computed based on the number of assigned PRBs and the target MCS, as described for LTE SISO.
- With Large delay CDD, the eNodeB transmits different information through the different antennas. Thus, two codewords can be used. However, since no specific precoding can be used, the MCS for both codewords is associated to a unique CQI value, which is calculated assuming transmission of two codewords. The achievable bitrate in this case can be computed based on the number of assigned PRBs and the target MCS, using the corresponding mappings between single layer TBS and multi-layer TBS (tables 7.1.7.2.2-1, 7.1.7.2.4-1 and 7.1.7.2.5-1 in TS 36.213).

Figure 2.14 details the process of PDSCH signal generation taking into account a single UE, and depicts how the UE-reported CSI is used at the eNB for both transmission schemes.
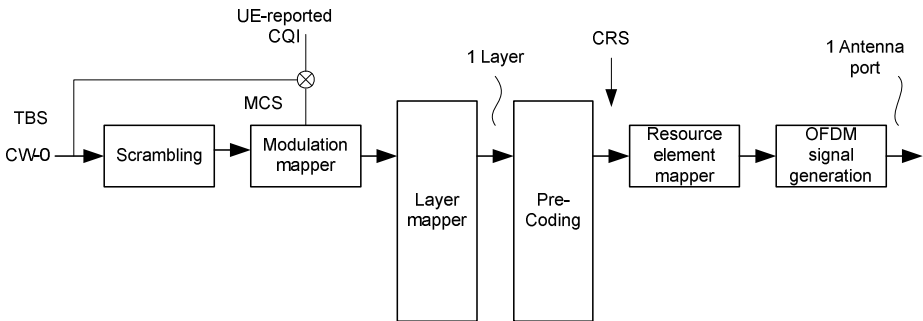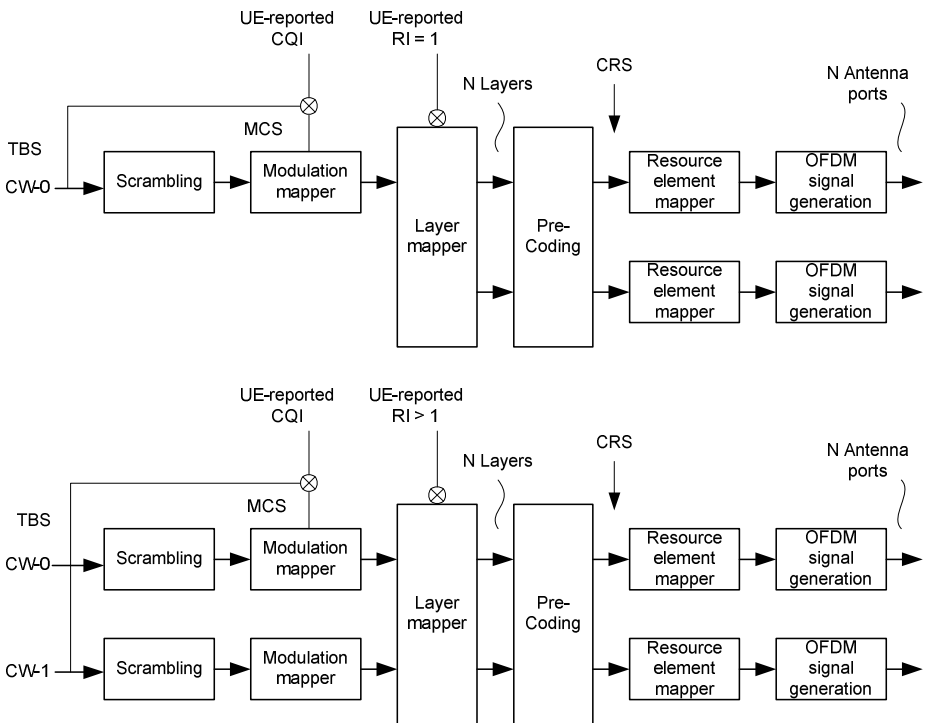

Figure 2.14 - CSI and PDSCH signal generation for TM3: TxD and large delay CDD.

Specifically, the CSI reporting modes that apply to TM 3 are illustrated in Figure 2.15, while detailed information about the reported data is provided in Table 2.10.
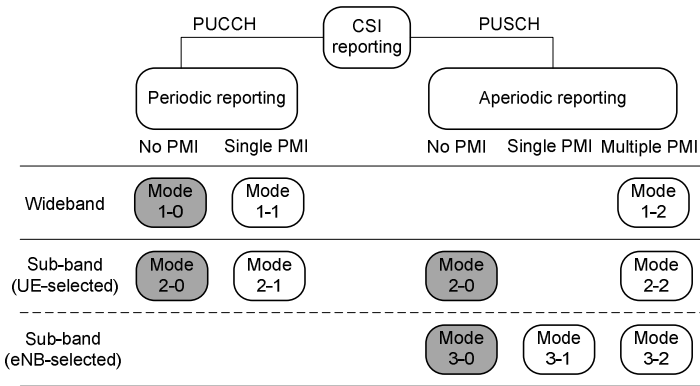
Figure 2.15 – Supported CSI reporting modes in LTE TM3.

Table 2.10 – CSI data in LTE TM3.

CSI Mode	CSI data
PERIODIC REPORTING OVER PDCCH	
Mode 1-0	In the subframe where RI is reported: • Type 3 report consisting of one RI, assuming transmission on set S sub-bands. In the subframe where CQI is reported: • Type 4 report with wideband CQI value, which is calculated only for CW-0 and assuming transmission on set S sub-bands.
Mode 2-0	In the subframe where RI is reported: • Type 3 report consisting of one RI, assuming transmission on set S sub-bands. In the subframe where wideband CQI is reported: • Type 4 report with wideband CQI value, which is calculated only for CW-0 and assuming transmission on set S sub-bands. In the subframe where CQI for the selected sub-bands is reported: • UE selects one preferred sub-band per bandwidth part. • One type 1 report per bandwidth part, including the CQI for CW-0 and for the selected sub-band. The label identifying the sub-band is also required.
APERIODIC REPORTING OVER PDSCH	
Mode 2-0	Sub-band CQI reporting: • UE selects a set of M preferred sub-bands. • Report one wideband CQI value, which is calculated for CW-0 and assuming transmission on set S sub-bands. • Report one CQI value reflecting transmission only over the M selected sub-bands and for CW-0.
Mode 3-0	Sub-band CQI reporting: • Report one wideband CQI value, which is calculated for CW-0 and assuming transmission on set S sub-bands. • Report one CQI value for each set S sub-band, which is calculated for CW-0 and assuming transmission only in that sub-band.

Transmission Mode 4

In TM4, only closed loop spatial multiplexing techniques are used, both for Rank=1 and for higher Ranks.

As illustrated in Figure 2.16, in this case the eNB assumes that the CSI feedback provided by the UE is accurate enough to provide detailed and updated information of the best modulation and coding scheme for each antenna. As a result, different MCS values can be applied to the two codewords and specific precoding matrices can be used for each layer in order to maximize the individual SNR.
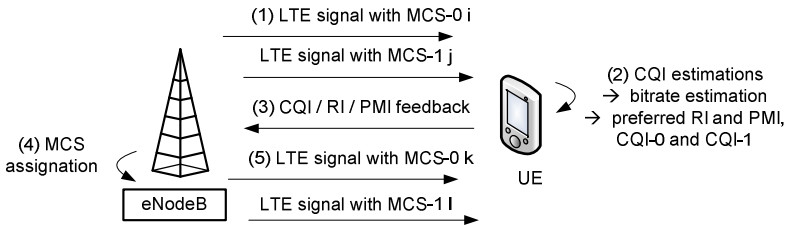
Figure 2.16 - AMC operation in LTE MIMO TM4.

CLSM in TM4 is a codebook based transmission scheme, which means that the UE is able to identify the best performing precoding matrix and the resulting CQI. This process can be implemented for the whole bandwidth (single wideband PMI) or in a per sub-band basis (sub-band PMI) to cope with frequency-selective fading.

Consequently, the UE is requested to report the PMI in addition to the CQI and RI values. Figure 2.17 illustrates the inclusion of CSI feedback in the modulation and coding process at the eNB.
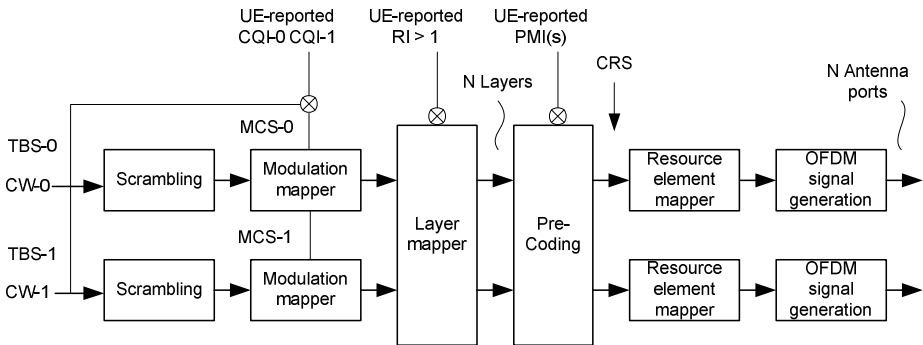
Figure 2.17 - CSI and PDSCH signal generation for TM3: CLSM.

Multiple CSI reporting options are available regarding the granularity of CQI and PMI and from the standpoint of wideband and sub-band values. Figure 2.18 shows the CSI reporting modes in TM 4, while Table 2.11 provides detailed information about the CSI data.
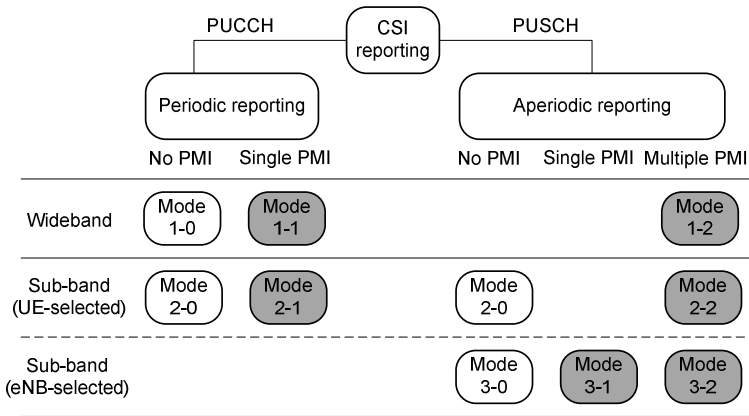
Figure 2.18 – Supported CSI reporting modes in LTE TM4.

Table 2.11 – CSI data in LTE TM4.

CSI Mode	CSI data
PERIODIC REPORTING OVER PDCCH	
Mode 1-1	In the subframe where RI is reported: • Type 3 report consisting of one RI, assuming transmission on set S sub-bands. In the subframe where CQI/PMI is reported: • A single precoding matrix is selected from the codebook subset assuming transmission on set S sub-bands. • Type 2 report consisting of: ○ The selected single PMI (wideband PMI). ○ One wideband CQI value for CW-0, which is calculated assuming the use of the single precoding matrix in all sub-bands and transmission on set S subbands. ○ When RI›1, an additional 3-bit wideband spatial differential CQI for CW-1 offset level.
Mode 2-1	In the subframe where RI is reported: • Type 3 report, as in Mode 1-1. In the subframe where wideband CQI/PMI is reported: • Type 4 report, as in Mode 1-1. In the subframe where CQI for the selected sub-bands is reported: • UE selects one preferred sub-band per bandwidth part. • One type 1 report per bandwidth part, consisting of: ○ One wideband CQI value for CW-0, which is calculated assuming the use of the single precoding matrix in the selected sub-band. The label identifying the sub-band is also required. ○ When RI›1, an additional 3-bit wideband spatial differential CQI for CW-1 offset level.

APERIODIC REPORTING OVER PDSCH	
Mode 3-1	Sub-band CQI reporting with single PMI: • A single precoding matrix is selected from the codebook subset assuming transmission on set S sub-bands. • Report one sub-band CQI value for CW-0 and for CW-1 and for each set S sub-band, which are calculated assuming the use of the single precoding matrix in all sub-bands and assuming transmission in the corresponding subband. • Report one wideband CQI value for CW-0 and for CW-1, which is calculated assuming the use of the single precoding matrix in all sub-bands and transmission on set S sub-bands. • Report the selected single PMI (wideband PMI).
Mode 1-2	Wideband CQI reporting with multiple PMI: • For each sub-band, a preferred precoding matrix is selected from the codebook subset assuming transmission only in the sub-band. • Report one wideband CQI value for CW-0 and for CW-1, which is calculated assuming the best precoding matrix in each sub-band and transmission on set S sub-bands. • Report the selected single PMI (wideband PMI) for each set S sub-band.

Mode 2-2	Sub-band CQI reporting with two PMIs (M sub-bands and S sub-bands):
	• For each sub-band, the UE makes a joint selection of joint selection of M preferred sub-bands and a single preferred precoding matrix from the codebook subset assuming transmission only in the M sub-bands.
	  ○ Report the selected single PMI (wideband PMI) for the M sub-bands.
	  ○ Report one CQI value for CW-0 and for CW-1, reflecting transmission only over the M preferred subbands and using the same single precoding matrix in each of the M subbands.
	• A single precoding matrix is also selected from the codebook subset assuming transmission on set S sub-bands
	  ○ Report the selected single PMI (wideband PMI) for all the set S sub-bands.
	  ○ Report one wideband CQI value for CW-0 and for CW-1, which is calculated assuming the use of the single precoding matrix in all sub-bands and transmission on set S sub-bands.

Mode 3-2	Sub-band CQI reporting with multiple PMI: • For each sub-band, a preferred precoding matrix is selected from the codebook subset assuming transmission only in the sub-band. • Report one wideband CQI value for CW-0 and for CW-1, which is calculated assuming the use of the corresponding selected precoding matrix in each sub-band and transmission on set S sub-bands. • Report one sub-band CQI value for CW-0 and for CW-1 and for each set S sub-band, reflecting transmission over the single sub-band and using the selected precoding matrix in the corresponding sub-band. • The selected single PMI (wideband PMI) for each set S sub-band.

It must be noted the difference between the required bits for reporting the CQI values in periodic and aperiodic modes. I-n the first case, 4 bits are used for each codeword. In the second case, the second codeword is encoded with 3 bits as an offset of the first codeword.

Concerning the reporting periodicity, PMI information is sent in the UL with the same periodicity than the CQI information. Yet, RI information is configured by the eNB as a multiple of the CQI/PMI reporting periodicity.

2.3.3   LTE-A CARRIER AGGREGATION

CA is used in LTE-A to increase the transmission bandwidth, and thus to increase the bitrate achievable for a user. The use of CA is dynamically configured for each user, and the LTE-A cell can support users with CA and users without CA simultaneously. Moreover, in order to keep backward compatibility with R8 and R9 UEs, CA is based on R8 and R9 LTE carriers and Transmission Modes.

CA is defined to ideally support the aggregation of up to five LTE carriers with bandwidths of 20 MHz each, for a total of 100 MHz in DL.

Carrier Aggregation with
Spatial Multiplexing
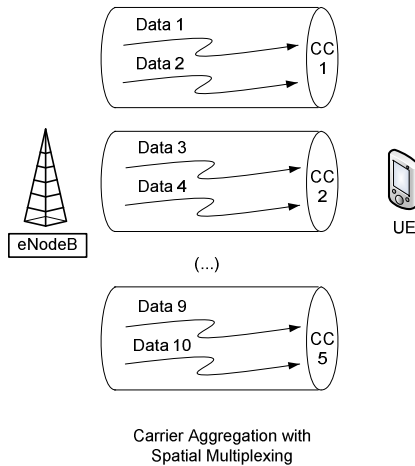
Figure 2.19 – Use of codewords in LTE-A Carrier Aggregation.

Each LTE carrier is denoted as Component Carrier (CC): one of them is configured as the Primary Component Carrier (PCC), associated to the Primary Cell (PCell), while the other carriers are known as Secondary Component Carrier (SCC), associated to any Secondary Cell (SCell), The SCCs are added and removed as required, while the PCC is only changed through handover procedures. The RRC connection is only handled by the PCell.

The PCell implements one PDCCH and one PUCCH, while any SCell may deploy a PDCCH or not, depending on UE capabilities. In case a SCell does not implement the PDCCH, the scheduling information for that SCell is delivered via another SCell PDCCH. This process is referred as cross-carrier scheduling in 3GPP R10 and does apply to the PDCCH.

None of the SCells implement the PUCCH, and therefore periodic CSI reporting must be performed through the PCell.

CA defines three types of bandwidth combinations:

- Intra-band contiguous CA.
- Inter-band CA.
- Intra-band non-contiguous CA.

The ideal configuration of 5x20 MHz is defined in 3GPP R10 for UE Cat. 8 devices, in order to support up to 3 Gbps in DL. The actual possible combinations for aggregating different bandwidths are defined as CA bandwidth classes in 3GPP TS 36.101, table 5.6A-1. However, the only applicable bandwidth aggregations are:

- R10 supports the implementation of "CA Bandwidth Class A" with 1 CC and "CA Bandwidth Class C" with 2 CCs, for up to 40 MHz in intra-band contiguous CA.
- R11 supports the implementation of "CA Bandwidth Class A" with 1 CC and "CA Bandwidth Class C" with 2 CCs, for up to 40 MHz in intra-band contiguous CA and inter-band CA.
- R12 supports the implementation of "CA Bandwidth Class A" with 1 CC, "CA Bandwidth Class B" and "CA Bandwidth Class C" with 2 CCs, and "CA Bandwidth Class D" with 3 CCs. In the latter case, CA supports up to 60 MHz in intra-band contiguous CA and inter-band CA.

Only a selected subset of LTE Bands are allowed to implement CA at the maximum bandwidth configuration The specific configurations for the possible combination of LTE Bands and supported bandwidths are specified in 3GPP TS 36.101, sections 5.5A and 5.6A.

As illustrated in Figure 2.20, the deployment of LTE-A Carrier Aggregation entails a unique logical anchor point in charge of coordinating the transmission throughout the different Component Carriers. Generally speaking, a Centralized BaseBand Unit (C-BBU) implements the digital functionalities and controls a series of Remote Heads Radio (RRH), which actually implement the LTE radio transmission functions.
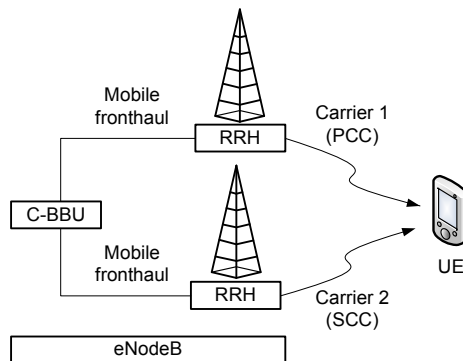
Figure 2.20 –Deployment strategy for LTE-A Carrier Aggregation.

Regarding Channel State Information, LTE-A Carrier Aggregation requires to maintain a different CSI process for each Component Carrier.

Since CA is based on R8-R9 LTE carriers for backward compatibility, the same CSI reporting schemes and reporting modes per each Transmission Mode are applicable. Likewise, the generation of CSI data is also performed based on the reception of Cell-specific Reference Signals.

Yet, a series of specific configurations apply to LTE-A CA.

- **Periodic CSI reporting**

Periodic CSI reporting is performed through the PUCCH of the PCC. Since the PCell is the only serving cell with PUCCH, the quality feedbacks associated to the rest of serving cells need to be reported at this unique UL channel by adding a carrier indicator field (CIF). Therefore, the scheduling and AMC functions are carried out in a centralized way without need for further synchronization between serving cells.

It must be noted that reporting CSI of different cells through a unique PUCCH increases the signalling overhead in the UL channel of the PCell. Additionally, periodic CSI reporting shares PUCCH resources with Hybrid Automatic Repeat Request (HARQ) processes. Since HARQ-ACK transmission are prioritized, periodic CSI reports may be discarded leading to system degradations.

On one hand, 3GPP R10 introduces a new PUCCH format 3 to support multiplexing of up to 10-bit HARQ-ACK in FDD (enough for five CCs) and CSI reports for different serving cells in a single uplink control information (UCI) information element.

On the other one, the CSI reporting period usually needs to be increased in compassion to other single-carrier LTE MIMO schemes. According to the minimum requirement for CSI reporting provided in 3GPP TS 36.101 section 9.6, the reporting periodicity for FDD systems is increased as shown in Table 2.12:

Table 2.12 – Example values for CQI / PMI reporting in CA according to 3GPP TS 36.101.

CSI	1 DL CC	2 DL CCs	3 DL CCs
CQI /PMI	5 ms	10 ms	20 ms

As a result, the degree of channel awareness at the eNB is likely decreased as more CCs are added to the LTE-A transmission. This issue may imply channel estimation errors especially for highly dynamic users or in fast fading situations, leading to transmission errors and decreased system throughput.

Alternatively, if the UE does not support simultaneous PUSCH and PUCCH transmissions and there is a PUSCH allocation in the related SCell, the periodic CSI reporting shall be performed through this SCell PUSCH.

- **Aperiodic CSI reporting**

Up to 3GPP R9, eNBs are able to request instantaneous CSI reports by activating the 1-bit "CQI request" filed in DCI Format 0 messages addressed to the targeted UE ([3GPP TS 36.212], section 5.3.3). Upon an aperiodic CSI report request, the UE shall transmit the information over the PUSCH allocation.

In 3GPP R10, this field is denoted as "CSI request" and becomes a 1-bit field for R9-compatible transmissions or a 2-bit field when UEs are configured with more than one DL cell. In case of 2.bit "CSI request" field, the configured value must be interpreted as shown in Table 2.13 when using any of the TM1-TM9.

Table 2.13 – Possible values for CSI request in LTE-A Carrier Aggregation.

CSI request field value in DCI Format 0 and 4	Aperiodic reporting
'00'	No aperiodic CSI report is triggered.
'01'	Aperiodic CSI report is triggered for the serving cell.
'10'	Aperiodic CSI report is triggered for a 1st set of serving cells.
'11'	Aperiodic CSI report is triggered for a 2nd set of serving cells.

When 'CSI request' is set to one, the UE must report the CSI feedback for the serving cell that transmitted the DCI message. Specific CSI configuration may be announced by each cell during as RRC connection parameters.

The other two CSI reporting schemes involve a set of serving cells. One or more SCells can be dynamically added or removed from the set of serving cells by means of RRC Connection Reconfiguration procedures. During this process, a SCell can be configured to make up a "set of serving cells" together with the PCell or with other SCells. Thus, the eNB may configure different sets of CCs and CSI feedback can be requested at the same time for different CCs.

The "CSI request" field is included in two different types of DCI messages. In addition to the DCI Format 0 already defined in R8-R9, a new DCI Format 4 is introduced in R10. While DCI Format 0 indicates the PUSCH grants for single antenna UL channels, DCI Format 4 is designed to support the assignation of PUSCH grants in multi-antenna UL channels (PUSCH transmission mode 2 supporting SU-MIMO). Both DCI formats are defined to support the 1-bit or 2-bit "CSI request" field.

2.4   CONCLUSIONS TO THE TECHNOLOGY REVIEW

This chapter provides an overall review of the LTE and LTE-A systems specified by the 3GPP, and which are the predominant technology for 4G broadband mobile communication networks. Beyond a simple technology review, the chapter focuses on:

- The analysis of the actual transmission techniques used in current commercial deployments.
- The implications of using AMC (Adaptive Modulation and Coding) based on CSI (Channel State Information) reporting.

According to the requirements imposed by the ITU-R for IMT-2020 systems, the downlink peak data rates expected in 4G systems are 1 Gbps for low mobility and 100 Mbps for high mobility patterns.

The analysis provided in Section 2.1 shows that LTE and LTE-A systems provide a scalable but complex solution, with many different possible configurations concerning the frequency and bandwidth of the cell, the Transmission Mode and associated transmission schemes used, the type and number of layers in a MIMO system, etc.

This requirement of 1 Gbps is only fulfilled by the 3GPP UE Category 8 devices in LTE-A, by considering 8x8 MIMO transmissions and the aggregation of five carriers of 20 MHz for a total of 100 MHz of bandwidth. However, UE Cat. 8 is more a theoretical solution than a commercial-grade product. To the date, only MIMO 2x2 systems are commercially deployed and the aggregation of only up to three carriers is further specified by 3GPP standards.

Therefore, although the terms 4G and 4G+ are being applied to LTE and LTE-A networks respectively, the LTE specification must be considered as a forerunner towards IMT-2020 systems and the LTE-A specifications are still progressing towards true IMT-2020 systems.

From the standpoint of achievable peak data rates, the following UE Categories are currently available in commercial mobile network deployments.

Table 2.14 – Commercial UE Categories and peak data rates (shadowed in grey).

UE Cat.	1	2	3	4	5	6	7	8	9	10	11	12
DL peak rate (Mbps)	10	50	100	150	300	300	300	3,000	450	450	600	600
UL peak rate (Mbps)	5	25	50	50	75	50	100	1,500	50	100	50	100

In R8-R9 systems, both UE Cat. 3 and UE Cat. 4 devices support MIMO 2x2 transmissions and up to 64QAM and 16QAM in DL and UL respectively. UE Cat.5, which introduces MIMO 4x4 in DL and 64QAM in UL, is not considered for commercial deployments.

The most widely adopted feature from the set of enhancements introduced for LTE-A in R10 and beyond is Carrier Aggregation, which supports up to 300 Mbps and 450 Mbps with DL 64QAM and the aggregation of two and three 20 MHz carriers respectively. Besides, the implementation of DL 256QAM makes it possible to reach 600 Mbps in DL with the aggregation of three LTE carriers.

The only possible MIMO transmission schemes are TxD, Large delay CDD (commonly referred to as OLSM) and CLSM with up to two codewords. The type of spatial multiplexing used is a function of how accurate the CSI feedback can be provided. Meanwhile, the use of one or two codewords in MIMO becomes a trade-off between resiliency and data rate. Under good SNR conditions, the proper reception of one codeword per layer can be expected. With worse SNR conditions, it may be preferable to transmit the same codeword in two different layers to increase the probability of correct reception.

In order to synchronize the transmission schemes between the eNB and the UE, two adaptive schemes are mainly used by the eNB:

- "Adaptive mode selection": the eNB may dynamically switch between different TMs through new RRC reconfiguration procedures.
- "Rank-adaptive transmission": the UE maintains an active RRC connection and the eNB may switch between any of the transmission schemes supported in the TM (or even between different Ranks for a same transmission scheme) based on the UE-provided CSI feedback.

Based on these adaptive schemes, each UE in the cell is configured to a unique TM with more than one possible transmission modes.

- TM3 supports dynamically switching between MIMO TxD and MIMO Large delay CDD for using one or two codewords respectively.
- TM4 supports dynamically switching between one or two codewords in MIMO CLSM.

Therefore, the CSI feedback process is also adapted according to the specific TM:

- In TM3, only the RI and CQI parameters are reported by the UE. The RI value indicates the preferred number of codewords, while the unique CQI value is used by the eNB to calculate the supported MCS. A unique CQI is reported, and thus the same MCS is used for both codewords.
- In TM4, the RI, CQI and PMI parameters are required for CSI. In this case two different CQI values can be reported, one for each codeword. Therefore, each codeword may use different MCS.

The specific methods for generating CQI values are not specified and are thus up to different vendor implementations. In a general sense, the reported CQI value should indicate the maximum achievable coding efficiency resulting in BLER values under the 10% threshold. Therefore, the CQI determines the maximum amount of data bits to include in each codeword, while the RI determines the number of simultaneous codewords. Therefore, both CSI parameters are significant for evaluating the performance of LTE transmissions.

Other relevant configuration parameters related to the CSI reporting are:

- The CSI reporting periodicity, which determines the accuracy of the CSI information available at the eNB from a temporal perspective. Reduced CSI reporting intervals entail a higher accuracy at the cost of increased UL signalling overhead. Therefore, the optimal CSI reporting value is a deployment issue and highly depends on the expected CSI dynamics over time. It must be noted that the RI parameter is reported in higher time intervals than the CQI and PMI parameters. Therefore, the AMC process is endowed with higher granularity than the "rank-adaptive transmission" scheme.
- CQI and PMI parameters can be reported as a unique wideband value for the whole transmission bandwidth, or as a set of sub-band values. Using wideband values reduces the UL signalling overhead, although the CSI accuracy may be worse in frequency-selective fading scenarios. Therefore, the adopted configuration determines the suitability of CSI from the frequency domain standpoint.

Taking into account the meaning of CQI and the possible direct mappings to MCS by the eNB, the accuracy of CQI values would determine the effectiveness of the AMC process. Overestimations of CQI result in increased BLER since the actual channel quality is worse than expected value. Underestimations of CQI lead to underutilization of the radio resources, since the estimated channel quality is lower than the actual one.

Finally, the impact of using Carrier Aggregation is mainly significant from the perspective of the CSI reporting periodicity. In summary, CSI reporting musty be implemented for each component carrier. However, only the primary carrier implements an UL control channel. Therefore, the UL signalling overhead would increase considerably unless the reporting intervals are increased.

As a conclusion, this chapter provides relevant information about the AMC and CSI feedback processes in LTE / LTE-A, with special focus on commercially available solutions. However, several CSI-related configuration parameters are not uniquely specified by the 3GPP standards. From an experimental point of view, it seems interesting to analyze the most probable values both for CSI configuration parameters and for the CSI parameters themselves.

3 ANALYSIS OF THE STATE OF THE ART

This chapter focuses on the analysis of publicly available information concerning CSI in LTE networks, the existing gaps, and the possible methodologies to gather relevant CSI information from real-world or experimental scenarios.

The analysis of the state of the art is divided in two main sections:

- First, Section 3.1 discusses the need for obtaining knowledge of the UE-generated CQI values and dynamics, in comparison to other LTE performance metrics. From this requisite, different alternatives are described as the main possible sources of real-world CSI information. Finally, different methods to derive CQI information from other performance metrics are discussed.
- Next, Section 3.2 focuses on the analysis of publicly available sources of information concerning real-world or experimental CSI data.

Finally, Section 3.3 provides the conclusions of the analysis of the state of the art, and states a series of challenges that need to be covered.

3.1   CQI AS KEY CSI PARAMETER

There is an increasing interest from the research community to study the performance of different proposals (e.g., channel-aware schedulers, channel-aware application servers, etc.) in real-world LTE scenarios. For example, several studies address the analysis of achievable performance in LTE networks from an application or transport protocol perspective.

- Concerning typical network performance metrics, [Laner-2012] and [Sommers-2012] provide an in-depth analysis of one-way delays in operational LTE networks. [Xu-2014] compares the performance of different types of modern cellular networks by means of laboratory and crowd-sourced end-to-end measurements. [Beyer-2013] focuses on the performance analysis in heterogeneous LTE networks, with macro-sites and small cells.
- [Huang-2013] presents a comprehensive study of the interactions between LTE radio characteristics and transport level protocols, identifying inefficiencies in the operation of TCP and the impact of network proxies.
- Concerning application-level studies, [Becker-2014] focuses on the performance of Hypertext Transfer Protocol (HTTP) over LTE and its root causes by profiling application-level data. Authors also identify the relevance of the use of transparent middleboxes. [Rivas-2013] addresses the delivery of VoIP services over LTE, and [Almohamedh-2014] relates the quality of mobile videos to the link level quality.

Despite the rapid growth in LTE deployments, researchers and end users have a limited understanding of the network performance and possible associated problems. Even mobile network operators do not fully understand the propagation and interference patterns affecting their networks, particularly in indoor areas not accessible to network operators for measurements [Kumar-2014]. Additionally, the interactions between radio performance and its use by applications and associated transport protocols require a thorough analysis [Huang-2013]. Due to these and other reasons, a better understanding of the LTE physical layer is required.

The quality of the radio channel may be estimated through a series of radio parameters [Almohamedh-2014] [Cainey-2014]:

- Received Signal Strength Indicator (RSSI) is the total power received per Resource Element (RE) (in dBm), including the combination of signals from serving cell, other neighbouring cells, co-channel and adjacent channel interferences.
- Reference Signal Received Power (RSRP) is the power associated to the CRS over the used bandwidth, in number of REs (in W).
- Reference Signal Receive Quality (RSRQ) is a measure of the quality of the signal, as ratio of the RSRP over the RSSI normalized to the used bandwidth.
- Signal-to-Interference and Noise Ratio (SINR), represents the ratio between the received signal (mainly CRS and PDSCH) and the sources of noise and

interference. Although not standardized by the 3GPP, most operators and UE vendors use this metric to derive the CQI values. Although not strictly correct, SINR is usually employed interchangeably with SNR (Signal-to-Noise Ratio).

Most of these radio parameters can be monitored in regular LTE smartphones though dedicated software (e.g., [Alvarez-2012] [Huang-2012] [Cainey-2014] and many other applications available in public repositories and stores), since many mobile OSs provide an API to gather these data from the LTE baseband modem.

Beyond all these power-related measurements, the key parameter to determine the performance of UEs in LTE is the CQI. This parameter determines the coding efficiency [3GPP-TS36.213] supported to meet the target BLER of 10%. Under good radio channel conditions, the CQI value reported by the UE to the eNB would be high, resulting in a high MCS index and better spectral efficiency [Nokia-2014]. In MIMO scenarios, RI is required in addition to CQI to fully understand the achievable system performance.

How UEs compute the CQI value is not standardized and is a vendor-dependent procedure. In fact, the 3GPP only provides a series of test points in different LTE cell characteristics with different AWGN and fast fading conditions [3GPP-TS36101]. The 3GPP only defines the CQI values that shall be reported by UEs in those conditions, together with the possible deviations. Unfortunately, CQI values cannot be generally accessed though commercial LTE devices and UEs specifically enabled for drive testing are required.

Because of this lack of understanding concerning real-world radio performance, most of the LTE-focused studies are based on different link-level and system-level simulators. Although well-known LTE simulators ([Mehlfuhrer-2011], [Piro-2011_a], [Piro-2011_b]) have been widely used in the past years, such tools may be of limited utility and lead to unreliable results [Landre-2013, Baguena-2015].

Therefore, in order to evaluate any channel-aware optimization proposal at different levels, it is important to analyze and characterize the real-world radio performance in different conditions and mobility patterns.

3.1.1   METHODS FOR COLLECTING CQI TRACES

Several methodologies can be used for capturing CSI traces and relevant statistics from real-world and experimental LTE systems.

1.   Operator traces.

Although obtaining CSI traces from mobile operators' networks may be complicated to obtain, it is indeed the best approach since these CSI traces will cover real-world conditions, multi-user scenarios and also the characteristics of commercial UEs. A possible limitation is the frequency of CSI reporting configured in the network.

2.   Network sniffing.

An alternative solution can be to monitor the air interface of LTE systems and extract relevant information of the CSI processes. Although this alternative covers most of the features cited in the previous point, the DL channel only provides information about the results of the AMC and not directly from the CSI operation.

3.   Field tests

Field tests are usually referred to the collection of performance metrics from a single UE in different locations of the cell. Traditionally, these types of tests have been performed with specialized commercial HW and SW with some kind of support from the HW vendor. Nowadays, many alternatives allow the extraction of some performance metrics from general purpose HW, such as smartphones, through the support offered by the mobile operating system. However, regular smartphones are not able to provide CQI values or statistics, and specialized HW and SW is still required.

4.   Network emulation

Although not providing really real-world CSI information, the use of LTE HW emulators allows analyzing the behaviour of commercial UE in certain radio conditions (e.g., [Nikaein-2014]). Additionally, some LTE emulators allow collecting all the CSI values for the whole test.

Section 3.2 includes several examples corresponding to different methodologies.

3.1.2   DERIVATION OF CQI FROM OTHER PARAMETERS

Provided that directly collecting CQI traces is not a trivial work and that it is mainly linked to vendor-enabled equipment or operator-supported scenarios, several alternatives are found in the literature to derive CQI values from other performance-related metrics.

CQI from MCS

The most straightforward way for estimating the UE-reported CQI is based on monitoring the MCS values assigned by the eNB to DL transmissions.

As described in Section 2.3.1 for SISO and Section 2.3.2 for MIMO, the eNB shall use the MCS that provides a coding efficiency closest to the coding efficiency associated to the latest reported CQI value. Thus, each combination of MCS and number of PRBs results in a specific coding efficiency, which may be easily mapped to the most accurate CQI.

Alternatively to computing the whole process every time, annex B.2.2.1 in 3GPP TR 37.901 [3GPP-TR37901] provides a series of tables mapping UE-reported CQIs and MCS values for different bandwidths and for SISO and 2x2 MIMO transmission schemes.

However, this mechanism entails a series of limitations that must be carefully taken into consideration.

First, the resulting coding efficiency is specific for each combination of MCS and number of PRBs assigned by the eNB. Therefore, a unique CQI value could result in different MCS value in function of the amount of radio resources assigned by the scheduling function of the eNB to the UE. Ideally, the number of assigned PRBs is also to be accounted for a perfect reverse-mapping between MCS and CQI. Nevertheless, in case of unavailability, the estimation error will be of one unit as much.

Second, it must be noted that UE Cat. 3 devices have a limited maximum TBS, which translates to an upper threshold in the assignable MCS. These threshold values are also reported in 3GPP TR 37.901 (annex B.2.2.1) for the different configurations. In case of UE Cat. 3 measurements, the higher range of CQI reports will converge into a single estimated CQI value.

Last but not least, non-standard operations of eNBs play an important role in this area. As reported e.g. in [Kumar-2014, Merz-2014], the eNB may implement a conservative MCS assignation under low utilization of radio resources. This way, the used modulation scheme is more robust and prevents possible BLER at the cost of using more PRBs for the same traffic demand. Additionally, eNBs usually implement specific algorithms to control the errors in the physical layer by reducing the MCS. Also in [Merz-2014], authors identify that the eNB may not follow the RI recommendations reported by UEs. This situation leads to higher utilization of TxD transmission schemes over spatial multiplexing transmission schemes.

One strategy to foster the ideal eNB operations involves triggering artificial bulk downloads, leading the cell to high utilization of radio resources as in [Merz-2014]. In that case, eNBs are likely to use the highest coding efficiency possible. Nevertheless, this approach entails active network monitoring and cannot be ensured in passive monitoring.

CQI from throughput

Many studies present performance studies in live LTE networks focused on the achievable download throughput. This metric provides an accurate estimate of the actually expected application-level performance, and has a clear relationship with the assigned MCS and the experienced radio quality. However, many parameters, configuration options at different levels of the protocol stack and network elements have also a great influence in these throughput measurements.

In order to infer CQI values from monitored throughput samples, all the requirements discussed before for the MCS metric need to be checked first. Additionally, inferring the

coding efficiency would require knowing the maximum achievable throughput at every moment, based on the assigned radio resources.

The need for accounting the assigned bandwidth, in terms of number of PRBs, is a relevant limitation for field test throughput measurements based on general purpose equipment. An alternative to specific field test HW/SW platforms is presented in [Ide-2013], where authors use a commercial real-time spectrum analyzer to determine the number of PRBs assigned to an UE. Although the UL direction is monitored in this case, the same procedure is applicable to DL transmissions. While this approach also requires highly specialized equipments, it may be an interesting alternative in some cases.

CQI from spectral efficiency

Other works gauge the performance in terms of spectral efficiency, which provides better approximations to the channel quality. The spectral efficiency represents the achievable bitrate normalized to the used bandwidth (in bits/s/Hz).

The spectral efficiency can be use d to estimate the coding efficiency assigned by eNBs to DL transmissions following expression (3.1).

$$CE = SE * CE\_max / SE\_max \qquad (3.1),$$

Being CE the estimated coding efficiency, SE the monitored spectral efficiency, SE_max the maximum spectral efficiency of the LTE cell corresponding to highest MCS, and CE_max the maximum coding efficiency corresponding to highest CQI.

The maximum spectral efficiency in a determined LTE cell can be determined by the maximum TBS), which at the same time is determined for each SISO/MIMO scheme by the combination of highest MCS index and highest number of PRBs allowed in the specific cell bandwidth. Table 3.1 shows the computed maximum spectral efficiency for 10, 15 and 20 MHz with 2 codewords in 2x2 MIMO.

Table 3.1 – Maximum spectral efficiency for different LTE cell bandwidths and transmission schemes.

Cell bandwidth	TBS	SEmax	TBS	SEmax	TBS	SEmax
	SISO		2x2 MIMO		4x4 MIMO	
10 MHz (50 PRBs)	36696	3.6696	75376	7.5376	146856	14.6856
15 MHz(75 PRBs)	55056	3.6704	110136	7.3424	220296	14.6864
20 MHz(100 PRBs)	75376	3.7688	149776	7.4888	299856	14.9928

Based on the maximum spectral efficiency and the coding efficiency defined for the maximum CQI value, the relationships as shown in Table 3.2can be inferred between the spectral efficiency and the different coding efficiencies for the whole set of CQIs.

As described before for the MCS, the mapping between spectral and CQI could only be ensured under controlled conditions, such as high cell loads, UE Cat. 4 device, etc. Since the spectral efficiency in a determined LTE cell depends on the used spectrum, the bandwidth occupied by the assigned PRBs is already included in these studies

Table 3.2 – Mapping of spectral efficiency and coding efficiency for 10-15-20 MHz.

CQI	mod	CE	SE 10MHz	SE 15MHz	SE 20MHz	SE 10MHz	SE 15MHz	SE 20MHz
			SISO			2x2 MIMO		
1	QPSK	0.1523	0.1006	0.1006	0.1033	0.2067	0.2013	0.2053
2	QPSK	0.2344	0.1549	0.1549	0.1590	0.3181	0.3098	0.3160
3	QPSK	0.3770	0.2491	0.2491	0.2558	0.5116	0.4983	0.5083
4	QPSK	0.6016	0.3974	0.3975	0.4082	0.8164	0.7952	0.8111
5	QPSK	0.8770	0.5794	0.5795	0.5950	1.1901	1.1592	1.1824
6	QPSK	1.1758	0.7768	0.7769	0.7978	1.5955	1.5542	1.5852
7	16QAM	1.4766	0.9755	0.9757	1.0019	2.0037	1.9518	1.9907
8	16QAM	1.9141	1.2645	1.2648	1.2987	2.5974	2.5301	2.5806
9	16QAM	2.4063	1.5897	1.5900	1.6326	3.2653	3.1807	3.2442
10	64QAM	2.7305	1.8038	1.8042	1.8526	3.7052	3.6093	3.6812
11	64QAM	3.3223	2.1948	2.1953	2.2541	4.5083	4.3915	4.4791
12	64QAM	3.9023	2.5780	2.5785	2.6477	5.2953	5.1582	5.2610
13	64QAM	4.5234	2.9883	2.9889	3.0691	6.1381	5.9792	6.0984
14	64QAM	5.1152	3.3793	3.3800	3.4706	6.9412	6.7615	6.8963
15	64QAM	5.5547	3.6696	3.6704	3.7688	7.5376	7.3424	7.4888

CQI from SNR

Generally speaking, CQI values are generated by UEs are based on the measured SNR of the pilot signals or CRSs. Since there is not a clear direct relationship between both metrics, most of the mapping proposals are based on previous experiments in controlled AWGN or fading conditions (e.g., [3GPP-TS36101]). In summary, these experiments take the target SNR as the configurable parameter in different transmission conditions (including the transmission scheme). For each SNR, the coding efficiency is increased until BLER

overpasses the 10% threshold. Through an iterative process, the whole map of matching points can be obtained.

However, this relationship may be complex in MIMO scenarios [Colom-2012] and its actual implementation is up to device vendors.

For example, the same effective SNR can be obtained with different contributions by each antenna. Hence, the proper identification of the channel quality at each antenna is critical for the determination of the requested transmission scheme and the specific CQI level to be reported. As shown in [Sevindik-2012], the correlation between SNR and CQI at different antennas depends on the experienced channel variability at each antenna. Therefore, different fading profiles would have different impact on the supported coding efficiency, and accurate CQI estimation becomes a complex process.

Even when CRS SNR is claimed to be a good estimator of the coding efficiency (figure 9 in [Merz-2014]), the range of CQI values monitored for a same SNR condition is usually wide. Thus, SNR values are not always an accurate estimator of the reported channel quality and CQI traces are generally preferred to analyze the experienced performance.

Additionally, most commercial UEs are endowed with additional logic to double check if performed CQI estimations are accurate enough. This usually means that UEs are able to account the HARQ results, and in case of increasing BLER more conservative CQI values are reported. This Outer Loop Link Adaptation (OLLA) is described e.g., in [Aho-2011].

CQI from RSRP, RSSI

CQI values are hardly accessible from higher layers in general purpose UEs. Likewise, some devices are capable of providing SNR values while many other UEs do not allow access to SNR statistics, or they are not detailed enough in MIMO scenarios. Therefore, some studies address the problem of inferring link quality from other radio metrics.

In [Slanina-2014], an almost linear relationship between CQI and RSRP values is depicted. However, these experiments are performed in a laboratory testbed and not in real-world commercial LTE networks. Specifically, authors use a PC-based software LTE network and a Universal Software Radio Peripheral (USRP) for the radio interface. The used UE is the USB dongle Huawei e398, which is a UE Cat. 3 device. Performance monitoring is carried out with Rohde&Schwarz Romes 4 software. The experiments are based on LTE Band 20 (800 MHz) and using four different bandwidths, namely 1.4, 3, 5 and 10 MHz. Additionally, the experiments are based on SISO transmissions and the applied fading channels are not detailed.

In [Landre-2013], authors propose a method to estimate SINR values from RSRP and RSSI measurements. The main contribution of this paper is a prediction method that relies on combining LTE link level simulations and LTE drive test measurements. In this case, field tests were performed with an UE Cat. 3 in two different LTE areas deployed at Band 7 (2.6

GHz). Reported results claim to properly simulate the predicted performance, based only on monitored RSSI and RSRP values, with the actual experienced performance.

Nevertheless, these relationships seem to be quite specific to the performed experiments and real-world scenarios are likely to exhibit different behaviours. For instance, in [Kumar-2014] authors describe the case where UEs report a very high RSSI and SNR value but a very low SINR. In this reported case, although the overall radio power is enough, the interference levels due to several eNBs significantly affects the reception of their CRSs and thus the channel estimation process is degraded.

3.2   ANALYSIS OF REPORTED CQI VALUES

In summary, it is evidenced that analyzing and characterizing the behaviour of CSI values in modern LTE networks is a very challenging but appealing problem. Therefore, this section aims at reviewing publicly available documents that deal with this problem, and identifies relevant findings and missing gaps. The analyzed studies are categorized according to the measurement methodology established in Section 3.1.1.

3.2.1   OPERATOR TRACES

In the White Paper "What is going on in Mobile Broadband Networks?: Smartphone Traffic Analysis and Solutions" released by Nokia networks in 2014, they provide an analysis of the performance experienced in a large number of deployed LTE networks [Nokia-2014].

According to average CQI values extracted from UE-provided CQI reports, they state that the typical CQI value in LTE networks ranges between 10 and 11. Logically, the reported CQI values depend on the network load and interference levels. This means that the eNB is able to use the highest modulation scheme 64QAM in the lower efficiency ranges.

Additionally, they identify a correlation between reported CQI values and network load, as shown in Figure 3.1.
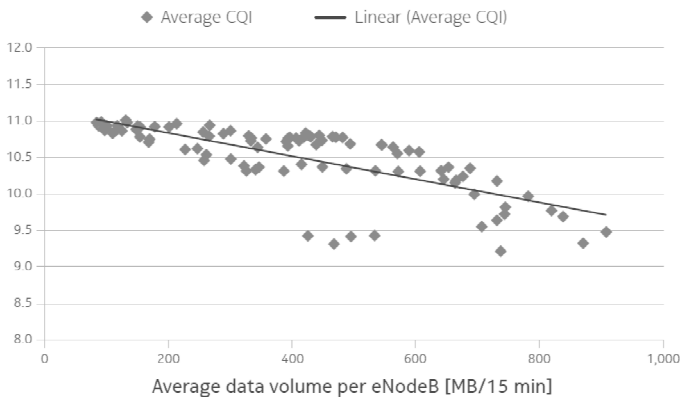
Figure 3.1 – Correlation between average CQI and network load [Nokia-2014].

The average CQI values range between 9.5 and 11, which falls in the edge between the highest 16QAM modulation scheme and the lowest 64QAM modulation scheme.

However, this white paper does not provide detailed information about the specific characteristics of the LTE cells, concerning e.g. the LTE Band and bandwidths. Moreover, only aggregated and averaged CQI statistics are gathered and the evolution of CQI over time cannot be inferred. Finally, neither the transmission scheme used by UEs nor the reported Rank in case of spatial multiplexing is specified in the report.

Alternatively to operator-provided traces, operator-supported approaches may involve the inclusion of monitoring probes inside the operators' networks.

Some examples of operator-assisted architectures are [Laner-2012] and [Huang-2013], where authors present a methodology for active and passive monitoring of deployed LTE networks respectively.
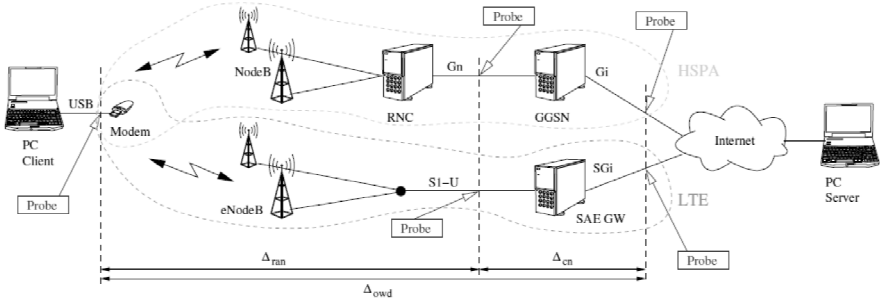
Figure 3.2 – Operator-assisted LTE monitoring [Laner-2012].
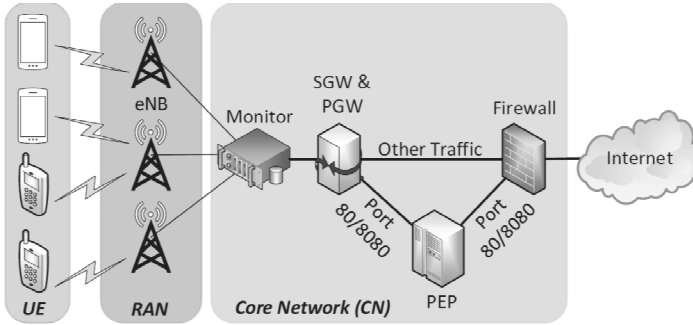
Figure 3.3 – Operator-assisted LTE monitoring [Huang-2013].

In both cases, the data collection point is located at the mobile backhaul, between the eNB and the SGW/PGW. Therefore, the radio-related information (such as reported CQI values) is not accessible and only application-level and transport-level statistics can be analyzed.

3.2.2   NETWORK SNIFFERS

Beyond commercial HW wireless protocol sniffers, the work presented in [Kumar-2014] is of special interest due to the use of accessible SW and affordable HW and for the quality of the research results provided.

In [Kumar-2014] authors introduce LTEye, claimed to be the first open platform to monitor the LTE physical layer and analyze the radio performance at a fine temporal and spatial granularity. This platform runs over Software Defined Radio (SDR) hardware to implement a passive sniffer without the need of either operators' support or users' private information.

LTEye demonstrates that the LTE physical layer can be passively monitored by accessing the information from common LTE control channels that contain metadata about UL and DL transmissions. However, general purpose hardware is likely unable to decode the LTE physical channel continuously in real-time and temporal snapshots shall be gathered in turn.

The information broadcasted within DCI messages over the PDCCH includes resource allocation in terms of assigned PRBs, modulation and coding rate based on assigned MCS, and DL/UL frame loss information according to "new data indicator (NDI)". In DCI messages indicating DL assignments, NDI represents if the TB is a HARQ retransmission. In DCI messages notifying UL grants, NDI represents if a TB needs to be retransmitted by the UE. This information is scrambled with the Cell Radio Network Temporary Identifier (C-RNTI) assigned to the user during the RRC session establishment. Therefore, LTEye is able to discriminate which DCI messages are addressed to different UEs.

Base on this platform, authors report the monitored LTE DL and UL channel quality for two different operators, both of them deployed at LTE Band 13 (700 MHz) and with DL/UL bandwidths of 10 MHz. Periodic measurements are performed with measurement time of 1 second and sampling period every 3 seconds Specifically, the link quality is assessed based on the average MCS assigned by eNBs to UEs. Figure 3.4 illustrates the average coding efficiency over time obtained from field measurements.
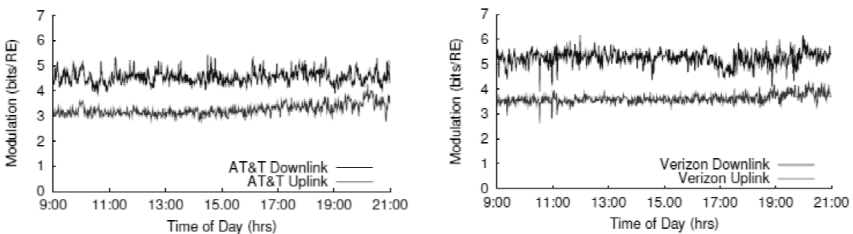
Figure 3.4 – Temporal evolution of averaged coding efficiency [Kumar-2014].

The average DL coding efficiency values for the whole set of samples are 4.56 and 5.23 (in bits/RE) respectively. According to Table 3.2, the former value would correspond to an average CQI close above 13. The latter value would provide an average CQI between 14 and 15. However, it must be noted that the MCS assignations may be conservative based on vendors' specifications. Therefore, the validity of these mappings is only guaranteed in case of high network loads, where eNBs use to apply the highest coding efficiency possible. In [Kumar-2014], the DL network utilization varies along time of day with averages of 25.20% and 58.18% respectively for each operator.

3.2.3   FIELD TESTING

Few studies provide detailed information concerning real-world CQI values obtained from field tests in using commercial LTE networks and UEs. The most relevant works identified are [Sevindik-2012], [Landre-2013] and [Merz-2014].

In [Sevindik-2012], authors illustrate the temporal evolution of CQI values in stationary and high user mobility conditions in one operational LTE network with 10MHz of bandwidth. The LTE network implements 2x2 MIMO DL transmission and statistics for the two codewords are provided. No information about the LTE Band or the TM (OLSM or CLSM) is provided. All the tests are performed in a suburban area and DL traffic is generated through accessing video sharing websites, with a total of 90 minutes of samples. No information about the LTE monitoring equipment is provided, in terms of UE type or field test SW.

Stationary measurements are carried out with a laptop inside a building. As illustrated in Figure 3.5, CQI values associated to both CWs are considerably high, in the range of 14 and 15. This behaviour is almost straightforward since the average SNR measured at both antennas is 27.7 and 27.2, with low deviation along the whole trace. Although no information about the RI is provided, RI=2 can be expected at those SNR values.
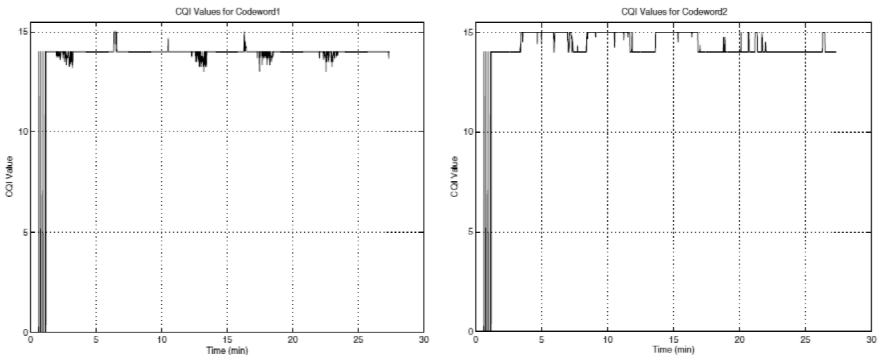
Figure 3.5 –Temporal evolution of CQI in stationary conditions [Sevindik-2012].

In this case, the correlation between the CQI values obtained for the two layers is reported to be 0.9872. This means that both antennas are in quite similar radio conditions. However, although the overall radio performance is quite favourable in stationary conditions, significant BLER values are exhibited along the whole temporal trace. The reported BLER is higher than the target 10% value for 14% of the time.
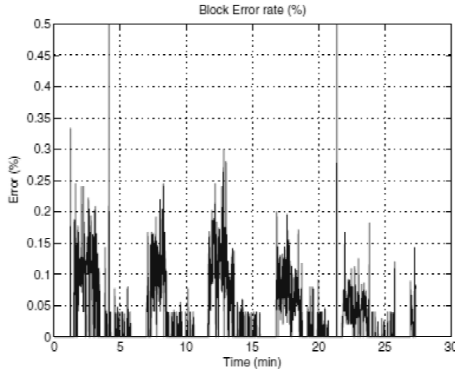
Figure 3.6 –Temporal evolution of BLER in stationary conditions [Sevindik-2012].

Concerning high mobility patterns, field tests are performed in a highway with an average user velocity around 70 km/h. In this case, only CQI values for one codeword are reported. As illustrated in Figure 3.7, the variability of CQI over time is significant. However, average CQI values or other CQI statistics are not provided. The correlation between monitored CQI and SNR values is 0.6580 and 0.8584 respectively for antenna 1 and 2. This means that the relationship between SNR and CQI is not so straightforward in case of high mobility. Moreover, the experienced radio conditions on each antenna are significantly different. In this case, antenna 2 is reported to experience less variable radio conditions.
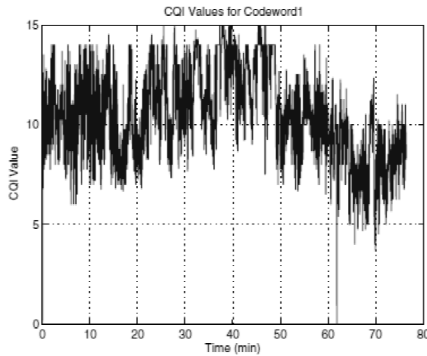
Figure 3.7 –Temporal evolution of CQI in high mobility conditions [Sevindik-2012].

Finally, the BLER monitored in mobility tests is presented in Figure 3.8. The average BLER accounts for 3.24%, with a standard deviation of 6.83%. The total time with BLER under the target 10% is 90%, which is higher than in the reported stationary conditions.
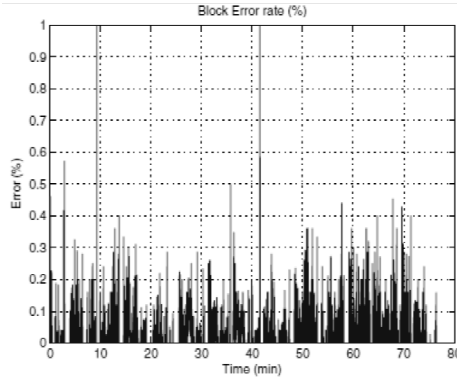
Figure 3.8 –Temporal evolution of BLER in high mobility conditions [Sevindik-2012].

In [Landre-2013], authors present the results of monitoring two different areas of an LTE network in its deployment phase. Field tests are carried out in LTE Band 7 (2.6 GHz), with 20 MHz cells supporting closed loop spatial multiplexing.

The performance results are focused on the application-level throughput. Yet, the controlled experiment conditions guarantee that the user is alone in the cell and that all the PRBs can be assigned to the test UE. Additionally, FTP-based traffic is enforced in the tests and accurate coding efficiencies can be assumed (ignoring transport layer inefficiencies). Therefore, the presented throughput values can be mapped to CQI values with limited error probability. Since the paper is more focused on the proposed prediction model than on the detailed analysis of field test results, only overall throughput values can be obtained.

Figure 3.9 shows the statistical characteristics of throughput, in terms of CCDF.
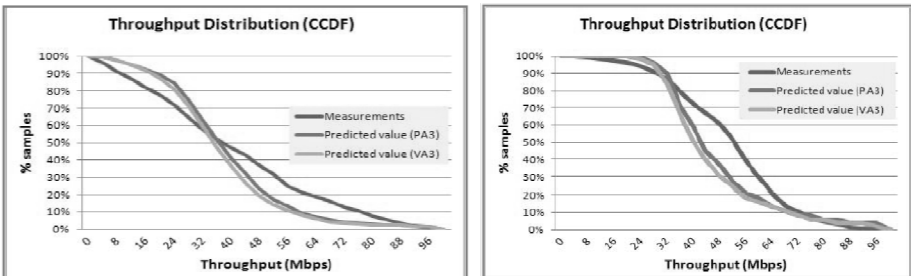
Figure 3.9 –CCDF of throughput in [Landre-2013].

According to the mapping established in Table 3.2, Table 3.3 presents the estimated CQI values corresponding to the reported throughput levels.

Table 3.3 – Mapping between monitored throughput and estimated CQI.

	Measured throughput (Mbps)	Estimated CQI in 2x2 MIMO	Measured throughput (Mbps)	Estimated CQI in 2x2 MIMO
	Area 1		Area 2	
Average	40	7.1	51	8
Median	37	6.7	53	8.2
Cell Centre (Q95)	85	10.5	80	10.3
Cell Edge (Q5)	5	1	23	4.8

In [Merz-2014], authors present the results of a series of field tests carried out to identify the physical effects of high speed patterns in LTE. Specifically, up to 200 Km/h velocities are reported. One of the merits of [Merz-2014] resides in the detailed explanation of the performed field tests. Two types of UEs have been used, being Cat.3 and Cat. 4 USB dongles. The operational LTE network monitored is deployed at LTE FDD Band 3 (frequency 1800 MHz) with cells using different bandwidths (10 MHz and 15 MHz) and implementing 2x2 MIMO in TM3. The commercial field test software used in Nemo Outdoor.

The performance metrics used in the study are:

- the spectral efficiency of the UE (in bit/s/Hz)
- the radio resources assigned to the UE (number of PRBs)
- the SNR for each antenna port (in dB)
- the distribution of MCS assigned to DL transmissions
- the distribution of Rank Indicators reported by UEs and assigned by eNB

Concerning RI, authors provide statistics of the use of RI=1 (single layer) and RI=2 (two layers) through the different measurement periods, and for both Cat. 3 and Cat. 4 devices. In Figure 3.10, each sample for the boxplot corresponds to the percentage of time for which the specific RI is used in a specific measurement period. The first leftmost graphs correspond to UE Cat. 4 device and the rightmost graphs to UE Cat. 3 device.

Some interesting findings about the use of RI are:

- In general, RI=2 is used in higher ratios of time. Thus, open loop spatial multiplexing behaves as a useful scheme even in high speed tests.
- UE Cat. 4 device estimates and requests RI=2 in higher ratios than UE Cat. 3, probably related to the chipset capabilities.
- The RI values assigned by eNBs do not follow the RI values reported by UEs.
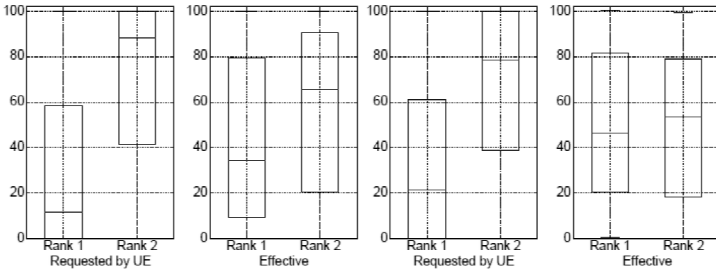
Figure 3.10 – Usage of RI at high speed in live LTE cells [Merz-2014].

Regarding CQI values, no direct information is provided by authors. However, they state that bulk traffic downloads are triggered to force high loads in eNBs. Thus, eNBs are expected to implement the highest coding efficiency possible as reported in CSI feedbacks. Therefore, an almost direct relationship can be established between the estimated CQI values and the MCS and spectral efficiency values.

Figure 3.11 and Figure 3.12 gather the information captured with the UE Cat. 4 device concerning the use of types of modulation and MCS values over the whole set of measurement periods. It must be recalled that information monitored by UE Cat. 3 devices is not representative at high ranges, due to the upper threshold imposed to MCS.

Based on Figure 3.11, and according to Table 3.2, the boxplot values can be directly mapped to a range of estimated CQI values. QPSK modulation is used for CQI values 1-6, 16QAM is used for CQI range 7-9 and 64QAM is used for CQI values in the range of 10-15. As can be observed, the probability of being in high CQI values is significant even at high speeds.
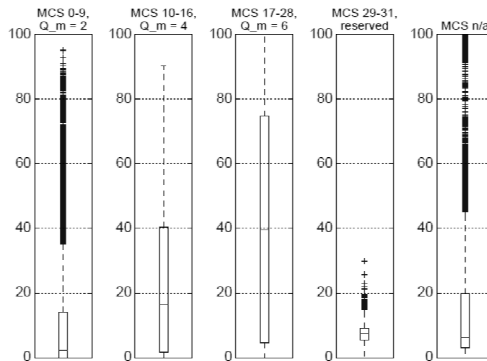
Figure 3.11 – Usage of modulations at high speed in live LTE cells [Merz-2014].
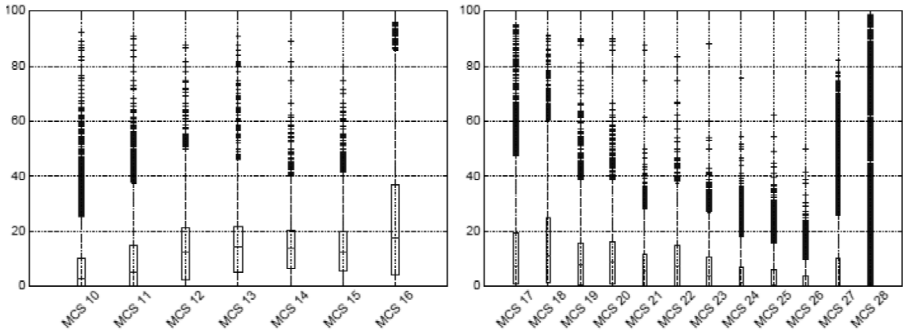
Figure 3.12 – Usage of MCS (per modulation) at high speed in live LTE cells [Merz-2014].

In order to get further insights of the specific MCS and CQI values, Figure 3.12 gathers the usage ratios of the different MCS values (normalized for the samples within each modulation order). At first sight, it seems that MCS values focus on the highest 16QAM values and lowest 64QAM values. However, there are measurement periods with almost 100% of usage for almost the whole range of MCS values.

In order to get a more detailed snapshot of the percentage of time where the different possible modulation schemes are used, CQI values are estimated from spectral efficiency values. Once again, the assumption of loaded eNBs allows estimating CQI values with spectral efficiency, although no information is provided about experienced BLER or transport-layer inefficiencies.

Figure 3.13 shows the ECDF of the spectral efficiency for the whole set of measurement periods.
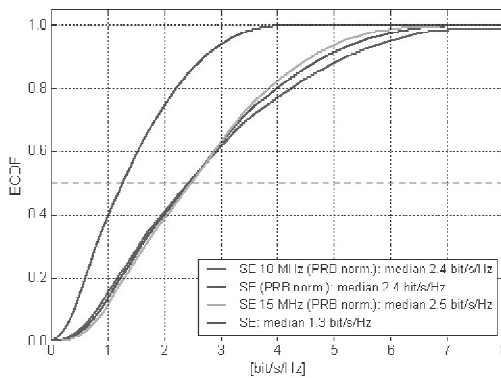
Figure 3.13 – Spectral efficiency in high speed field tests [Merz-2014].

As can be observed, the median value of the normalized spectral efficiency is similar for both types of LTE cells (10 MHz and 15 MHz cells), being between 2.4 and 2.5 bits/s/Hz. However, 10 MHz cells exhibit more disperse values with higher number of samples in the lower and higher ranges. The mapping between the spectral efficiency and the coding efficiency is provided in Table 3.2 for different types of cell bandwidths and transmission schemes. Taking as reference the normalized spectral efficiency values averaged for both types of cells (10 MHz and 15 MHz bandwidths), an averaged value of the spectral efficiency is also used as shown in Table 1.1.

Table 3.4 – Mapping of average spectral efficiency and coding efficiency for 10-15 MHz.

CQI	modulation	CE	SE (average)
1	QPSK	0.1523	0.2040
2	QPSK	0.2344	0.3140
3	QPSK	0.3770	0.5050
4	QPSK	0.6016	0.8058
5	QPSK	0.8770	1.1747
6	QPSK	1.1758	1.5749
7	16QAM	1.4766	1.9778
8	16QAM	1.9141	2.5638
9	16QAM	2.4063	3.2230
10	64QAM	2.7305	3.6572
11	64QAM	3.3223	4.4499
12	64QAM	3.9023	5.2268
13	64QAM	4.5234	6.0587
14	64QAM	5.1152	6.8513
15	64QAM	5.5547	7.4400

As a result, the estimated CQI values reported by UEs in high speed field tests are summarized in Figure 3.14 and Table 3.5.

Table 3.5 – Mapping of spectral efficiency to CQI.

	Median	90th percentile	99th percentile
Spectral efficiency (bits/s/Hz) [Merz-2014]	2.4	4.8	6.4
Estimated average CQI value	7.76	11.52	13.52
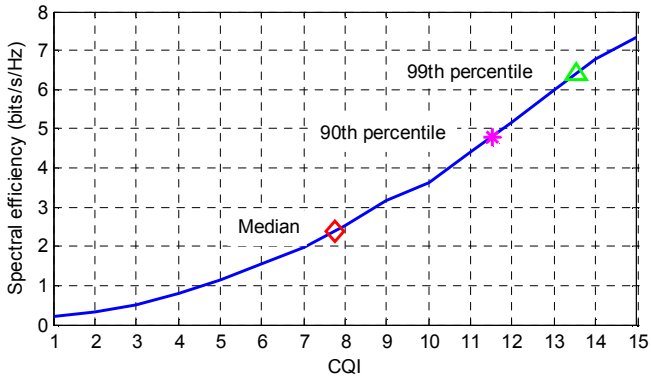
Figure 3.14 – Mapping of spectral efficiency to estimated CQI.

3.3   CONCLUSIONS TO LTE CSI REPORTING

From the analysis of the state of the art, it is evidenced that understanding the insights of CSI processes in live LTE networks is a challenging but appealing topic nowadays. However, the amount of publicly available information is limited, and most of the available documents lack of certain context information to fully understand the exact meaning of the monitored CSI values.

The first part of the chapter is devoted to the analysis of possible sources of information for performance evaluation in terms of CSI and the relation to other radio performance metrics. The second part of the chapter provides an analysis of the most significant reports available in the literature concerning the monitored CSI in live LTE networks.

As explained in Chapter 2, the key CSI parameters that determine the performance level achievable by a user in LTE systems are RI and CQI. The former determines the number of codewords that can be simultaneously used by the eNB in MIMO transmissions, while the latter determines the maximum coding efficiency supported in those codewords (and thus, the maximum MCS that can be assigned to DL transmissions to each user). The combination of both parameters establishes the maximum amount of user data than can be transmitted per TTI.

However, gathering CSI data is not an easy and affordable task for most of the research community. From a general perspective, actual CSI data can only be accessed in three ways:

- Access at the UE side. Gathering CSI data from UEs requires the use of specific HW, since commercial UEs do not provide access to this kind of low-level CSI information. Additionally, these vendor-enabled devices are usually commercialized through specialized field testing SW tools, which also hide the interface with the HW.
- Access at the eNB side. In 4G architectures, CSI information provided by UEs is only available at the eNB. Therefore, this methodology requires the support of the mobile operator / eNB vendor. Multi-UE CSI information could be simultaneously accessed in live operational contexts, although the CSI accuracy would be limited to the actually configured CSI reporting period.
- Access at the air interface. It is shown that the LTE control channel can be sniffed to gain access to control information associated to all the UEs in a cell. However, the analyzed works target the DL control channel and therefore the collected metrics are related to result of the AMC process (i.e., the MCS and the number of assigned PRBs). Although AMC takes CSI information as an input, the intrinsic relationship is not always direct.

Since accessing CSI information is not an easy task nowadays, several initiatives try to characterize the performance of live LTE networks with general-purpose UE devices, mainly focused on the CQI parameter. Some applications claim to report CQI values, although they

only implement the request to the mobile operating system where the actual CQI value is not available. Other studies try to infer the value of CQI from a series of heterogeneous measurable parameters.

However, inferring CQI values from different performance metrics entail a series of drawbacks that may lead to misinterpretations of the performance achievable by a user:

- Most of the commercial devices provide access to live RSRP, RSSI and RSRQ values. However, the literature shows that there is not always a direct relationship between these parameters and the reported CQI.
- Many commercial LTE devices also report SNR values through the mobile operating system. Although SNR is claimed to be a good estimator of the coding efficiency, several issues must be considered:
  - Mapping SNR to CQI may be complex in MIMO scenarios where the contribution of each antenna to the wideband SNR is not clear. This effect is especially problematic when the fading conditions have quite variable impact on each reception antenna.
  - Additionally, commercial UEs are likely to incorporate an Outer Loop Link Adaptation function to cope with imperfect CSI reporting. Results provided in Figure 3.5 seem to be in line with this behaviour, reflecting short periods of lower CQI when high BLER is experienced.
  - As a result of these issues, the range of CQI values monitored for a same SNR condition is usually wide.
- The outcome of the AMC process can be gathered by sniffing the DL control channel of the LTE cell. The analysis of the assigned MCS values over time could be taken as a reference for the estimated CQI values reported by the UEs sharing the same cell. However, the literature reports that following the CSI feedback is not mandatory and eNBs may use conservative MCS assignations when there are enough radio resources.
- Similarly, different application-level metrics such as throughput and spectral efficiency can be used as a reference to estimate the CQI levels reported by UEs. As in the previous case, these mappings are only valid if the eNB follows the recommended AMC operation, e.g. under high radio resource usage for a unique UE in the cell.

Although the analysis of the state of the art discourages the estimation of CQI values from other performance metrics in a general sense, it is interesting to provide a further detailed study on the subject.

Additionally, even in the case that CQI values are properly monitored or inferred, two issues would remain open:

- The RI value must be also gathered to properly understand the impact of CQI values on application-level performance.

- The periodicity and reliability of CQI measurements / estimations need to be further evaluated.

From the analysis of CSI values reported in different studies, the most relevant conclusions and open issues can be summarized as follows:

- Many of the CSI studies focus on the CQI parameter, without providing the required information about the RI parameter.
- Other studies provide information about both RI and CQI parameters, but mainly from a general statistical perspective and without properly correlating the possible CQI values to the RI values.
- None of the analyzed studies provide any information about PMI reporting. Thus, TM3 can be assumed as the predominant mode in commercial mobile broadband networks.
- None of the studies provides information about the CQI reporting mode, in terms of wideband / sub-band and periodic / aperiodic feedbacks.
- Different studies lack of the necessary information about the LTE Band, the LTE bandwidth, the user mobility, etc. Therefore, the reported statistical CQI values are not comparable.
- Although some studies illustrate the evolution of CQI over time for specific mobility conditions, the periodicity of the measurements are not provided. Additionally, none of the studies provides a characterization of the variability of CQI or RI values over time.
- Surprisingly, the BLER values experienced in stationary conditions are found to be higher than the BLER in stationary conditions in [Sevindik-2012]. A possible explanation is associated to the use of OLLA functions under considerable BLER conditions, which leads to a more conservative CQI estimation by the UE.
- There are not clear evidences about the correlation between the SNR experienced by the two antennas in MIMO systems. Some experiments seem to indicate that both antennas experience similar channel quality levels, while other results seem to illustrate the opposite.
- Finally, none of the studies provides CSI data in Carrier Aggregation systems. Therefore, the possible impact of using different LTE Bands and of the increased CSI reporting intervals cannot be evaluated.

As a result, it is concluded that not only accessing CSI information is a complex task for most of the research community, but also the outcome of the CSI feedback processes are not properly characterized with a sufficient level of detail from studies in live LTE networks. The direct consequence is that most of the LTE-focused research studies are based on easy CQI mappings from complex radio models, which may not lead to accurate system-level simulations.

Hence, the key challenge for the rest of the document is aimed at providing more structured and detailed insights of the CSI processes monitored from commercially available LTE networks.

4 FIELD TESTING IN LTE

The review of the LTE technology (Chapter 2) identifies the motivation for a better understanding of the CSI (Channel State Information) procedures experienced in real-world deployments, and their possible impact in the AMC (Adaptive Modulation and Coding) operation in LTE systems.

From the analysis of commercial LTE networks currently deployed worldwide, the range of possible LTE Transmission Modes seems to be limited to TM1-TM4. Determining the TM is critical for understanding the CSI procedures, since different CSI parameters may be required from the set of CQI, RI and PMI.

The analysis of the state of the art (Chapter 3) illustrates the increasing interest by the research community towards fully understanding the values and characteristics of the CSI parameters experienced in live LTE networks. However, most of the analyzed studies are limited to the CQI parameter, and do not provide enough information concerning the MIMO scheme or the dynamics of the multi-layer transmission.

With these antecedents in mind, this section presents the main outcomes of a series of experiments carried out through field tests. The main motivations of these tests can be summarized in the following open questions:

- Which is the predominant LTE TM and transmission scheme in different conditions?
- Which is the behaviour of the RI parameter in different conditions? How strong is the correlation of the two reception antennas in MIMO systems?
- Is it really possible to infer CQI values from other performance metrics such as RSSI, RSRP, RSRQ or SNR?
- Is it really possible to infer CQI values from the monitored DL MCS assignations?
- Is it possible to characterize the temporal evolution of CSI values? How often and how quick are CQI/RI/PMI variations? And how deep does CQI varies over time?
- Do eNBs follow exactly the CSI information provided by UEs in terms of RI/CQI for the MCS assignations?
- Although CSI values should be generated from the quality of the Reference Signals, is there any impact of the DL data? This is, can field tests be performed without DL data transfers properly?
- Which is the impact of different context parameters such as the mobility pattern or the modulation used for DL data?

This chapter is organized as follows.

- Section 4.1 provides a description of the data set, explaining the followed field testing methodology and the main results concerning the CSI-related configuration parameters.
- Section 4.2 revisits the analysis of possible relationships between different radio performance metrics and the CQI values, by taking into account the observed values.
- Likewise, Section 4.3 evaluates the possible relationships between the CSI reported by UEs with the MCS values assigned by eNBs with real-world commercial equipments.
- Section 4.4 focuses on the characterization of the CSI values gathered from field tests, identifying the most significant results and the possible limitations.
- Finally, Section 4.5 summarizes the most relevant outcomes of the chapter.

4.1 DESCRIPTION OF THE DATA SET

As explained before, although field testing is a resource and time consuming measurement methodology, it is the only way to gather the required CSI information from outside the mobile operator networks.

Field tests have been performed in different live LTE networks. CSI information was gathered in different mobility patterns and different cities in the North of Spain, using commercial LTE cells deployed in the 2.6 GHz band (LTE Band 7) with 20 MHz of bandwidth.

The test equipment consisted of a laptop connected to the LTE network with a Samsung GT-B3730 USB dongle and running ASCOM TEMS Investigation© as drive test tool. The USB LTE dongle is enabled by the vendor to make CSI information available for the SW. However, these CSI values are reported with a sampling period of 1 s. Although the sampling period can be configured to lower values in the field test SW, CSI values would be repeated within the 1 s period.

The used USB dongle is an LTE Category 3 device, which imposes a series of constraints in the measurements. First, Category 3 devices are capable of operating in SISO and MIMO with a maximum of two layers for spatial multiplexing in the downlink. Since October 2014, several deployments in Spain support LTE-A with Carrier Aggregation of 40 MHz, by mixing downlink transmissions from 1.8 GHz and 2.6 GHz bands. However, Category 6 or higher devices are required to support CA and therefore the downlink bandwidth is limited to 20 MHz with Category 3 devices.

Secondly, Category 3 devices are limited to support up to 75 Mbps in the downlink with one layer, and 100 Mbps with two spatial layers in MIMO. This limitation imposes a restriction in the MCS value that can be assigned to an UE in MIMO (MCS of 23 for 20 MHz cells). Category 4 devices do not impose this limitation, and therefore 150 Mbps could be achieved in downlink. However, this effect does not impact the generation and reporting of CQI values since the limitation is applied during the AMC decision in the eNB.

Monitored LTE networks are configured to operate with Transmission Mode 3. Thus, the involved CSI parameters are RI and CQI. The CQI reporting periodicity is configured to 5 ms, and wideband CQI reports are used. The RI reporting periodicity is configured to 80ms. The former value determines the granularity of CQI measurements at the eNB, while the latter value limits the frequency for switching between transmission schemes.

Table 4.1 – Summary of relevant field test information.

LTE Band	LTE bandwidth	UE Category	Transmission Mode	CQI reporting periodicity	RI reporting periodicity	SW CSI periodicity
Band 7	20 MHz	UE Cat. 3	TM3	5 ms	80 ms	1 s

In order to capture CSI information in different conditions, the following mobility patterns have been defined:

- Static mobility pattern. Field tests are performed in single locations without moving the laptop or the USB dongle. For diversity purposes, static tests include indoor and outdoor locations. Indoor locations include buildings of four to six floors, with positions close to the window. Outdoor locations include open air positioning in open spaces and in narrow streets between buildings of seven to ten floors.
- Pedestrian mobility pattern. Field tests are carried out with the laptop on the hands of a user moving at pedestrian speeds of around 5 km/h in wide streets and open spaces within cities.
- Vehicular mobility pattern. Field tests are performed inside a car wandering within the cities. Therefore, drive tests are limited to speeds of up to 50 km/h. The collection of CSI data is not interrupted when the vehicle is stopped (e.g. in semaphores or intersections), and thus the vehicular data set also includes static data.

Figure 4.1 presents an overview of the field test data in terms of the different performance metrics, i.e. RSSI, RSRP, RSRQ, SNR and CQI. The Probability Mass Distribution (PMF) of the different parameters allows making a first evaluation of the diversity of the field tests.

As can be observed in the SNR plots, wide ranges of quality conditions are included in the data set. For pedestrian and vehicular data sets, there are considerable amount of samples in a continuous range from 0 dB to 30 dB, and even including up to -10 dB samples. As can be observed, the probability of samples is not equally distributed and exhibits biased patterns towards the low SNR and high SNR ranges respectively for pedestrian and vehicular mobility patterns. This effect must not be considered as a direct behaviour of the mobility patterns, but as a direct result of the locations in the experimental data set.

The sample probabilities in the static mobility pattern are more discontinuous and exhibit a considerable amount of samples only in certain SNR values. Again, this is a direct outcome of the empirical field tests, since each static test covers only a limited range of SNR. Obtaining a continuous data set would entail looking for specific locations with the desired SNR and performing the collection of CSI data in those locations.

As a first conclusion, the visual inspection of performance metrics provides some direct relationships between tendencies (e.g., CQI-SNR- RSSI-RSRP in the pedestrian data set), while other parameters exhibit a non-direct relationship (e.g., between CQI-SNR and RSSI-RSRP in the vehicular data set).

As a second conclusion for the rest of the section, it must be noted that using a heterogeneous data set means that the RI and CQI values obtained for each mobility pattern cannot be taken as absolute reference values and some equalization ort homogenization process is required.
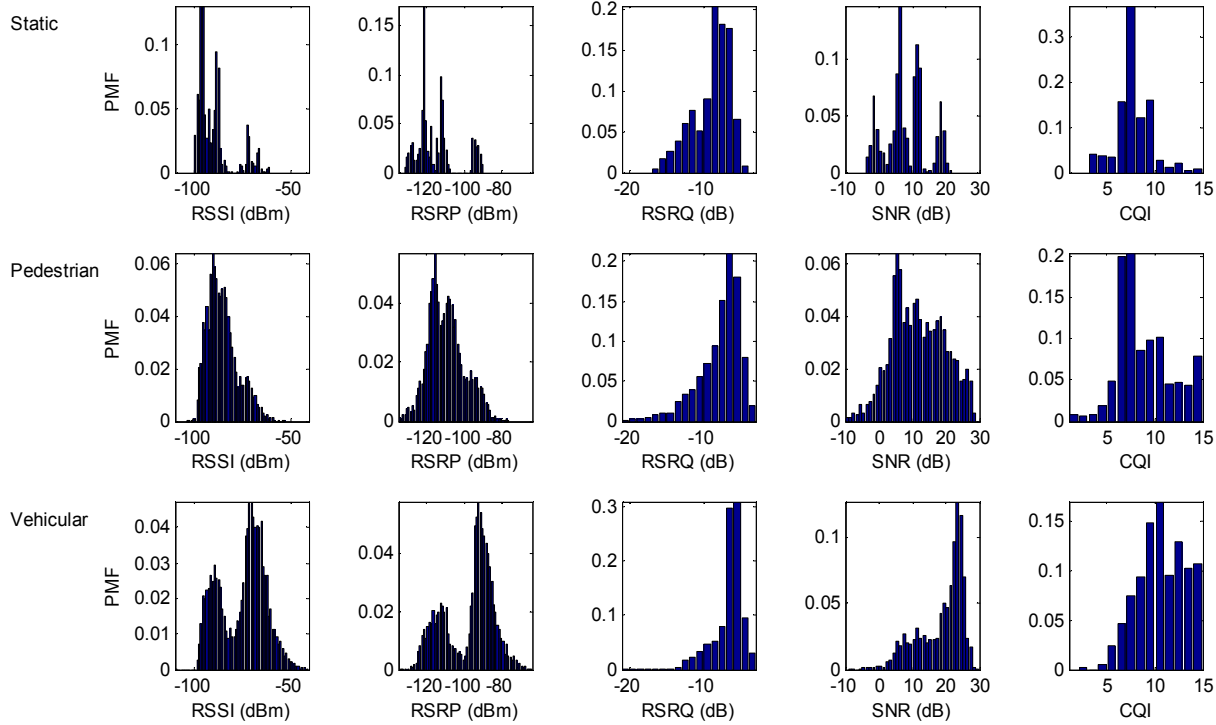
4.2   IMPACT OF RADIO PARAMETERS ON CSI

First of all, this section analyzes the relationships between the different radio parameters reported by UEs with the key parameter CQI. Initially, RSSI / RSRP / RSRQ / SNR parameters are compared to CQI from an overall perspective. After analyzing the impact of the RI parameter in these mappings, a more accurate analysis is provided per RI and mobility patterns.

4.2.1   ANALYSIS OF RAW TRACES

In order to inspect whether CQI values can be inferred from other typical radio parameters such as RSSI, RSRP, RSRQ and SNR, this section provides the visual representation of these relationships for the different mobility patterns considered.

Figure 4.2 gathers the scatter plots of CQI against RSSI, RSRP, RSRQ and SNR for the whole dataset of the field test traces regarding static measurements. Figure 4.3 and Figure 4.4 gather similar results for the field test traces concerning pedestrian and vehicular mobility profiles respectively.
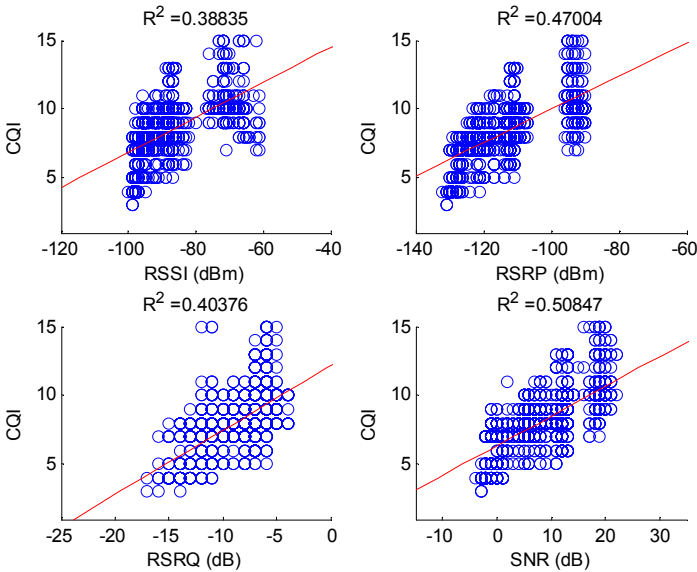
Figure 4.2 –Relation of different radio parameters and CQI for static pattern.
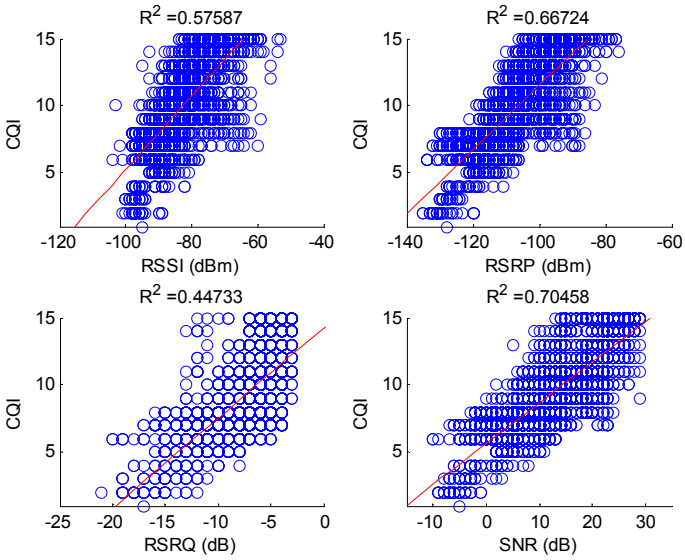
Figure 4.3 –Relation of different radio parameters and CQI for pedestrian pattern.
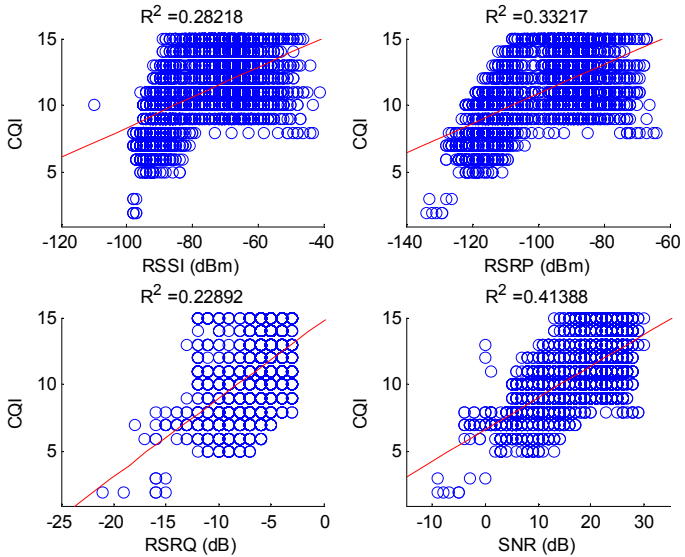
Figure 4.4 –Relation of different radio parameters and CQI for vehicular pattern.

As illustrated, none of the radio parameters provide accurate mappings to CQI for any of the mobility patterns. In overall, it can be observed that a single value in the x axis results in possible CQI values with 5 to 10 units of variability.

Since scatter plots do not provide any significant information about the number of occurrences of each x-y point, Figure 4.2-Figure 4.4 also include the results of performing linear fittings to the datasets. The red lines in these figures correspond to the best fitting function, while the coefficient of determination (denoted by R^2) represents the proportion of the variance in the CQI variable that is predictable from the independent variable.

Table 4.2 – Summary of R^2 values for different mappings.

Mobility pattern	Radio parameter			
	RSSI	RSRP	RSRQ	SNR
Static	0.38835	0.47004	0.40376	0.50847
Pedestrian	0.57587	0.66724	0.44733	0.70458
Vehicular	0.28218	0.33217	0.22892	0.41388

From the analyzed parameters, the SNR seems to be the best fitting parameter, followed by the RSRP. However, the resulting fittings obtained from the gathered datasets are not accurate enough to provide good estimations of CQI from any of the analyzed radio parameters.

4.2.2   IMPACT OF RI

As explained in Chapter 2, the transmission scheme in TM3 allows dynamically switching between one and two transmission layers depending on the highest estimated DL bitrate in each mode. This effect has a direct impact on how the SNR is assigned to the estimated reception conditions.

In TxD (RI=1 in TM3), one layer is mapped to two reception antennas. Therefore, the transmission is more resilient and the probability of correctly decoding the information is higher. In OLSM (RI=2 in TM3), two layers are mapped to two reception antennas and the required SNR for the proper decoding of the two layers increases.

Additionally, the different reception conditions of each antenna port add further complexity to the mappings. The challenging issue is to understand how each reception antenna contributes to the overall SNR, and how this power sharing results on different achievable CQI levels in the two antennas.

As an example, Figure 4.5 illustrates an excerpt of 310 s from a drive test trace obtained in static conditions.
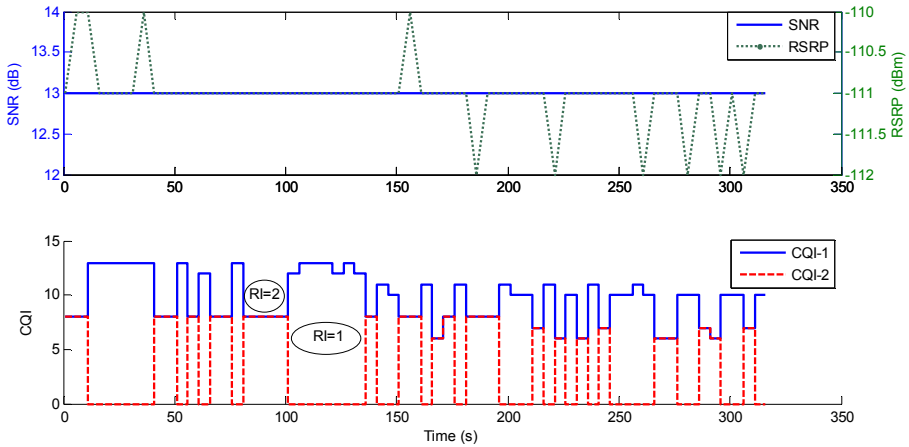
Figure 4.5 –Excerpt of field test trace with different transmission layers.

The first subplot shows the RSRP and SNR values reported by the device, since those parameters seem to provide the best fittings for the used dataset. In these static measurements, the SNR provides a constant value of 13 dB. It must be noted that only one SNR value is reported by the used UE, and therefore the reception condition of each antenna cannot be directly identified. Meanwhile, the RSRP values are also quite constant, with a variation of one dB above and below the mean value.

The second subplot shows the collected CQI values reported by the UE for the two antennas. It can be observed that the second CQI value (CQI-2 in the figure) is either zero or the same as the first CQI value. This effect must be understood by taking into account the instantaneous transmission scheme. UEs are in charge of generating both CQI values and estimating the most beneficial transmission scheme that maximizes the downlink bitrate. From that estimation, UEs report a single CQI value together with the preferred RI.

For RI=1, CQI values reported by UEs are associated to the best channel condition from the two antennas. For RI=2, CQI values reported by UEs are associated to the best condition achievable at the two antennas simultaneously, which is the worst of the two channel conditions. Thus, it must be noted that CQI-1 and CQI-2 values reported by the drive test tool are not directly those estimated for the two antennas. Instead, CQI traces include some periods of individual CQI values and some periods of the maximum CQI achievable at both antennas at the same time.

As a result, based on the radio performance experienced by two different reception antennas, the MIMO scheme varies along time as illustrated in Figure 4.5. As can be observed, the same value of SNR and RSRP can provide different reported CQI values directly related to the transmission scheme.

The main implication of this effect is the complexity to characterize the behaviour of CQI values directly from raw CQI traces. Since different fading conditions may affect to different antennas, similar SNR values may result on higher or lower CQI-1 values if RI=1 or RI=2.

4.2.3   ANALYSIS OF FILTERED TRACES

In order to determine if the rank-adaptive transmission plays a critical role in the analyzed mappings, Figure 4.6 illustrates the scatter plots between SNR and CQI in function of the RI parameter for the different mobility patterns considered. Additionally, the figures present the best fitting linear functions and the goodness of fit based on the R^2 coefficient.
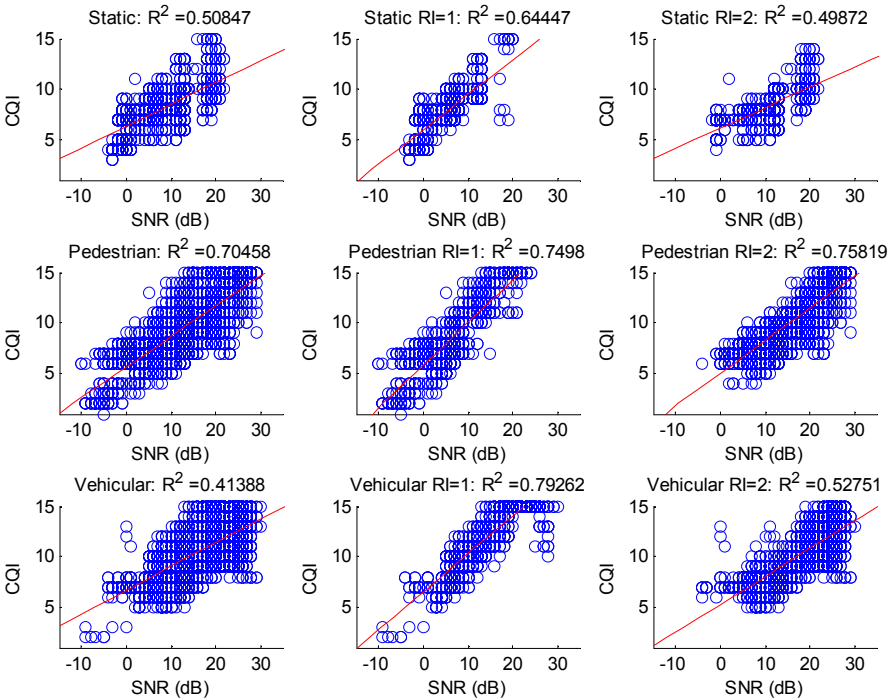
Figure 4.6 – Relation of SNR and CQI for different mobility patterns and LTE transmission schemes.

The first column represent the results from the raw traces including RI=1 and RI=2 transmissions, as presented in Figure 4.2-Figure 4.4. The second and third columns represent those traces with RI=1 and RI=2 respectively.

Table 4.3 summarizes the goodness of fit for the different cases:

Table 4.3 – Summary of R^2 values for SNR-CQI mappings.

Mobility pattern	Number of transmission layers		
	Raw	RI=1	RI=2
Static	0.50847	0.64447	0.49872
Pedestrian	0.70458	0.7498	0.75819
Vehicular	0.41388	0.79262	0.52751

As can be observed, the filtered traces result in better estimations of CQI from SNR, especially for the case of RI=1.

The possible explanation for this effect is related to the different transmission schemes. Initially, RI=1 is expected in low SNR ranges in order to enhance the transmission resiliency, while RI=2 is expected in high SNR ranges to increase the transmission efficiency. However, Figure 4.6 illustrates that both RI values are possible all over most of the SNR range.

This effect must be associated to the different reception quality of the two antennas. The probability of finding RI=1 in high SNR values seems to indicate that the SNR in one antenna is considerably higher to the SNR in the other antenna. Therefore, the estimated DL throughput associated to the estimated MCS using the best antenna is higher than the estimated DL throughput using the MCS of the worst antenna for the two layers.

As a result, the relevance of identifying the RI parameter associated to other CSI parameters such as CQI is shown. Nevertheless, none of the fittings provide sufficiently accurate results to determine a linear relationship between SNR and CQI in this experimental dataset.

4.3   RELATIONSHIP BETWEEN CQI AND MCS

Following with the analysis about mapping CQI to other parameters, this section focuses on the relationships between CQI and MCS. Similar to the previous section, the analysis of raw traces is first presented and the impact of different context parameters is analyzed later.

4.3.1   ANALYSIS OF RAW TRACES

Figure 4.7 illustrates the scatter plots between the variables CQI and MCS for the whole dataset and for each of the mobility profiles. Additionally, each plot includes a representation of the CQI to MCS mapping standardized by the 3GPP.
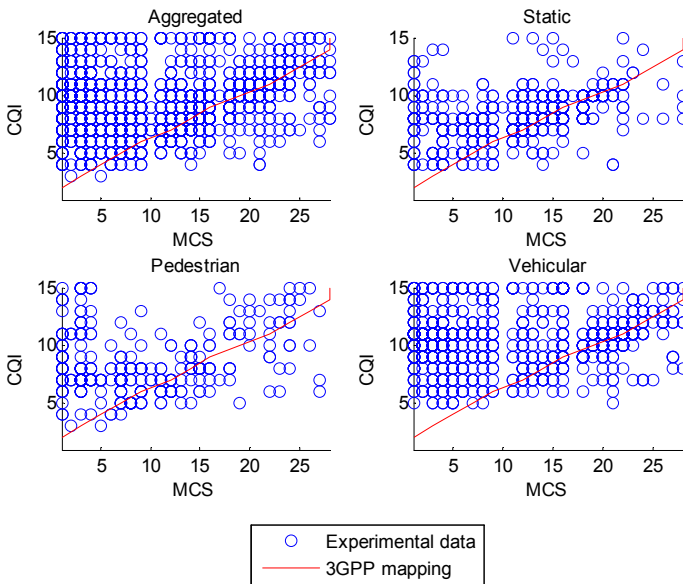
Figure 4.7 – Relation of MCS and CQI for different mobility patterns.

Generally speaking, the assigned MCS values are not a proper indicator of the reported CQI value. A wide range of CQI values is associated to each individual MCS value. Most of the CQI samples are above the expected value according to the 3GPP specifications. Moreover, there are CQI samples below the expected value.

The next subsections analyze the possible impact of different context parameters in these relationships. Section 4.3.2 focuses on the possible impact of the RI parameter, while Section 4.3.3 studies the effects of the cell load in the MCS assigned by the eNodeB.

4.3.2   IMPACT OF RI

Figure 4.8 depicts a segment of 14 s corresponding to a field test trace under static monitoring conditions and with greedy source DL traffic from second 11 to 22.
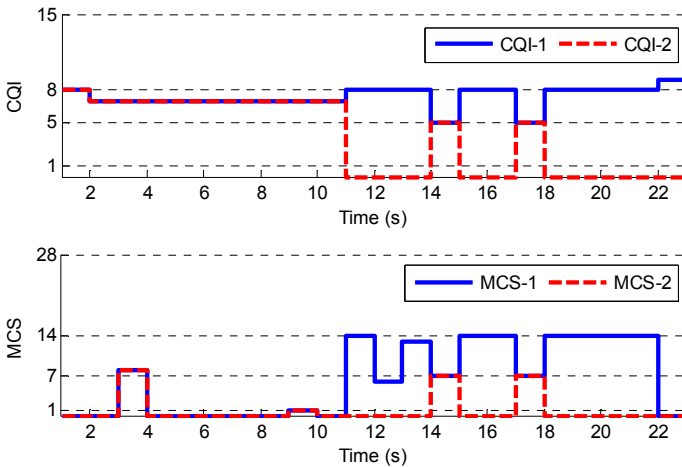
Figure 4.8 – Excerpt of field test trace with different RI and MCS.

This figure exemplifies different effects to take into account.

- The first and last second of the trace correspond to periods without traffic assignment, and thus MCS is set to 0. However, the CQI value is still reported to the eNodeB while the UE is in Connected state. As a result, those samples with MCS set to 0 must be deleted from the analysis.
- The RI parameter does not seem to have a direct impact on the CQI to MCS mappings. Most of the time with CQI reported as 8, the MCS is set to 14 by the eNodeB. And those periods with reported CQI = 5, the MCS is set to 7 by the eNodeB. Regardless RI=1 or RI=2, both mappings match the expected values according to the 3GPP.
- During the period of CQI = 7, there are two seconds with MCS set to 8 and 1.

As exemplified in Figure 4.9, the RI parameter does not seem to have a direct impact of the mappings between MCS and CQI by itself. Both RI=1 and RI=2 situations may and may not follow the standard 3GPP mappings, based on other contextual factors.
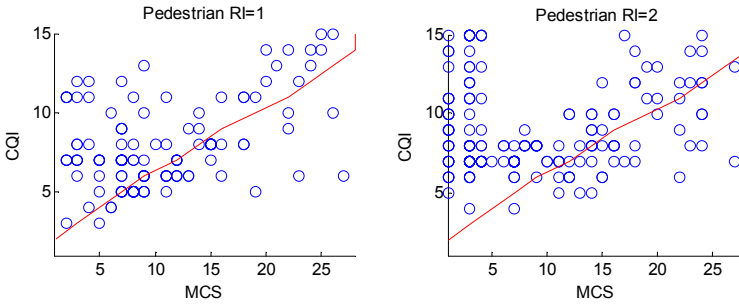
Figure 4.9 – Relation of MCS and CQI for pedestrian mobility pattern and different transmission schemes.

4.3.3 IMPACT OF PRB AND DL THROUGHPUT

Figure 4.10 and Figure 4.11 illustrate the relationships of MCS and CQI in function of the assigned DL bandwidth and the achieved DL throughput.
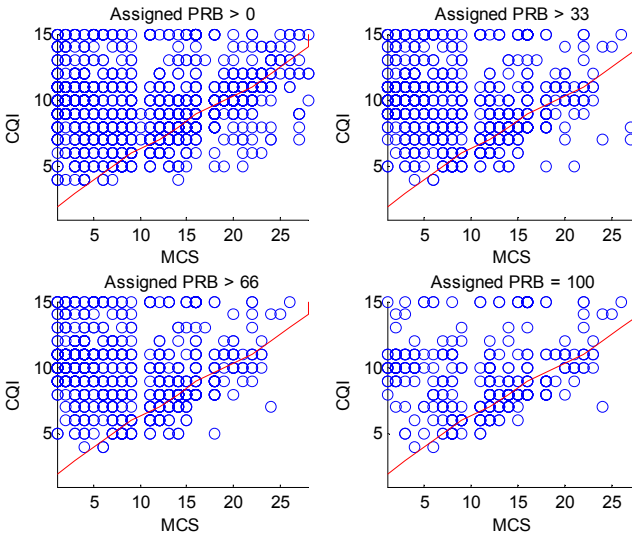
Figure 4.10 – Relation of MCS and CQI for different number of assigned PRBs.
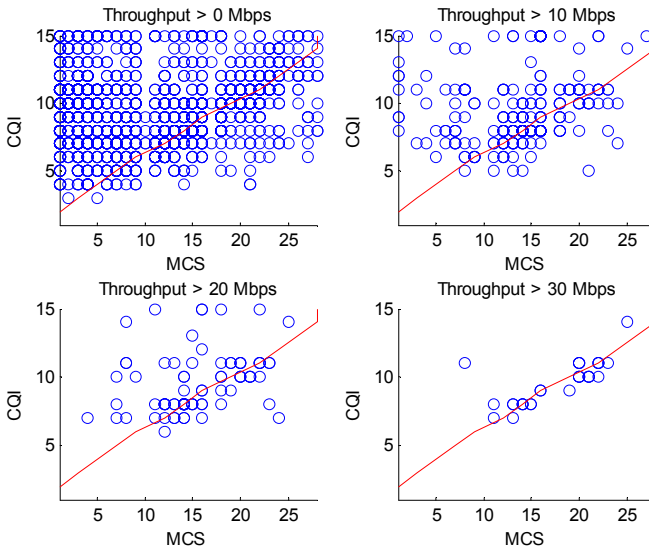
Figure 4.11 – Relation of MCS and CQI for different DL throughputs.

In the first case, the CQI samples are closer to the expected value as the number of assigned PRBs increases. This is an interesting aspect, since the assigned PRBs can be monitored by identifying the used bandwidth with a spectral analyzer. However, the relationship is not accurate enough to perform a proper prediction of the CQI based on the monitored MCS.

The main reason for this effect is associated to the behaviour of the monitored eNodeBs. While there are sufficient PRBs available in the cell to cope with all the traffic demands, the eNodeB may decide to schedule DL transmissions with a lower MCS while increasing the number of assigned PRBs. In this way, the transmissions are more resilient to transmission errors and the performance of other users is not compromised. Therefore, the probability of experiencing the expected mappings even when the number of PRBs is 100 will depend on the ratio of samples using high traffic demands.

This effect is better depicted in Figure 4.11, where the evolution of the CQI to MCS mappings are illustrated for increasing traffic demands. In this way, using greedy sources in the field test measurements may guarantee a correct estimation of the CQI based on the monitored MCS.

Unfortunately, a minimum DL throughput cannot be established for passive monitoring, since this value actually depends on the achievable CQI level.

4.4   CHARACTERIZING LTE MIMO CHANNELS

Once illustrated the difficulty of inferring CQI values from other related LTE parameters, this section focuses on the analysis of CSI traces gathered from field testing in different conditions. The main objective of this section is to determine if CSI parameters can be characterized to some extent, bearing in mind its possible application to future LTE studies.

As a reminder, the reader should note that the analyses provided in this section correspond to a series of LTE cells deployed at 2.6 GHz and with 20 MHz and operating inTM3. The generalization of these results to other types of LTE cells should be further studied. Additionally, it must be noted that the reporting granularity of the field test toolset used is limited to 1 s. Related sub-second analyses are provided in Chapter 5.

As an illustrative example of the experimental CSI data, Figure 4.12 shows an excerpt of 160 s from a field test trace obtained in pedestrian conditions. The upper subplot shows the evolution of the SNR over time, while the lower subplot depicts the resulting CSI parameters.

Since this LTE cell operates in TM3, the relevant CSI parameters to be reported by the UE are RI and CQI. The former indicates the preferred number of layers in MIMO transmissions, leading to TxD or OLSM for RI=1 and RI=2 respectively. The latter indicates the estimated quality of DL transmissions and should determine the modulation and coding efficiency implemented by the eNodeB for that UE.
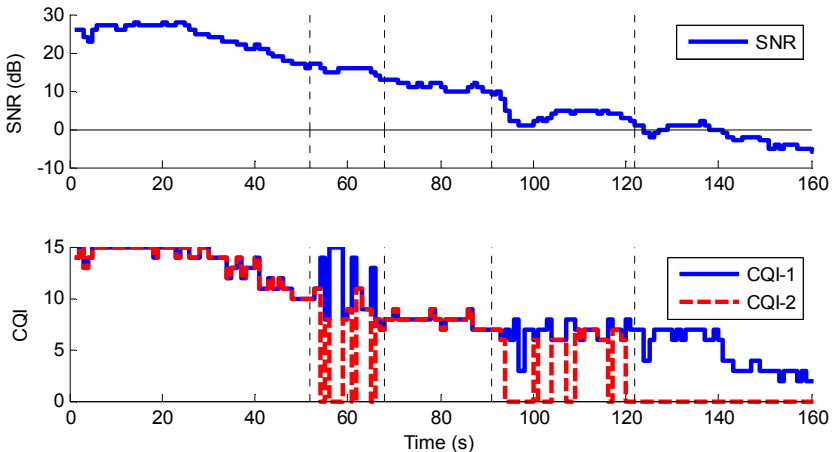
Figure 4.12 – Excerpt of field test trace with RI areas.

This figure illustrates five different areas of operation:

- In the first area corresponding to the highest SNR conditions, the two CQI values internally reported by the UE (CQI-1 and CQI-2) are equal. This means that the UE would report RI=2 and CQI-1 value to the eNodeB.
- In the fifth area corresponding to lowest SNR values, CQI-2 is always 0. This means that the UE selects RI=1 for DL transmissions with the CQI-1 value.
- The areas second to fourth correspond to intermediate SNR values, and different behaviours are identified. In the second and fourth areas, the RI parameter dynamically changes between 1 and 2. Meanwhile, the third area present constant value of RI=2.

Additionally, areas two and four show different CQI patterns:

- In the second area, CQI values for RI=1 and quite higher than CQI values for RI=2. Generally speaking, this would mean that the SNR values associated to both reception antennas are quite different, being both them quite variable in the range of 1 s. These effects would explain the quick variability in RI.
- In the fourth area, the quality conditions of the two antennas are lower. Again, only a relevant variability of CQI over time at least at one antenna may explain the high variability in RI.

As a result, different questions remain open for understanding the experimental behaviour of LTE traces:

- The behaviour and variability of RI over time should be analyzed, as well as its relation with the monitored SNR.
- The behaviour and variability of CQI over time should be analyzed for each RI value, as well as its relation with the monitored SNR.

4.4.1 COARSE-GRAIN RI CHARACTERISTICS

The rank-adaptive transmission in TM3 allows dynamically switching between RI=1 and RI=2 MIMO schemes, leading to one-layer TxD and two-layer OLSM respectively. The eNodeB decides the specific transmission scheme based on the CSI feedback provided by the UE in terms of RI.

As explained in Section 4.1, the monitored LTE cells are configured to request RI reporting every 80 ms. However, the CSI values provided by the field test toolset is limited to a granularity of 1 s. It is assumed that the RI value reported internally by the field test toolset corresponds to the value with higher occurrences in the sampling period. Due to this limitation, the statistical properties analyzed in this section are referred to as coarse-grain characteristics.

Figure 4.13 illustrates the PMF of the experimental samples in the whole dataset for the different relevant radio quality parameters, identifying the proportions of each value that correspond to RI=1 and RI=2.
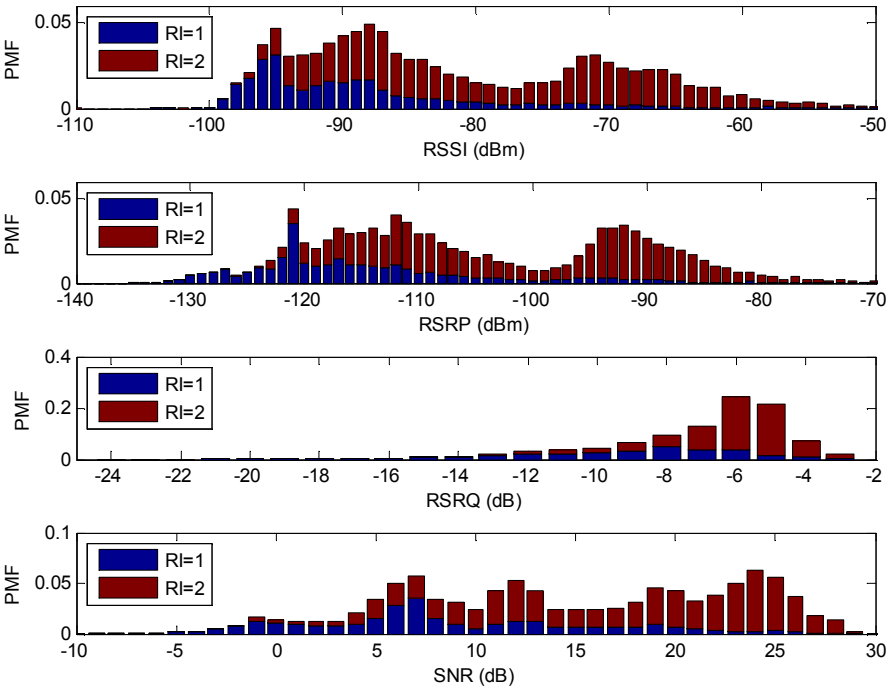
Figure 4.13 – PMF of RI=1 and RI=2 for RSSI, RSRP, RSRQ and SNR.

From a general standpoint, it can be observed the prevalence of RI=1 in the lower values of RSSI, RSRP, RSRQ and SNR, while the use of RI=2 becomes widespread in the higher ranges.

In order to identify the effect of the different mobility patterns in the use of RI, Figure 4.14 gathers the PMF of the samples for the static, pedestrian and vehicular mobility patterns. As in the previous case, each value in the PMF is split into the contribution of RI=1 and RI=2.

For a better understanding of the prevalent value along the whole range of experienced SNR values, Figure 4.15 simply plots the ratio of RI=2 occurrences in steps of 3 dB.

While the static and pedestrian patterns clearly show an increasing trend in the use of RI=2 as SNR raises, the vehicular pattern exhibits a significant use of RI=2 even at low SNR values.
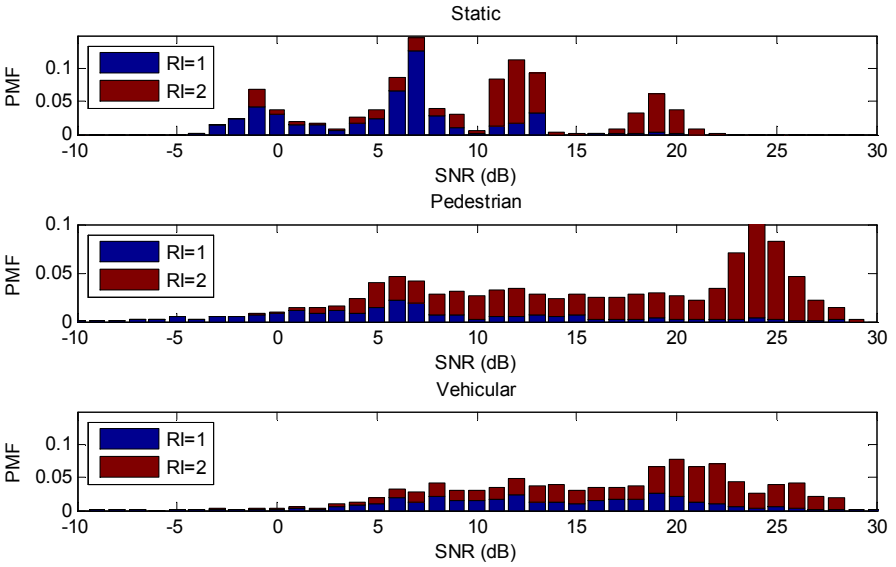
Figure 4.14 – PMF of RI=1 and RI=2 for SNR per mobility patterns.
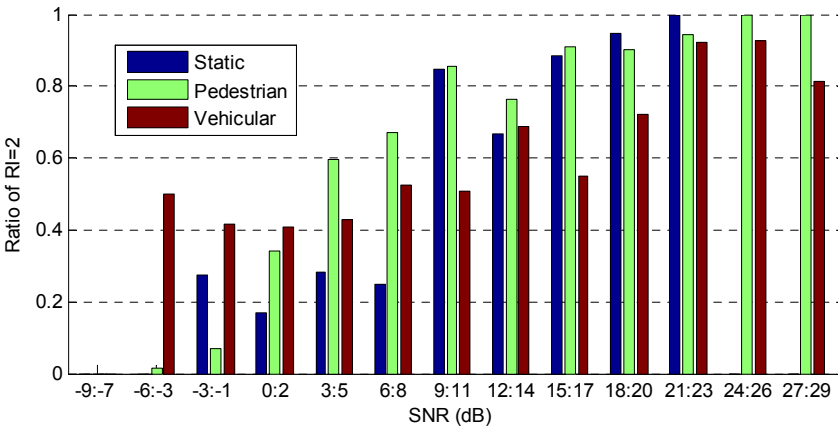
Figure 4.15 – Ratio of RI=2 for different SNR ranges and per mobility patterns.

The SNR thresholds representing the value where the prevalence of RI changes from RI=1 to RI=2 are 8.5 dB, 3.5 dB and 12.5 dB respectively for the static, pedestrian and vehicular patterns.

4.4.2   TEMPORAL VARIABILITY OF COARSE-GRAIN RI

Beyond how much UEs request the use of TxD and OLSM for different SNR ranges, another open issue is how long these transmission schemes remain active over time.

As explained before, the used field test toolset does not allow going into details at sub-second periods. Although it is not possible to know if a single RI value means that the same RI is maintained during the whole second, it is still interesting to understand the periods of time for which the same RI remains prevalent. Furthermore, it is also interesting to analyze if the different mobility patterns have an impact on these durations.

For this aim, Figure 4.16 represents the burstlengths of the same RI value in terms of ECDF. An RI burstlength is thus defined as the period of time with the same RI value. Burstlength values are illustrated for the two possible RI values and for the three different mobility patterns considered.
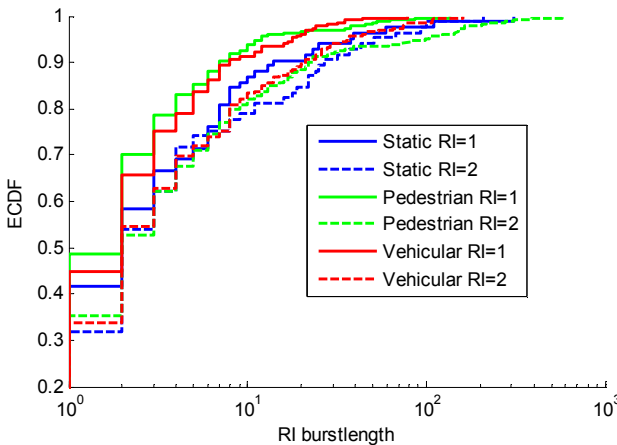
Figure 4.16 – ECDF of RI burstlength for RI=1 and RI=2 and per mobility patterns.

The general trend shows that RI burstlengths are higher for RI=2. This means that the probability of staying in OLSM transmission scheme is higher than the probability of staying in TxD. However, static measurements with RI=1 get closer to RI=2 traces beyond 4 s of burstlength. The average RI burstlengths are summarized in Table 4.4.

RI burstlengths of 1 mean that the transmission scheme changes immediately between the two alternatives. This happens between 42% and 48% of times for RI=1, while it is reduced between 31% and 35% of times for RI=2.

Table 4.4 – Average RI burstlengths.

Mobility pattern	Number of transmission layers	
	RI=1	RI=2
Static	10.21 s	11.60 s
Pedestrian	4.42 s	16.83 s
Vehicular	4.1o s	8.42 s

In order to identify the impact of the different RI prevalence situations, Figure 4.17 represents the ECDF of RI burstlengths taking into account the SNR thresholds previously identified (8.5 dB, 3.5 dB and 12.5 dB respectively for static, pedestrian and vehicular). The dotted lines represent those SNR ranges where the specific RI is not prevalent.
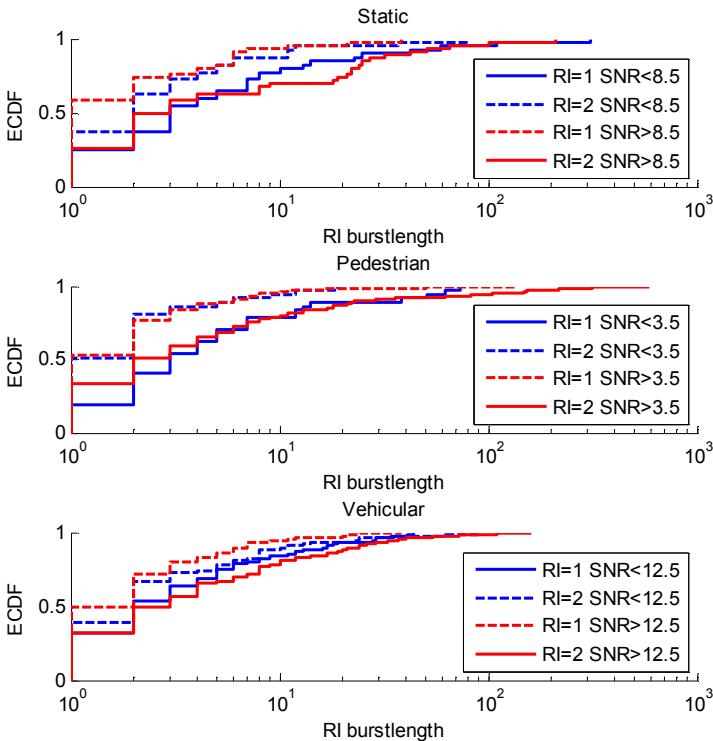
Figure 4.17 – ECDF of RI burstlength for RI=1 and RI=2 in different SNR ranges and per mobility patterns.

From a visual inspection of the general trends, the transmission schemes are more resilient to remain in the same MIMO strategy in the SNR range where each RI predominates.

The average duration of the periods in the same RI for each SNR range are gathered in Table 4.5. As can be observed, the average burstlengths for RI = 2 over the SNR thresholds are considerably higher to RI = 1 periods. Foe SNR conditions below the threshold, the difference in average values is lower as expected from the analysis of the aggregated probabilities.

Table 4.5 – Average RI burstlengths in different SNR ranges.

Mobility pattern	Number of transmission layers and SNR range			
	SNR ‹ SNR_{th}		SNR ›SNR_{th}	
	RI=1	RI=2	RI=1	RI=2
Static	17.50 s	5.65 s	3.44 s	16.44 s
Pedestrian	9.78 s	6.49 s	3.36 s	18.75 s
Vehicular	5.92 s	5.72 s	3.01 s	9.33 s

4.4.3 COARSE-GRAIN CQI CHARACTERISTICS

Similarly to the case of RI parameter, coarse grain CQI traces with 1 s of sampling period are analyzed in this section.

As explained in Section 4.1, the monitored LTE cells are configured to request CQI reporting every 5 ms. However, due to the limitations of the CSI values provided by the field test toolset, it is assumed that the logged CQI values correspond to some statistical value of the whole CQI trace over the previous 1 s period.

From Figure 4.1, it is clear that the measurement samples are not equally distributed across different mobility patterns. Thus, a raw comparison of CQI values in different conditions would result on unfair results. Likewise, the statistical properties of the raw CQI traces cannot be used to characterize a generalized behaviour, since the results would be biased by the specific probabilities of the reception conditions in the dataset.

As a first step, Figure 4.18 presents again the scatter plots between SNR and resulting CQI values from Figure 4.6. Since scatter plots do not provide accurate information about the number of occurrences for each point, Figure 4.18 also includes the histograms of both SNR and CQI parameters.
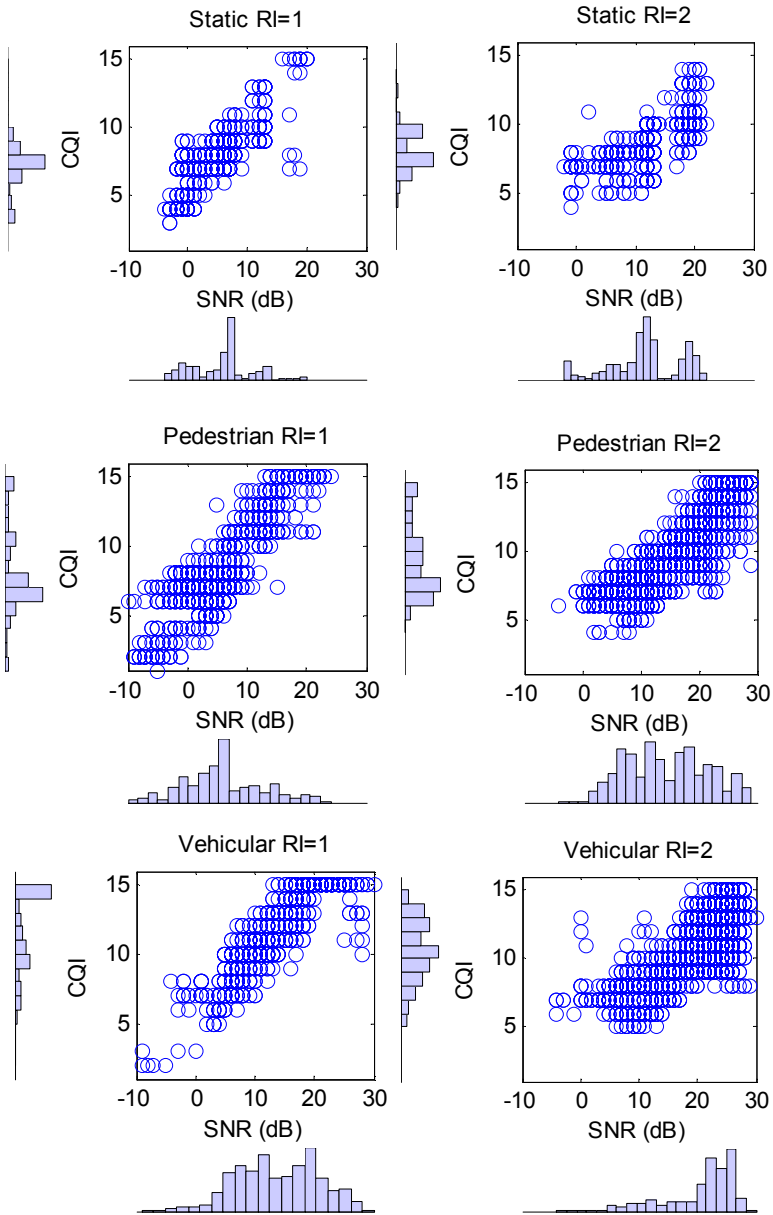
Figure 4.18 – Scatter plots and histograms of CQI and SNR for different RI values and mobility patterns.

In fact, the presented histograms are not significant regarding the ratio of occurrences for each scatter point. For example, the vehicular subset with RI=1 exhibits a high number of samples with CQI=15. Those CQI values are associated to SNR values in the range form 13 dB to 30 dB, but it is not possible to visually identify the contribution of each SNR to the total value.

As a step forward, Figure 4.19 includes a representation of these contributions through coloured scatter points. The legend of the colour bar has been on purpose deleted, since the maximum value is different for each subplot. For simplicity and clarity, only the pedestrian and vehicular subsets are shown. Additionally, the ECDF of SNR values are included since this brings relevant information about the SNR values with higher number of measurement samples.
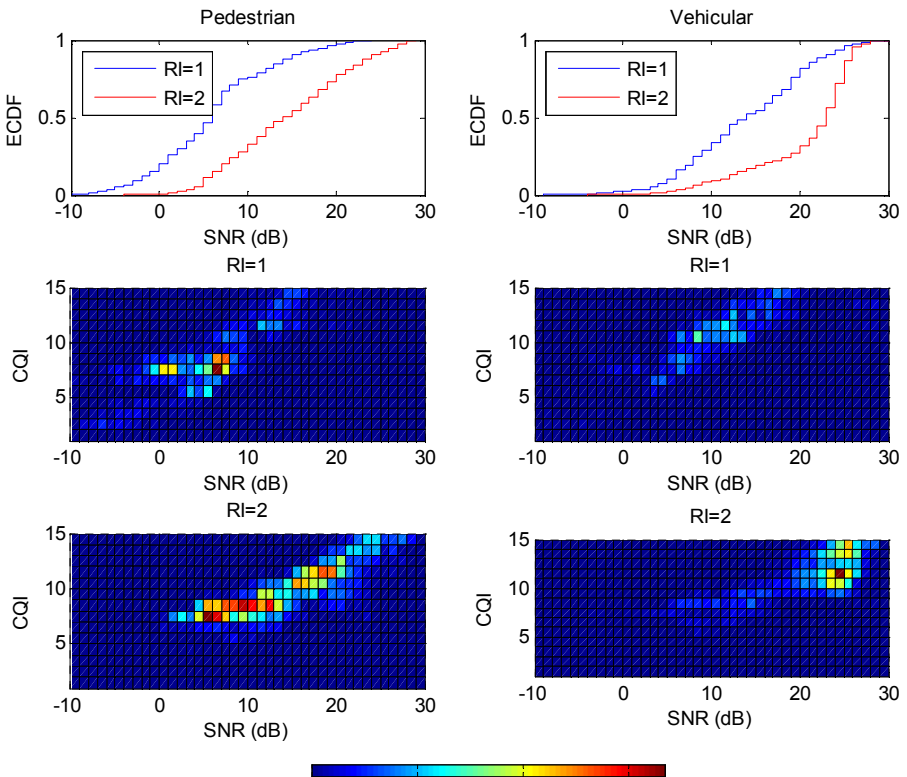
Figure 4.19 – Scatter plots of CQI and SNR with coloured number of occurrences for pedestrian and vehicular mobility patterns.

In order to present statistically comparable and generalizable CQI results, the number of samples in different SNR values should be similar within a representative range. In that way, the sample of CQI values could include representative CQI average and deviation values avoiding biased results due to non heterogeneous SNR probabilities.

For this aim, the whole monitored SNR range from -10 dB to 30 dB is split into three different ranges:

- -10 dB to 4 dB, representing low SNR values with prevalent RI=1.
- 5 dB to 19 dB, representing medium SNR values without any prevalent RI.
- 20 dB to 30 dB, representing high SNR values with prevalent RI=2.

Although the performed static measurements do not provide heterogeneous sampling frequencies in any relevant range, their results are also included.

Figure 3.1 gathers the results for the lower range of SNR.
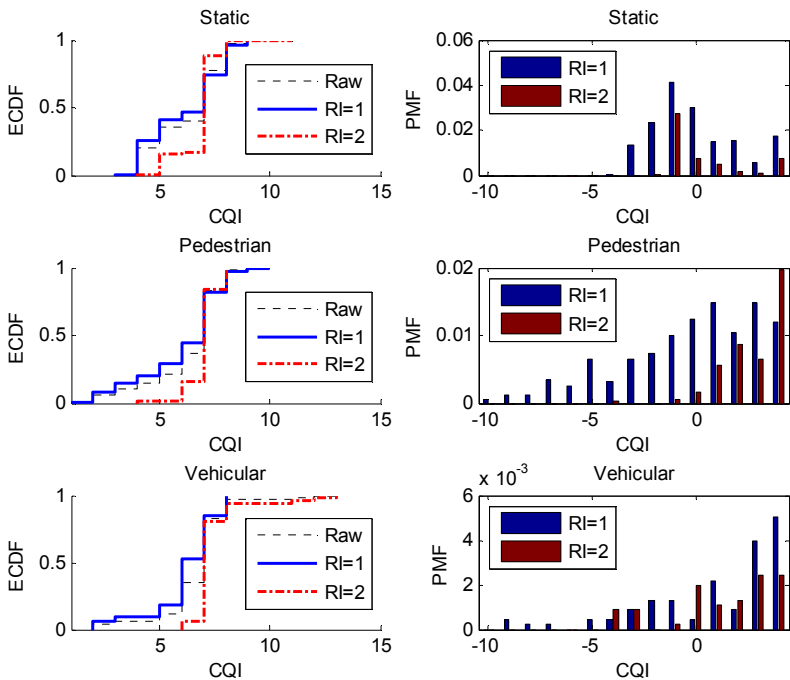
Figure 4.20 –ECDF and PMF of CQI for SNR = {-10:4}.

For RI=2, most of the SNR values are in the range of -1 dB to 4 dB leading to most of the CQI values falling between 6 and 8. For RI=1, the PMF of SNR is more disperse over the whole range, leading to more variable CQI values. Anyway, the upper threshold in both cases tend to CQI=8. The 95% of CQI samples are below this threshold in all the analyzed conditions.

Figure 4.21 illustrates the CQI results for the medium range of SNR values.
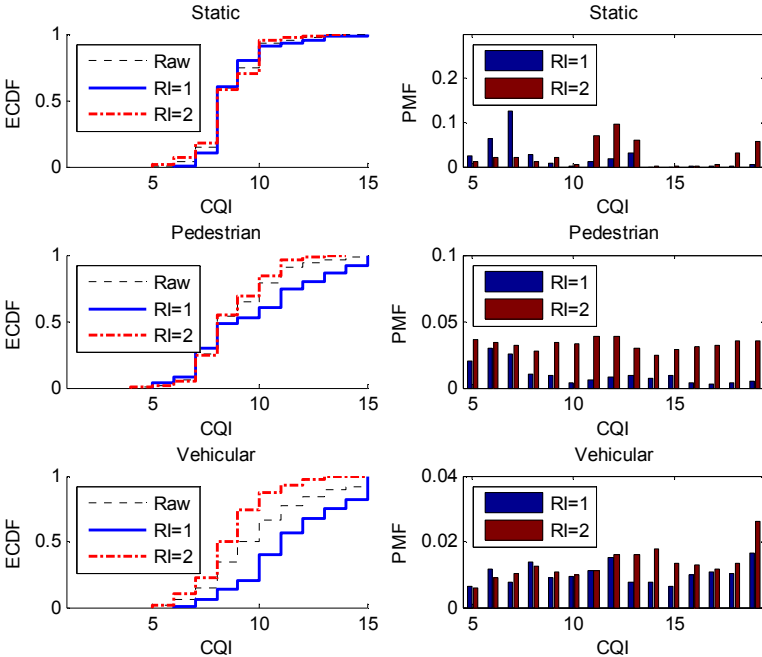
Figure 4.21 – ECDF and PMF of CQI for SNR = {5:19}

For the static case, the CQI for both RI values exhibit a quite similar behaviour. Since the SNR distributions are not comparable, it is interesting to understand the specific conditions that lead to similar CQI results in different RI values.

For example, taking only into account the SNR values associated to CQI=8, the experimental average SNR is 6.82 dB for RI=1 and 10.33 dB for RI=2. This means that, in this range and for the static measurements, there is an almost 4 dB of difference to reach the same CQI value for the RI=1 and RI=2. Translated to achievable DL throughput, CQI=8 would lead to 25.5 Mbps for RI=1 and 51 Mbps for RI=2 in ideal conditions.

For the pedestrian and vehicular subsets, the PMF of measurement samples is more heterogeneous over the selected SNR range. In both cases, it is observed that CQI values for RI=1 are considerably higher than CQI values for RI=2, also with different ECDF shapes.

Table 4.6 summarized the average SNR and CQI values in this intermediate SNR range. As expected from the visual inspection, the subset of RI=1 in the pedestrian case exhibits a higher probability of lower SNR values up to 7 dB. Therefore, the average value is quite lower. Even in those conditions, the average CQI for RI=1 is higher than for RI=2. In the vehicular case, similar SNR average values lead to quite different average CQI values.

Table 4.6 – Average SNR and CQI values for SNR= {5:19}.

Mobility pattern	Number of transmission layers			
	RI=1		RI=2	
	SNR	CQI	SNR	CQI
Pedestrian	9.45	9.64	13.03	8.64
Vehicular	12.30	11.38	11.93	8.66

Finally, Figure 4.22 provides the results for the higher range of SNR values. In this case, the number of RI=1 samples is quite low in all cases, most of them leading to CQI=15 samples. For RI=2, more than 90% of the samples are above CQI=9 in all cases.
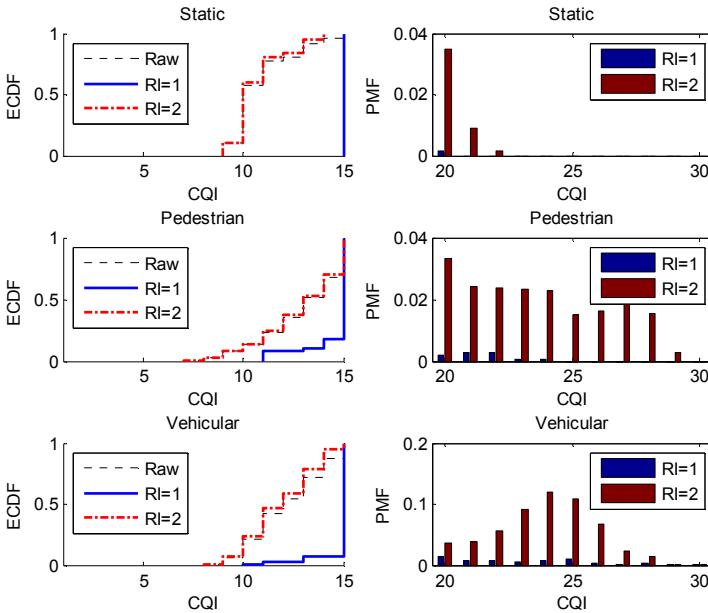
Figure 4.22 – ECDF and PMF of CQI for SNR = {20:30}.

4.4.4   TEMPORAL VARIABILITY OF COARSE-GRAIN CQI

In addition to the absolute CQI values in different reception conditions, the study of the temporal variability of CQI values provides the necessary information to understand how quickly and how much the channel quality varies over time.

In this sense, it is commonly assumed that the wireless channel in mobile broadband networks is intrinsically associated to fast and significant variations. However, from the analysis provided in Chapter 3, there is no clear evidence that quantifies this effect in live LTE networks.

As discussed in Section 4.2, a proper analysis of reported CQI values needs to separate the CSI samples according to the possible RI values. Moreover, likewise to the RI analysis, the coarse grain CQI values are evaluated for each mobility patter.

Figure 4.23 illustrates the duration of time periods with a constant CQI value. As can be observed, the probability that the CQI value varies from one second to the next one is around 60% for most of the combinations. Additionally, the burst duration is lower than 10 s for more than the 90% of times for all the combinations of RI and mobility pattern. It must be noted that for all the cases, around 23% of changes in the reported CQI value are also associated to changes in the RI value. Therefore, those variations can be explained due to a change in the experienced channel quality of any of the reception antennas.
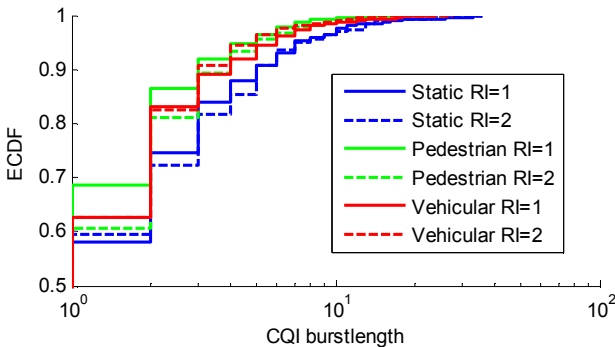
Figure 4.23 – ECDF of CQI burstlength for RI=1 and RI=2 and per mobility patterns.

In order to capture the possible impact of different CQI levels in the experienced burstlengths, Figure 4.24 illustrates the outcomes for CQI ranges. These CQI ranges aggregate CQI values based on the target coding efficiency, according to Table 2.7.
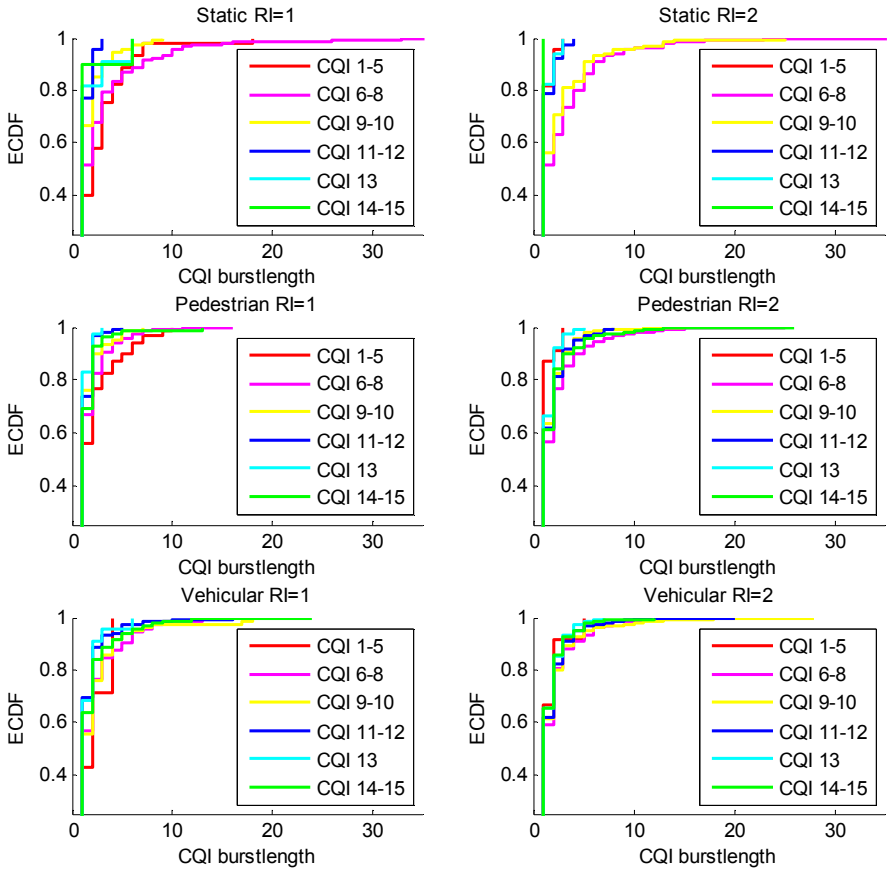
Figure 4.24 – ECDF of CQI burstlength for RI=1 and RI=2 and per mobility patterns, and per coding efficiency range.

Beyond the frequency of CQI changes, the amplitude of CQI changes is also a significant parameter to understand the dynamicity of the wireless channel. Since this chapter deals with coarse-grain CQI values, these results are especially relevant for macroscopic operations such as application-level rate adaptations.

Figure 4.25 illustrates the probabilities of the CQI variation amplitude between consecutive samples. Most of the scenarios evaluated quite stable conditions between consecutive CG-CSI samples, with maximum variations of 1 or 2 units above of below the current CQI value. The most variable conditions are found for RI = 1 with pedestrian mobility pattern and for RI = 2 in static conditions.
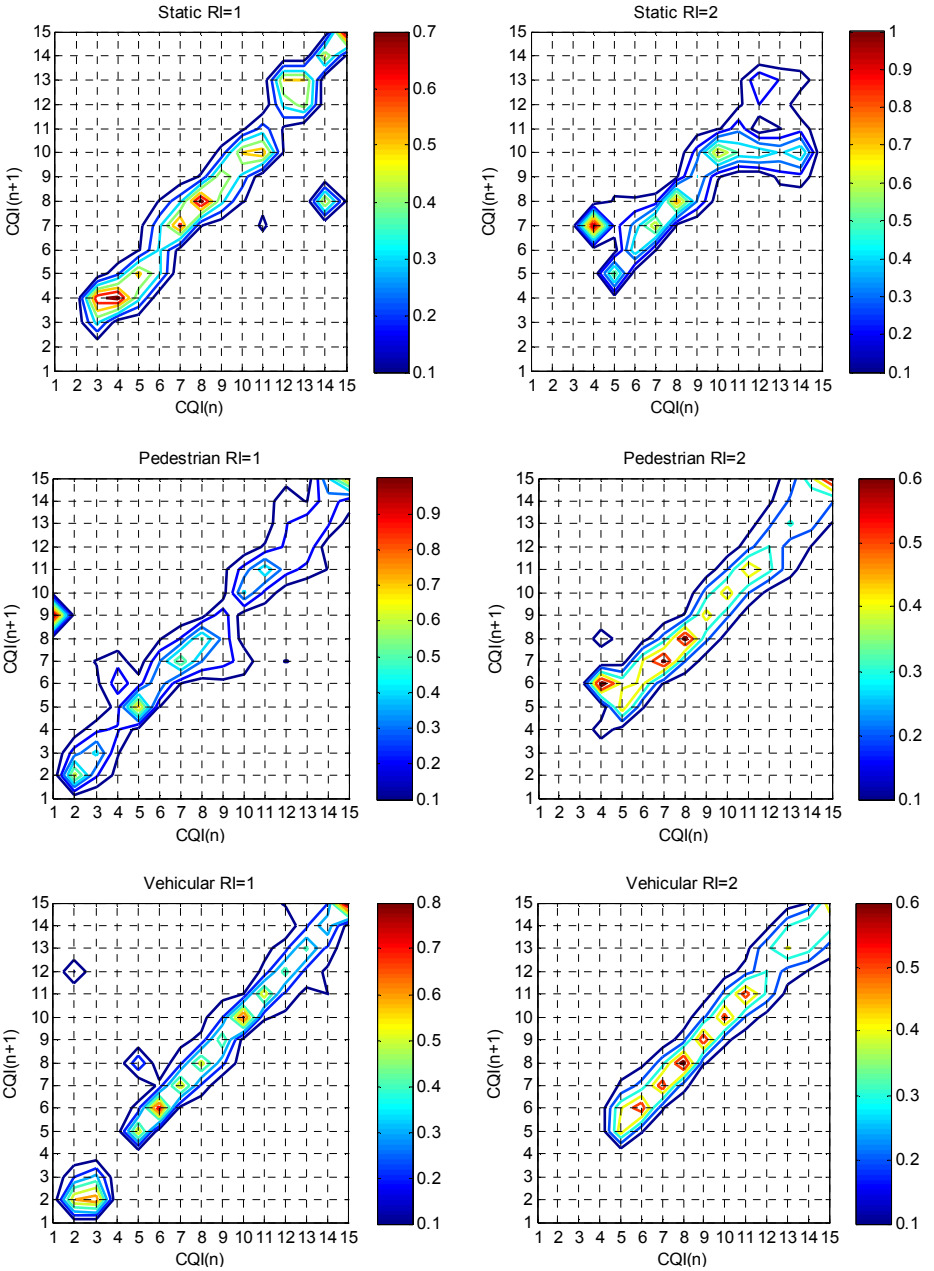
Figure 4.25 – Probability of CQI evolution between two consecutive samples.

Figure 4.26 and Figure 4.27 gathers the obtained results for the vehicular mobility pattern and for RI = 1 and RI = 2 respectively. In this case, the probabilities of moving from one CQI value to any CQI value is represented for different time hops, from 1 s to 19 s in steps of 2 s.
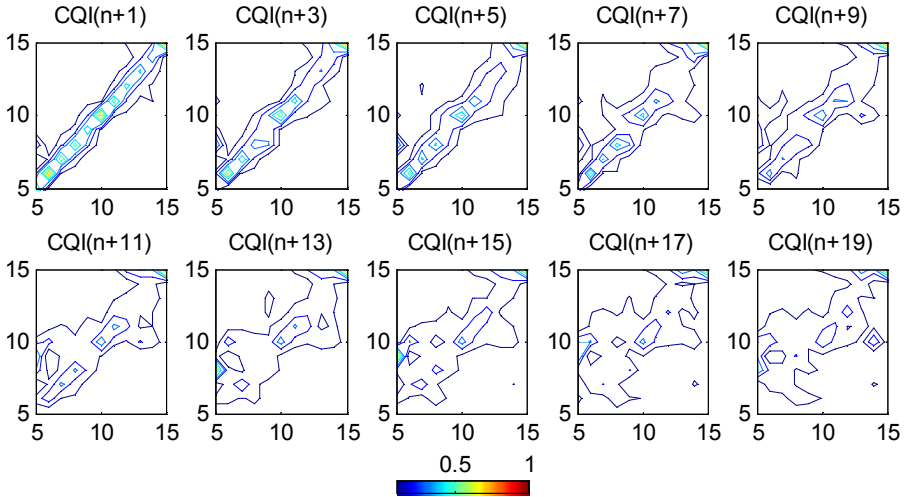
Figure 4.26 – Evolution of CQI variation amplitude over time, for vehicular RI =1.
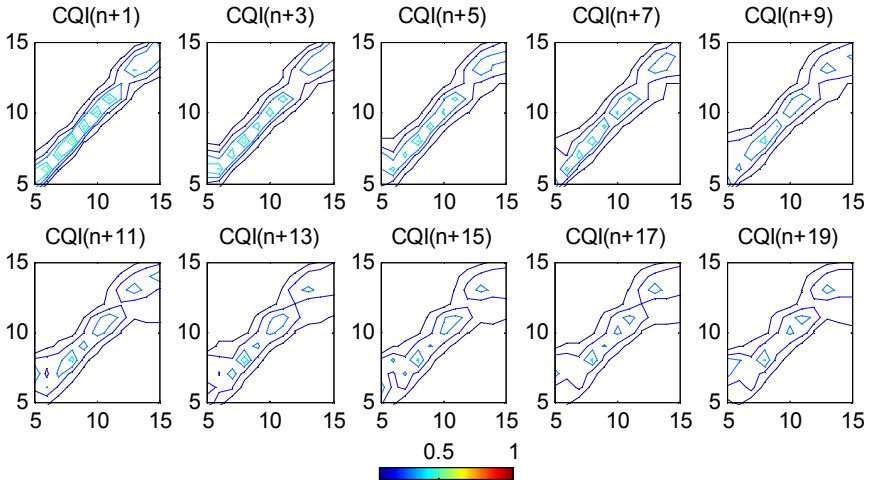
Figure 4.27 – Evolution of CQI variation amplitude over time, for vehicular RI =2.

In order to understand the evolution of CQI over time, a similar approach has been followed by increasing the number of seconds between two CSI samples. In this way, the expected CQI values at different future instants can be estimated.

In the case of vehicular mobility and RI = 1, the amplitude of CQI variations becomes considerable from a difference of five seconds. From that point, it is quite difficult to estimate the future CQI value from the current value.

For vehicular mobility and RI = 2, the CQI variability remains lower for the whole range of times, and especially for the medium CQI range of values. The upper and lower CQI ranges reach a variability of up to 5 units.

4.5   CONCLUSIONS TO FIELD TESTS

This chapter is aimed at providing a step beyond the state of the art concerning the understanding and characterization of downlink data channels in live LTE networks, in terms of the experienced channel quality.

Concretely, CSI information has been collected from a series of field tests in several commercially available LTE networks. The objective of this work is to better understand the actual performance of LTE systems in real-world conditions, in order e.g. to evaluate the suitability of CSI models commonly used by the research community. Therefore, the use of commercial LTE networks and commercial UEs is mandatory.

The current status of the technology makes it possible to use research-focused eNBs and UEs interchangeably. Although some effects of the air interface can be modelled and different signal performance metrics can be obtained, Chapter 3 shows that commercial equipments usually incorporate a series of functionalities that guide the CSI-AMC operation beyond the standardized procedures. Thus, although the result becomes more vendor-specific, this chapter makes only use of commercial equipments and focuses on commercial-grade performance evaluation.

Specifically, field tests have been carried out in different live LTE networks deployed in LTE Band 7 at 2.6 GHz and with 20 MHz of bandwidth. For completeness of the CSI sample, different mobility and traffic patterns have been used. The test equipment consists of a laptop with a Samsung GT-B3730 USB dongle, which is an UE Cat. 3 device enabled by the vendor to report CSI information to the laptop. ASCOM TEMS Investigation is used to retrieve CSI information from the UE.

As a first conclusion, it must be noted that the applicability of the outcomes of this chapter is only ensured for the specific context conditions. It remains for further study if these results can be generalized to other LTE bands / bandwidths or other commercial UEs.

From the basic analysis of the monitored networks, several open questions can be answered:

- Most of the captured DL transmissions are based on the TM3 transmission mode, which supports MIMO transmissions with one or two codewords for increased resiliency and capacity respectively.
    - ○ "Adaptive mode selection" is barely used in specific conditions, performing the RRC Reconfiguration procedure to SISO.
    - ○ The outcome of the "rank-adaptive transmission" procedure entails that almost 30% of the CSI samples correspond to TxD (one codeword) and more than 70% of the CSI samples are associated to Large Delay CDD (two codewords).

- Only periodic CSI reporting is observed in the collected data set, including RI and wideband CQI values.
- The monitored CQI reporting periodicity is 5 ms.
- The monitored RI reporting periodicity is 80 ms.

Although these CSI reporting granularity values may result in frequent variations in RI and CQI values, the CSI data set is restricted to 1 s of minimum variability. This is, both RI and CQI values are constant for at least 1 s and they always vary in intervals of an integer number of seconds. This effect seems to be more related to the performance of the field test HW than to the actual CSI variability. As a conclusion, this matter remains for further study in next chapters of the document.

Regarding the outcomes of the field tests, the chapter is divided in two main areas:

- Section 4.2 and Section 4.3 are aimed at checking if the collected CSI data set makes it possible to propose a valid relationship between the monitored CQI values and other performance-related parameters (i.e., RSSI, RSRP, RSRQ, SNR) or AMC-related outcomes (i.e., MCS and number of assigned PRBs).
- Section 4.4 focuses on characterizing the behaviour of the collected MIMO CSI parameters. Due to the limitation in the CSI sampling frequency, these parameters have been denoted as Coarse-Grain CSI metrics, i.e., Coarse-Grain CQI (CG-CQI) and Coarse-Grain RI (CG-RI).

According to the collected CSI data set, the relationships between CQI and other performance metric are not trivial. The main conclusions can be summarized as follows:

- The estimation of CQI values from other radio performance parameters is not possible in general. The quality of linear fitting improves considerably if the RI value is considered, although the outcome is not accurate enough for generalized CQI estimations.
    - o The simple visual inspection of Figure 4.2-Figure 4.4 illustrates that each individual RSSI, RSRP, RSRQ and SNR value is associated to a wide range of reported CQI values (with 5 to 10 units of variability).
    - o Although a linear matching tendency is more or less followed in the scatter plots, the coefficients of determination shown in Table 1.1 determine the inaccuracy of the linear fittings.
    - o After isolating the CQI samples per RI=1 and RI=2, the range of reported CQI values per each radio metric is reduced, and the coefficients of determination are increased to some extent.
- Similarly, the prediction of CQI values from monitored MCS values does not provide a direct relationship unless intensive usage of radio resources is required.
    - o In general, the scatter plots in Figure 4.7 shows a wide range of possible CQI values per each MCS value, with higher variability towards higher CQI values for each MCS.

- In this case, applying an isolated analysis per RI value does not enhance the CQI estimations.
- According to Figure 4.10, the relationship between MCS and CQI provides closer values when high number of PRBs are used. However, there are still many samples where the full assignation of PRBs is associated to reduced coding efficiency. According to Figure 4.11, only high data rate conditions guarantee a more direct relationship.

- The correlation of the channel quality levels experienced by each of the two reception antennas seems to exhibit different behaviours in different conditions.
  - According to Table 1.1 and Table 4.3, the overall trend is that the relationship between CQI and SNR is lower for RI =2. Without taking into account other possible effects, this trend can be explained assuming that the contribution of each antenna to the overall wideband SNR is more variable in RI =2. In TM3 RI = 2, the reported CQI needs to cope with the target coding efficiency and target BLER for the worse antenna condition. Therefore, it would be expected to find a more direct relationship between the worse antenna SNR and the reported CQI, but the contribution of the better antenna to the overall SNR makes the final relationship less predictable.

Regarding the characterization of LTE DL MIMO data channels, the collected CSI data set allows stressing the following conclusions:

- CG-RI
  - From a general perspective, RI = 1 prevails under low SNR conditions and RI = 2 prevails under high SNR conditions. A similar trend is observed for the rest of radio performance metrics RSSI, RSRP and RSRQ.
  - Concerning the different mobility patterns, the vehicular field tests exhibit the highest heterogeneity with considerable RI = 2 samples at low SNR conditions and RI = 1 samples at medium SNR conditions.
  - The ratio of RI = 2 samples account for 51%, 73% and 77% for static, pedestrian and vehicular conditions respectively. However, it must be noted that the lower ratio for static conditions can be due to the higher number of samples at low SNR conditions.
  - As shown in Figure 4.12, RI can exhibit large periods of constant RI value and some periods where the RI value switches quickly between RI = 1 and RI = 2.
  - Figure 4.16 illustrates that the periods with the same RI value vary from one second to one hundred of seconds, depending on the mobility pattern.
  - In general, RI = 2 samples exhibit higher probability to remain in the same state, especially for high SNR values.

- CG-CQI
  - In general, RI = 2 samples provide lower CQI values even when these CSI samples are more probable to happen at higher SNR conditions.
  - In general, RI = 1 samples provide higher CQI values even when these CSI samples are more probable to happens at lower SNR conditions.
  - Nonetheless, there are periods with RI = 2 with high CQI values (Figure 4.22) and periods with RI = 1 with low CQI values (Figure 4.20).
  - From a temporal perspective, CQI values are likely to change the value from one second to the following second with a probability of around 60% in most of the evaluated conditions.
  - Most of the time periods with constant CQI values are lower than 10 s.
  - Concerning the amplitude of the CQI variations, the collected data set does not exhibit high probabilities of deep variations of CQI between two consecutive CQI samples. The most variable conditions are found to be the static measurements with RI = 2 and the pedestrian mobility patterns with RI = 1.
  - Concerning the evolution of CQI over more than one second periods, the subset with RI = 2 samples tend to be less significant variations.

It must be noted that the CG-CSI values show the prevalence of RI and CQI values over the whole period of 1 s. Thus, these outcomes must be understood from a macroscopic standpoint and do not prevent other behaviours at sub-second level.

5 LTE EMULATION TESTS

Once identified the coarse-grain characteristics of the CSI parameters, this section deals with the identification of the fine-grain patterns at sub-second level. As cited in Chapter 4, the used toolset for field test measurements is only able to provide information of the CQI / RI dynamics at the scope of one second.

Although this information may be suitable for defining the macroscopic behaviour of CSI in real-world use cases, more detailed information is required by other applicability cases such as the definition of novel LTE schedulers, which operate at TTI level.

Therefore, the main objectives of this section are introduced through a series of questions that are unresolved in the analysis of the state of the art:

- Which is the relationship between the coarse-grain CSI and the fine-grain CSI values?
- How reliable are the coarse-grain CSI characterizations provided by the field test tools? Are these characterizations well-suited as inputs for macroscopic problems?
- How reliable are the coarse-grain CSI statistics at sub-second level? How quick and how much CSI values vary within the second period?
- Which is the actual impact of several well-known radio fading profiles into real-world UEs? Is it possible to infer some type of relationship between the reported CSI and other parameters? Are the results comparable with state of the art LTE simulators?
- Can we expect any significant impact on the operation of LTE HARQ processes? Is it possible to recommend any CRR value for different fading / mobility patterns?

5.1 DESCRIPTION OF THE DATA SET

A commercial LTE emulator, the Aeroflex 7100 LTE emulator, has been used in order collect fine-grain CSI traces from real devices up to the practical limit of 2ms in CRR. This emulator performs the role of the eNodeB, since it creates the LTE radio signal and all the necessary LTE protocol events to support the attachment and registration of any LTE device through a radiofrequency cable or over the air.

In order to reproduce the overall radio conditions of the field tests described in Chapter 4, the LTE emulator is properly configured with the monitored LTE radio characteristics in terms of frequency, bandwidth, power levels, etc. In these conditions, the Samsung GT-B3730 dongle is connected to the LTE emulation system as represented in Figure 5.1. The scope of these experiments has been constricted to the evaluation of the empirical fine-grain CQI values in LTE SISO conditions (RI=1). Therefore, the dynamics of the RI parameter are not considered in this document.
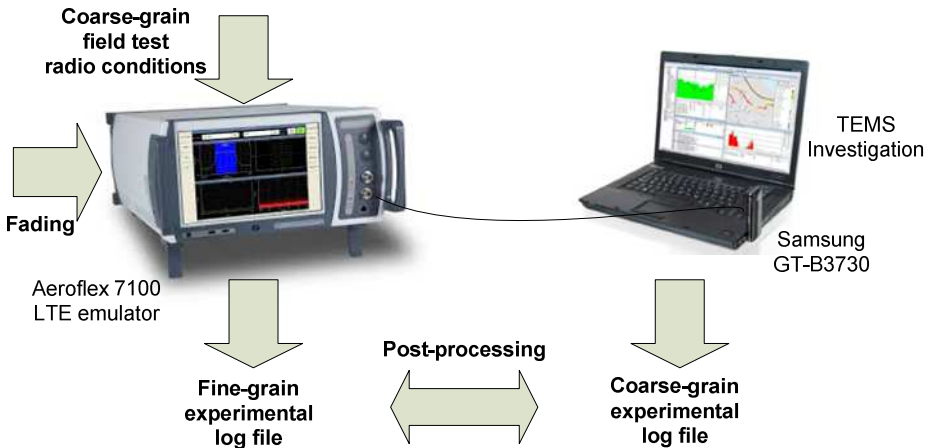
Figure 5.1 –Testbed for realistic LTE experiments.

Under this experimental framework, different coarse-grain radio conditions are configured and the resulting CQI values provided by the UE are collected. First, a certain level of SNR is configured by introducing AWGN to the LTE signal. Afterwards, different fading conditions are added to the resulting radio signal.

The LTE emulator is configured to request CQI reports from the UE every 2 ms, and the received CQI values are logged by the emulator and saved to a file for further offline processing. At the same time, TEMS Investigation is used at the laptop to collect coarse-

grain statistics in the different experimental conditions in order to check reported coarse-grain values against real-world fine-grain data.

Two families of experiments are reported in this document:

- Section 5.2 - The first set of experiments evaluates the behaviour of the UE under different Test Points for LTE, based on the fading profiles established in 3GPP TR 37.901. In this case, the AWGN SNR conditions are configured a priori and not modified during the experiment.
- Section 5.3 - In the second set of experiments, the Aeroflex 7100 Test System Application Programming Interface (API) is used in order to dynamically modify the target AWGN SNR according to the coarse-grain SNR values collected in the field tests.

5.2 3GPP TEST POINTS

Table 5.5.4.5-2 in 3GPP TR 37.901 [3GPP-TR37901] establishes a series of radio conditions that cover most of the propagation scenarios experienced in LTE field tests.

- The static test point resembles the situation without fading or AWGN interferences.
- The Extended Pedestrian A (EPA) profile introduces high variability in the CQI, and therefore in the MCS and the assigned TBS.
- The Extended Vehicular A (EVA), which occurs frequently in LTE deployments, is evaluated in good and medium SNR conditions (20 dB and 10 dB) and with different Doppler frequency values (from 5 Hz to 200 Hz). Higher Doppler frequencies are associated to higher LTE carrier frequencies.
- The Extended Terrestrial Urban (ETU) profile is evaluated at poor reception conditions (0 dB) and in medium to very high Doppler frequencies.

Based on these configurations, the test points defined in Table 5.1 are proposed for carrying out a series of emulation experiments in different reception conditions. The purpose of these experiments is twofold: evaluating the behaviour of a commercial UE in these conditions and comparing the CSI results obtained from the emulator and from the field test software.

These AWGN SNR and fading conditions have been configured in the Aeroflex 7100 LTE emulation system to analyze the behaviour of the UE in heterogeneous channel conditions. For each test, the UE is registered to the network and CQI values are gathered over 2 minutes. Considering the reporting frequency of 2 ms, a total of 60,000 CQI samples are gathered for each test point. At the same time, the coarse-grain CQI values at 1 second of periodicity are collected with the field test software for comparison with fine-grain results.

Table 5.1 –Proposed LTE Test Points for stationary experiments.

Test Point ID	SNR	Speed	Doppler frequency	Description
Static	20dB	0 km/h	0 Hz	Static conditions at high SNR.
EPA5	20dB	5 km/h	12 Hz	Low Doppler frequency at high SNR.
EVA5	10dB	5 km/h	12 Hz	Low Doppler frequency at medium SNR.
EVA70	20 dB	70 km/h	172 Hz	High Doppler frequency at high SNR.
EVA200	20 dB	200 km/h	492 Hz	Very high Doppler frequency at high SNR.
ETU70	0dB	70 km/h	172 Hz	High Doppler frequency at poor SNR.
ETU300	0dB	300 km/h	738 Hz	Very high Doppler frequency at poor SNR.

5.2.1   FINE-GRAIN CQI STATISTICS

All the experiments in this section are carried out at a cell frequency of 2.6 GHz and with a bandwidth of 20 MHz. The emulator is configured to assign all the DL PRBs to the single UE, and the AMC is configured to dynamically adapt to the reported CQI values.

Figure 5.2 provides the results obtained for the 2 minutes CQI traces with a target SNR of 20 dB and without any fading channel. Two CQI traces are illustrated: the blue lines represent the CQI values provided by the UE at 2 ms of periodicity (denoted as "7100" in the figure) and the red lines represent the CQI values provided by the field test software at 1 s of periodicity (denoted as "TEMS" in the figure).

Additionally, the SNR values monitored at the LTE emulator and at the UE are provided.
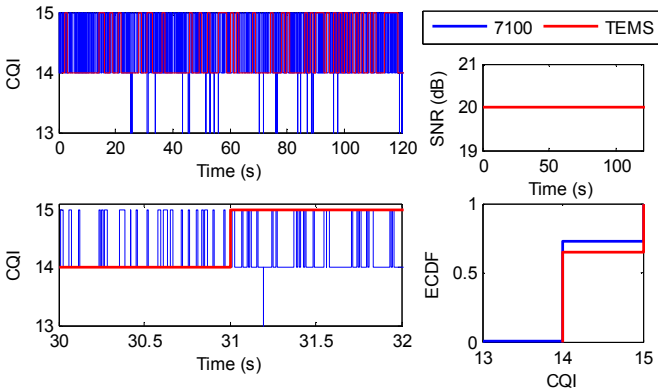
Figure 5.2 –Experimental results for "static" test point.

As can be observed in the upper-right subplot, the monitored SNR value is completely stable at the target value of 20 dB. With these SNR conditions, the upper-left subplot shows that the coarse-grain CQI values fluctuate between 14 and 15 along the whole trace The fine-grain CQI values are also mainly within those two values, with some CQI values going down to 13.

To better understand the relationships between the coarse-grain and fine-grain CQI values, the lower-left subplot illustrates an excerpt of 2 seconds of the traces. It is clear that the variations of the CQI at sub-second level are significant even with no additional fading. Moreover, the ECDF of both traces is represented in the lower-right subplot. As can be observed, the coarse-grain CQI trace exhibits slightly lower ratio of CQI = 15 values.

Figure 5.3 gathers the experimental results for the rest of LTE Test Points in Table 5.1.
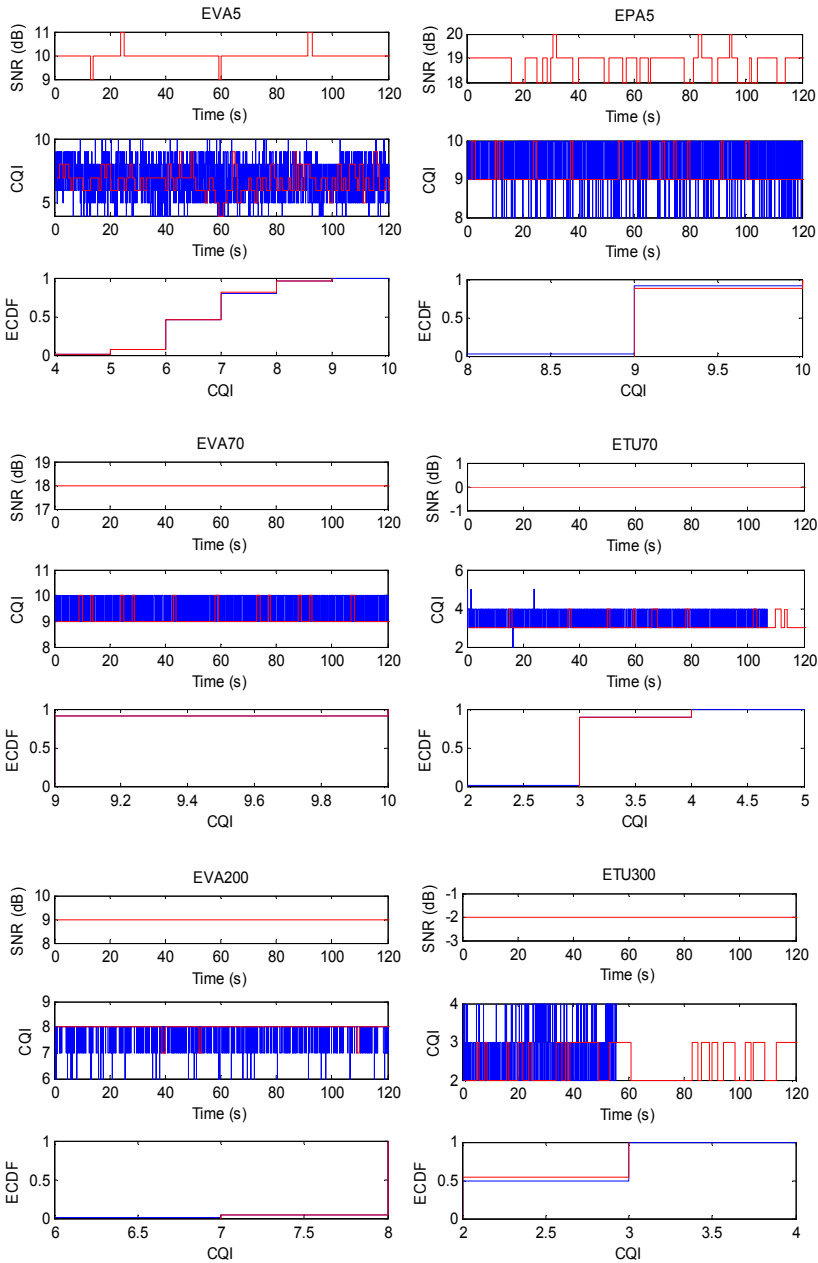
Figure 5.3 – Experimental results for LTE test points with fading.

For each LTE Test Point, three subplots are included: the SNR values monitored by the field test software, the monitored CQI traces at coarse-grain and fine-grain, and the ECDFs of both CQI traces.

As a first relevant outcome, it can be stated that the ECDF values of the coarse-grain and fine-grain CQI values are quite close in all the experiments. Therefore, the coarse-grain CQI values can be considered a good estimator of the macroscopic behaviour of the channel quality, although it is observed that the sub-second CQI dynamics are much more variable.

Taking as reference the different test points with AWGN SNR = 20 dB, the different effects of the fading profiles are clearly identified. For the case without fading shown in Figure 5.2, the measured SNR is also 20 dB for the whole trace. When EPA5 is added, the measured SNR fluctuates between 18 and 20 dB. Meanwhile, EVA70 results in a measured SNR of 18 dB for the whole trace. However, this effect is not directly mapped to the generated CQI values since in both cases most of the fine-grain values correspond to CQI = 9, with even a slightly higher result for EVA70. Likewise, adding EVA200 significantly decreases the monitored SNR to 9 db, while the reported CSI values are mostly CQI = 8.

Concerning the impact of the CQI dynamics into the TBS, and thus into the DL throughput, Figure 5.4 shows the throughput measured at the physical LTE layer of the UE for the different test points with AWGN SNR configured to 20 dB. In addition to the different traces, Figure 5.4 includes the maximum throughput achievable according to the main component of the CQI.
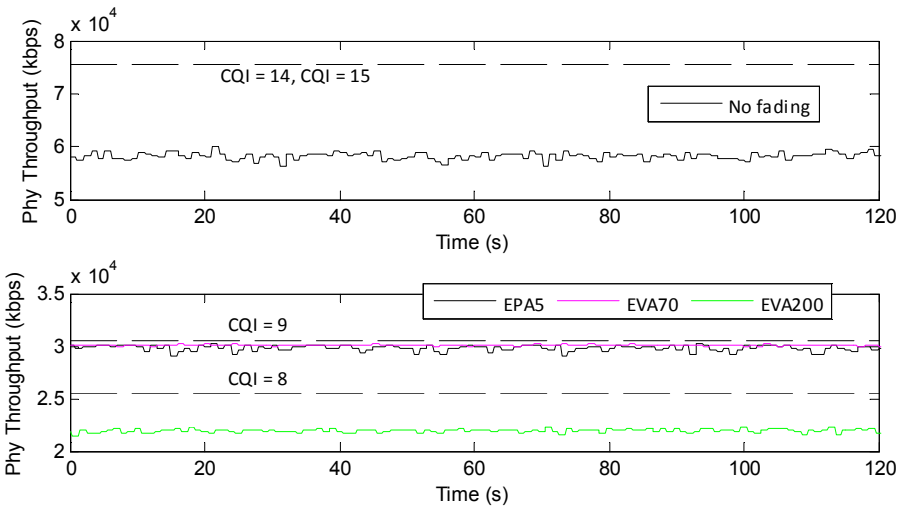
Figure 5.4 –Physical throughput for test points at AWGN SNR = 20 dB.

For the case without additional fading, the main components of CQI are 14 and 15. Therefore, according to table B.2.2.1-11 in [3GPP-TR37901], the assigned MCS would be 27 for a maximum of 75,376 kbps in DL with SISO transmissions. However, it is clear that this target throughput value cannot be reached even when BLER values do not increase significantly.

As expected b the descriptions in Table 5.1, EPA5 results in more variable TBS values and more variable DL physical throughputs compared to EVA70. Yet, both traces achieve DL throughputs close to the upper limit associated to CQI = 9. However, EVA200 is not able to approximate the limit of CQI = 8, likely due to incurred BLER or conservative MCS assignments.

Coming back to Figure 5.3, EVA5 fading results in quite constant monitored SNR values equal to the configured 10 dB, with slight variations to 11and 9 dB. However, CQI values exhibit a significant variability both at coarse-grain and fine-grain values. The average CQI value becomes 6.72 and 6.66 respectively for fine-grain and coarse-grain values, with CQI variations between 4 and 10. In terms of physical throughput, the average value results in 16.48 Mbps, with maximum and minimum values of 19.36 Mbps and 14.48 Mbps.

Finally, the two test points based on ETU fading profile are associated to very stringent radio conditions with AWGN SNR configured to 0 dB. In both cases, the reported CQI values are below 4, and the associated DL BLER values are 28.03% and 53.93% in average for ETU70 and ETU300 respectively. There, as can be observed, the LTE channels are severely degraded and even the CQI reports cannot arrive at the LTE emulator.

5.2.2   IMPACT OF THE FADING PROFILE ON LTE PROCEDURES

Beyond the basic inspection of the CQI behaviour at sub-second level, this section is aimed at providing a preliminary evaluation of the possible implications of these CQI patterns into the typical operation of LTE systems through three different experiments.

To cover the range of propagation conditions, the border test points are selected and compared. On one hand, the static test point is chosen as a reference with no additional fading and provides quite stable CQI conditions over time. On the other hand, EVA5 seems to be the fading profile that results in highest CQI variations.

As a first experiment, the evolution of the reported CQI levels while increasing the AWGN SNR is evaluated. Although several studies in the literature deal with this relationship (e.g., [Kawser-2012] and [Chen-2011]), the underlying experiments need to be carried out for each specific radio configuration in terms of frequency, bandwidth and transmission scheme.

Two main tests have been scheduled over the testbed presented in Figure 5.1. First, the AWGN SNR is configured to 0 dB and is incremented in steps of 1 dB up to 22 dB without

any additional fading. For each SNR point, a fine-grain CQI trace of 60 s is gathered and the average CQI value selected. The same process is then repeated for the second test, adding EVA5 fading to the LTE signal.

The obtained results are summarized in Figure 5.5. As can be observed, the CQI values generated by the UE are always higher with AWGN than with EVA5 for the same SNR value. This fact confirms that the generation of CQI is not only dependent on the SNR, and therefore generic mapping models cannot be generally applied. In the selected cases, the difference in CQI estimation is of up to 3 values.
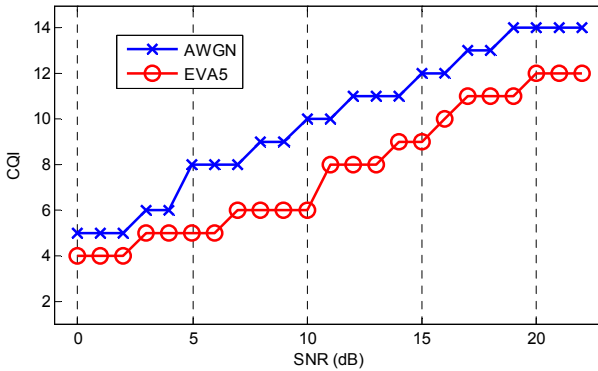
Figure 5.5 –Evolution of CQI with increasing SNR for AWGN and EVA5.

The second analysis in this section focuses on the implications of the dynamics of coarse-grain and fine-grain CQI values into the LTE AMC procedure.

Theoretically, the CQI value reported from the UE to the eNB is used to determine the MCS assigned to the next DL transmission. For the case of SISO transmissions and full PRB allocation to the UE, table B.2.2.1-11 in [3GPP-TR37901] provides a direct mapping between CQI and MCS. These MCS values can be further mapped to the actual TBS based on tables 7.1.7.1-1 and 7.1.7.2.1-1 of [3GPP-TS36213]. For the case of MIMO transmissions, table B.2.2.1-12 of [3GPP-TR37901] and tables 7.1.7.1-1, 7.1.7.2.1-1 and 7.1.7.2.2-1 of [3GPP-TS36213] can be used. Based on the definition of CQI, the target BLER for each operational point is 10%, which practically means that the expected BLER will remain below 10% if the previous CQI-MCS-TBS mappings are performed.

Two main questions arise in this respect:

- How do CQI dynamics affect this procedure? In case that the CQI evolves to a lower value, it is expected that the assigned MCS would entail a higher BLER.
- How severe is the assignation of a MCS higher than the corresponding MCS according to the actual channel quality?

For the first question, Figure 5.6 depicts the outcome of CQI dynamics concerning the CSI reporting loop. For both AWGN and EVA5 test points, the ECDF of the difference between consecutive CQI values is shown.
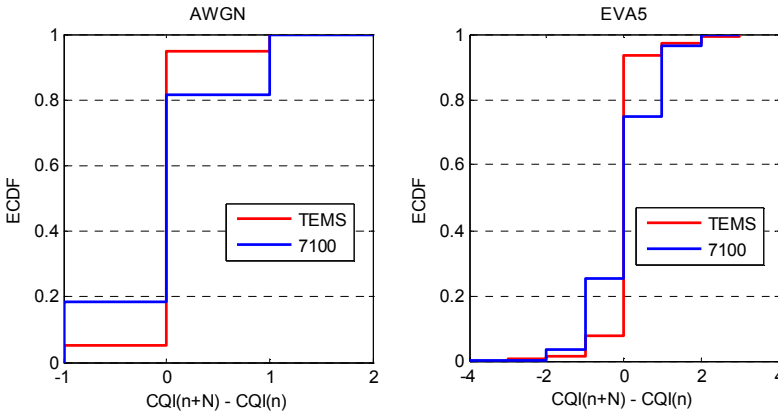
Figure 5.6 –Difference between consecutive CQI values for AWGN and EVA5.

For fine-grain CQI, this difference is obtained by taking the reference of 8 TTIs of CQI delay according to the HARQ loop. The probability of making overrated MCS assignments is evaluated by means of the ratio of samples where the future CQI value is lower than the CQI available at the LTE emulator. The AWGN CQI trace results in 18.59% of expected erroneous assignments, while the EVA5 CQI trace increases up to 25.36%. As a first conclusion, it is observed that the channel conditions with EVA5 fading results in higher expected overestimations of CQI compared to the AWGN channel.

Additionally, these ratios are considerable higher compared to the coarse-grain CQI values, which provides 5.03% and 7.92% of expected overestimations for AWGN and EVA5 respectively. Therefore, the coarse-grain CQI values cannot be considered a good estimator of CQI dynamics for sub-second level procedures.

For the question regarding the impact of these overestimations on the actual experienced BLER, a new set of experiments have been performed with the LTE emulator and the commercial UE.

For these tests, the AWGN SNR is increased in steps of 1 dB, from 0 dB to 22 dB in the case of no additional fading and from 3 dB to 22 dB in the case of adding EVA5 fading. For each test point, the predominant CQI is captured. And for each SNR value, the MCS is manually increased in steps of 1 until the BLER values significantly overpasses the target BLER. For each combination of SNR and MCS, the experimental average BLER is recorded.

Figure 5.7 and Figure 5.8 gathers the obtained results for AWGN and EVA5 radio channels.
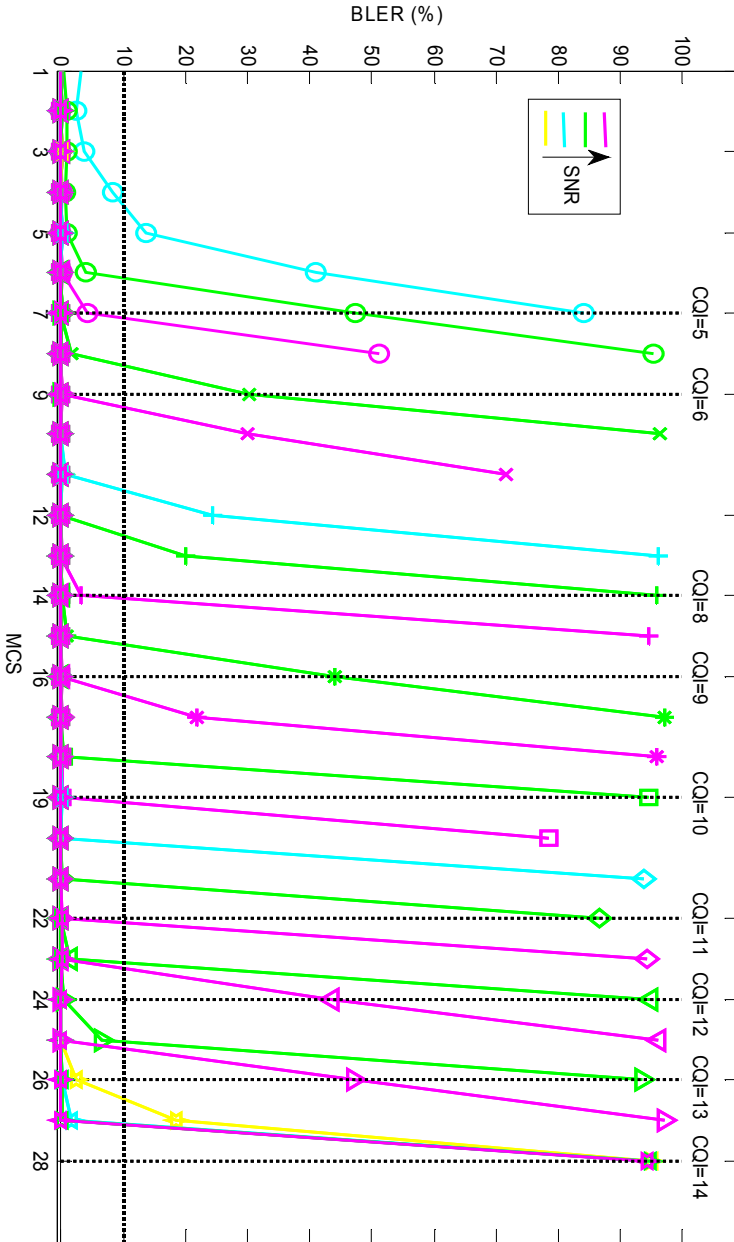
Figure 5.7 –Impact of CQI overestimation for AWGN.
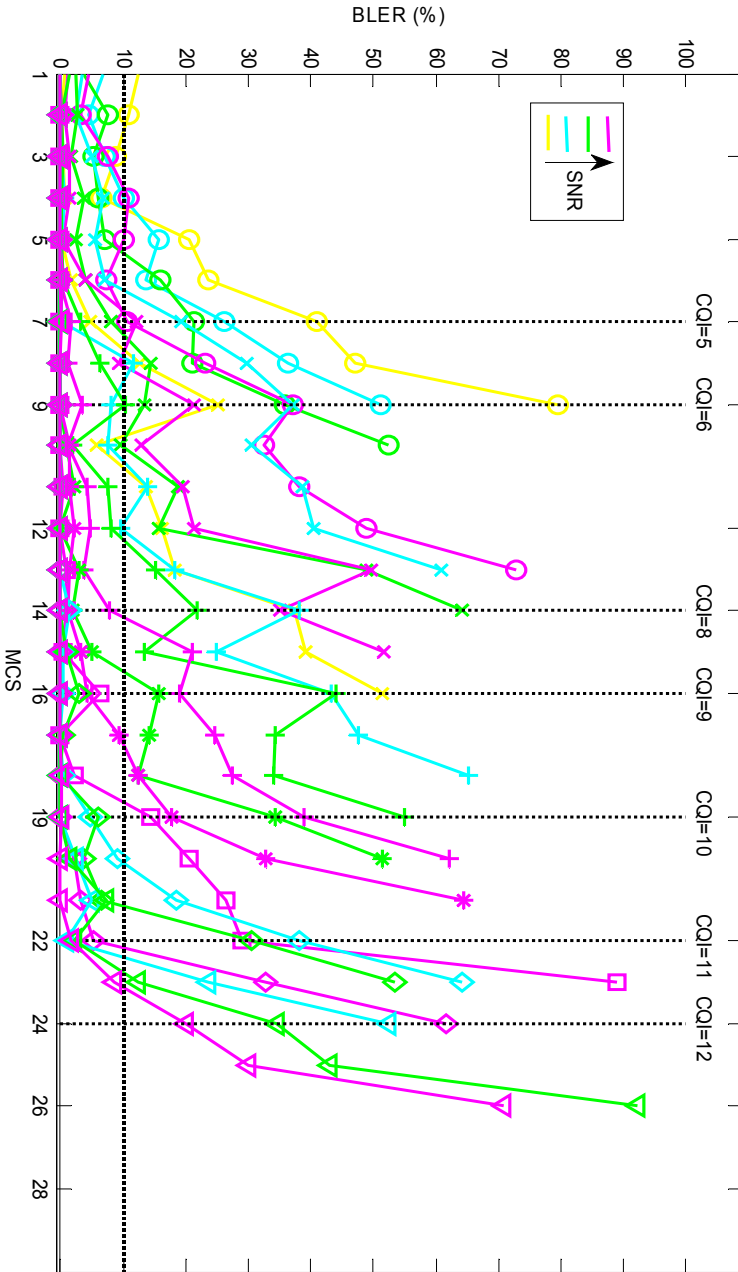
Figure 5.8 – Impact of CQI overestimation for EVA5.

For each CQI value obtained in the experiments, a range between 2 and 4 consecutive SNR values can be associated. Therefore, rather than including the exact value of SNR, Figure 5.7and Figure 5.8 use a colour code to represent the incremental SNR tests resulting in the same CQI value. The actual SNR value can be obtained taking into account that 1 dB is increased between two consecutive lines. Additionally, all the lines corresponding to the same CQI value use the same marker for a better identification of the common ranges. Finally, for each obtained CQI value, the target MCS is represented as a vertical dotted line.

In order to illustrate the interpretation of results, the case of CQI = 5 and AWGN is analyzed. Three different SNR conditions provide a predominant value of CQI = 5, corresponding to SNR = 0, SNR = 1 and SNR = 2. According to the direct mappings between previously cited, an MCS of 7 would be expected for this CQI value. However, only the line of SNR = 2 copes with the target BLER of 10% at MCS = 7. For SNR = 1 and SNR = 0, the experienced average BLER at MCS = 7 increases to almost 50% and 85% respectively. For SNR = 1, MCS = 6 would be required, while SNR = 0 would require MCS = 4 to remain below the target 10% BLER.

A similar behaviour is experienced for AWGN u p to CQI = 11. For higher CQI values, the supported MCS is even lower to the theoretical one corresponding to the reported CQI.

Two main conclusions can be inferred from these results:

- According to these experiments, only the reported CQI is not a sufficient estimator for the eNB in order to cope with the target BLER value.
- The BLER increases abruptly when the MCS goes beyond the actual supported value.

For channel conditions with additional EVA5 fading, the exhibited patterns concerning the relationships between SNR, CQI, MCS and BLER are quite different and more irregular.

First of all, it must be taken into account that the CQI values obtained for EVA5 in Figure 5.3 are quite variable and thus average CQI values may be rough estimations of the channel quality.

This being noticed, the following outcomes can be summarized from the results in Figure 5.8:

- For the same upper threshold of SNR, the reported CQI is limited to 12 in EVA5, compared to CQI = 14 in AWGN.
- The BLER experienced for the target MCS corresponding to each CQI ranges between 5% and 20% in average. And these BLER values do not follow a clear evolution with the average CQI.
- For different MCS values higher than the expected one, the increase of BLER is less abrupt than in the case of AWGN.

Therefore, in overall it seems that AWGN channels provide more controlled environments than fading-added radio channels such as EVA5.

In summary, according to Figure 5.6, Figure 5.7and Figure 5.8, it would be expected that some level of BLER is found in the experimental traces obtained for the 3GPP LTE Test Points. However, as shown in Figure 5.9, only the ETU test points associated to severe SNR conditions exhibit considerable BLER values.
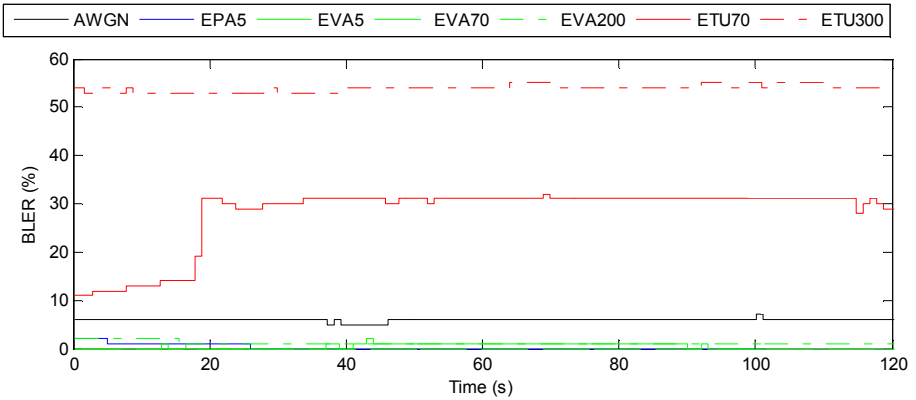
Figure 5.9 –Evolution of BLER with increasing SNR for AWGN and EVA5.

Therefore, the question remaining relates to AMC implemented by the eNB, or by the LTE emulator in this case, in order to cope with these possible problems. As illustrated in Figure 5.10, the assigned MCS values are in general lower to the expected ones due to the direct mappings.
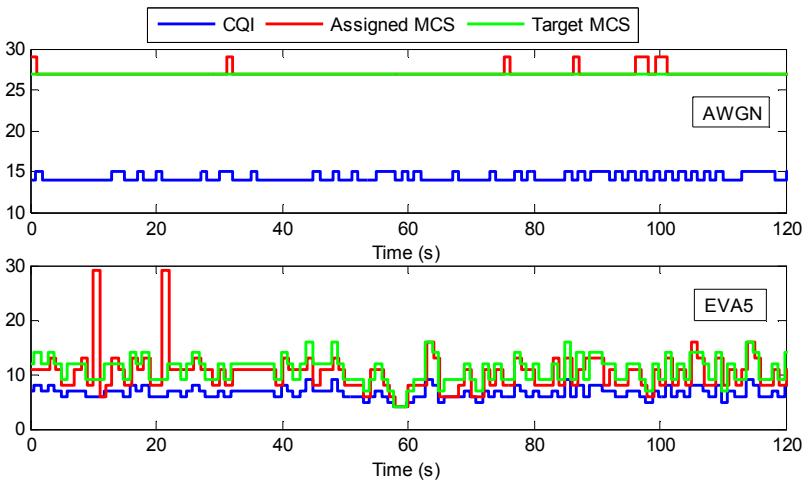
Figure 5.10 –CQI values and experimental and target MCS values for AWGN and EVA5.

5.3   CHARACTERIZING LTE MIMO CHANNELS

This section describes a series of experiments performed with the LTE emulation system aimed at resembling the field test scenarios described in Chapter 4. Since the field test toolset is not able of providing CSI information at sub-second, these experiments intend to infer some level of fine-grain CQI patterns from the LTE emulations.

Specifically, based on the testbed described in Figure 5.1, the following methodology is implemented:

1. A laptop running the commercial UE is connected and registered to the LTE emulator through a RF cable.
2. The AWGN SNR in the LTE emulator is programmatically configured at steps of one second, according to the wideband SNR values monitored in field tests.
3. Based on the profiles described in Table 5.1, different fading profiles are added to the generated LTE signal in different tests.
4. The fine-grain CQI traces obtained at the LTE emulator (from CSI reports uploaded by the commercial UE) are compared with the coarse-grain CQI traces obtained at the laptop (from CSI reports provided by TEMS Investigation).
5. The fine-grain CQI traces obtained in emulation are compared to the coarse-grain CQI traces obtained from field tests.}

Figure 5.11 illustrates an excerpt of 260 s from a drive test trace obtained from TEMS Investigation, which has been used in the LTE emulation experiments.
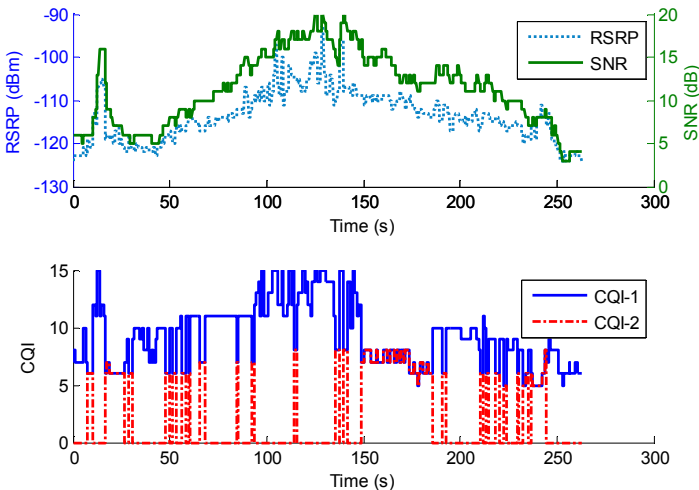
Figure 5.11 – Example trace from field testing in LTE MIMO.

As can be observed, the wideband SNR captured in this field test ranges from 3 dB to 20 dB, resulting in UE-generated CQI values from 4 to 15. In this excerpt it is observed that different RI values predominate in different time slots, leading to RI = 1 and RI = 2 MIMO transmission slots. Since there is not a direct way of isolating the contributions of each antenna to the wideband SNR, the same SNR trace is used in the LTE emulations and the results with different fading profiles are compared to the isolated RI = 1 and RI = 2 traces.

Figure 5.12 illustrates the statistical characteristics of the isolated RI = 1 and RI = 2 traces for the trace excerpt shown in Figure 5.11.
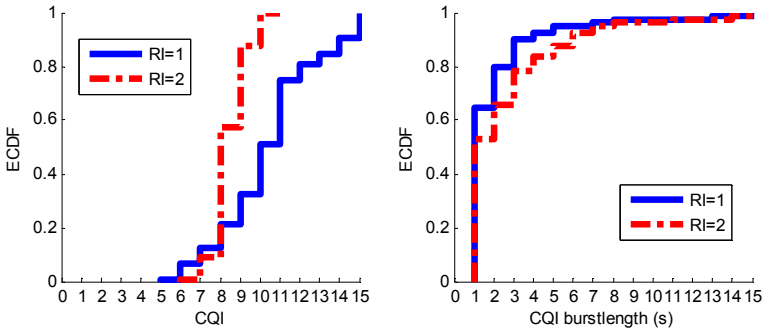
Figure 5.12 –Characteristics of CQI from field tests for RI=1 and RI=2.

The left plot in Figure 5.12 illustrates the ECDF of CQI values. As can be observed, RI = 2 periods provide lower CQI values than RI = 1 periods. Although this fact is observed in most of the performed drive tests, several scenarios provide high CQI values also for RI = 2, when both antennas experience good channel conditions at the same time.

In order to provide some further evidence of the different characteristics experienced by CQI in both transmission schemes, the right plot in Figure 5.12 shows the ECDF of monitored CQI burstlengths. At this time scale, CQI values seem to be less variable for RI = 2 periods than RI = 1 periods although for both of them maximum burstlengths are around 15 s.

5.3.1   FINE-GRAIN CQI STATISTICS

Figure 5.13 illustrates the obtained experimental coarse-grain results in terms of CQI ECDF (upper plot) and CQI burstlength ECDF (lower plot) as reported by TEMS Investigation. This figure also includes the statistical properties of the selected field test CQI traces, separated between RI = 1 and RI = 2 periods.
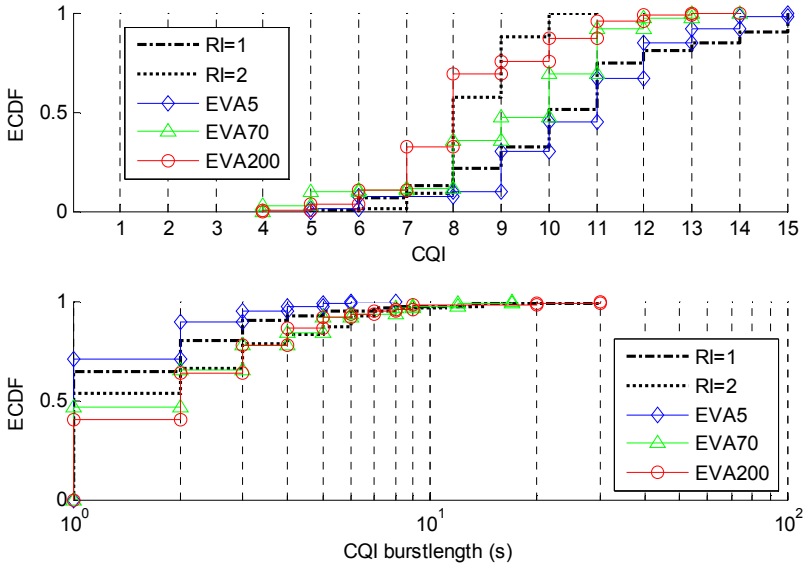
Figure 5.13 –Field test traces vs. 3GPP fading channels.

As expected, none of the propagation conditions perfectly matches any of the real-world traces. However, some specific trends are observed as follows:

- CQI traces in MIMO RI = 1 periods are closer to EVA5 fading condition in both CQI and CQI burstlength first order statistics.
- CQI traces in MIMO RI = 2 periods are closer to EVA70 and EVA200 fading conditions in both statistics.

These results can be interpreted considering the LTE Transmission Mode 3 and possible switching between the two alternative transmission schemes. As explained before, RI = 1 is used when one of the antennas experiences a significant better channel condition compared to the other antenna. In this case, it seems that the best antenna follows a less severe fading condition such as EVA5.

RI = 2 is used when the estimated bitrate using two layers in the worst radio condition achieves a higher bitrate than a unique layer through the best antenna. Therefore, RI = 2 CQI traces are associated to the more severe fading condition of the two antennas. Although high CQI values have been monitored in RI = 2, most of the field test experiments provide lower CQI values and are therefore associated to more severe fading conditions.

5.3.2 TEMPORAL VARIABILITY OF FINE-GRAIN CQI

In order to infer the possible behaviour of CQI at sub-second level, the experimental CQI traces reported by the Samsung GT-B3730 are captured at the LTE emulator and compared to the coarse-grain CQI traces.

Figure 5.14 illustrates the results of the actual CQI traces at 2 ms of reporting period.
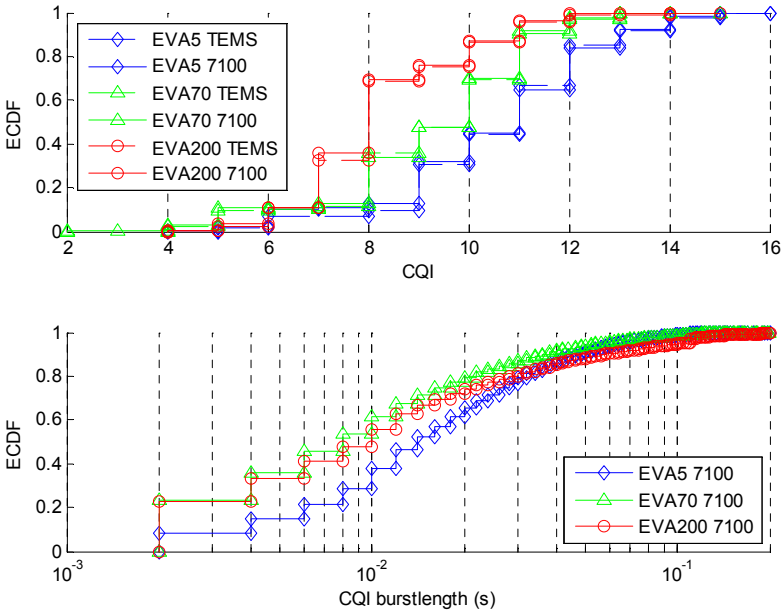
Figure 5.14 –Burstlength of CQI traces at LTE frame level.

The upper plot confirms that aggregated CQI values reported by TEMS and actual CQI values reported by UE to the eNodeB follow similar statistics. However, CQI values over time are much more variable than coarse-grain reports. The lower plot illustrates the ECDF of CQI burstlengths and confirms that burstlengths beyond 200 ms are hardly probable in any scenario.

Additionally, as expected from results in Section 5.2, it is observed that EVA5 fading channels exhibit higher burstlengths than the other two fading conditions. These characteristics may be exploited by channel-aware scheduling strategies to optimize the performance of the cell avoiding low-level retransmissions due to fast channel variability.

5.4   CONCLUSIONS TO EMULATION TESTS

From Chapter 4, the main characteristics of the coarse-grain CSI parameters are analyzed. These CG-RI and CG-CQI parameters can be obtained with a periodicity of one second, although it is shown that the actual CSI reporting periodicity is configured to 5 ms and 80 ms for CQI and RI respectively.

Understanding the characteristics of these CG-CSI parameters can be useful for macroscopic purposes, such as transport- and application-level dynamic configurations. However, other types of research studies require a more detailed knowledge of the sub-second dynamics of the CSI parameters. For example, the design and evaluation of novel LTE scheduling algorithms could benefit from an improved knowledge of the CSI dynamics at AMC time scales.

Since this type of fine grain CSI (FG-CSI) values cannot be easily collected from commercial equipments, this chapter presents a methodology to somehow infer the detailed behaviour of CSI data up to 2 ms of periodicity, which Is the practical limit imposed by the 3GPP.

As illustrated in Figure 5.1 the proposed methodology is based on the use of an LTE emulator, the Aeroflex 7100 Digital Radio Test Set, and the same CSI monitoring toolset as in the field tests. The LTE emulator is configured to resemble the coarse grain radio conditions gathered from field tests and different fading patterns are further added to the generated signal. From each emulation test, the CG-CSI values are available from the TEMS Investigation SW and the FG-CSI values are collected from the Aeroflex 7100 equipment with the required granularity.

In order to limit the scope of the study, this chapter focuses on the Fine Grain CQI (FG-CQI) values. Different families of emulation tests have been carried out aimed at better understanding the relationships of the CG-CQI and FG-CQI values:

- By comparing the CG-CQI and FG-CQI values generated in controlled emulation tests, it is possible to understand the sub-second CQI dynamics for the reported CG-CQI traces.
- By analyzing the behaviour of CSI and AMC procedures in different operational points, the impact of different fading profiles into the results generated by the commercial UE can be evaluated.
- By comparing the CG-CQI traces collected from field tests in Chapter 4 and from experimental tests in this chapter, the real-world CSI can be characterized to some extent. Although it is not possible to validate the inferred outcomes, some tendencies can be assumed for the collected data set.

Although the proposed methodology introduces several uncertainties in the process, the obtained FG-CQI values at least provide some reference patterns of the possible real-world behaviours.

From the perspective of the analyzed CSI patterns, the obtained results confirm that the behaviour at sub-second level is quite more variable than the coarse-grain CQI dynamics observed from the field tests. In this family of tests, each test point is configured with of a constant AWGN SNR value and a specific fading profile. Therefore, the observed CSI patterns are mainly due to the effect of fading. Figure 5.3 shows the temporal evolution of the CG-CQI reported by the field test SW and the actual FG-CQI values collected at the LTE emulator from the UE-generated CSI reports.

The main results observed from the first family of emulation tests are:

- Most of the test points provide a FG-CQI variability amplitude of one unit above or below the CG-CQI reported.
- EVA5 fading profile introduces the highest FG-CQI variability over the reported CG-CQI value. In this case, a prevalent CG-CQI of 4 may include up to FG-CQI values of 9. Thus, this fading profile is selected to further analysis of the possible impact on the standard AMC procedure.
- The effect of the most severe fading conditions is somehow different to the expected behaviour. Theoretically, higher frequency values would lead to more variability in the channel quality. However, the experiments performed indicate that the overall SNR is decreased considerably resulting in lower but les variable CQI values.
- From a macroscopic standpoint, the comparison of the CG-CQI and FG-CQI ECDFs shows quite similar values. Hence, it can be assumed that CG-CQI values can be valid for high level estimation of the achievable throughput.

The impact of the different fading profiles on the CQI values and the implications of the CQI dynamics on the AMC process are also analyzed with the second family of emulation tests. In this case, the LTE emulator is configured to apply different SNR conditions with EVA5 fading and without fading. Besides, the configuration of the LTE emulator is modified to apply manual and automatic MCS assignations.

The main results observed from the second family of emulation tests are:

- As shown in Figure 5.5, the same level of SNR configured results in quite different CQI levels at the UE, with up to 4 units of difference.
- When the CQI report available at the eNB for MCS determination is higher than the actual CQI value at the UE, a CQI overestimation occurs. Figure 5.6 shows that the static condition results in around 18% of CQI overestimations, with a maximum difference of one unit. Adding EVA5 increases the ratio of CQI overestimations to 25% with CQI differences of up to four units.
- The effect of working with CQI miss-estimations is analyzed in Figure 5.7andFigure 5.8. By forcing the LTE emulator to assign MCS values different to the corresponding one, the BLER value is analyzed with and without fading.
  - In AWGN conditions, the relationship is quite clear. Even in the highest SNR for each CQI value, applying the correct MCS results in BLER lower

than 10%, and applying higher MCS values increases the BLER significantly. Therefore, the CSI-based AMC process is quite coherent and stable.
  - o However, adding EVA5 fading results in less predictable results, with higher BLER values even for the correct MCS and less disruptive BLER values with higher MCS assignations.
- Figure 5.9 and Figure 5.10 show how the AMC algorithm implemented in the LTE emulator is able to keep the BLER values below the target 10% for the EVA5 test, by using lower MCS values.

Finally, the third family of emulation tests allows inferring the possible characteristics of the real-world CQI patterns. In this case, the LTE emulator is configured to follow the coarse grain radio condition of a subset of the field test CSI samples. By comparing the CG-CQI values provided by the field test SW in the emulation test and the CG-CQI values obtained in the actual field test, the main CQI patterns are inferred. Besides, the FG-CQI values associated to that emulation test is used to evaluate the estimated FG-CQI characteristics.

The main results observed from the third family of emulation tests are:

- Figure 5.13 shows that the CG-CQI values associated to RI = 1 in the field tests are closer to the CG-CQI values associated to the emulated EVA5 fading profile. A similar conclusion can be extracted for the duration of the time periods with constant CG-CQI value.
- Contrarily, the CG-CQI values associated to RI = 2 in the field tests are closer to the CG-CQI values associated to the emulated EVA70 and EVA200 fading profiles.
- Figure 5.14 shows that the statistics of the CG-CQI values obtained in the emulation tests are also quite close to the FG-CQI values obtained in the same emulation tests. Therefore, the CG-CQI parameter can be considered a good overall estimator of the achievable throughput also when the SNR is modified over time.
- Figure 5.14 also shows the dynamics of the FG-CQI values obtained from the emulation tests. In summary, EVA5 fading profile provides more variable CQI values in the time domain of milliseconds. The behaviour of EVA70 and EVA200 are more similar exhibit less variable conditions.
- As a result, the outcomes of these emulation tests show the tendency that real-world RI = 1 CSI samples are closer to fading profiles with lower Doppler frequency and real-world RI = 2 CSI samples are closer to fading profiles with higher Doppler frequency values.

In general, these finding are in line with the assumptions made in Chapter 4, which pointed out that RI = 1 is only selected by the UE when one reception antenna is in much better signal conditions than the other reception antenna. For RI = 2 samples, the lower of the two CQI values at each antenna has to be reported In TM3. Hence, the probability of experiencing lower CQI values in RI = 2 is higher, since the probability that the two antennas are in very good channel quality conditions is lower.

6 IMPACT OF CSI DYNAMICS ON LTE AND BEYOND

Previous sections have been focused on the analysis of CSI (Channel State Information), as gathered from commercial UEs and real-world and emulated 4G LTE networks. From this analysis, the dynamics of two key CSI parameters (namely RI and CQI) have been derived taking into account the temporal variability and the magnitude of variations.

This section makes use of the obtained information in order to infer the implications of CSI variability in the overall performance of 4G systems, including recent architectural evolutions towards 5G.

Specifically, the analysis addresses the relevance of partial and delayed CQI information in different contexts of use. The challenges studied can be summarized in the following problems:

- Classical 4G LTE architectures:
    - o Study of the proper selection of CQI reporting periodicity as a critical input for the scheduling functions at the 4G LTE eNB, taking into account the characterized CSI patterns.
- Evolved 4G LTE architectures, with centralized functions.
    - o Study of the joint impact of CQI reporting periodicity and CQI delay into the eNB scheduling functions, taking into account the characterized CSI patterns.
- Evolved 4G LTE architectures, with edge computing service instances.
    - o Study of the impact of coarse-grain CSI awareness in edge traffic conforming elements.

Section 6.1 provides further details on the addressed network architectures and the open research challenges.

Section 6.2 presents the selected case studies and the underlying rationale. It must be noted that the previous scenarios would entail a huge number of case studies concerning different types of traffic, scheduling algorithms, etc. Therefore, in this document these scenarios have been mapped to a limited set of four individual case studies.

Finally, Sections 6.3-6.6 present the detailed evaluation of each case study.

6.1 RESEARCH CHALLENGES CONCERNING CSI PATTERNS

In order to illustrate a series of open research challenges identified for study, this section provides a description of each item including a review of the underlying technology and the open issues.

The research challenges have been classified in the following categories:

- Challenge #1: Partially available CSI at eNB.
- Challenge #2: Joint impact of partially available and delayed CSI at eNB.
- Challenge #3: Coarse-grain CSI-awareness in edge computing applications.

6.1.1 CHALLENGE #1: PARTIALLY AVAILABLE CSI AT ENB

Historically, the RRM (Radio Resource Management) functions in cellular networks have evolved towards more user-centric schemes. RRM elements are nowadays able to perform enhanced channel-aware scheduling decisions based on real-time feedback provided by UEs. In this way, cellular networks can meet the objectives of maximizing the efficiency of radio resources while coping with multi-user resource sharing.

As explained in Chapter 2, the evolution of RRM from 3G to 4G broadband mobile networks is mainly based on two aspects:

- The RRM logic is moved towards the radio interface. In 3G UMTS, the RNC (Radio Network Controller) is the element in charge of RRM and controls a series of Node Bs within the RAN. Meanwhile, in 4G LTE the RRM and other functions are placed at the eNodeB with direct access to channel quality feedbacks provided by UEs.
- The TTI (Transmission Time Interval) is reduced to support a quicker reaction to instantaneous channel conditions in the multi-user context. In 3G UMTS the possible TTI values are from 10 ms to 80 ms. It was reduced to 2 ms in the transitional HSDPA technology, and, finally, configured to 1 ms in 4G LTE.

Although the resulting RRM solution maximizes the efficiency of the radio spectrum usage, running optimal RRM functions faces some performance issues. First, using high granularity in CSI feedbacks may overhead the UL channels with signalling information. Second, running advanced scheduling logic at TTI level may entail high computational requirements, with the associated deployment costs.

Focusing on the downlink of a 4G network, LTE radio resources are divided in radio PRBs, which are assigned to multiple users both in time and frequency [Capozzi-2013]. The channel capacity associated to a PRB evolves over time due to the intrinsic variability of the medium. The classical issue in current RAN, including 4G LTE networks, is related to the

problem of how to handle the assignment of shared radio resources among multiple mobile users in order to maximize the overall service experience. As illustrated in Chapter 2, the overall performance of 4G LTE networks is based on CSI. The RI parameters provides information about the preferred MIMO transmission scheme, and the CQI parameter is intended to notify the highest supported modulation scheme and coding rate.

In the last years, the problem of multi-user scheduling in variable channel conditions in heterogeneous contexts has been largely studied [Fouziya-2014]. Most of these works are based on the introduction of service- and channel-awareness in the scheduling function of the eNodeB, considering channel-awareness as fine-grain CQI feedbacks provided by mobile devices.

Channel- aware schedulers keep knowledge about the channel state information of the different users, in order to allocate the required resources and also to introduce fairness aspects in the multi-user problem. In time-varying channel conditions, such schedulers take advantage of the channel awareness or opportunistic gains to improve the performance of the system, e.g. the overall achieved throughput.

However, in real-world deployments, reliable instantaneous channel information will not always be available for each user at every decision slot. Regarding CQI reporting, two significant configuration parameters need to be taken into account:

- The CRR (CQI Reporting Rate), as the number of milliseconds between two consecutive CSI reports generated by a UE. A high periodicity provides better channel-awareness, at the cost of higher signalling overload in uplink channels. On the contrary, lower periodicities may lead to inaccurate channel state estimations at the scheduling decision elements.
    - According to table 7.2.2-1A in [3GPP-TS36213], possible values of CRR values are {2, 5, 10, 20, 40, 80 and 160} ms.
- The CQI delay between CSI report generation and its availability for application at the RRM element. This value is directly related to the HARQ loop time, which depends on the radio transmission time (i.e., the TTI) and the LTE frame processing times at the eNB and UE.
    - Assuming processing times of around 3 ms, the HARQ loop time (and consequently the CQI delay) becomes 8 ms in typical LTE FDD systems [3GPP-TR37901].

Although [3GPP-TR37901] recommends a reporting periodicity of 5 ms for several LTE DL performance tests, the most accurate selection would entail an analysis of the channel variability in different contexts of use.

Therefore, it is interesting to perform a comprehensive study of the most accurate CRR value for different contexts of use, taking into account the different mobility patterns analyzed in Chapter 4 and the obtained CQI patterns.

6.1.2   CHALLENGE #2: DELAYED CSI AT ENB

In the framework of evolved 4G LTE architectures and future 5G mobile networks, different proposals are emerging aimed at overcoming the capacity limitations of current RAN. The concept of Network Sortwarization is being proposed to move some RAN-related functions back to shared HW elements with high computational capacities, taking into account several trends such as SDR (Software Defined Radio), Software Defined Networking (SDN) and Network Function Virtualization (NFV).

In order to identify the impact of Network Sortwarization on the CSI procedure, different proposals and their impact on the standard HARQ procedure need to be understood.

A Centralized RAN system concentrates different processing resources together to form a pool in a central data centre. This aggregation of HW resources in shared locations not only reduces deployment costs, but also leverages low latency connections between different RAN processing units enabling a series of enhanced capabilities such as advanced RRM coordination and interference management [ChihLin-2014]. When these resources run over virtualized infrastructures, adding flexible and scalable HW resource management capabilities, the Centralized RAN becomes a Cloud RAN (C-RAN) [Wu-2015].

According to 3GPP terminology, the higher degree of centralization entails a network architecture where all the baseband processing is made by BBU (BaseBand Units) at centralized data centres, and radio signals are exchanged with the RRH (Remote Radio Heads) over high-speed low-latency connections (making up the mobile fronthaul).

However, as explained in [Rost-2014], the requirements of the fronthaul in terms of high data throughput and low delays makes that this fully centralized solution is only achievable with optical fibre connections nowadays. Since this technology is not available everywhere, and its complete deployment entails costly operations, other alternatives for partial centralization are also considered.

Figure 6.1 illustrates different alternatives for the centralization of RAN functions.

a) fully centralized RAN   b) partially centralized RAN
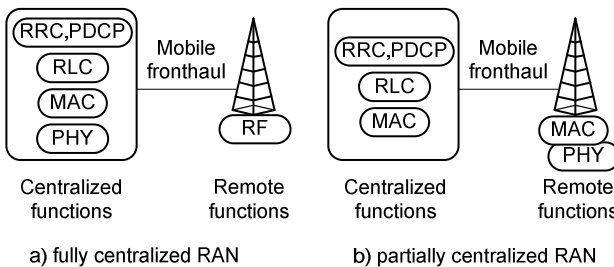
Figure 6.1 – Fully centralized vs. partially centralized RAN.

The NGMN Alliance released a document concerning the fronthaul requirements associated to the centralization of the MAC entity [NGMN-2015]. In order to cope with the typical HARQ timing of 8 ms, only fronthauls of up to 250 μs (in terms of one-way latency) are acceptable. Higher latency fronthauls require the application of HARQ interleaving, in order to delay the HARQ process. In [NGMN-2015], an extra delay for the HARQ process is considered in the range between 1 and 8 TTIs (this is, 1 ms to 8 ms), leading to mobile fronthauls of 0.5 ms to 4 ms of one-way latency. Figure 6.2 illustrates the effect of HARQ interleaving with a fronthaul of 4 ms.
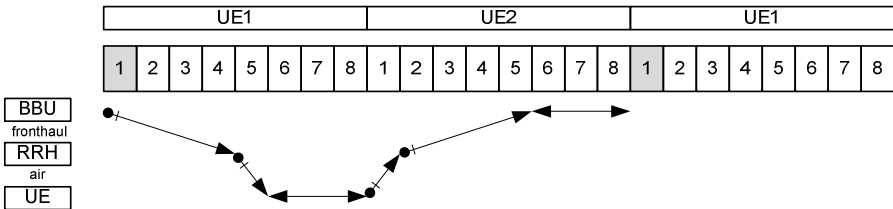
Figure 6.2 – Extra HARQ delay due to interleaving.

Of course, it must be noted that delaying the HARQ process may have an influence in the system performance. A single UE may use up to 8 HARQ processes in order to keep continuous data transmission. Therefore, using HARQ interleaving means that the maximum datarate achievable for a single UE is reduced. The overall system performance could not be affected in multi-user scenarios, since different UEs would fill in the gaps generated in the train of HARQ processes. Moreover, HARQ retransmissions are also affected by the additional delay.

Similarly, the Small Cell Forum performed a comprehensive analysis including other possible splits between centralized and remote functions [SCF-2015_a, SCF-2015_b]. Concerning the MAC-PHY split, the conclusion for the standard HARQ processing is the same than in the NGMN case: fronthauls of up to 250 μs are acceptable. With one HARQ interleave (8 ms of extra delay), fronthauls of 2 ms are acceptable; with two HARQ interleaves (16 ms of extra delay), fronthauls of up to 6 ms may be acceptable (if the influence to single-user performance is accepted).

Additionally, a MAC split is analyzed separating the MAC scheduling functions and the MAC HARQ functions. In this case, the turnaround time of scheduling to HARQ report is the critical parameter for the fronthaul delay requirements, leading to up to 6 ms of one-way latency.

All these technological constraints have also a clear impact in the CSI-driven RRM procedure. Delaying the HARQ process means that the CSI estimation is applied a number of TTIs beyond its reception at the eNB. In this context, it is interesting to analyze from a general perspective how far the RRM functions can be moved from the remote radio units in terms of delay, taking into account the characteristics of CSI previously analyzed.

6.1.3 CHALLENGE #3: NON IDEAL CSI-AWARENESS IN EDGE COMPUTING APPLICATIONS

The current trends towards "cloudification" of the RAN, enabling scalable and flexible centralization of RAN functions, also allows reusing the available HW infrastructure for deploying service instances at the edge of the mobile network. In this way, networked applications could support low latency requirements and accurate CSI awareness, in order to dynamically adapt the service delivery to the current user context.

One of the emerging technologies to cope with more personalized and user-centric service provisioning is the novel Mobile Edge Computing (MEC) industry initiative [MEC-2014], a promising approach to solve these types of problems from an operator-supported approach. This initiative proposes that mobile network operators would provide an API to third-party partners, offering them access to critical characteristics such as location-awareness and network context information. This information may be exploited to develop proximity-enabled services with close-to-zero latency characteristics, in order to optimize the management of future mobile multimedia networks.

Regardless the adopted architecture for C-RAN, MEC-driven service instances must be deployed over the cloud resources available at the RAN. Thus, the degree of coupling between service-level instances and RRM functions may differ, as depicted in Figure 6.3.

a) fully centralized RAN   b) partially centralized RAN
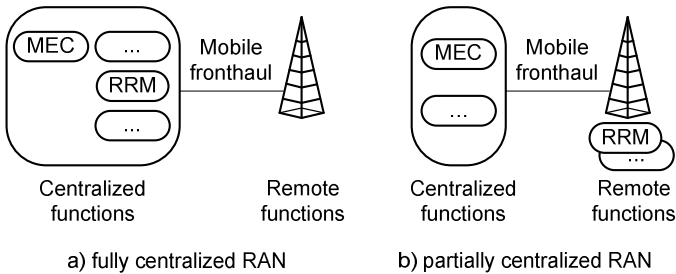
Figure 6.3 – MEC location in fully centralized vs. partially centralized RAN.

In this context, the CSI periodicity made available to the MEC instances is of great relevance. On one hand, a high degree of granularity, similar to the CSI reporting period configured at the UEs, would provide enhanced channel awareness to the applications. On the other hand, this feedback could entail a high data volume in the interface between the cloud RRM function and the MEC instance.

As a result, it seems interesting to study the relationships between the fine-grain and coarse-grain CSI feedbacks, and the impact of the determined CSI patterns in current 4G LTE deployments in this relationship.

6.2 SELECTED CASE STUDIES

From the multiple heterogeneous research targets associated to the identified challenges, in this document four specific case studies are addressed.

Table 5.1 enumerates the selected case studies, their definition and target objectives and the related research challenge.

In order to reduce the number of studies, each case study has been addressed from a standalone perspective, using different CSI patterns, scheduling functions and traffic patterns. Therefore, although the common objective is to analyze the impact of the identified CSI dynamics in different traffic handling functions, all the obtained results must be individually analyzed or must be carefully compared, taking into account the different contexts of use.

Additionally, Table 5.1 includes a citation to different publications where each case study has been detailed, gathering the problem statement and main results of each area.

Table 6.1 – List of Case Studies.

Case Study	Objective	Challenge addressed	Reference
#1: IMPACT OF CSI DYNAMICS ON ENB SCHEDULING FUNCTIONS.	To study the feasibility of using different CRR values with the identified CQI patterns, and its impact on the cell performance with classical eNB scheduling functions.	Challenge #1	[Fajardo-2015_a]
#2: IMPACT OF CSI DYNAMICS ON CENTRALIZED ENB SCHEDULING FUNCTIONS.	To study the feasibility of using different CRR and CQI delay values with the identified CQI patterns, and its impact on the cell performance in novel Centralized RAN architectures.	Challenge #2	[Fajardo-2015_c]
#3: IMPACT OF CSI DYNAMICS ON MOBILE EDGE FLOW SCHEDULING.	To study the macroscopic dynamics of CQI and the feasibility of using lower degree of CQI reporting values in edge computing applications, aimed at: general purpose flow scheduling.	Challenge #3	[Fajardo-2015_b]
#4: IMPACT OF CSI DYNAMICS ON MOBILE EDGE MULTIMEDIA DELIVERY.	To study the macroscopic dynamics of CQI and the feasibility of using lower degree of CQI reporting values in novel multimedia delivery systems based on mobile edge computing.	Challenge #3	[Fajardo-2015_d]

6.2.1 DEFINITION OF CASE STUDY #1: IMPACT OF CSI DYNAMICS ON ENB SCHEDULING FUNCTIONS

In order to evaluate the impact of the obtained channel characteristics into classical LTE scheduling functions, this case study presents the results of introducing the experimental CQI traces into system simulations, instead of using synthetic / simulation-based traces.

For this aim, the analysis deals with the performance of well-known scheduling algorithms such as Round Robin (RR), Best CQI (BC) and Proportional Fair (PF) under the obtained LTE MIMO channel conditions. The three scheduling strategies are somehow channel-aware, since they implement awareness of multi-user CQI values for adaptive modulation and coding.

Specifically, the study focuses on the impact of CRR in a controlled simulation-driven LTE scenario due to the significance of CQI feedback granularity in variable radio channels.

In order to limit the number of parameters affecting the results, UEs have been simulated as greedy sources. In this way, the specific traffic demands do not influence the resource sharing process.

Multi-user simulations are performed with two classes of users. The first class of users follow a channel model based on the RI = 1 and RI = 2 CSI samples obtained in Chapter 5.

6.2.2 DEFINITION OF CASE STUDY #2: IMPACT OF CSI DYNAMICS ON CENTRALIZED ENB SCHEDULING FUNCTIONS

This case study analyzes the impact of moving the resource scheduling logic along the RAN with special focus on the associated inaccuracy in CSI. In order to contextualize the study in real-world deployments, CSI information obtained from live 4G networks is used to analyze the associated radio performance variability.

Several works in the literature aim at analyzing or/and proposing existing or new/enhanced scheduling schemes in the context of partially and inaccurate observable wireless channels (see for example [Ahmad-2014], [Basukala-2010], [Ahmad-2013], [Taboada-2012_a], [Taboada-2012_b], [Schwarz-2013]). However, none of the analyzed works combine the use of real-world CQI values with a comprehensive study of both CQI periodicity and CQI delay parameters.

Therefore, this case study discusses the expected performance in different combinations of CQI delay and CRR. For this aim, a series of simulations have been performed including mobile multimedia transmissions and typical scheduling algorithms, such as RR, BC and PF. Static and mobile users are considered in this case.

6.2.3   DEFINITION OF CASE STUDY #3: IMPACT OF CSI DYNAMICS ON MOBILE EDGE FLOW SCHEDULING

Taking into account several recent research results [Fouziya-2014], flow- and channel-aware scheduling policies are able to maximize the performance in dynamic wireless scenarios such as LTE. Unfortunately most of the advanced scheduling functions proposed in the scientific literature are driven by complex mathematical logic. The associated complexity prevents its implementation in real-world eNodeB elements, which need to determine the multi-user traffic assignments every TTI slot of 1 ms.

This case study focuses on the network-assisted optimization of downlink traffic flows in scenarios with multiple mobile users. Rather than applying complex scheduling logics at the eNodeB elements, this case study analyzes the possibility to deploy user-aware service instances within the C-RAN in order to optimize the delivery of traffic flows based on close-to-the-user channel-awareness (as depicted in Figure 6.3 b). In this sense, this case study deals with a two-round channel-aware scheduling process, comprising an advanced traffic conformance deployed as a MEC instance and a classical scheduler at the eNB RRM module. The former will make use of CG-CQI values for channel awareness, while the latter is able to use the FG-CQI values reported by UEs.

As a reference for performance target, the scheduling policy proposed to drive the cloud-enabled traffic shaping is based on background work [Taboada-2014_a], which defines a near-optimal index policy named Attained Service dependent Potential Improvement (ASPI). ASPI solves the opportunistic scheduling problem for general file size distributions and multiple channel states, restricted to i.i.d. channels and single user transmissions. In this case study, ASPI is applied to multi-user simultaneous transmissions leading to Multi-user Attained Service Potential Improvement (MASPI), and its performance under the obtained CSI patterns is evaluated.

Performance evaluation is made by comparing the delay results of three different architectures:

- eNB running classical scheduling policy aimed at maximizing cell throughput.
- eNB running novel scheduling policy aimed at optimizing mean flow delays.
- MEC function running novel scheduling policy aimed at optimizing mean flow delays together with eNB running classical scheduling policy aimed at maximizing cell throughput.

6.2.4 DEFINITION OF CASE STUDY #4: IMPACT OF CSI DYNAMICS ON MOBILE EDGE MULTIMEDIA DELIVERY

Nowadays, Dynamic Adaptive Streaming over HTTP (DASH) is the predominant technology for multimedia delivery in the Internet, also including the mobile Internet [Seufert-2015]. In general, dynamic content delivery reacts to the specific network conditions based on quick client-driven decisions ([Sieber-2013], [Muller-2012]). However, client-driven adaptations are individually driven and the combined effects of sharing radio resources are not fully considered [Famaey-2013].

Different proposals aim at optimizing the transmission of multimedia content over the Internet by including intelligent nodes within the provision chain ([Grafl-2013], [Bouten-2014]), with special interest in mobile environments. In general, different adaptation points may be available over the provision chain.

In the context of optimal multimedia delivery in 4G mobile networks, different proposals address the need for adding network-assisted adaptation to better cope with the problem of fairness between multiple users [Famaey-2013]. However, network-assisted adaptation elements lack of accurate radio channel awareness, which hinders the optimal delivery of media sessions in 4G networks. Therefore, none of these proposals define the interaction with the resource allocation and scheduling mechanisms of underlying radio networks.

The current evolution aims at including service adaptation capabilities into the 5G cloud-enabled RAN in order to integrate mobile user awareness and enhance adaptation responsiveness [Soldani-2015]. In this way, specific radio performance parameters could be used to drive the optimization process.

This case study focuses on the mobile network-assisted adaptation of media flows in the context of DASH- Scalable Video Coding (SVC) [Sanchez-2011], aimed at maximizing the overall QoE in scenarios where multiple mobile users are accessing multimedia content at the same time through a shared radio access.

In order to achieve this objective, the case study proposes a novel architecture intended to exploit both the content awareness and the user context awareness. This proposal includes a network element, denoted as Mobile Edge-DASH Adaptation Function (ME-DAF), which is located within the C-RAN (Cloud Radio Access Network) [Wu-2015] following the novel MEC (Mobile Edge Computing) principles [MEC-2014]. ME-DAF integrates media caching and QoE-driven traffic conforming capabilities.

As in the previous case study, the interactions of the FG-CQI and GCG-CQI reporting need to be studied, with special focus on the CQI temporal patterns obtained in previous sections.

6.2.5   DEFINITION OF THE SIMULATION ENVIRONMENT

In order to better understand the implications of the observed CQI values at different temporal scales, two types of studies are proposed for each case study:

- First, the possible impact of CQI dynamics into the adaptive scheduling functions is analyzed from a standalone perspective, considering a unique user in the cell with greedy downlink traffic.
- Second, a more comprehensive analysis is performed taking into account the possible effect of different scheduling algorithms in multi-user environments. In this case, system level simulations are carried out to resemble realistic traffic patterns and radio resource sharing schemes.

The suitability of using well-known LTE simulators has been evaluated from different perspectives.

The main advantages of these simulators are:

- They provide comparable and verifiable results.
- They include specific models at different layers of the protocol stack, covering the implications of different protocol configurations.

However, a series of limitations of deficiencies have been detected that dissuade the adoption of any of these LTE simulators:

- The analyzed simulators do not allow a dynamic switching of transmission schemes within a Transmission Mode. A specific MIMO transmission scheme is configured as an input for the simulation, and the number of used codewords is constant all over the simulation.
- The temporal evolution of CQI values obtained in simulations is not even comparable to the CQI patterns identified in Chapter 5.
- CSI information is usually retrieved by the eNB on demand and without properly modelling the CSI process and the effects of the CSI reporting delay.

Figure 6.4 provides a comparative analysis of the effects of the different CSI dynamics into the AMC process. As a simple exercise, the figure illustrates the "expected BLER" as a result of having inaccurate CQI information in the eNB at the time of performing AMC decisions. In other words, transmission errors are directly considered when the CQI available at the eNB for a UE is higher than the actual CQI value experienced by the UE when the DL transmission is eventually received.

Figure 6.4 – Comparative analysis of expected BLER based on the observed FG-CQI.and ns3 simulation traces.

The figure includes the results obtained from three main sources of CQI values:

- FG-CQI values obtained from the LTE emulation tests.
- CQI values logged from ns3 simulator using the Mutual Information (MI) scheme for mapping SNR to CQI.
- CQI values logged from ns3 simulator using the SNR to CQI mapping in [Piro-2011_b].

Based on the characteristics obtained in Chapter 5, two fading patterns are considered: EVA with low Doppler frequency (EVA$_{LD}$) and EVA with high Doppler frequency (EVA$_{HD}$).

As can be observed, there are significant differences between the experimental and the simulation-driven CQI values:

- The effect of increasing the CRR value is more relevant in the experimental traces.
- The effect of increasing the CQI delay is also more relevant in the experimental traces.
- For low Doppler frequency, simulation-driven CQI dynamics are quite stable over CRR and CQI delay. The UE-provided CQI values are much more variable.
- For high Doppler frequency, simulation-driven and UE-provided CQI dynamics are more similar in shape. However, UE-provided CQI values provide lower expected error rates since they result in less variable CQI traces.

As a result of all these issues, a new simulation framework has been implemented from scratch for multi-user performance evaluation. Although the developed simulation

framework has some limitations (e.g. in a proper modelling of HARQ or TCP layers), it is better suited for the analysis of CSI dynamics and their impact on the AMC process.

The basic LTE simulation environment is implemented in MATLAB, and the obtained LTE MIMO CQI traces are configured as input vectors for the event-driven simulation.

The main features considered in the simulation code are the effect of different multi-user scheduling strategies and the effect of retransmissions due to inaccurate channel estimations associated to CRR and CQI delay values.

As typical in current LTE networks, the simulation uses scheduling decisions and transmission slots of 1 ms. Since LTE cells of 20 MHz are assumed, the scheduler needs to determine how to assign a total of 100 PRBs among the different users at each transmission slot. For AMC, the eNB needs also to determine the MCS and the TBS for each user according to [TS36213]. In our case, MCS values directly depend on the reported CQI values.

Application-level data arrives at the eNB following different traffic models. This traffic is placed in a unique DL transmission queue and data segments are transmitted to each UE based on the allocated transmission slots.

Different scheduling algorithms are implemented. Round Robin schemes perform the assignation on PRBs first and the AMC in a second step. However, traffic- and channel-aware schedulers need to include the target MCS and TBS in the PRB assignation procedure.

For a simple modeling of the transmission errors, all the DL transmissions with an MCS value higher than the value associated to the actual CQI are considered erroneous. The affected Transport Block is therefore placed in a retransmissions queue with higher priority to the normal data queue. Consequently, erroneous transmissions are retransmitted in the next available transmission opportunity.

The probability of correctly receiving a retransmission follows the same scheme that initial transmissions. This means that the simulator does not consider the additive reception schemes proposed by modern HARQ schemes.

6.3   CASE STUDY #1: IMPACT OF CSI DYNAMICS ON ENB SCHEDULING FUNCTIONS

The system architecture considered for this case study is illustrated in Figure 6.5, and it includes the classical LTE network elements involving one eNB and one UE.
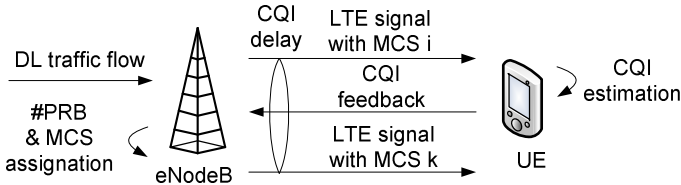
Figure 6.5 – System architecture for Case Study #1.

Figure 6.5 depicts the case where the UE generates a CSI report just after the reception of DL LTE data. Therefore, the CSI reporting follows the same timing of the HARQ process, resulting on 8 ms of CQI delay. This situation resembles both the best case in periodic CSI reporting, where the HARQ answer overlaps with the CSI reporting, and aperiodic CSI reporting, where the eNB may request on-demand CSI reports when required.

Considering the general operation of periodic CSI reporting, the UE will not be always able to provide CSI reports for every consecutive DL transmission, and therefore the CQI value would be further delayed.

Two types of CQI traces have been used in this case study, as illustrated in Figure 6.6. These traces have been generated following the methodology presented in Chapter 5, and using the same SNR profile for the AWGN pattern.

Both traces resemble a user moving from the edge to the centre of an LTE cell, and going back to the cell edge. The difference between the traces resides in the fading channel associated to the experiments.

The upper plot in Figure 6.6 resembles a mobility pattern with aggressive fading pattern, represented by Extended Vehicular A with High Doppler frequency (EVA_{HD}). Meanwhile, the lower plot in Figure 6.6 resembles a mobility pattern with lower speed, represented by Extended Vehicular A with Low Doppler frequency (EVA_{LD}).

As can be observed, EVA_{HD} results in decreased channel quality, providing lower CQI values. While EVA_{LD} reaches the maximum CQI at the cell centre, EVA_{HD} is not able to provide these high channel quality states. Additionally, it must be noted that EVA_{LD} is associated to less variable CQI values.
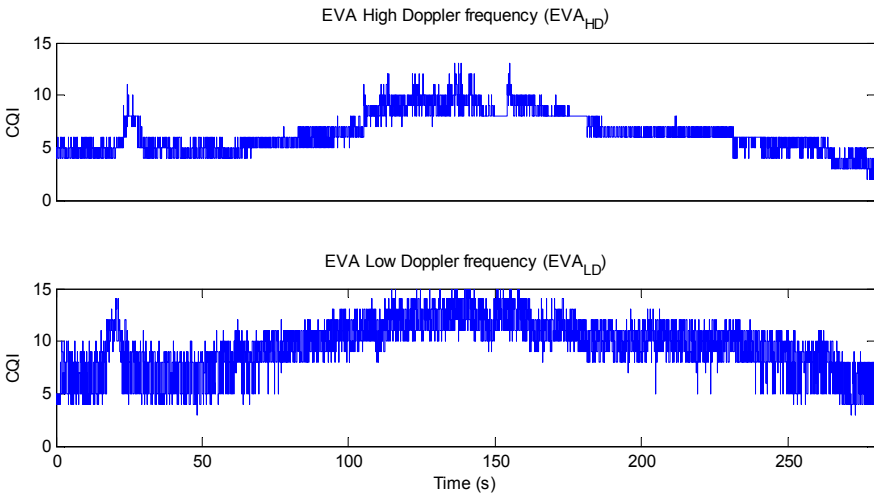
Figure 6.6 – CQI traces for Case Study #1.

6.3.1   SINGLE USER ANALYSIS

First of all, the reference performance achievable by a single user is evaluated by simple processing of the CQI traces. This case assumes that only one UE is served by the eNB, and that the UE behaves as a greedy consumer of traffic. Therefore, the UE would receive the maximum amount of data allowed by the channel quality at every TTI.

In this way, the results are based only on the characteristics of the CQI traces (for both EVA_{HD} and EVA_{LD}) and the intrinsic behaviour of the LTE technology.

As a first step, the analysis focuses on the ratio of TTI slots where a HARQ NACK can be estimated. For simplicity, a HARQ process is assumed to provide error if the CQI estimation available at the eNB is higher than the actual values in the CQI trace. This assumption would mean that the eNB assigns the maximum MCS associated to the UE-reported CQI, and that every transmission with an MCS higher than the supporter MCS results in a transmission error. On the contrary, every transmission with an MCS lower or equal to the supporter MCS would result in an error-free transmission (instead of the 10% of BLER rule).

In order to capture the impact of the CQI dynamics, different values of CRR and CQI delays are considered:

- CRR = [2, 5, 10, 20, 40, 80, 160] ms
- CQI delay = [1, 4, 8] ms

It must be noted that the first two values of the CQI delay parameter are not possible in real-world LTE FDD deployments where the CQI delay is configured to 8 ms. However, these data sets are interesting for comparison of the ideal situation with the actual one. A CQI delay of 1 ms means that the eNB is able to get the CQI value generated by the UE immediately without further processing or transmission delays. Increasing the CQI delay to 4 ms takes into account DL and UL transmission times of 1 ms, and processing times of 1 ms at both the eNB and the UE.

Additionally, two CQI reporting schemes are evaluated. On one hand, "CQI value" represents the case where the instantaneous CQI value is reported by the UE. On the other hand, "CQI median" means that the UE reports the median CQI value during the CRR period.

Figure 6.7 gathers the obtained results, gathering the average ratio of estimated HARQ NACK for each combination of values.
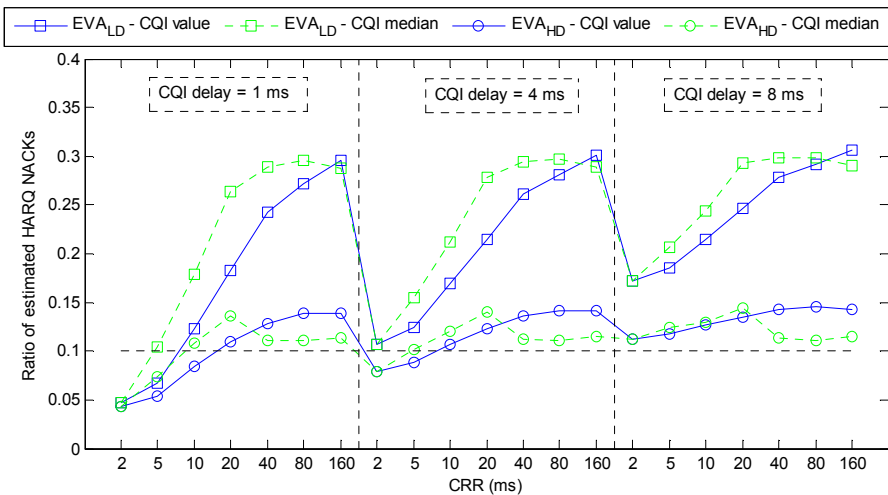
Figure 6.7 – Expected BLER for Case Study #1.

In a general sense, it can be observed how EVA_{HD} traces result in lower error ratios compared to the EVA_{LD} traces. This effect seems to be a direct consequence of lower CQI variability of the EVA_{HD} trace, likely associate to a more conservative assignation of CQIs at the UE,

Taking into account the results of Chapter 4, periods with RI=1 are generally more probable with fading patterns with low Doppler frequencies and higher CQI values, while RI=2 becomes more probable with higher Doppler frequencies and lower CQI values. Therefore, as a general remark, results seem to confirm that higher CQI values are associated to higher error rates.

Concerning the CRR value, it can be observed that error ratios increase with the CQI reporting periodicity when instantaneous CQI values are reported. However, this trend is decreased and even inverted after CRR = 20 ms when median CQI values are used.

Regarding the evolution of expected errors with the value of CQI delay, it must be noted that the more variable channel only provides accurate values at low CRR values (below 10 ms of periodicity) even at the ideal CQI delay of 1 ms. For the typical value of 8 ms, a direct AMC mapping would provide theoretical error rates beyond 15% even for almost instantaneous reporting (CRR = 2 ms). Less variable channels result in estimated error rates between 10% and 15% for the whole set of CRR values, supporting the use of high CRR.

Beyond this simple estimation of HARQ NACKs, an analysis of the lost transmission opportunities provides a better understanding of the impact of the CQI patterns on AMC outcomes. For this aim, different throughout-related metrics are introduced:

- "Error throughput", as the throughput associated to the whole set of TBS that need to be retransmitted due to HARQ NACKs, i.e., due to overestimation of CQI.
- "Wasted throughput", which is the throughput associated to the difference between the TBS associated to the estimated CQI and the TBS that could be actually transmitted according to the current channel status. In other words, it is the throughput lost due to underestimation of CQI
- "Lost throughput", defined as the aggregation of the "error throughput" and the "wasted throughput".

Figure 6.8 presents the obtained results in terms of ratio of the total "effective throughput", which is the data rate eventually received by the UE for instantaneous CQI reporting.
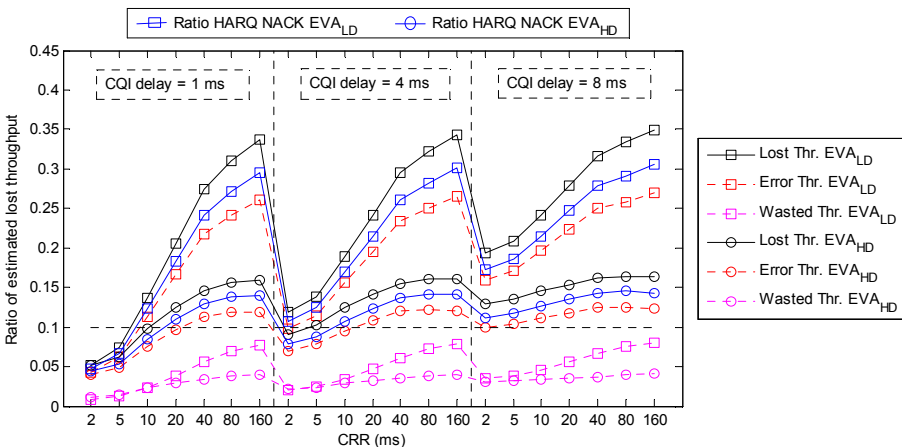
Figure 6.8 – Expected wasted throughput for Case Study #1.

In addition to the different throughput metrics, Figure 6.8 also includes the ratios of estimated HARQ NACKs as a reference.

In general, the main contribution to the "lost throughput" is the "error throughput" and the "lost throughput" is slightly superior to the ratio of HARQ NACKs, especially at high CRR values.

6.3.2   MULTI-USER SIMULATIONS

In order to evaluate the impact of the obtained channel characteristics in multi-user contexts, this section presents the results of the introduction of experimental CQI traces into the analysis of LTE eNB scheduling strategies.

For this aim, this section analyzes the performance of well-known scheduling algorithms under the obtained LTE channel conditions. Specifically, two classes of users are configured regarding the channel characteristics: the first class of users follow the obtained EVA_{LD} channel trace and the second class of users follow the obtained EVA_{HD} channel trace.

All the users are configured with LTE MIMO using RI=2 continuously (up to ~150 Mbps in DL).

In this case, the CQI delay parameter is fixed to 3 ms, caused by the CQI measurement at the UE side, the CQI feedback transmission and the CQI processing at the eNodeB, and the analysis focuses on the impact of CRR in a controlled simulation-driven LTE scenario.

Table 1.1 summarizes the main simulation parameters used in this case study.

Table 6.2 – Simulation parameters for Case Study #1.

Parameter	Value
Transmission Time Interval (TTI)	1 ms
Number of Resource Blocks (PRB)	100
LTE Transmission Mode	MIMO OLSM
Traffic model	Greedy sources
Scheduling algorithms	BC, RR, PF (w = 100 ms)
CQI Reporting Rate	2, 5, 10, 20, 40, 80, 160 ms
CQI delay	3 ms
Number of UEs	20 UEs, in two classes
Channel model	EVA_{LD}, EVA_{HD}
Simulation length	1,000 s

The scheduling policies used in the experiments are:

- RR (Round Robin): With this discipline, the RBs are fairly shared among users.
- BC (Best CQI): This policy assigns RBs fairly among the users with the estimated highest instantaneous CQI.
- PF (Proportional Fair): This discipline consists in assigning RBs fairly among the users with the highest ratio of the estimated current transmission rate and the current averaged throughput for a window of 100 ms (without taking into account retransmitted bits).

Simulations are performed for 1,000 s of length, considering 20 greedy traffic sinks in the cell, each traffic source corresponding to a mobile user. 10 UEs follow the EVA$_{LD}$ channel and 10 UEs follow the EVA$_{HD}$ channel

The focus of the study is the achievable aggregated cell throughput, as a measure to evaluate the performance of the different scheduling strategies under the described LTE channel characteristics and CRR configurations.

First, Figure 6.9 analyzes the results for the aggregate values taking into account the two considered classes of users.

Left-graph in Figure 6.9 shows the results for the effective throughput, which refers to correctly transmitted data (without taking into account retransmissions). The right-graph of Figure 6.9 illustrates the total amount of traffic used in the cell for retransmissions due to inaccurate channel estimations at the eNodeB.
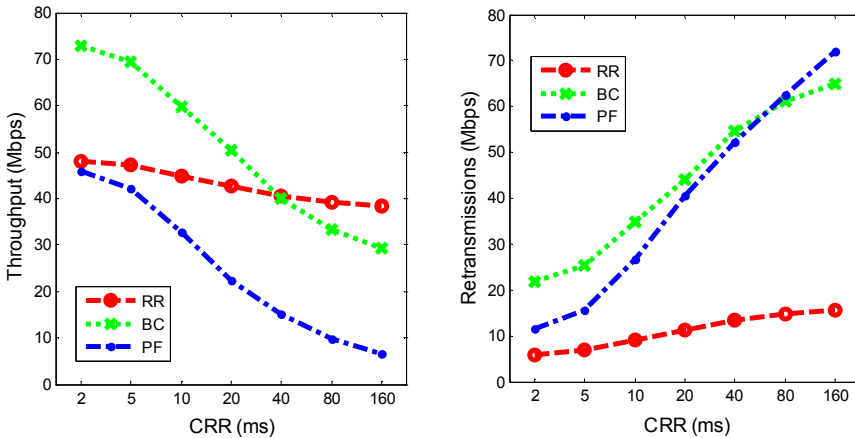
Figure 6.9 – Effective throughput (left) and wasted throughput caused by retransmissions (right).

As can be observed, channel-aware disciplines exhibit severe degradations as CRR increases, while RR shows a more stable performance. Furthermore, it is clear that channel-aware policies cause more retransmissions than RR; with a notable increase with the CRR value.

This effect is mainly associated to the inherent behaviour of the analyzed schedulers. Channel-aware schedulers prioritize the transmission of traffic associated to users with high CQI values. However, those channel states exhibit more variability and the probability to transit to channel states with lower CQI is high. As a result, the eNodeB would overestimate the transmission capacity for those users leading to higher error probability in the transmissions. In the case of RR, users are selected regardless their channel condition. As cited before, users with lower CQI values are associated to less variable channel states, thus leading to lower transmission capacity but lower error probability.

As a result, the overall performance of BC provides higher bitrates in the lower CRR values (up to CRR=20 ms) and exhibits more severe degradations for higher CRR values where the probability of inaccurate CQI estimations increase.

Beyond aggregate cell performance values, Figure 6.10 illustrates the throughput results of the two classes of users; the left-graph belongs to users in better channel conditions (EVA_{LD}) and right-graph belongs to users in worse channel conditions (EVA_{HD}).

EVA_{LD} results in higher CQI values compared to the EVA_{HD} channel model. The left-graph shows the prominent improvement of BC for the class of users in good channel conditions, while users in bad channel conditions are penalized. In these conditions, RR behaves as the fairest scheduler and the most reliable against high CRR values.
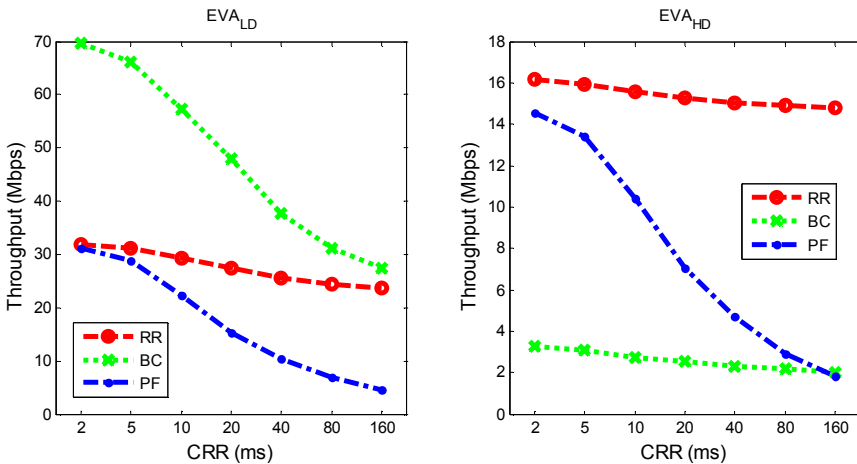
Figure 6.10 – Per-class effective throughput.

6.4 CASE STUDY #2: IMPACT OF CSI DYNAMICS ON CENTRALIZED ENB SCHEDULING FUNCTIONS

The system architecture considered in this case study is illustrated in Figure 6.11, including the split of the eNB into BBU and RRH elements and the mobile fronthaul. As can be observed, the CQI delay adds the latency associated to the fronthaul segment both in the UL and DL directions. The rest of the LTE operation is similar to the Case study #1.
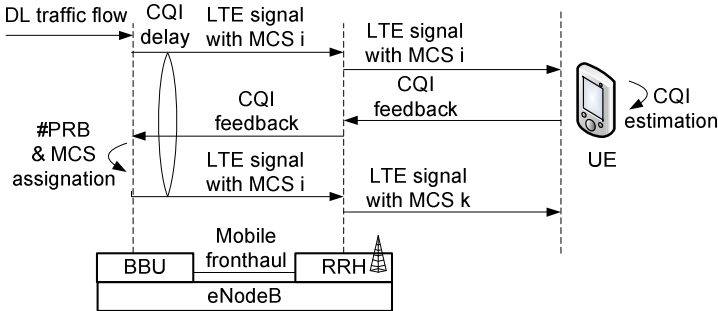
Figure 6.11 – System architecture for Case Study #2.

Figure 6.12 illustrates the specific CQI traces used in this case study.
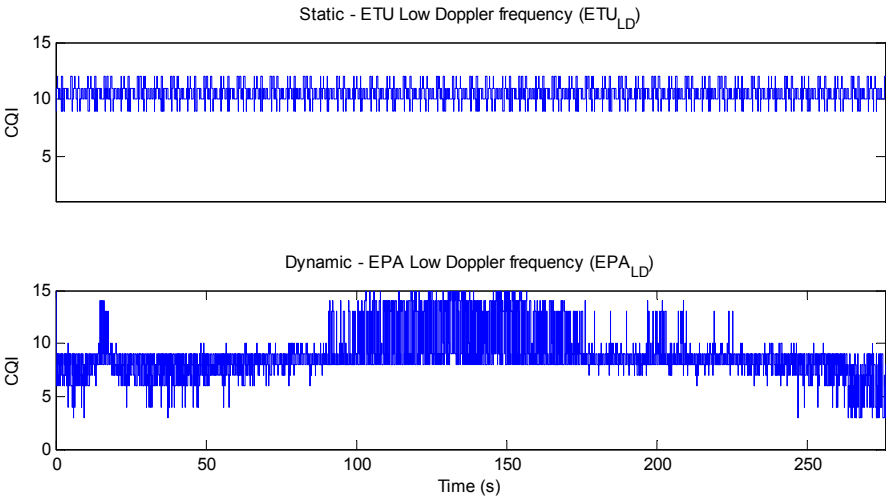
Figure 6.12 – CQI traces for Case Study #2.

Two types of CQI traces have been used in this case study, which have been generated following the methodology presented in Chapter 5. A first CQI trace is based on modelling a static user, with a fixed SNR value and Extended Typical Urban fading channel with low Doppler frequency (ETU$_{LD}$). In this case, the obtained CQI values vary between 9 and 12. Besides, a mobile user is characterized following the same SNR profile for the AWGN pattern as in Case Study #1, but applying an Extended Pedestrian A fading model with low Doppler frequency.

6.4.1   SINGLE USER ANALYSIS

Similarly to Case Study #1, the maximum performance expected for an individual user is evaluated through the inspection of CQI traces. Therefore, both traces have been sampled at CRR intervals and delayed by CQI delay in order to generate the estimated CQI value at eNB. Afterwards, this CQI value is compared to the actual CQI value available at the corresponding TTI in order determine if a transmission is assumed as error-free or erroneous due to the variable channel conditions.

Besides the CQI delay values analyzed in Case Study #1, this case study introduces two new CQI delay values for evaluation. The complete set of CQI delay values are listed in Table 6.3:

Table 6.3 – CQI delay values in Case Study #2.

CQI delay	Description
1 ms	Ideal case, where the UE is assumed to generate the CQI value without further processing delays and the eNB is assumed to obtain the CQI value immediately.
4 ms	Almost ideal case, where the processing delays at UE and eNB are reduced to 1 ms.
8 ms	Typical LTE procedure, with 8 HARQ processes and 8 ms of HARQ delay. No fronthaul delay is considered.
16 ms	Standardized LTE procedure with HARQ interleaving, The fronthaul supports one-way delays of up to 4 ms.
24 ms	Standardized LTE procedure with two HARQ interleaves, The fronthaul supports one-way delays of up to 8 ms.

The expected HARQ NACK ratios obtained are presented in Figure 6.13. For simplicity and clearness, the values corresponding to CRR 2 ms and 5 ms have been omitted.
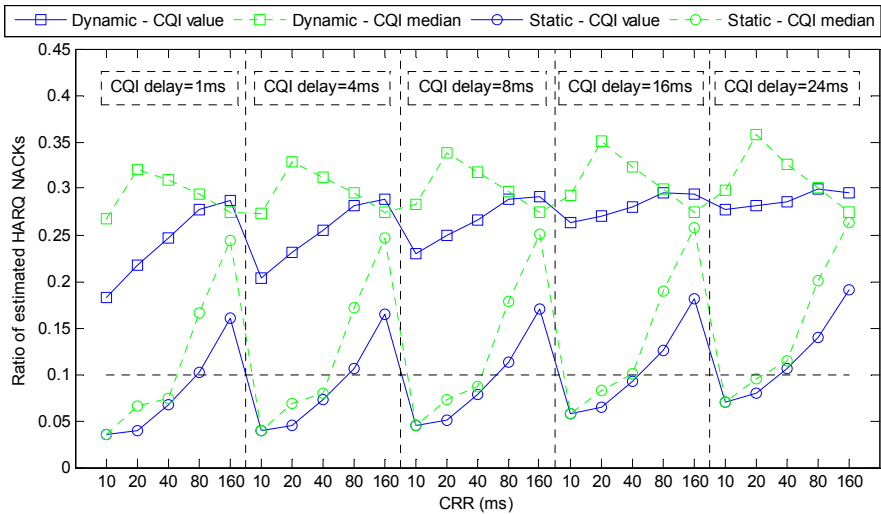
Figure 6.13 – Expected BLER for Case Study #2.

Compared to the CQI traces used in Case Study #1, it is noted that EPA_{LD} behaves very similarly to EVA_{LD} for both instantaneous and median CQI reporting. On the contrary, the considered static pattern exhibits a more gradual evolution of the error ratios over the different CQI delay values.

Regarding the EPA_{LD} trace, the two new CQI delay values introduced to consider different fronthaul latencies are very similar, with expected error ratios between 25% and 30% assuming direct AMC operation.

Regarding the static ETU_{LD} trace, results indicate a progressive increment in the expected HARQ NACKs with the CQI delay. Focusing on the last three values, the overall conclusion is that using one HARQ interleave (extra 8 ms in the HARQ loop) introduces around 1.5% of additional error rate due to the dynamics of the CQI values. Meanwhile, two HARQ interleaves (extra 16 ms in the HARQ loop) results in around 3% of additional error rate due to the dynamics of the CQI values.

It must be noted that these results are associated to greedy traffic sinks, since users receive the maximum achievable amount of data at every TTI. For the analysis of individually achievable throughputs, the limitations in the number of HARQ processes should be taken into account. Additionally, more realistic simulations are presented in Section 6.4.2, considering multi-user scenarios with specific traffic patterns.

6.4.2 MULTI-USER SIMULATIONS

This section evaluates the impact of the analyzed CQI channels in multi-user scenarios, with more realistic traffic demands. Specifically, multimedia traffic patterns have been used for this study. As in the previous case study, the overall performance is evaluated in terms of achieved throughput for each type of user. Additionally, this section introduces a multimedia quality metric in terms of the ratio of correctly received media segments. From simulation results, the best performing scheduler can be identified for different CQI configurations and different user mobility patterns.

The simulation framework is the same as in Case Study #1, taking the CQI traces as inputs for the channel state in the simulations. Table 6.4 gathers the main simulation parameters for this case study. The simulation time for each test point is 1,000 s. All the users are served by a unique LTE cell of 20 MHz operating at high load. In this case, all the UEs are configured to use SISO transmissions in order to reduce the number of users required.

Table 6.4 – Simulation parameters for Case Study #2.

Parameter	Value
Transmission Time Interval (TTI)	1 ms
Number of Resource Blocks (PRB)	100
LTE Transmission Mode	SISO
Traffic model	Multimedia traffic based on sequence of media segments: • GOP = 2 s • Poisson-distributed arrivals Four media flows: • Encoding bitrate = {100, 300, 650, 1700}kbps • Pareto-distributed segment sizes
Scheduling algorithms	BC, RR, PF (w = 1 s)
CQI Reporting Rate	2, 5, 10, 20, 50 ms
CQI delay	2, 10, 20, 40 ms
Number of UEs	17 UEs
Channel model	Dynamic mobility pattern: EPA_{LD} Static mobility pattern: four classes, based on ETU_{LD}
Simulation length	1,000 s

In this section, traffic demands are based on continuous media sessions of variable bitrate. Each media session can be made up of up to four media flows, which are characterized by their average encoding bitrates. In order to consider a wide range of multimedia services such as radio, music, Standard Definition video and High Definition video, media sessions range from 100 kbps up to 1.7 Mbps.

According to the modern DASH transmission scheme, each media session is composed of a series of media segments, which are transmitted consecutively over time for media continuity. For instance, every Group of Pictures (GOP) in an encoded video results in one different media segment. Assuming variable bitrate flows, media segments of different media sessions are characterized by their size distribution and arrival process. Specifically, four types of media flows are considered for each UE, with average bitrates of 100 kbps, 300 kbps, 650 kbps and 1.7 Mbps respectively. Media segments of each session arrive according to a Poisson process with a mean rate λ of 2 s. The size distribution of media segments for the aggregate of the four media sessions follows a Pareto distribution with a mean of 170 KB (scale parameter = $2.292 \cdot 10^{-7}$ and shape parameter=3.974).

Media segments are generated in different media sources and arrive at the RRM element in their path towards the destination mobile user. These media segments are enqueued, and the RRM scheduler decides how many bits are selected to transmit to each user in each TTI.

Regarding the LTE scheduling policies, the same descriptions as in Case Study #1 apply here. For Proportional Fair, it must be noted that the window for averaging the transmitted throughput is increased to 1 s in this case since the overall DL data rates are considerably lower. Another specific feature in this case study is that schedulers implement some kind of flow awareness through a flow-driven discard timer. It is assumed that a media segment should be downloaded on time for its smooth playout [Hossfeld-2012]. Otherwise, it is useless to continue with the transmission of those segments. In this way, media segments that are not fully transmitted before 10 s are discarded [3GPP-TS26247].

With the purpose of analyzing the joint impact of the CRR and the CQI delay in radio resource allocation, five CRR values (2, 5, 10, 20, 50; in ms) and four CQI delay values (2, 10, 20, 40; in ms) are considered in the study.

Case Study #2 deals with two scenarios. First, the "dynamic scenario" involves a series of users following the EPA$_{LD}$ channel pattern with random start point. A second "static scenario" includes four classes of users, randomly associated to one of four different channel traces. The different CQI channels are generated from the ETULD channel, directly applying a constant offset to the CQI values. Figure 6.14 depicts the different channels.
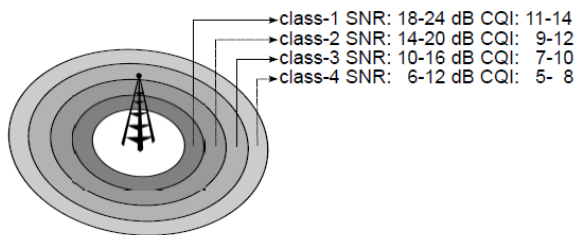
Figure 6.14 – Artificial CQI channels for the "static scenario".

In order to study the performance of the scheduling algorithms under severe congestion settings, high network loads with 17 users are considered.

For each scenario, the performance analysis is made for the considered combinations of CQI delays/CRRs and for the three scheduling algorithms. First, the performance is gauged in terms of "effective throughput", which refers to the rate associated to the received media segments, and the "error throughput", as the wasted throughput due to HARQ retransmissions. Second, the percentage of received media segments is evaluated as a critical metric for multimedia quality assessment.

- **"Dynamic scenario"**

In this first family of simulations all the users in the cell follow the same channel distribution, which corresponds to the variable SNR joint with the EPA$_{LD}$ fading profile. Figure 6.15 shows the aggregated performance results in terms of effective throughput for the different scheduling policies, CRR and CQI delay values.
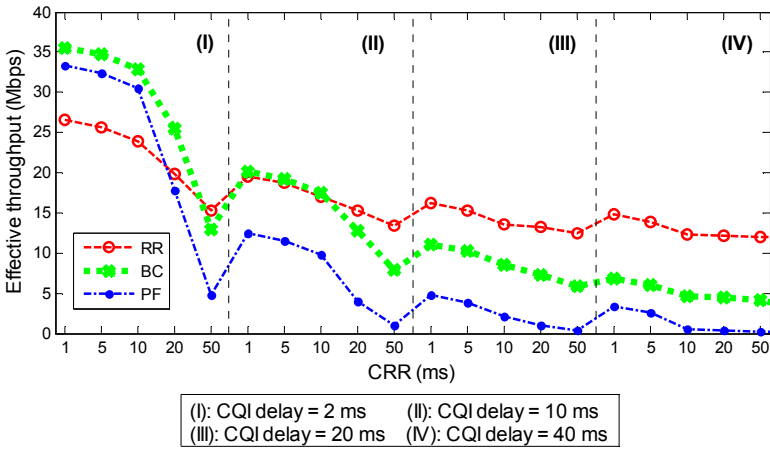
Figure 6.15 – Effective throughput for the dynamic scenario.

In general, opportunistic policies outperform RR for CQI delay = 1 ms until CRR = 20 ms. However, the decrease of throughput as CRR and CQI delay increases is relevant for BC and PF. On the other hand, the throughput deterioration for CRR=50 ms is remarkable for the first two CQI delay values.

For CQI delay close to the standard HARQ time, BC and RR exhibit similar behaviours up to CRR = 10 ms. For higher CQI delays, RR provides a more stable performance. Of course, these results are only valid for a single-class, where all users share channel characteristics

For higher CQI delays, RR provides a more stable performance. Of course, these results are only valid for a single-class, where all users share similar channel characteristics. Figure 6.16 shows the wasted throughput due to retransmissions. It is worth mentioning that BC and PF cause fewer retransmissions than RR in the lowest CQI delay considered until CRR=10 ms. Nevertheless, for the rest of analyzed points the worsening of those two channel-aware policies in this wasted throughput terms is notable.
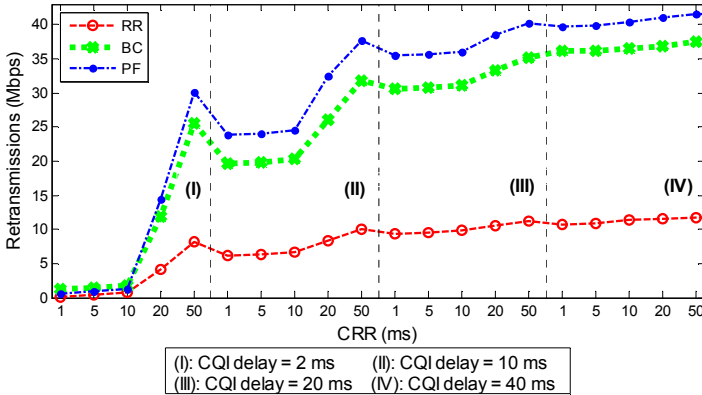
Figure 6.16 – Wasted throughput caused by retransmission for the dynamic scenario.

As depicted in Figure 6.17, similarly to the presented behaviour for the effective throughput, BC outperforms RR in the percentage of received media segments in the first CQI delay range until the CRR is 20 ms. Nonetheless, RR achieves the highest multimedia quality in the remaining combinations.
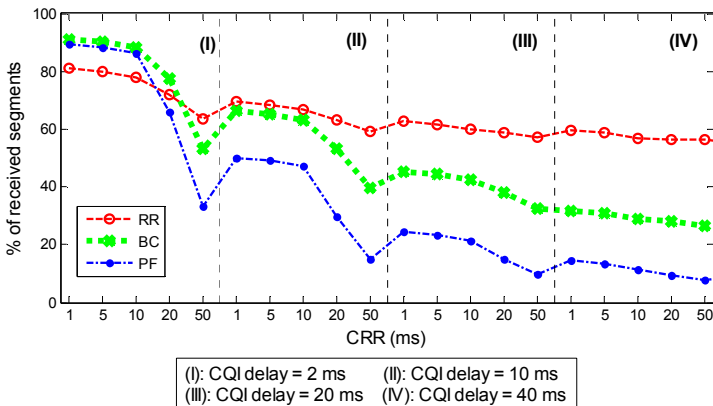
Figure 6.17 – Percentage of received media segments for the dynamic scenario.

- **"Static scenario"**

This scenario analyzes the performance of the proposed schedulers under less variable channel models. Furthermore, this is a multi-class setting in terms of CQI, where user classes would differ due to the UE location in the cell. Under low mobility conditions, Figure 6.18 shows that BC is the best candidate in terms of effective throughput for the whole set of CQI delays/CRRs, and achieves less severe degradations among CQI delay ranges in comparison with the previous scenario. As shown in Figure 6.19, the throughput wasted due to retransmissions is generally lower in this scenario.
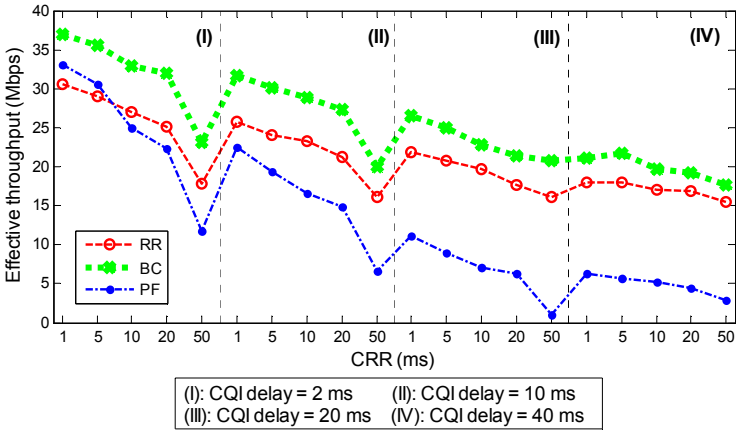
Figure 6.18 – Effective throughput for the static scenario.
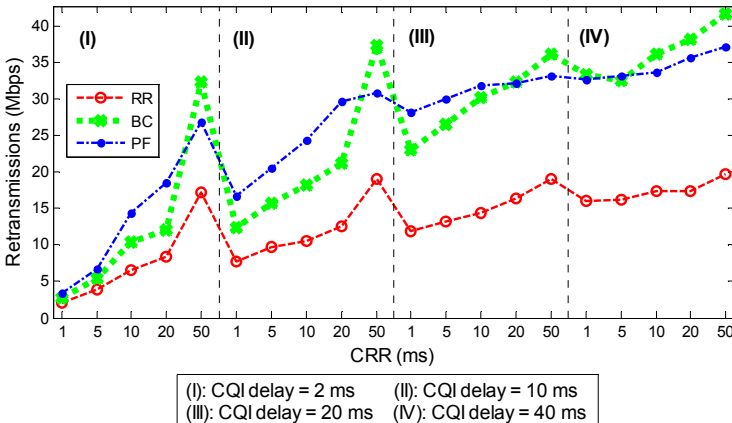
Figure 6.19 – Wasted throughput caused by retransmissions for the static scenario.

Besides, Figure 6.20 summarizes the per-class behaviour in received media segments terms for each scheduling discipline.

From the plots of the different policies it can be observed that RR and PF are remarkably fairer between classes than BC. However, for BC in the first two CQI delay ranges, except for CRR=50 ms, the percentages of received media segments for the best two classes are extraordinary (for the best class in all the analyzed points). Therefore, when choosing among schedulers, it would depend on the degree of fairness it is expected to achieve.
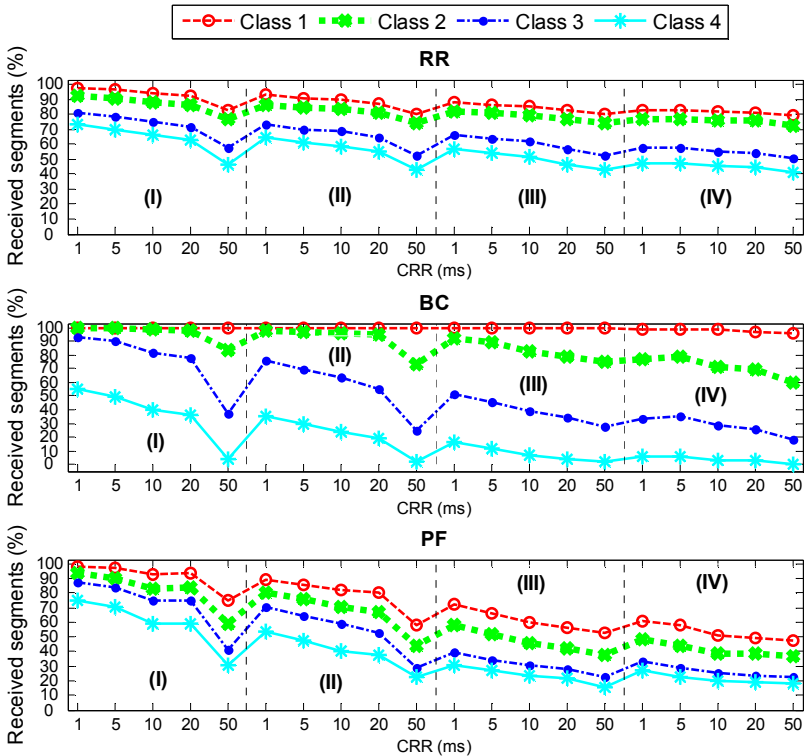
Figure 6.20 – Percentage of received media segments for the static scenario.

6.5   CASE STUDY #3: IMPACT OF CSI DYNAMICS ON MOBILE EDGE FLOW SCHEDULING

In order to implement the mobile edge computing functionalities proposed for Case Study #3, a new functional element is introduced and denoted as Mobile Edge Scheduler (MESch), aimed to handle with the DL traffic within the MEC architecture. Figure 6.21 illustrates the overall network architecture proposed for this case study.
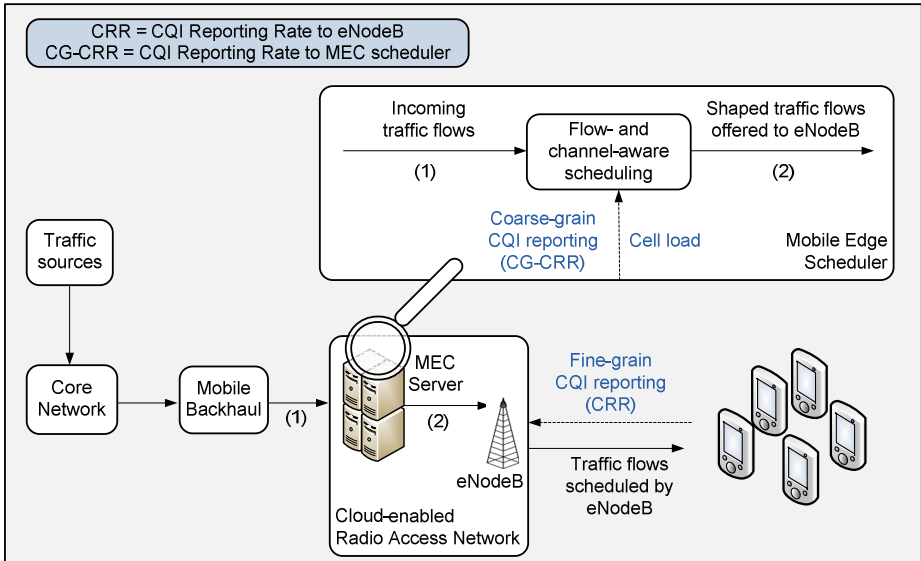
Figure 6.21 – System architecture for Case Study #3.

From a general perspective, it is assumed that a number of Internet traffic sources deliver traffic flows towards the mobile end users following arbitrary flow distributions. These flows traverse the Internet segments and the mobile backhaul before arriving at the RAN. In emerging C-RAN architectures, Internet applications would be able to gather users' channel feedbacks to some extent in order to optimize their traffic delivery to mobile users.

As illustrated in Figure 6.21, the key element in the MEC industry initiative is the MEC Server, which is integrated into the mobile operators' RAN in order to provide value-added capabilities to third party developers [MEC-2014]. In the case of LTE, the MEC Server is directly integrated into the eNodeB. The MEC Server is based on cloud computing principles to run third-party applications over a common hardware infrastructure. These applications may range from lightweight monitoring instances, which would provide relevant RAN-

related information to optimize external OTT servers, to more complex applications, intended to handle and modify the traffic to/from the mobile users at RAN level.

Upon this MEC Server element, the proposed MESch is deployed as an intelligent node aimed at optimizing the traffic delivery to multiple mobile users. MESch is included in the service provisioning chain, enabling the required flow awareness concepts. At the same time, MESch interacts with the MEC Server in order to retrieve cell and user context information, such as the cell load or per-user radio performance statistics.

 MESch implements a flow- and channel-aware scheduling policy in order to maximize the service experience. This module combines flow awareness, user context awareness and cell status awareness, in order to run the required intelligent scheduling logic. The output of MESch can be seen as a series of decomposed traffic flows, properly segmented in chunks according to the optimization logic and being forwarded to the eNodeB for its delivery to the end users. Thus, the eNodeB will run a more basic scheduling logic at TTI level and making transmission decisions based on the updated channel feedbacks reported by the mobile devices. The whole operating mode, with two concatenated scheduling functions with non-ideal shared channel awareness, entails a series of limitations to be analyzed.

The MEC API is the designated interface for retrieving cell statistics and individual channel quality information through the Radio Network Information Services (RNIS). In multi-user scenarios, the CQI feedback granularity may entail a high load in the interface between MEC Server and MESch. Thus, a coarse-grain feedback statistic is defined in Figure 6.21 as CG-CRR. The suitable value of this CG-CRR is one of the open issues evaluated in this case study.

In this case study, all the users are associated to the same CQI trace according to the mobile pattern with EVA_{LD} as described in Case Study #1. Figure 6.22 illustrates this CQI trace, and one example of sampling these CQI values with averaged values at one second periods.
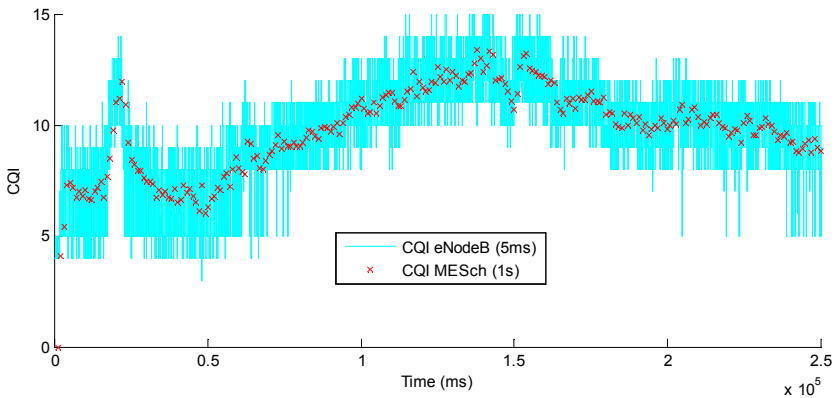
Figure 6.22 – CQI traces at eNodeB and MESch for Case Study #3.

6.5.1 SINGLE USER ANALYSIS

As a first exercise, Figure 6.23 shows the outcomes of applying the delayed CQI estimations at CG-CRR level compared to the actual CQI values in the EVA$_{LD}$ radio channel. In this example, CG-CQI values are generated by double sampling process. First, the UE feedbacks the median CQI values with CRR = 5 ms, and the eNB generates a CG-CQI value at CR-CRR = 1 s by simply copying the instantaneous available CQI value.

The effects of inaccurate CQI estimation are just gauged in terms of expected achievable throughput and actually achievable throughput. Since greedy traffic sinks are used for single-user analysis, this difference of throughputs is computed for the whole train of TTIs and the average difference value is obtained.

In Figure 6.23, the average differential throughput over the whole CQI trace is plotted as a single point. For each CG-CRR value, a total of 50 points are represented associated to different initial TTIs within the trace. Additionally, the average of all results is illustrated for the positive values and for the negative values.

As can be observed, the overall trend is that increasing the CG-CRR leads to higher average miss-estimations of the available throughout, and especially to higher variance in the results.
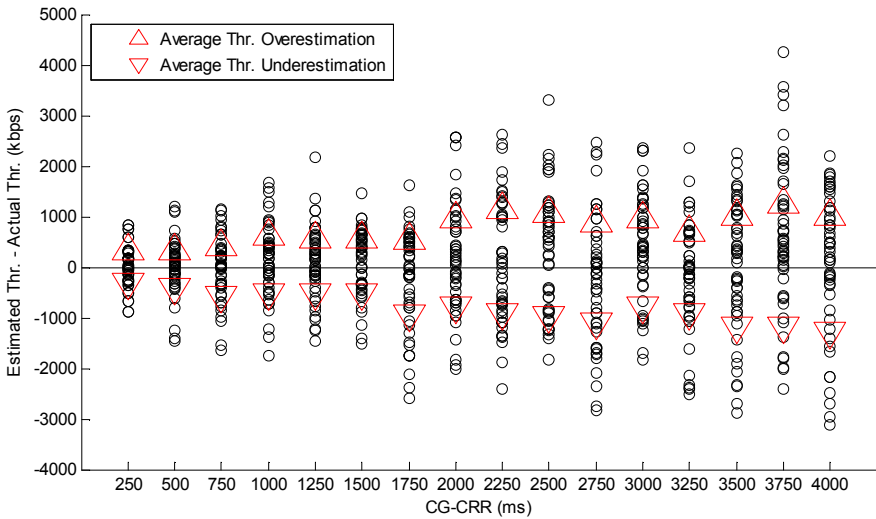
Figure 6.23 – Average throughput miss-estimations for EVA$_{LD}$ and CG-CRR based on instantaneous CQI values.

Positive average values mean that the achievable throughput estimated by MESch is higher to the actual achievable throughput, and therefore the eNB would need to cope with traffic demands that cannot be allocated to the mobile user. Negative average values mean that the estimated throughput values at MESch are lower than the achievable throughput due to the channel quality, and therefore some radio capability would be unused in average.

Figure 6.24 illustrates the average miss-estimations in terms of throughput for both instantaneous and median CG-CQI values. In this case, median CG-CQI values are generated by computing the median value of the CQI values available at the eNB over 1 s period, which at the same time are median values of the UE-generated instantaneous CQI values over 5 ms periods.

In Figure 6.24, throughput miss-estimation is defined as the average of the absolute values of the average throughput resulting from each individual test, regardless they are overestimations or underestimations. It must be noted that throughput estimations are carried out for LTE users with MIMO transmission scheme and direct CQI to MCS mapping.

As can be observed, median CG-CRR values provide better estimations than individual CG-CRR values, enhancing the performance in almost 50% in many CG-CRR values. These results are in line with those found in the previous case studies, where instantaneous CQI values provided better performance only for low CRR values.
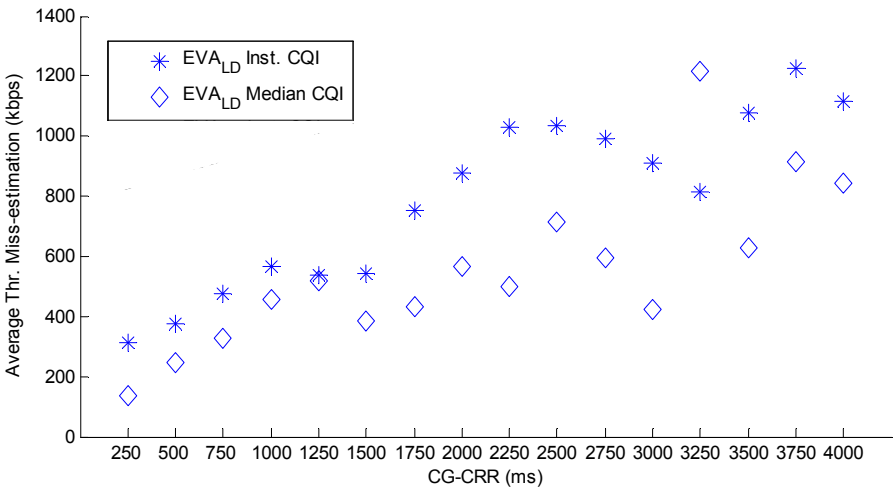
Figure 6.24 – Average throughput miss-estimations for EVA$_{LD}$ and CG-CRR based on instantaneous and median CQI values.

In order to better understand the impact of these average throughout miss-estimation values over the total throughput, and to better capture the dynamics of the miss-estimations over the whole CQI trace, Figure 6.25 represents the outcomes of two different experiments. Both experiments are carried out over the same EVA$_{LD}$ pattern, with LTE MIMO and CG-CRR = 1s; the only difference the initial TTI to start generating the median CQI values at CRR and CG-CRR.

At steps of 1 s, Figure 6.25 illustrates the average achievable DL throughput according to the actual channel CQI ("Actual Thr." in blue), the estimated achievable DL throughput according to the latest available CG-CQI ("Estimated Thr." in purple), and the instantaneous difference between both values ("Miss-estimation" in black).
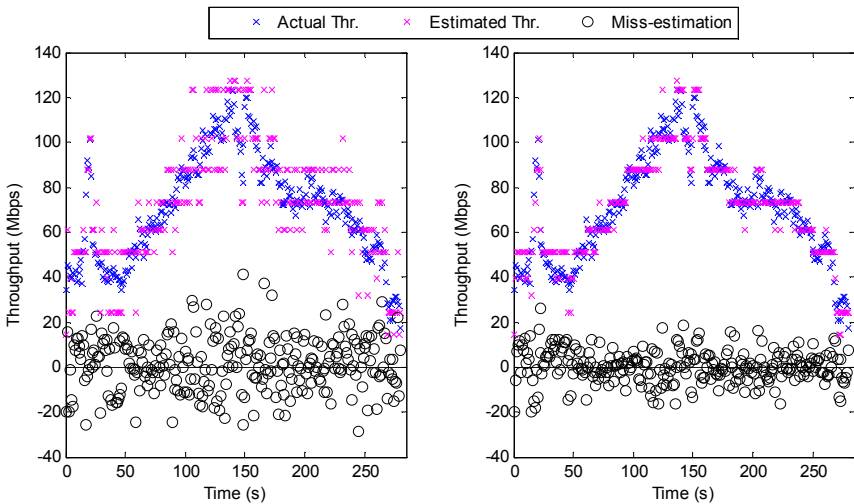
Figure 6.25 – Temporal evolution of throughput estimation for EVA5 at CG-CRR=1s.

6.5.2   MULTI-USER SIMULATIONS

Going beyond simple outcomes based on trace analytics, system level simulations may provide a better understanding of the eventual interactions between the CQI and CG-CQI values, and the effects of the double scheduling process.

As described in the system architecture for Case Study #3, the MESch element does not really perform as an LTE scheduler but as a traffic conforming element that takes the reported CG-CQI values as an input to estimate users' quality status. As a result, throughput over-estimations would lead to eNB congestion effects, where traffic should be placed into transmission queues until the required radio resources are available. Additionally, the effect

of over-estimation and under-estimation in multi-user scenarios need to be taken into evaluated.

Based on the common simulation framework, the MESch node has been integrated as a C-RAN element with access to CG-CQI statistics. The proposed MESch includes a novel scheduling algorithm aimed at orchestrating the delivery of traffic flows to the different users present in the mobile cell. As a result, different flows (i.e., HTTP objects, media segments) arrive at the MESch, which needs to prioritize the delivery of these flows to minimize the overall mean flow delay. For this aim, the MESch takes into consideration the averaged radio conditions of each user in a CG-CRR period, as well as the current flow size-related information. The flow sizes are a priori unknown to the scheduler, but the flow size distribution of the traffic is known.

Table 6.5 gathers the main simulation parameters for the case study.

Table 6.5 – Simulation parameters for Case Study #3.

Parameter	Value
Transmission Time Interval (TTI)	1 ms
Number of Resource Blocks (PRB)	100
LTE Transmission Mode	MISO OLSM
Traffic model	Poisson arrivals. Pareto flow sizes.
Scheduling algorithms	BC for eNB, MASPI for MESch
CQI Reporting Rate	CRR = 5 ms CG-CRR = 1 s
CQI delay	3 ms
Number of UEs	20 UEs, in two classes
Channel model	EVA_{LD}
Simulation length	1,000 s

Regarding traffic demands, Pareto distributed flow sizes are considered. It is known that Internet traffic flows are properly modelled by means of Pareto distributions [Thompson-1997]. In this case, the traffic is configured to a mean flow size of 5 Mbit and a shape parameter of 1.3. These flows arrive according to a Poisson process, whose rate determines the network load. Six network states are considered: low load (ρ=0.25, 0.375), medium load (ρ =0.5, 0.75) and high load (ρ =0.9, 0.95).

As cited before, the reference performance is associated to the MASPI scheduling policy, which is based on previous work [Taboada-2014_b]. The resulting performance of the different flow scheduling alternatives is evaluated in terms of mean delay of the following different approaches:

- Classical eNodeB scheduler (eNodeB(BC)): eNodeB running Best CQI (BC) discipline. This discipline gives priority to those users with higher reported CQI values.
- Near-optimal eNodeB scheduler (eNodeB(MASPI)): eNodeB running MASPI scheduler. This discipline aims at prioritizing those flows with lower expected time to finish.
- The novel two-stage proposal (MESch-eNodeB(BC)): MASPI running at MESch and classical BC policy at eNodeB.

BC is a channel-aware scheduling policy in the sense that it applies AMC to select the most suitable MCS for each UE based on the reported CQI at CRR = 5 ms. Similarly, MASPI incorporates the coarse-grain channel awareness at CG-CRR = 1 s for decision making. Additionally, MASPI takes into account the monitored BLER (Block Error Rate) and applies conservative MCS assignations when required in order to mitigate the effect of radio retransmissions under highly variable radio channel conditions.

The performance is analyzed in terms of delay for the described scenario, considering delay as the total time since the reception of a flow until its complete transmission to the mobile user. For that aim, results focus on the mean delay of the three schemes under study for the considered network loads. In addition to the mean value, the 95% confidence intervals are included.

Figure 6.26 collects the mean delay results of the analyzed LTE settings. As can be observed, on the one hand, the proposed two-phase scheduling proposal behaves notably better than a classical scheduler at the eNodeB such as BC. On the other hand, MESch-eNodeB(BC) provides worse results than a near-optimal eNodeB scheduling solution such as MASPI with BLER awareness. Moreover, it is worth to mention that both the difference in mean delay among schedulers and the confidence intervals increase with the network load value.
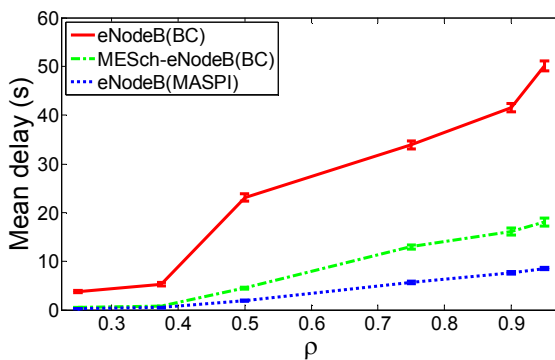
Figure 6.26 – Mean delay results.

Therefore, the average delays achieved with this proposal enhance those obtained with eNodeB(BC), while not requiring high computing capabilities in the eNodeB hardware. These results are in the same scale as those achieved by the one-phase MASPI solution at the eNodeB, even if MESch-eNodeB(BC) makes use of more uncertain channel information due to the CG-CRR parameter. As a result, it can be stated the CG-CQI feedback scheme behaves quite well even for the highly variable EVA$_{LD}$ channel evaluated.

Table 6.6 to Table 6.8 show the detailed results for three representative test points, corresponding to low, medium and high radio network loads. Three parameters are shown for each test scenario: the ratio of completed flows in the simulation time, the average BLER through the whole simulation and the average flow delay experienced due to the additional MESch node. Logically, the latter value is only significant for the MESch-eNodeB(BC) case.

As can be observed, the ratio of flows completely transmitted to the UE follows the same behaviour than the average delays. For all the considered network loads, eNodeB(MASPI) and eNodeB(BC) provide the lowest and highest values respectively. The proposed MESch-eNodeB(BC) scheme achieves intermediate results.

Similarly, it is observed that experienced BLER is higher for eNodeB(BC), while eNodeB(MASPI) reduces the BLER significantly. The enhancement achieved in the proposed MESch-eNodeB(BC) scheme is considerable at low network loads, and converges to eNodeB(BC) at high loads.

Finally, it is remarkable that the average flow delay due to the added MESch scheduling phase also increases with the network load, reaching up to 1.5 seconds at high network load conditions.

Table 6.6 – Detailed results for ρ = 0.25.

	Finished flows	BLER	MESch delay
eNodeB(BC)	0.9805	0.2186	-
MESch-eNodeB(BC)	0.9991	0.1467	0.2061
eNodeB(MASPI)	0.9994	0.0932	-

Table 6.7 – Detailed results for ρ = 0.75.

	Finished flows	BLER	MESch delay
eNodeB(BC)	0.9531	0.3019	-
MESch-eNodeB(BC)	0.9755	0.1709	0.6731
eNodeB(MASPI)	0.9896	0.1029	-

Table 6.8 – Detailed results for $\rho = 0.95$.

	Finished flows	BLER	MESch delay
eNodeB(BC)	0.9299	0.3047	-
MESch-eNodeB(BC)	0.9549	0.3072	1.4491
eNodeB(MASPI)	0.9892	0.1176	-

The proposed MESch-eNodeB(BC) provides accurate performance outcomes, exhibiting average flow delays that are closer to the near-optimal eNodeB(MASPI) scheduling policy than to the classical eNodeB(BC) policy. At the same time, the complexity of the radio head is reduced to BC scheme and the complex logic is deployed at the cloud facilities of the RAN. As expected, eNodeB(MASPI) provides the lowest mean delays for the complete set of traffic flows. While the proposed architecture provides higher mean delays compared to eNodeB(MASPI), it significantly improves the results of the simple eNodeB(BC) approach.

The total transmission delays in the proposed architecture are the combination of the scheduling function at MESch and the scheduling function at eNodeB. The first contribution provides slightly higher delay values than eNodeB(MASPI). Although the scheduling logic is the same, the results of MESch cannot capture the effects of radio retransmissions due to the variability of radio channels. The second contribution provides significantly lower average delay values compared to eNodeB(BC). MESch decomposes the Pareto traffic into a new train of flow segments according to the actual flow and channel characteristics. Thus, for example, heavy flows associated to users in good channel conditions may be delayed by MESch preventing higher delays for other flows with higher probability to finish.

6.6 CASE STUDY #4: IMPACT OF CSI DYNAMICS ON MOBILE EDGE MULTIMEDIA DELIVERY

Taking as reference the network architecture described in Case Study #3, this case study proposes a similar solution focused on enhancing the delivery of multimedia traffic in multi-user scenarios. Specifically, DASH services based on SVC are evaluated.

The proposed novel ME-DAF (Mobile Edge – DASH Adaptation Function) functional element runs as a service instance over the MEC Server, making the most out of two convergent trends: the multi-layer enabled Dynamic Adaptive Streaming over HTTP and the Mobile Edge Computing.

Figure 6.27 illustrates the overall network architecture of the resulting solution.
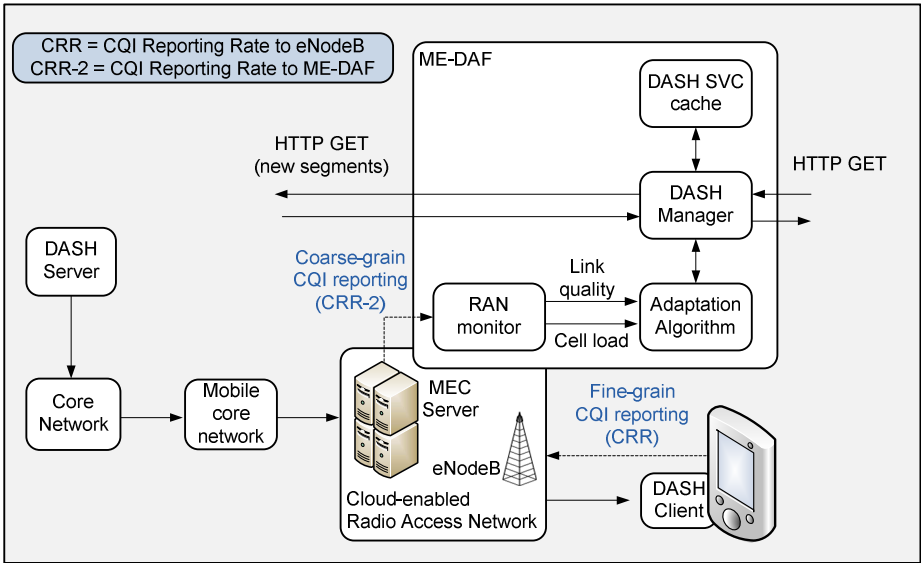
Figure 6.27 – System architecture for Case Study #4.

Similarly to the case of MESch in Case Study #3, ME-DAF interacts with the MEC Server in order to retrieve cell and user context information, such as the cell load or per-user radio performance statistics. Besides, ME-DAF is designed as a RAN-enabled service instance able to capture and manage the HTTP transactions of the associated customers. Depending on the business model, ME-DAF could be deployed to operate for a specific OTT operator or for a mobile network operator (including virtual operators).

The proposed ME-DAF is aimed at orchestrating the delivery of HTTP objects to the different multimedia users present in the cell. According to the state of the art, multi-layer enabled client devices would select the best achievable media representation at each time. In case of sudden individual radio degradations or cell saturation, an element such as ME-DAF would be able to cope with the dynamic adaptation of sessions. As a result, different media segment requests arrive at ME-DAF, which needs to prioritize the delivery of HTTP objects to maximize the overall performance. Consequently, ME-DAF adds multi-user service logic over the traditional standalone client-driven adaptation approach, being able to prioritize and/or drop different HTTP transactions according to a QoE-driven fair scheduling of radio resources.

For this aim, ME-DAF takes into consideration the significance of each media segment (base layer and enhancement layers), the current radio conditions of each user (and thus, the actual achievable quality), and the available resources in the cell for the service.

Figure 6.27 illustrates the main functional modules of ME-DAF:

- DASH Manager is in charge of handling media segment requests from the different clients, triggering HTTP caching functions in order to increase both the network efficiency in the wired elements and the user-experienced latency. In this sense, DASH Manager is responsible of replying to HTTP GET requests made by the mobile users, and forwarding these requests to the external media source when the content is not previously cached. The DASH Manager also analyzes the SVC-enabled MPD files and instructs the Adaptation Algorithm module with the flow-level characteristics of the traffic. Finally, it implements the decisions of the Adaptation Algorithm and performs the media delivery towards the end users.
- DASH SVC cache module is in charge of storing and serving media segments as instructed by DASH Manager.
- The Adaptation Algorithm is in charge of making QoE-driven scheduling decisions in order to maximize the service experience. This module combines content awareness, user context awareness and cell status awareness. In this way, the ME-DAF is able to exploit the benefits of the multi-layer media delivery to incorporate network-assisted adaptations to the client-driven approach. In order to perform the channel aware estimations, the Adaptation Algorithm is fed with low-level detailed information provided by the MEC Server. Being the most radio technology-dependent part of ME-DAF, the Adaptation Algorithm module needs to be adapted to each specific deployment.
- The RAN Monitor module is in charge of implementing the MEC API to interact with the MEC Server in order to retrieve cell statistics and individual channel state information (CSI), which is provided by means of CQI (Channel Quality Indicator) in LTE. CSI is reported by UEs to eNodeB at CRR (CQI Reporting Rate), usually configured to low values (e.g., 5 ms). In multi-user scenarios, this feedback granularity would entail a high traffic volume in the interface between MEC Server and ME-DAF RAN Monitor. Thus, the coarse-grain feedback statistic is also used in Figure 6.27 as CRR-2.

In this case study, two classes of users are defined, based on the assigned CQI channel. First, "class-1" users are associated to the EVA$_{LD}$ channel as described in Case Study #3. Second, "class-2" users are associated to a new channel that provides lower and less variable CQI values.

Figure 6.28 illustrates both CQI traces, as well as the sampled CQI traces available at the ME-DAF at CG-CRR periodicity.
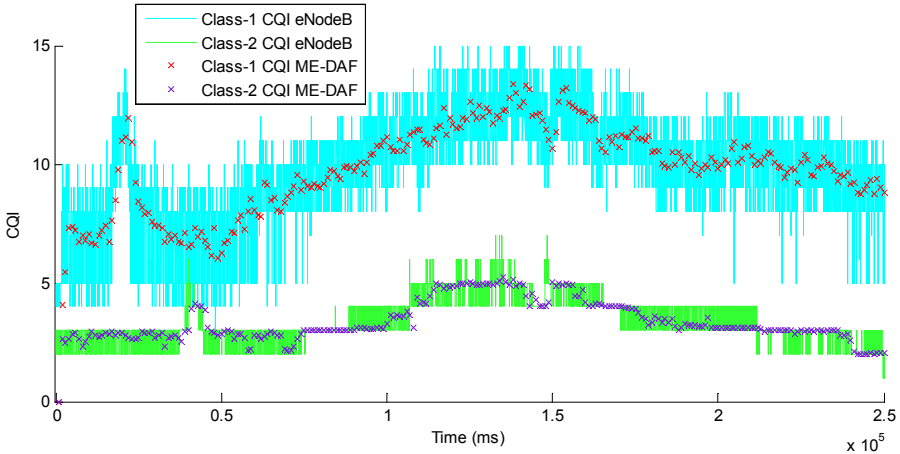
Figure 6.28 – CQI traces at eNodeB and ME-DAF.

6.6.1 SINGLE USER ANALYSIS

Besides the analysis already provided for the "class-1" users in Section 6.5.1, this section focuses on the results for the "class-2" users and on the compassion between the two types of channels.

Similarly to Figure 6.23, Figure 6.29 gathers the average differential throughput over the whole CQI trace for different CG-CRR values. Additionally, the average of all results is illustrated for the positive values and for the negative values.

Figure 6.30 provides the aggregated outcomes for the two types of channel, and for the instantaneous and median CG-CQI methods. The general trend is that throughput estimations are worse as the CG-CRR value increase. Yet, since the "class-2" channel is less variable and with lower CQI values, lower miss-estimations are found in the achievable throughput. Moreover, the same trend is observed concerning the benefits of using median CR-CQI values instead of instantaneous values.
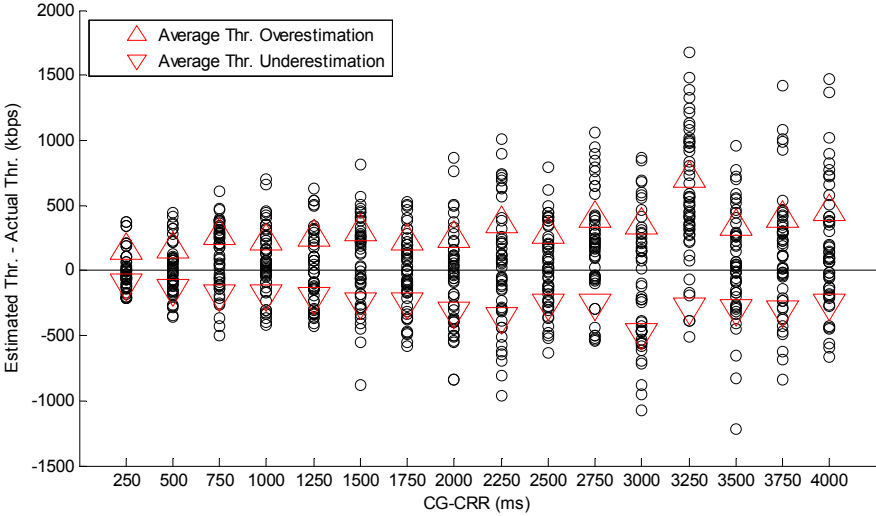
Figure 6.29 – Average throughput miss-estimations for "class-2" and CG-CRR based on instantaneous CQI values.
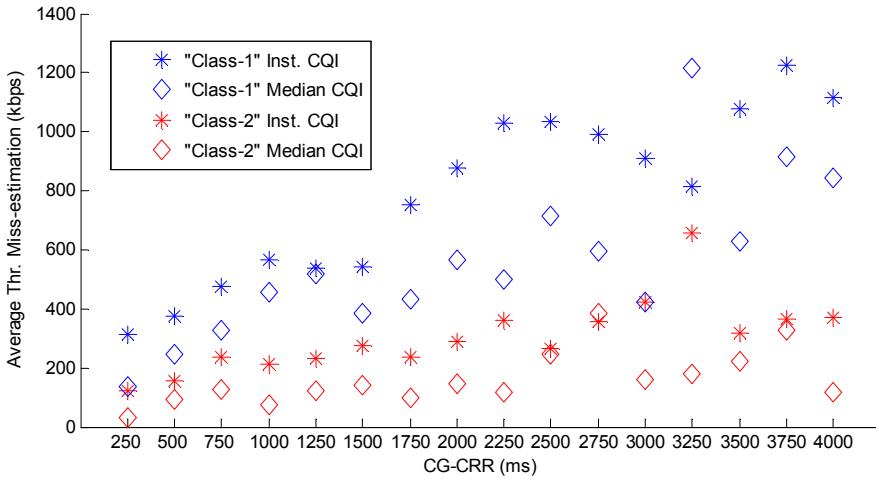
Figure 6.30 – Average throughput miss-estimations for CG-CRR based on instantaneous and median CQI values.

6.6.2   MULTI-USER SIMULATIONS

This section analyzes the performance of the proposed ME-DAF element under DASH-SVC transmissions in modern cellular networks, comparing the achieved performance in terms of QoE and with special focus in the impact of the defined CG-CQI parameter. Table 6.9 gathers the main simulation parameters for the case study, which have been applied through the common simulation framework.

<div align="center">Table 6.9 – Simulation parameters for Case Study #4.</div>

Parameter	Value
Transmission Time Interval (TTI)	1 ms
Number of Resource Blocks (PRB)	100
LTE Transmission Mode	MISO OLSM
Traffic model	Multimedia traffic based on sequence of media segments: • GOP = 2 s • Poisson-distributed arrivals Audio: • Encoding bitrate = 100 kbps Three SVC layers: • Encoding bitrates L0-L2= {295.88, , 646.52, 1690.64} kbps
Scheduling algorithms	BC, LC
CQI Reporting Rate	CRR = 5 ms CG-CRR = 1 s
CQI delay	8 ms
Number of UEs	20 UEs, in two classes
Channel model	"Class-1"based on EVA$_{LD}$. "Class-2" based on modified EVA$_{LD.}$
Simulation length	1,000 s

Traffic demands are made up of a fixed number of UEs in the cell accessing different SVC video sessions. Each video session is composed of series of Group of Pictures (GOPs), and each GOP comprises a base video layer (L0) and two enhancement video layers (L1 and L2). GOP length is configured to 2s and flow size distributions are characterized from traces provided in [Sieber-2013]. The mean size of base layer, first enhancement layer and second enhancement layer are 73.97 KB, 161.63 KB and 422.66 KB respectively. Taking into account the GOP size, the average video bitrates for each aggregated layer are 295.9 kbps, 942.4 kbps and 2,633.04 kbps. Audio-related information is included as another media representation, considering exponentially distributed audio segment sizes with mean size of 25 KB (for an average of 100 kbps). Therefore, the whole video stream would require an average of 2,733.04 kbps for its complete transmission.

The achieved performance in terms of QoE is gauged for the following approaches:

- eNodeB scheduling strategy, without further higher-layer adaptations, aimed at analyzing the application-level impact of LTE schedulers in scenarios with shared radio resources. Two types of eNodeB scheduling functions are evaluated:
  - BC (Best CQI). The scheduling function prioritizes those UEs with better radio conditions, i.e. higher reported CQI values. Thus, the objective is to maximize the overall achieved throughput of the cell at the cost of reduced fairness between UEs.
  - Layer CQI (LC). The scheduling function schedules the transmission of base layers first and the transmission of enhancement layers later [11]. Within each priority class, the scheduler applies BC principles among UEs. This type of eNodeB aims at maximizing the number of UEs with a minimum level of quality.
- Combined client-driven adaptation and eNodeB scheduling, aimed at gauging the improvement of DASH clients in the considered network conditions. The clients implement typical buffer-aware adaptation capabilities, forcing them to decrease the requested video quality upon foreseeing buffer starvation situations.
- Complex ME-DAF based adaptations, jointly to client-driven adaptations over the considered eNodeB scheduling strategies, aimed at evaluating the enhancements of the proposed architecture. Two types of radio feedback parameters are evaluated, leading to two ME-DAF implementations:
  - CQI-aware MEC (C-MEC): ME-DAF receives periodic CQI values for every involved UE.
  - CQI- and BLER-aware MEC (CB-MEC). In addition to CQI, the MEC Server is able to trigger individual information when UEs experience high BLER due to high mobility patterns.

The implemented LTE schedulers (BC and LC) arrange the transmissions of multi-user traffic at every TTI of 1ms, allocating the set of available PRBs according to traffic demands and CSI reports. Based on the reported CQI values, eNodeB applies AMC to select the most suitable MCS for each UE according to 3GPP TS 36.213 [3GPP-TS36213]. Additionally, eNodeB applies conservative MCS assignations when high BLER is detected in order to mitigate the effect of radio retransmissions under highly variable radio channel conditions.

Two classes of UEs are considered, resembling better (Class-1 UEs) and worse (Class-2 UEs) channel conditions. Taking into account both CQI traces and video patterns, simulation results with 20 mobile users equally assigned to Class-1 and Class-2 UEs are performed. In this scenario, the considered LTE cell is forced to congestion and the different media adaptation algorithms can be evaluated in severe load conditions.

CQI traces at eNodeB provide a granularity of 5 ms, while CQI traces available at ME-DAF are generated at 1 s granularity. Average CQI values are 9.47 and 3.36 for Class-1 and Class-2 UEs respectively, resulting in average data rates of 67,326.56 kbps and 13,651.2 kbps.

Among the different QoE influence factors [Seufert-2015], in the context of this paper the QoE for each user is determined by the subjective quality associated to the achieved content bitrate and gauged according to [Sieber-2013] and [Zinner-2010]. From a QoE perspective, a media segment should be downloaded on time for its smooth playout. The trade-off between responsiveness and smoothness is driven by the client buffer size, which establishes the maximum transmission delay tolerable to avoid video stalling and re-buffering effects [Seufert-2015]. In our case, the buffer size is configured to 10 s and video segments with higher transmission delays are discarded. The playable video representation is then mapped to QoE following SSIM values provided in [Sieber-2013] and Mean Opinion Score (MOS) mappings proposed in [Zinner-2010]. Although being a subjective metric in nature, MOS is typically also used as a metric to estimate the impact of different objectively measurable aspects in the QoE. In [Seufert-2015], several references are analyzed to show how MOS can be properly mapped to initial playout delay and video stalling patterns, image quality encoding levels, image spatial resolution and image temporal resolution. In summary, MOS levels achievable for each video representation are configured to: 3 for L0, 3.5 for L1 and 5 for L2. In case only audio or no media segment is received, MOS value of 2 and 1 are assigned respectively.

Finally, the adaptation algorithm implemented for performance evaluation falls in the field of traditional multi-objective optimization. The problem becomes a single-objective utility function considering averaged MOS scores for the set of users, constrained by the minimum acceptable MOS level of 3. The algorithm takes as inputs the overall available RBs and CQI values for each user, while the set of allowed content bitrates is a system parameter. The optimization vector is composed by the number of RBs for each user, constrained by the possible content bitrates and the current MCS.

Figure 6.31 shows the ratio of correctly received video segments in function of different media representations (i.e., audio, video base layer and video enhancement layers). Each subplot includes all the information concerning the evaluated approaches. "eNodeB" denotes the case where only eNodeB scheduling influences the transmission of media flows. "Client" denotes the case where UEs implement client-driven adaptations. Finally, "C-MEC" and "CB-MEC" represent the two proposed ME-DAF approaches. For each scheduling policy (BC and LC), results for Class-1 UEs, Class-2 UEs and aggregated values are offered.

As can be observed, BC-driven eNodeB transmissions result on clear unfairness between UE classes. While Class-1 UEs receive 100% of media segments at highest quality level, Class-2 UEs do not reach a sufficient quality level since they receive less than 50% of media segments belonging to audio and video base layer. Thus, one-half of mobile customers would be clearly unsatisfied with the service.

LC-driven eNodeB provides the inverse trend. In this case, eNodeB tries to transmit higher priority media segments (i.e., audio and video base layer) until they are discarded due to application-level playout threshold. Therefore, 100% of audio and base layer media segments properly arrive at Class-1 and Class-2 clients. Consequently, eNodeB tries to

deliver L1 for Class-2 UEs before L2 for Class-1 UEs, which leads to inefficient use of radio resources. In this case, only 20% of L2 video segments are delivered to Class-1 UEs.
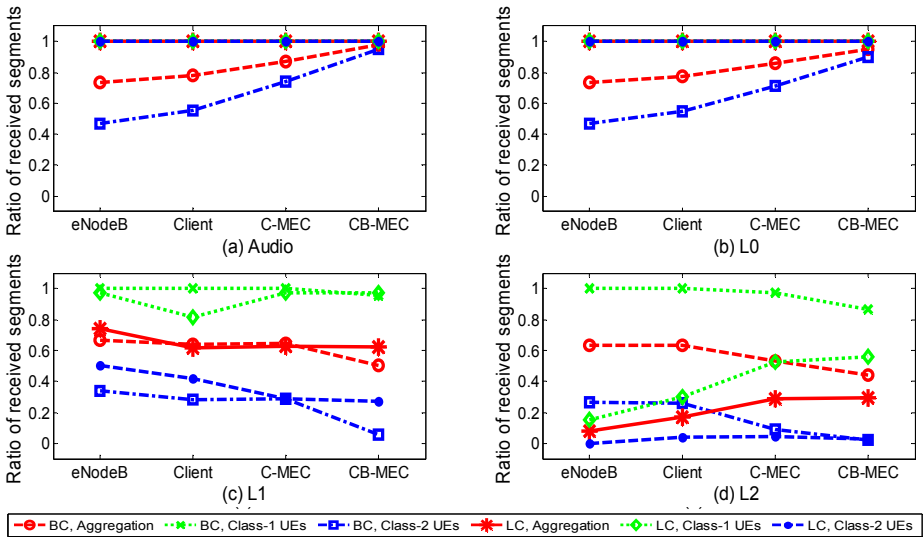
Figure 6.31 – Ratio of correctly received media segments: a) audio; b) base layer (L0); c) enhancement layer 1 (L1); d) enhancement layer 2 (L2).

Client-driven buffer-aware adaptation enhances the quality of media sessions to some extent, through a better use of the assigned radio resources. Under BC-driven eNodeB conditions, only Class-2 UEs need to dynamically adapt the requested media quality. As a result, Class-2 UEs avoid requesting L1 media segments to allow the transmission of L0 segments of consecutive GOPs. Under LC-driven eNodeB, both Class-1 and Class-2 UEs need to apply quality adaptations and the behavior is similar to the previous case.

In order to better understand the effect of these results on QoE, Figure 6.32 illustrates the mapping of the playable quality levels into MOS scale. Additionally, MOS allows a better understanding of the behavior and effect of ME-DAF.

The proposed scenario illustrates the limitations of individual decision making in client-driven adaptations, and the lack of QoE awareness in eNodeB scheduling policies. The proposed ME-DAF scheme approximates the optimal solution in terms of QoE. Under BC-driven eNodeB, ME-DAF is capable of dropping L2 media segments for Class-1 UEs in benefit of Class-2 UEs, which are able to reach the established lower MOS threshold. Under LC-driven eNodeB, ME-DAF is capable of dropping L1 media segments for Class-2 UEs in benefit of Class-1 UEs, which experience an increase on the number of received L2 media segments.

As a result, the optimal solution is approximated by different fronts, showing the efficient performance of the proposed ME-DAF adaptation approach in different LTE deployment scenarios.
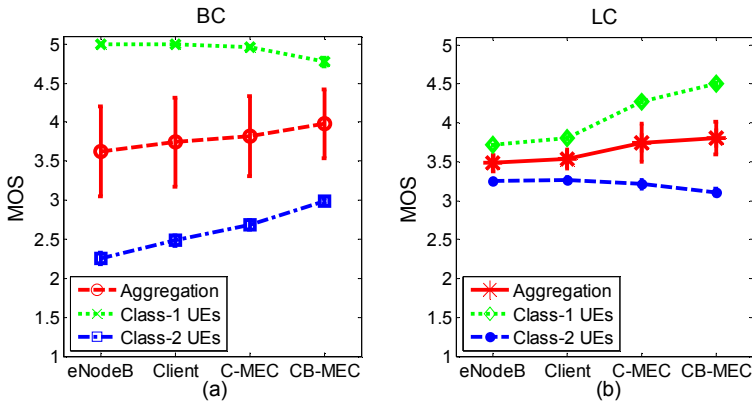
Figure 6.32 – Resulting MOS: a) eNodeB Best CQI; b) eNodeB Layer CQI.

It is shown that ME-DAF is capable of conforming media sessions to maximize the average QoE, taking as constraint the minimum quality threshold. As a result, the proposed multi-user adaptation algorithm is well-suited to exploit the awareness of dynamic radio conditions in multi-user mobile multimedia scenarios through the use of the defined CG-CRR values.

6.7   CONCLUSIONS TO IMPACT OF CSI DYNAMICS

The performance evaluation carried out in this chapter takes as inputs the different results obtained from the previous chapters:

- From Chapter 4, the CSI traces collected from field testing provide the main characteristics of the temporal evolution of CQI in different conditions. Since these CSI samples are gathered at one second periodicity, only CG-CQI values are characterized from field tests.
- From Chapter 5, the previous CG-CQI traces have been used to characterize the possible temporal evolution of CQI at millisecond scales. Since the CQI values obtained from the emulations tests are gathered at two millisecond periodicity, FG-CQI values can somehow be characterized.

In summary, the main contribution of Chapter 6 deals with the evaluation of the implications that the observed CG- and FG-CQI dynamics have into different traffic scheduling entities in traditional and novel LTE architectures.

Three main research challenges have been identified and studied in this chapter:

- Challenge #1: Partially available CSI at eNB.

At the time scale of milliseconds, a classical LTE eNB faces the problem of dealing with partially observable CSI values. At each TTI, the eNB needs to determine the MCS for DL transmissions for each UE. However, each UE reports the CQI value at a specific periodic interval, which is configured by the eNB in the range from 2 ms to 160 ms. Depending on the CRR and the FG-CQI dynamics, the CSI information available for the AMC operation may be inaccurate leading to either transmission errors or inefficient usage of radio resources. Additionally, each HARQ process has a loop tie of 8 ms due to different transmission and processing delays. Therefore, the generated CQI reports are available to the eNB with a delayed amount of time.

- Challenge #2: Joint impact of partially available and delayed CSI at eNB.

This challenge deals with the possibility of using novel centralized eNB architectures, and the case where the fronthaul introduces further delays in the HARQ processes and in the CSI processes. Similarly to the previous challenge, the dynamics of the FG-CQI is evaluated by taking into account these extra CQI delays.

- Challenge #3: Coarse-grain CSI-awareness in edge computing applications.

The last challenge copes with novel mobile edge computing architectures, where some service instances make use of some CSI information to accommodate the scheduling of the service-level flows to the channel status of the different users. In this case, the usability of

CG-CQI values as guidance for application-level scheduling is evaluated. Therefore, not only the dynamics of the FG-CQI but also the correlation to the CG-CQI values need to be better understood.

From these research challenges, four specific case studies have been evaluated.

1. Case Study #1: Impact of CSI dynamics on eNB scheduling functions.
2. Case Study #2: Impact of CSI dynamics on centralized eNB scheduling functions.
3. Case Study #3: Impact of CSI dynamics on mobile edge flow scheduling.
4. Case Study #4: Impact of CSI dynamics on mobile edge multimedia delivery.

For each case study, two types of analysis are performed:

- Analysis of the implications of the CQI dynamics from a standalone perspective, considering a unique user in the cell with greedy downlink traffic.
- Simulation-driven analysis of the implications of the CQI dynamics from a multi-user perspective, taking into account different traffic profiles and resource sharing algorithms. For this aim, and in order to issues found in well-known LTE simulators, a new simulation framework has been implemented from scratch.

Different fading patterns have been utilized in the different case studies. As a general rule, performance results are considered proper for the AMC process if the resulting transmission errors remain below the target BLER of 10%.

The most relevant conclusions obtained from the analysis of the case studies can be summarized in the following items:

1. Case Study #1 uses two wireless channels based on EVA fading profile, a good quality channel with low Doppler frequency and a bad quality channel with high Doppler frequency.

- As expected from previous conclusions, the EVA_{LD} channel is associated to a higher variability of the CQI values, and thus the probability of transmission errors in higher than in EVA_{HD}.
- In general, using instantaneous CQI values is better for low CRR values, while at higher CRR values the median CQI provides a better performance. For EVA_{HD}, the threshold is around 20 ms, while in EVA_{LD} it raises to 160 ms.
- For ideal CSI reporting with CQI delay of just 1 ms, EVA_{HD} provides accurate performance up to CRR = 10 ms, while EVA_{LD} only support up to CRR = 5 ms.
- For a standard CQI delay of 8 ms, none of the analyzed channels would cope with the target BLER of 10%. EVA_{HD} varies between 10% and 15% for whole CRR range, while EVA_{LD} exhibits an increasing tendency for the whole CRR range from 15% to 30%. These results tend to confirm the need to implement an outer loop link adaptation scheme in these wireless conditions.

- From multi-user simulations, it is observed that CQI-aware scheduling disciplines degrade their performance as CRR increases, while uniform distribution of resources exhibits a more stable behaviour over the range of CRRs. The main reason behind this behaviour is that CQI-aware schedulers tend to assign transmission slots to those user with high CQI at the specific TTI, and those states have higher probability of leading to transmission errors.
- From a general perspective of cell performance based on the aggregated throughput, Best CQI policy offers a better behaviour up to CRR = 20 ms. After that point, the number of required radio retransmissions degrade the performance below the Round Robin approach.

2. Case Study #2 uses two wireless channels: a static pattern based on ETULD fading profile, and a dynamic pattern based on EPALD fading profile. In this case, the CQI delay is allowed to increase beyond the typical 8 ms.

- For CQI delays higher than 8 ms and up to 24 ms, the expected transmission errors tend to homogenize around 30% for the whole range of CRR values in the dynamic mobility pattern.
- For the static case, the increasing tendencies within each CQI delay are similar for all the CQI delays analyzed, with a higher initial value for each increasing CQI delay.
- For the static case, even CQI delays of 24 ms are properly supported with up to CRR = 20 ms.
- The multi-user simulations with multimedia traffic tend to confirm the same range of values.
- With low mobility multi-class users, Best CQI always behaves better since the CQI variability is low and the required radio retransmissions are also low.
- In high mobility scenarios, Best CQI achieves higher average throughput for up to CRR=20 ms when the RRM logic is at the eNodeB. Meanwhile, it only achieves higher throughput up to CRR=10 ms for CQI delays beyond 8 ms. For the rest of configurations, the high variability of CQI values increases the retransmissions due to inaccurate CQI estimations and Round Robin performs better.

3. Case Study #3 uses only one wireless channel, based on the EVA_{LD} fading profile. The CG-CQI values used to drive the service-level scheduling are based on aggregated FG-CQI values.

- The single-user analysis indicates the relevance of using the median CQI value for CG-CQI values instead of instantaneous FG-CQI values.
- Also from the single-user analysis, it is shown that the macroscopic throughput estimation remains in reasonable values up to 1.5 s of integration period for the EVA_{LD} channel.

- The multi-user simulations demonstrate the possibility of performing intelligent service-level scheduling of flows at mobile edge computing instances. The use of the CG-CQI parameter allows proper decision making at the edge of the mobile network.

4. Case Study #4 uses two wireless channels, the first one based on the EVA$_{LD}$ fading profile and the second one with lower CQI values and lower amplitude of temporal CQI variations. The CG-CQI values used to drive the service-level scheduling are also based on aggregated FG-CQI values.

- The single-user analysis indicates the benefits of using the median CQI value for CG-CQI values also for the lower variability wireless channel.
- The macroscopic throughput estimations tend to exhibit accurate performance values until 2 s of integration period in this case.
- The multi-user simulations demonstrate once again the possibility of performing intelligent service-level scheduling of multimedia flows at mobile edge computing instances, through the use of the CG-CQI parameter.

7   CONCLUSIONS

7.1   OVERVIEW OF THE PERFORMED ACTIVITIES

This document gathers the most significant results of a series of activities carried out towards better understating the CSI (Channel State Indication) processes in live 4G LTE networks. From the outcomes presented along the different sections, the key CSI parameters are characterized at the time scopes of seconds and milliseconds. These different sampling scales determine the different flavours of the CSI parameters, which have been denoted as CG-CSI (coarse grain CSI, at one second periodicity) and FG-CSI (fine grain CSI, at two milliseconds of periodicity).

Two main objectives have been fulfilled with the presented results:

- First, the **characterization of the CG-CSI and FG-CSI parameters** provides evidences about the actual variability of the wireless channel in commercial-grade scenarios. The level of variability of the channel quality is determined by two main aspects: the periodicity of quality variations and the amplitude of those variations. The quantification of those two characteristics helps understanding the possible impact of the wireless channel in different contexts of use.
- Second, the different case studies presented in the evaluation section analyze the **impact of the observed CSI values into different traffic scheduling elements**. Different network architectures have been evaluated, including traditional 4G LTE networks and novel architecture designs dealing with the centralization of the eNB and with mobile edge computing features.

To attain these two objectives, three main types of research activities have been required:

- **Detailed evaluation of the different CSI measurement methodologies**, analyzing the statistical significance of the CSI values that can be gathered from the different available mechanisms, and trying to get the most of each world in a coordinated approach. This point includes the proper management of the related tools such as the field testing tools and the LTE emulator.
- **Handling of statistical processing tools**, in order to analyze the collected CSI data sets and to characterize the relevant CSI parameters at different temporal scales.
- Research activities related to the **evolution of the network architectures** in broadband mobile networks. In this point, the detailed analysis of the different channel-aware traffic scheduling elements and the possible implications of the CG-CSI and FG-CSI parameters are of utmost importance.

The contents of the document have been organized in seven chapters:

- **Chapter 1** provides the introduction to the work, including the scope and the main motivations that led to these research activities.
- **Chapter 2** provides a review of the technology concerning mobile broadband networks, analyzing the technical features involved in the different 3GPP Releases and positioning the current state of the available commercial deployments. Among other features, this chapter specially focuses on the involved CSI feedbacking mechanisms and the relationship with the AMC (Adaptive Modulation and Coding) procedures. As a main conclusion, it is observed that commercial deployments are based on MIMO 2x2 with predominance of TM3 (Transmission Mode 3). The enhancements of peak data rates are associated to CA (Carrier Aggregation) of different LTE Bands. Therefore, commercial UEs must follow the CSI procedures associated to those LTE features.
- **Chapter 3** analyzes the current state of the art of the scientific literature related to gathering CSI data. First, the chapter identifies different performance metrics from radio to application levels and establishes the possible relationships with the CSI parameters. In summary, it is observed that CSI values cannot be reliably inferred from other metrics and specific CSI measurements are actually required for the estimation of the performance. Second, the chapter reviews the most relevant studies dealing with live CSI data. In overall, it is concluded that most of the studies do not provide the sufficient information about the collected CSI data (in terms of sampling periodicity, relationships between CQI and RI, etc.) or about the context of use.
- **Chapter 4** details the adopted field testing methodology and provides the obtained results. Although significant findings are obtained concerning the CQI and RI metrics, these results are limited to a sampling periodicity of one second. The CG-RI and CG-CQI parameters are characterized for stationary measurements and for different mobility patterns (pedestrian and urban vehicular).
- **Chapter 5** specifies the methodology adopted for the emulation tests, as a basis to resemble the real-world reception conditions and try to infer the sub-second CQI values and temporal patterns. In summary, two different tendencies have been identified concerning the possible fading effects associated to the different MIMO transmission schemes.
- **Chapter 6** evaluates the implications of the observed CG-CSI and FG-CSI patterns into different traffic scheduling elements at different locations of the network architecture and at different levels of the protocol stack. The analysis has been organized in three research challenges and four case studies. For each case study, the individual and multi-user implications have been studied.
- **Chapter 7** proved the main conclusions to the document, identifying the most relevant outcomes and possible future research lines. The main contributions of the document are established from the methodological perspective and from the standpoint of the CSI characterization.

7.2   MAIN CONTRIBUTIONS

7.2.1   CSI MEASUREMENT METHODOLOGY

Chapter 3 identifies four different methods for collecting CSI traces in live LTE networks:

1.   Gathering CSI data from mobile network operators.
2.   Sniffing the LTE air interface.
3.   Performing field tests.
4.   LTE network emulation.

The first method implies directly accessing the eNB for gathering the CSI feedbacks of the different UEs. In 3G UMTS networks, some performance metrics such as BLER can be obtained from the wired segments connecting the UMTS NodeB and the UMTS Radio Network Controller. However, in LTE networks all the CSI and AMC-related information remains at the eNB and therefore it can only be collected from there. Unfortunately, eNBs are not expected to extract or even store this kind of CSI information with the required granularity, mainly due to the associated processing and memory overheads. In novel centralized LTE architectures, it could be possible to include a probe in the high speed fronthaul to passively capture this kind of data. However, even in that case the CSI values would be sampled to the CSI reporting periodicity usually configured higher than the lower threshold of 2 ms.

Concerning the second approach, the analyzed works show that network sniffers are capable of extracting some performance metrics from the DL control information. However, the AMC-related information is not sufficient to directly infer the CSI values since eNBs do not need to directly follow the CSI information.

Field testing has been proven to supply significant and accurate information about the CSI values that a UE experiences along time. Yet, the CSI sampling periodicity of commercial field test toolsets is two orders of magnitude higher than the actual CSI reporting periodicity.

Finally, although LTE network emulation is not actually a method for collecting CSI data from live networks, it is considered in the analysis since it allows making use of commercial UEs. This way, the specific vendor-dependent CSI procedures and algorithms can be considered through emulation tests.

Taking into account the advantages and drawbacks of each method, a novel methodology is proposed to characterize the behaviour of the CSI parameters at the highest sampling frequency possible. As illustrated in Figure 5.13, the proposed methodology integrates the results from field testing into LTE emulation tests.
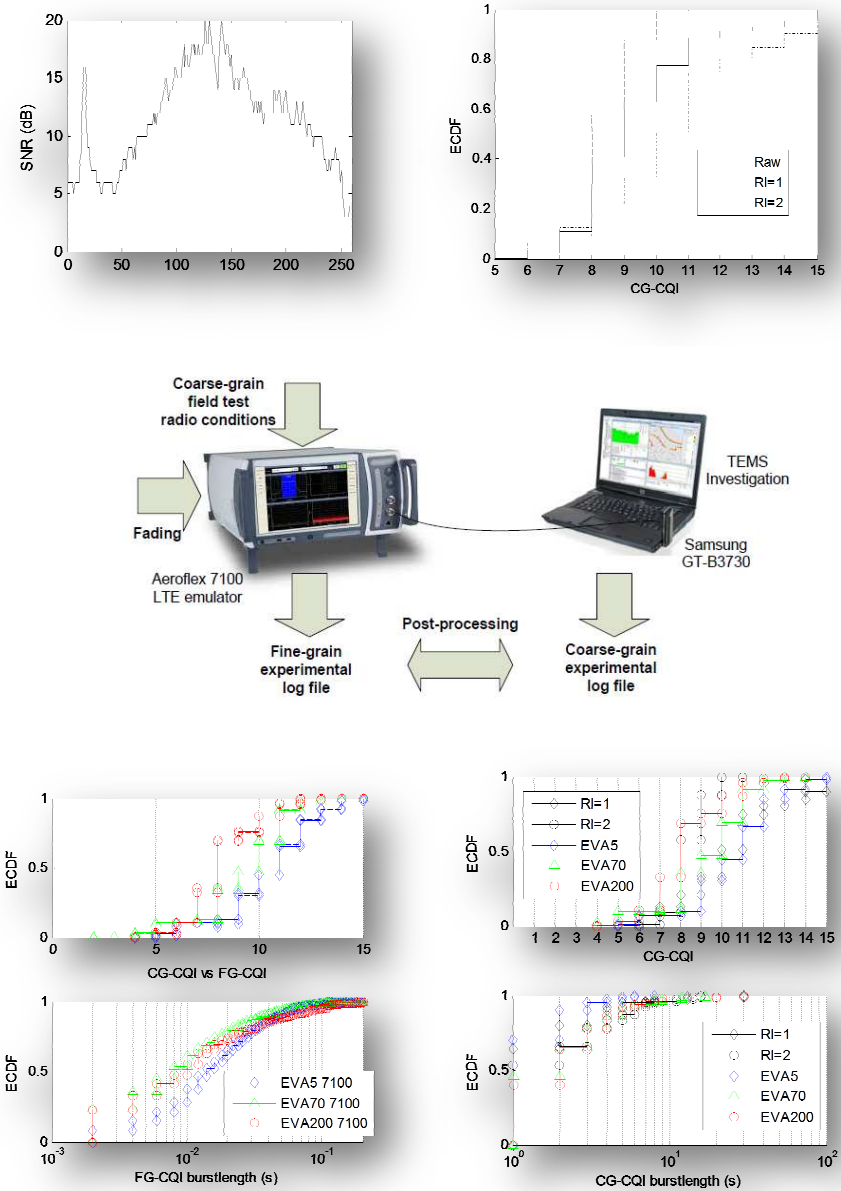
Figure 7.1 –Mixed CSI collecting methodology.

The procedure of the proposed combined methodology can be summarized in the following steps:

- **Field tests provide the temporal evolution of coarse grain radio conditions** (in terms of RSSI, RSRP, RSRQ and SNR) and of the resulting CQI values. From a detailed analysis, the CG-CQI values are obtained for each MIMO transmission scheme supported (identified as RI=1 and RI=2 traces in Figure 5.13).
- The **LTE emulator is properly configured to follow the radio conditions experienced by the UE in field tests**. Basically, the RSRP is initially configured to the monitored one, and the AWGN component is dynamically varied over time following the collected SNR values from field tests.
- In these conditions, **the LTE signal is transmitted to the same commercial UE** in order to evaluate its response in terms of CG-CQI. In this case, the LTE emulator is configured to request periodic CSI reports every 2 ms and all the CSI values are logged. In order to evaluate different possible channel conditions, a series of fading patterns are added to the LTE signal.
- For each emulation test, **the resulting CG-CQI values are statistically compared to the RI=1 and RI=2 traces** obtained from field tests. If the statistical properties of both the CQI values and the CQI burstlength values share similar tendencies, the FG-CQI values of the relevant emulation test is selected for further analysis. The statistical values of the FG-CQI and CG-CQI metrics are shown to be quite similar for each emulation test.

The main conclusions to the proposed methodology to characterize the CSI values are:

- **CQI** values are characterized at **2 ms of sampling periodicity**.
- The **suitability of the obtained FG-CQI values** can be evaluated based on the statistical analysis of CG-CQI values obtained from the field tests, and the CG-CQI and FG-CQI values obtained from the emulation tests.
- The FG-CSI data are not collected from actual live conditions, and thus there is **no evidence** that the obtained FG-CQI values are in consonance with the experienced patterns in commercial usages.

Beyond the proposed methodology, the performed activities have been useful to derive a series of conclusions about the CSI measurement tests. These findings can be summarized in a series of recommendations as presented in Table 7.1.

Table 7.1 – Main findings about the CSI measurement methodology.

Open issue	Obtained answer
Which is the predominant LTE TM and transmission scheme in different conditions?	From the analysis of the scientific literature and from the monitored commercial networks, the predominance of TM3 is stated. Therefore, all the field testing outcomes should provide information about both CSI parameters, RI and CQI. The values of CQI must be interpreted taking also into account the values of RI.
Although CSI values should be generated from the quality of the Reference Signals, is there any impact of the DL data? This is, can field tests be performed properly without DL data transfers?	There is no evidence about the way commercial UEs generate the CSI values. However, from the literature review and from the experiments carried out, it can be assumed that some kind of OLLA (Outer Link Level Adaptation) is likely to be used in order to cope with several inefficiencies of the CSI feedbacking procedure, which leads to different CQI values. These additional considerations at the UE are based on monitoring the result of the inaccurate AMC, in terms of BLER. Therefore, since the amount of DL data has an impact on the BLER, it is recommended to use actual DL traffic in the CSI measurements. Beyond pure CSI monitoring, the use of intensive DL data is recommended when CQI values are inferred from other performance metrics such as the application-level throughput or the assigned MCS.
Which is the impact of different context parameters such as the mobility pattern or the modulation used for DL data?	The impact of the mobility has been clearly identified though the different results concerning the stationary measurements and the pedestrian and vehicular mobility patterns. Not only the characteristics of CQI are different, but also the usage of the different transmission schemes differ for the different mobility patterns analyzed. Concerning the characteristics of the DL transmissions, both the number of assigned PRBs and the modulation scheme seem to have a direct impact on the CSI reporting. On one hand, if wideband CQI is used for CSI reporting, the specific characteristics in different sub-bands are not taken into account. Therefore, using higher DL bandwidth (in terms of number of PRBs) increases the probability of inaccurate AMC decisions. And, as explained before, the BLER may have a relevant impact of the generated CQI values. On the other hand, using modulation schemes with lower coding efficiency leads to increased resiliency against channel errors. Therefore, it is clear that the modulation and coding scheme assigned to DL transmissions have a direct impact on the BLER, and thus on the reported CQI values.

7.2.2 UNDERSTANDING LIVE CSI VALUES

The main reasons that motivated these research activities were related to the lack of a clear understanding of the CSI values that can be expected in real-world LTE commercial usages. Additionally, there is an uncertainty about the suitability of the CQI generating models presented in the literature and used in several well-known simulation tools.

These uncertainties have been translated to a series of open questions that have been addressed through the document.

Table 5.1 gathers the list of open issues and the answers obtained from the most significant outcomes of this PhD work.

<p align="center">**Table 7.2 – Main findings about the CSI values.**</p>

Open issue	Obtained answer
Which is the behaviour of the RI parameter in different conditions? How strong is the correlation of the two reception antennas in MIMO systems?	As expected, the value of RI significantly depends on the channel quality conditions. In general, RI = 1 predominates at low SNR values, where more resilient transmissions are required. RI = 2 is more likely used with high SNR conditions, where the spatial multiplexing features can be used to transmit two codewords at the same time. The behaviour of RI is slightly different for each mobility pattern evaluated. In static measurements and pedestrian mobility, this trend is clearly observed. Under vehicular mobility, the use of RI = 2 is also considerable at low SNR values and RI = 1 is observed also at very high SNR values. The SNR values where the predominant RI value switches from RI = 1 to RI =2 is measured to 8.5 dB, 3.5 dB and 12.5 dB respectively for the static, pedestrian and vehicular patterns. With regard to the correlation of the channel quality levels experienced by each of the two reception antennas, the overall trend seems to indicate that the relationship between CQI and SNR is lower for RI =2. Thus, the quality of estimations of the CQI value from SNR values is lower for RI = 2.
Is it really possible to infer CQI values from other performance metrics such as RSSI, RSRP, RSRQ or SNR?	The estimation of CQI values from other radio performance parameters such as RSSI, RSRP, RSRQ and SNR is not possible in general. Although a linear matching tendency is more or less followed in the scatter plots, each individual RSSI, RSRP, RSRQ and SNR value is associated to a wide range of reported CQI values (with 5 to 10 units of variability). The quality of linear fitting improves considerably if the RI value is considered, although the outcome is not accurate enough for generalized CQI estimations.
Is it really possible to infer CQI values from the monitored DL MCS assignations?	Similarly, the prediction of CQI values from monitored MCS values does not provide a direct relationship unless intensive usage of radio resources is required.

Do eNBs follow the CSI information provided by UEs in terms of RI/CQI for the MCS assignations?	In general, the scatter plots shows a wide range of possible CQI values per each MCS value, with higher variability towards higher CQI values for each MCS. Additionally, this uncertainty remains even applying an isolated analysis per RI value.
	From the coarse grain values obtained in the field tests, it is observed that the transmission scheme configured by the eNB is usually (but not always) in accordance with the reported RI value. However, these coarse grain values are statistical samples of the actual values and the actual relationship at 80 ms of periodicity cannot be observed.
	For the CQI parameter, it is clearly observed that the eNB-assigned MCS does not generally follow the maximum coding rate supported by the reported CQI values.
How reliable are the coarse-grain CSI characterizations provided by the field test tools? Are these characterizations well-suited as inputs for macroscopic problems?	From a macroscopic standpoint, the comparison of the CG-CQI and FG-CQI ECDFs shows quite similar values. Hence, it can be assumed that CG-CQI values can be valid for high level estimation of the achievable throughput.
Is it possible to characterize the temporal evolution of CSI values? How often and how quick are CQI/RI/PMI variations? And how deep does CQI varies over time? Which is the relationship between the coarse-grain CSI and the fine-grain CSI values? How reliable are the coarse-grain CSI statistics at sub-second level? How quick and how much CSI values vary within the second period?	The MIMO transmission scheme could be changed every 80 ms. From the coarse grain values obtained in field tests, RI = 1 is observed to change immediately to RI = 2 in the following second with 40%-50% of probability. For RI = 2, this probability is reduced to 30%-40%.
	From a coarse grain perspective, CQI values obtained from field tests are likely to change the value from one second to the following second with a probability of around 60% in most of the evaluated conditions Most of the time periods with constant CQI values are lower than 10 s.
	Concerning the amplitude of the CQI variations, the collected data set does not exhibit high probabilities of deep variations of CQI between two consecutive CQI samples. In general, most of the times CQI evolves to one unit above or below the current value.
	The most variable conditions are found to be the static measurements with RI = 2 and the pedestrian mobility patterns with RI = 1. In those cases, CQI variations of several units are observed.
	Concerning the evolution of CQI over more than one second periods, the case of vehicular mobility has been analyzed. For RI = 1 samples, the amplitude of CQI variations becomes considerable from a difference of five seconds. From that point, it is quite difficult to estimate the future CQI value from the current value. The subset with RI = 2 samples tend to be less significant variations.
	Beyond the temporal variability of CSI parameters at one second level, the sub-second dynamics have been analyzed based on artificial test points.
	In general, it is observed that CQI values change multiple times within a second for all the fading profiles evaluated. Most of the test points provide a FG-CQI variability amplitude of one unit above or below the CG-CQI reported. EVA5 fading profile introduces the highest FG-CQI variability over the reported CG-CQI value. In this case, a prevalent CG-CQI of 4 may include up to FG-CQI values of 9.

	In summary, fading profiles with low Doppler frequency provides more variable CQI values in the time domain of milliseconds. Fading profiles with high Doppler frequency result in lower CQI values but exhibit less variable conditions.
Which is the actual impact of several well-known radio fading profiles into real-world UEs? Is it possible to infer some type of relationship between the reported CSI and other parameters?	From a statistical perspective, the CG-CQI values associated to RI = 1 in the field tests exhibit a closer relation to the CG-CQI values associated to fading profiles with low Doppler frequency in the emulated tests. Contrarily, the CG-CQI values associated to RI = 2 in the field tests are closer to the CG-CQI values associated to high Doppler fading profiles in the emulated tests. This relationship is observed for both the CG-CQI values and for the duration of the time periods with constant CG-CQI value.
Are the results comparable with state of the art LTE simulators?	The observed FG-CQI characteristics from the commercial UE are quite different to the expected CQI values obtained from general-purpose simulators or from state-of-the-art SNR to CQI mappings.
Can we expect any significant impact on the operation of LTE HARQ processes? Is it possible to recommend any CRR value for different fading / mobility patterns?	From the results presented in the evaluation chapter, the observed FG-CQI dynamics would have a significant impact in the AMC process. Based on the evaluation of CQI reporting periodicity and possible CQI delay values, the inaccurate CQI information available at the eNB would lead to CQI miss-estimations. CQI overestimations would result in transmission errors and increased BLER, while CQI underestimations would result in inefficient use of radio resources. The CQI inaccuracy is especially relevant for pedestrian and vehicular mobility patterns, where BLER values would range from 15% to 30%. Therefore, it is observed that the bare CSI reporting mechanism would entail inefficiencies in the AMC process, and evidences that commercial UEs and eNBs are likely to implement additional control measures to overcome the problem.

7.3   SCOPE OF THE WORK, ACKNOWLEDGMENTS AND OBTAINED RESULTS

This section provides an overall analysis of the research activities presented in this document, including the background status, the research lines and projects involved and the main progress and the main scientific merits achieved.

- Scope of the work and institutional acknowledgements

The research activities leading to the results presented in this document have been performed in the Networking, Quality and Security (NQaS) research group of the University of the Basque Country (UPV/EHU). Most of the members are affiliated to the Department of Communications Engineering and work in the Faculty of Engineering of Bilbao.

This work is integrated in one the long-lasting core research lines of the NQaS group. As can be easily shown in the PhD applicant publication record, mobile networks behaviour modelling and NGN architectures have been a core part of his research from 2005. However, in terms of LTE and beyond technologies the specific timeframe for performing the presented activities can be restricted from early 2014 to the end of 2015.

The core activities of the presented work are involved in the research lines associated to the project "QoEverage - QoE-aware optimization mechanisms for next generation networks and services", led by Dr. Fidel Liberal and funded by the Spanish Ministerio de Economia y Competitividad (MINECO) under grant TEC2013-46766-R. The timeframe of the "QoEverage" project is from January 2014 to December 2016.

The PhD applicant has been hired for the "QoEverage" project from January 2015 to October 2015. In this period, most of the research activities were performed including the majority of the field testing and emulation experiments and their further processing and analysis.

In addition to "QoEverage" project, the presented outcomes also include feedback and contributions from the research work carried out in the scope of the "SESAME: Small cEllS coordinAtion for Multi-tenancy and Edge services" project. SESAME is a cooperative project funded by the European Commission from the H2020 programme under grant agreement No 671596 in the framework of the 5G-PPP. The timeframe of the "SESAME" project is from July 2015 to December 2017, and the participation of the NQaS group of the UPV/EHU is led by Dr. Fidel Liberal.

The PhD applicant has received funds from the "SESAME" project from November 2015 to the finalization of this document. The inputs from the "SESAME" project are related to the novel architectures proposed for mobile broadband networks with centralized processing functions, and contributed to the definition of the second and third research challenge described in the evaluation chapter.

- Individual acknowledgments

Beyond the institutional acknowledgments, the credits of this document must include several colleagues who actively participated in the research activities presented in the document:

- o To Dr. Fidel Liberal, as PhD supervisor and principal researcher of the cited projects, who actively participated in the whole process of conception, development and identification of the main results, and also provided valuable editorial reviews to the document.
- o To Dr. Ianire Taboada, who collaborated in the different research papers resulting from these research results, and specially for providing the MATLAB environment for multi-user simulations.
- o To Ander Carreño, flash collaborator in the NQaS group, whose committed efforts to deal with the LTE emulator tests are more than appreciated.
- o To Eneko Atxutegi, who contributed to understanding the CSI reporting procedure in ns3 and provided the performed the required comparative simulations.
- o To Mikel Ramos, for the efficient translation to Basque language.

- Research background and research outcomes

First of all, the outcomes from the performed research activities contributed for a better understanding of the specific channel-aware traffic management capabilities in LTE / LTE-A networks, and specially focused on the commercially available features.

Integrated into the broader area of "next-generation mobile networks: performance evaluation and management techniques", the results of this PhD contribute in three main research lines:

- o Performance evaluation of networked services, with especial focus on real-time multimedia services.
- o Optimization techniques for mobile traffic scheduling at the eNB.
- o Cross-layer adaptation mechanisms for maximizing the QoE of mobile multimedia services.

The PhD applicant has been collaborating in these three research topics since 2007, with special involvement in the first and third items. Although not directly linked to the core activities of this PhD work, the outcomes presented could not had been possible without the utilization of all the previously obtained skills. Table 7.3 gathers the most relevant research results that have been used as background for this PhD work, and the relation to the presented work.

Table 7.3 – Research background and relation to the PhD work.

List of background journal papers related to the contents of the PhD work
Jose Oscar Fajardo, Fidel Liberal, Is-Haka Mkwawa, Lingfen Sun , Harilaos Koumaras, "QoE-driven dynamic management proposals for 3G VoIP services", Computer Communications, Volume 33, Issue 14. Pages 1707-1724, September 2010. http://dx.doi.org/10.1016/j.comcom.2010.04.004
Relation to the PhD work: Performance analysis of VoIP services over live 3G UMTS networks, using a third-party BLER model that captures the performance experienced in commercial networks. Study of mappings between UMTS RLC performance and application-level performance for AMR voice services, including the specific encapsulation of voice frames.
Asiya Khan, Lingfen Sun, Emmanuel Ifeachor, Jose Oscar Fajardo, Fidel Liberal, Harilaos Koumaras, "Video Quality Prediction Models Based on Video Content Dynamics for H.264 Video over UMTS Networks", International Journal of Digital Multimedia Broadcasting, Volume 2010. Special Issue on 'IP and Broadcasting Systems Convergence, 2010. http://dx.doi.org/10.1155/2010/608138
Relation to the PhD work: Performance analysis of video services over live 3G UMTS networks, using a third-party BLER model that captures the performance experienced in commercial networks. Study of mappings between UMTS RLC performance and application-level performance for RTP-based H.264 video services, including the analysis of the impact of the frame sizes.
Gustavo Florido, Fidel Liberal, Jose Oscar Fajardo, "QoS-oriented Admission Control in HSDPA Networks", Network Protocols and Algorithms", Volume 1, Issue 1. Pages 52-61, 2009. http://dx.doi.org/10.5296/npa.v1i1.178
Relation to the PhD work: Understanding of the impact of HSDPA technology into mobile service provisioning, with special focus on the novel scheduling functions moved to the base stations.
Ianire Taboada, Fidel Liberal, Jose Oscar Fajardo, Urtzi Ayesta, "QoE–aware optimization of multimedia flow scheduling", Computer Communications, Volume 36, Issue 15. Pages 1629-1638, July 2013. http://dx.doi.org/10.1016/j.comcom.2013.06.007
Relation to the PhD work: Understanding of the impact of LTE technology into mobile service provisioning, with special focus on the novel AMC procedures and scheduling functions allocated at the eNBs.
Fidel Liberal, Ianire Taboada, Jose Oscar Fajardo, "A lightweight network state estimation mechanism in ARQ-based wireless networks", Telecommunication Systems, Volume 57, Issue 2, pp 137-157, October 2014. http://dx.doi.org/10.1007/s11235-013-9810-2
Relation to the PhD work: Analytical modelling of the performance metrics associated to the ARQ procedures designed to overcome possible radio transmission errors in mobile networks. Analysis of the effects into service-level metrics. ARQ may also be configured in LTE at RLC level.
Jose Oscar Fajardo, Ianire Taboada, Fidel Liberal, "QoE-driven and network-aware adaptation capabilities in mobile multimedia applications", Multimedia Tools and Applications (MTAP), Volume 70, Issue 1, pp 311-332, May 2014.http://dx.doi.org/10.1007/s11042-011-0825-y
Relation to the PhD work: General management model for mobile networks that includes cross-layer monitoring and cross-layer adaptation capabilities for maximizing the QoE in multi-user service delivery environments. Understanding of the required CSI metrics to drive the cross-layer decision making.

Concerning the specific scientific outcomes beyond this document, Table 7.4 lists the scientific publications achieved up to the date and identifies the specific area of focus. As can be observed, each publication is related to one of the case studies proposed for the evaluation of the impact of CSI dynamics on different scheduling functions.

Table 7.4 – Resulting publications and relation to the PhD work.

Scientific publication	Relation to the PhD work
Conference paper and Book chapter (Q2 SJR) Jose Oscar Fajardo, Ianire Taboada, Fidel Liberal, "Analysis of CQI traces from LTE MIMO deployments and impact on classical schedulers" 13th International Conference on Wired and Wireless Internet Communications (WWIC), Malaga, Spain, May 25-27, 2015. Wired/Wireless Internet Communications, Volume 9071 of the series Lecture Notes in Computer Science, pp. 60-73, 23 August 2015. http://dx.doi.org/10.1007/978-3-319-22572-2_5	This paper presents the main results of the novel CSI collection methodology, combining the outcomes from field testing with tailored LTE emulation tests. Additionally, the main finding concerning the necessity of indicating the RI (this is, the specific MIMO transmission scheme) is presented. Finally, the paper covers the results from the Case Study #1 in what concerns to the multi-user simulations and the impact of the observed CSI patterns in different classical LTE scheduling algorithms.
Conference paper Jose Oscar Fajardo, Ianire Taboada, Fidel Liberal "Joint impact of CQI feedback delay and CQI reporting rate on channel-aware scheduling" XII edición de las Jornadas de Ingeniería Telemática (JITEL), Palma de Mallorca, Spain, October 14-16, 2015.	This paper gathers the main results obtained from Case study #2, presenting the challenge of periodic and delayed CSI values in a centralized eNB architecture.
Conference paper and Book chapter (Q4 SJR) Jose Oscar Fajardo, Ianire Taboada, Fidel Liberal "Radio-Aware Service-Level Scheduling to Minimize Downlink Traffic Delay Through Mobile Edge Computing" 7th EAI International Conference on Mobile Networks and Management (MONAMI 2015), Santander, Spain, September 16–18, 2015. Mobile Networks and Management, LNICST 158, chapter 10, pp. 1-14, November 2015. http://dx.doi.org/10.1007/978-3-319-26925-2_10	This paper covers the main research proposals and CSI-related outcomes obtained from Case Study #3. First, the challenges associated to the novel mobile edge computing paradigm are analyzed. Later, the specific proposal designed in Case Study #3 is presented, which is aimed at implementing some kind of channel-aware flow scheduling function at the centralized eNB, while the specific RRM remains at the remote unit. Finally, the implications of using CG-CQI values are evaluated.
Journal paper (Q1 JCR, Q1 SJR) Jose Oscar Fajardo, Ianire Taboada, Fidel Liberal "Improving Content Delivery Efficiency through Multi-Layer Mobile Edge Adaptation" IEEE Network Magazine, Feature topic Quality-of-Experience (QoE)-Aware Design in Next-Generation Wireless Networks, November 2015. http://dx.doi.org/10.1109/MNET.2015.7340423	This paper covers the results associated to Case Study #4. After providing a chronological review of adaptive multimedia delivery mechanisms, the paper illustrates an innovative solution based on mobile edge computing. The benefits of incorporating channel awareness into the multi-user multimedia scheduling are discussed, and the impact of using CG-CQI values is gauged.

7.4 APPLICABILITY OF RESULTS, LIMITATIONS AND FUTURE RESEARCH LINES

The proposed CSI gathering methodology provides an indirect way of inferring CSI values when they cannot be directly accessed from commercial UEs or from commercial eNBs. This approach, with its advantages and drawbacks previously analyzed, can be interesting for researchers working in the same area of CSI modelling.

Additionally, the recommendations identified in Table 7.1 can be of interest for researchers planning to perform CSI collecting activities and with no previous expertise in the field.

Concerning the obtained CG-CSI data, several statistics and identified trends can be significant for other researchers working in the same area and for engineers working in the field of channel-aware mobile traffic management.

Some topics of possible interest are:

- The CG-RI patterns at different SNR ranges and different mobility conditions.
- The temporal evolution of CG-CQI values and the analysis about the commonly assumed fast quality variations associated to radio channels.
- The possible use of CG-CQI values for service-level traffic management.
- The temporal evolution of FG-CQI values and the analysis about the commonly assumed fast quality variations associated to radio channels.
- The possible use of FG-CQI statistics for defining novel traffic scheduling algorithms.

It must be noted that the present document only provides some kind of characterization of the CSI parameters at different time scales. However, it does not propose a specific model for the artificial generation of CSI traces. The former allows identifying tendencies and overall patterns, while the latter is usually understood as a formal definition of the intrinsic characteristics that can be provided for a generalized usage. Due to several possible limitations, a proper generalized modelling of CSI data is not recommendable at this stage.

The main possible limitations identified for the obtained results apply to the areas of field testing and LTE emulation. For each limitation, possible future actions are also identified:

- **Field test have been performed in different commercial LTE cells belonging to different LTE operators in Spain**. However, the field test toolset is only one, made including a specific commercial UE enabled by the vendor to facilitate CSI data. Therefore, since the CSI generation involves vendor-specific algorithms, it is expected that other commercial UEs perform differently and exhibit different CSI values under similar radio conditions.

- o Performing field tests with many different UEs in different contexts of use is a very time consuming task, and requires the availability of different vendor-enabled devices. However, the selected emulation tests can be carried out with different UEs, and their actual CSI reports can be collected at the LTE emulator for comparison purposes.
  - o Although there is no evidence that other commercial UEs would behave similarly, the overall conclusions about the possible behaviour of CSI parameters against state-of-the-art simulators are still valid.
- **Field tests have been performed over LTE networks in Band 7, deployed at 2.6 GHz, and with transmission bandwidths of 20 MHz**. It is expected that lower frequency bands result in better propagation conditions. However, one cannot directly extrapolate if this would result just in better radio conditions and enhanced CSI values, or if the associated temporal variations of the CSI parameters would also be highly affected.
  - o Therefore, the specific CSI values can only be considered for the specific context of use, and other contexts of use should be further studied.
- **Understanding the performance in modern LTE-A networks with Carrier Aggregation requires a better understanding of the CSI patterns in different LTE Bands.** Additionally, further evidence of the configured CSI reporting periodicity is required.

Concerning the multi-user simulations carried out for performance evaluation, the simulation framework has been specifically developed from scratch instead of using well-known LTE simulators. Although the latter would provide more comparable results, a series of limitations of deficiencies have been detected that dissuade their adoption. First, the analyzed simulators do not allow a dynamic switching of transmission schemes within a Transmission Mode. Second, the temporal evolution of CQI values obtained in simulations is not even comparable to the CQI patterns identified in this document. Finally, CSI information is usually retrieved by the eNB on demand and without properly modelling the CSI delay. Therefore, although the developed simulation framework has some limitations (e.g. in a proper modelling of HARQ or TCP layers), it is better suited for the analysis of CSI dynamics and their impact on the AMC process.

From the standpoint of the LTE system structure, the present document covers the possible impact of the observed CSI dynamics in three network architectures: classical LTE architecture, novel LTE architectures with centralized (possibly virtualized) eNB functions, and novel architectures of mobile edge computing in LTE networks.

Besides the possible enhancements to the current research activities, the present document can serve as an input for future LTE deployments. Although the commercial exploitation of other LTE transmission schemes are not currently expected, many studies nowadays focus on the experimental CSI evaluation of technologies such as MIMO 4x4, beamforming, multi-user MIMO and CoMP (Coordinated MultiPoint) transmissions.

Future 5G networks will also bring new challenges in the field of CSI monitoring, including radio technologies such as millimeter wave (mmWave), new small cell heterogeneous architectures and the use of NFV (Network Function Virtualization).

REFERENCES

- <u>Normative and general-purpose references</u>

[3GPP-Rel]   3rd Generation Partnership Project (3GPP), Releases
                    http://www.3gpp.org/specifications/67-releases (last accessed on November 2015)

[3GPP-TR37901]   3rd Generation Partnership Project (3GPP), TR 37.901. "Technical Specification
                    Group Radio Access Network; User Equipment (UE) application layer data
                    throughput performance".
                    URL: http://www.3gpp.org/dynareport/37901.htm

[3GPP-TS26247]   3rd Generation Partnership Project (3GPP), TS 26.247. "Transparent end-to-end
                    Packet-switched Streaming Service (PSS); Progressive Download and Dynamic
                    Adaptive Streaming over HTTP (3GP-DASH)".
                    URL: http://www.3gpp.org/DynaReport/26247.htm

[3GPP-TS36101]   3rd Generation Partnership Project (3GPP), TS 36.101. "Evolved Universal Terrestrial
                    Radio Access (E-UTRA); User Equipment (UE) radio transmission and reception".
                    URL: http://www.3gpp.org/dynareport/36101.htm

[3GPP-TS36211]   3rd Generation Partnership Project (3GPP), TS 36.211. "Evolved Universal Terrestrial
                    Radio Access (E-UTRA); Physical channels and modulation".
                    URL: http://www.3gpp.org/dynareport/36211.htm

[3GPP-TS36212]   3rd Generation Partnership Project (3GPP), TS 36.212. "Evolved Universal Terrestrial
                    Radio Access (E-UTRA); Multiplexing and channel coding".
                    URL: http://www.3gpp.org/dynareport/36212.htm

[3GPP-TS36213]   3rd Generation Partnership Project (3GPP), TS 36.213. "Evolved Universal Terrestrial
                    Radio Access (E-UTRA); Physical layer procedures".
                    URL: http://www.3gpp.org/dynareport/36213.htm

[3GPP-TS36306]   3rd Generation Partnership Project (3GPP), TS 36.306. "Evolved Universal Terrestrial
                    Radio Access (E-UTRA); User Equipment (UE) radio access capabilities".
                    URL: http://www.3gpp.org/dynareport/36306.htm

[GSA-2015]   GSA , "Evolution to LTE report", version of October 13, 2015.
                    http://www.gsacom.com/downloads/pdf/Evolution_to_LTE_report_131015.php4
                    (last accessed on November 2015)

[ITU-M2012]   International Telecommunications Union (ITU), M.2012, "Detailed specifications of
                    the terrestrial radio interfaces of International Mobile Telecommunications
                    Advanced (IMT-Advanced)".
                    URL: https://www.itu.int/rec/R-REC-M.2012

[NGMN-2015]   Next Generation Mobile Networks (NGMN) Alliance, "Project RAN Evolution: Further Study on Critical C-RAN Technologies", March 2015. URL: https://www.ngmn.org/publications/all-downloads/article/project-ran-evolution-further-study-on-critical-c-ran-technologies.html (last accessed on November 2015)

[Nokia-2014]   Nokia Networks, White Paper: "What is going on in Mobile Broadband Networks?"(2014) http://www.gsacom.com/downloads/pdf/Nokia_smartphone_traffic_white_paper_2014.php4 (last accessed on November 2015)

[MEC-2014]   European Telecommunications Standards Institute (ETSI) Industry Specification Group (ISG) Mobile Edge Computing (MEC), "Mobile-Edge Computing Introductory Technical White Paper", September 2014. URL: https://portal.etsi.org/Portals/0/TBpages/MEC/Docs/Mobile-edge_Computing_-_Introductory_Technical_White_Paper_V1%2018-09-14.pdf (last accessed on November 2015)

[SCF-2015_a]   Small Cell Forum (SCF), Document 106.05.1.01, "Virtualization for Small Cells: Overview", June 2015. URL: http://scf.io/doc/106

[SCF-2015_b]   Small Cell Forum (SCF), Document 159.05.1.01, "Small Cell Virtualization Functional Splits and Use Cases", June 2015. URL: http://scf.io/doc/159

[Wikipedia-LTE1] Wikipedia, "List of LTE networks". https://en.wikipedia.org/wiki/List_of_LTE_networks (last accessed on November 2015)

- ## Scientific publications

[Ahmad-2013]   A. Ahmad, M. Assaad, "Optimal power and subcarriers allocation in downlink OFDMA system with imperfect channel knowledge", Optimization and Engineering, vol. 14, no. 3, pp. 477–499, 2013.
DOI: 10.1007/s11081-011-9181-z

[Ahmad-2014]   A. Ahmad, N. Ul Hassan, N. Shah, "Robust channel quality indicator reporting for multi-carrier and multi-user systems", Computer Networks, vol. 74, pp. 78–88, 2014.
DOI: 10.1016/j.comnet.2014.09.007

[Aho-2011]   K. Aho, O. Alanen, J. Kaikkonen, "CQI Reporting Imperfections and their Consequences in LTE Networks", In Proc. The Tenth International Conference on Networks (ICN 2011), pp. 241-245, 2011.
URL:
https://www.thinkmind.org/index.php?view=article&articleid=icn_2011_12_10_10192

[Almohamedh-2014] H. Almohamedh, F. Al Qurashi, I. Kostanic, "Mobile Videos Quality Measurements for Long Term Evolution (LTE) Network, " In Proc. Int'l Conf. IP, Comp. Vision, and Pattern Recognition (IPCV'14), pp. 505-509, 2014.
URL:
http://research.fit.edu/wice/documents/Mobile%20Videos%20Quality%20Measurements%20for%20Long%20Term.pdf

[Alvarez-2012]   A. Alvarez, A. Diaz, P. Merino, F.J. Rivas, "Field measurements of mobile services with Android smartphones", In Proc. 2012 IEEE Consumer Communications and Networking Conference (CCNC), pp. 105-109, 2012.
DOI: 10.1109/CCNC.2012.6181066

[Baguena-2015]   M. Baguena Albaladejo, D.J. Leith, P.Manzoni, "Measurement-Based Modelling of LTE Performance in Dublin City", CoRR, abs/1506.02804, 2015.
URL: http://arxiv.org/abs/1506.02804

[Basukala-2010] R. Basukala, H.A.M. Ramli, K. Sandrasegaran, L. Chen, "Impact of CQI feedback rate/delay on scheduling video streaming services in LTE downlink", In 2010 12th IEEE International Conference on Communication Technology (ICCT), pp. 1349–1352, 2010.
DOI: 10.1109/ICCT.2010.5689046

[Becker-2014]   N. Becker, A. Rizk, M. Fidler: "A measurement study on the application-level performance of LTE", In: Proc. 2014 IFIP Networking Conference, pp. 1-9, 2014.
DOI: 10.1109/IFIPNetworking.2014.6857113

[Beyer-2013]   J. Bayer, J. Belschner, J. Chen, O. Klein, R. Linz, J. Muller, Y. Xiang, X. Zhao, "Performance Measurement Results Obtained in a Heterogeneous LTE Field Trial Network", In Proc. 2013 IEEE 77th Vehicular Technology Conference (VTC Spring), pp- 1-5, 2013.
DOI: 10.1109/VTCSpring.2013.6692705

[Bouten-2014]   N. Bouten, S. Latré, J. Famaey, W. Van Leekwijck, F. De Turck, "In-Network Quality Optimization for Adaptive Video Streaming Services", IEEE Transactions on Multimedia, vol. 16, no. 8, pp. 2281-2293, 2014.
DOI: 10.1109/TMM.2014.2362856

[Cainey-2014]   J. Cainey, B. Gill, S. Johnston, J. Robinson, S. Westwood, "Modelling Download Throughput of LTE Networks", In Proc. 2014 IEEE 39th Conference on Local Computer Networks Workshops (LCN Workshops), pp. 623-628, 2014.
DOI: 10.1109/LCNW.2014.6927712

[Capozzi-2013]   F. Capozzi, G Piro, L.A. Grieco, G. Boggia, P. Camarda, "Downlink Packet Scheduling in LTE Cellular Networks: Key Design Issues and a Survey", IEEE Communications Surveys & Tutorials, vol. 15, no. 2, pp. 678–700, 2013.
DOI: 10.1109/SURV.2012.060912.00100

[Chen-2011]   X. Chen, H. Yi, H. Luo, H. Yu, H. Wang, "A Novel CQI Calculation Scheme in LTE\LTEA Systems", In Proc. 2011 International Conference on Wireless Communications and Signal Processing (WCSP), pp. 1-5, 2011.
DOI: 10.1109/WCSP.2011.6096767

[ChihLin-2014]   I. Chih-Lin, J. Huang, R. Duan, C. Cui, J. Jiang, L. Li, "Recent Progress on C-RAN Centralization and Cloudification", IEEE Access, vol. 2, pp. 1030-1039, 2014.
DOI: 10.1109/ACCESS.2014.2351411

[Colom-2012]   J. Colom-Ikuno, S. Pendl, M. Simko, M. Rupp, "Accurate SINR estimation model for system level simulation of LTE networks", In Proc. 2012 IEEE International Conference on Communications (ICC), pp. 1471-1475, 2012.
DOI: 10.1109/ICC.2012.6364098

[ElNashar-2014]   A. ElNashar, M. El-Saidny, M. Sherif, "Design, Deployment and Performance of 4G-LTE Networks: A Practical Approach", ed. Wiley, ISBN: 978-1-118-68321-7, 608 pages, 2014.
DOI: 10.1002/9781118703434

[Hossfeld-2012]   T. Hossfeld, S. Egger, R. Schatz, M. Fiedler, K. Masuch, C. Lorentzen, "Initial Delay vs. Interruptions: Between the Devil and the Deep Blue Sea", In Proc. of the 2012 Fourth International Workshop on Quality of Multimedia Experience (QoMEX), pp. 1–6, 2012.
DOI: 10.1109/QoMEX.2012.6263849

[Huang-2012]   J. Huang, F. Qian, A. Gerber, F. Park, Z. Morley Mao, S. Sen, O. Spatscheck, "A close examination of performance and power characteristics of 4G LTE networks", In Proc. 10th international conference on Mobile systems, applications, and services (MobiSys '12), pp. 225-238, 2012.
DOI: 10.1145/2307636.2307658

[Huang-2013]   J. Huang, F. Qian, Y. Guo, Y. Zhou, Q. Xu, Z. Morley Mao, S. Sen, O. Spatscheck, "An in-depth study of LTE: effect of network protocol and application behavior on performance", In Proc. ACM SIGCOMM 2013 conference on SIGCOMM (SIGCOMM '13), pp. 363-374, 2013.
DOI: 10.1145/2486001.2486006

[Ide-2013]   C. Ide, B. Dusza, C. Wietfeld, "Performance of Channel-Aware M2M Communications based on LTE Network Measurements", In Proc. 2013 IEEE 24th International Symposium on Personal Indoor and Mobile Radio Communications (PIMRC), pp. 1614-1618, 2013.
DOI: 10.1109/PIMRC.2013.6666400

[Fajardo-2015_a] J.O. Fajardo, I. Taboada, F. Liberal, "Analysis of CQI traces from LTE MIMO deployments and impact on classical schedulers", In Proc. 13th International Conference on Wired and Wireless Internet Communications (WWIC), pp. 60-73, 2015.
DOI: 10.1007/978-3-319-22572-2_5

[Fajardo-2015_b] J.O. Fajardo, I. Taboada, F. Liberal, "Joint impact of CQI feedback delay and CQI reporting rate on channel-aware scheduling", In Proc. XII edición de las Jornadas de Ingeniería Telemática (JITEL), 2015.

[Fajardo-2015_c] J.O. Fajardo, I. Taboada, F. Liberal, "Radio-Aware Service-Level Scheduling to Minimize Downlink Traffic Delay Through Mobile Edge Computing", In Proc. 7th EAI International Conference on Mobile Networks and Management (MONAMI 2015), 2015.
DOI: 10.1007/978-3-319-26925-2_10

[Fajardo-2015_d] J.O. Fajardo, I. Taboada, F. Liberal, "Improving Content Delivery Efficiency through Multi-Layer Mobile Edge Adaptation", IEEE Network Magazine, vol. 29, no. 6, 2015.
DOI: 10.1109/MNET.2015.7340423

[Famaey-2013]   J. Famaey, S. Latre, N. Bouten, W. Van de Meerssche, B. De Vleeschauwer, W. Van Leekwijck, F. De Turck, "On the merits of SVC-based HTTP adaptive streaming", In Proc. IFIP/IEEE International Symposium on Integrated Network Management, pp. 419–426, 2013.
URL: http://ieeexplore.ieee.org/xpls/abs_all.jsp?arnumber=6573013

[Fouziya-2014]   S. Fouziya Sulthana, R. Nakkeeran, "Study of Downlink Scheduling Algorithms in LTE Networks", Journal of Networks, vol. 9, no. 12, pp. 3381-3391, 2014.
DOI: 10.4304/jnw.9.12.3381-3391

[Grafl-2013]   M. Grafl, C. Timmerer, H. Hellwagner, G. Xilouris, G. Gardikis, D. Renzi, S. Battista, E. Borcoci, D. Negru, "Scalable Media Coding Enabling Content-Aware Networking", IEEE MultiMedia, vol. 20, no. 2, pp. 30-41, 2013.
DOI: 10.1109/MMUL.2012.57

[Kawser-2012]   M. T. Kawser, N.I.B. Hamid, M.N. Hasan, M.S. Alam, M.M. Rahman, "Downlink SNR to CQI Mapping for Different Multiple Antenna Techniques in LTE", International Journal of Information and Electronics Engineering, vol. 2, no. 5, pp. 757-760, 2012.
DOI: 10.7763/IJIEE.2012.V2.201

[Kumar-2014]   S. Kumar, E. Hamed, D. Katabi, L.E. Li, "LTE Radio Analytics Made Easy and Accessible", In Proc. ACM SIGCOMM 2014, pp. 211-222, 2014.
DOI: 10.1145/2645884.2645891

[Muller-2012]   C. Muller, D. Renzi, S. Lederer, S. Battista, C. Timmerer, "Using Scalable Video Coding for Dynamic Adaptive Streaming over HTTP in mobile environments", In Proc. IEEE 20th European Signal Processing Conference (EUSIPCO), pp. 2208–2212, 2012.
URL:
http://ieeexplore.ieee.org/xpl/articleDetails.jsp?reload=true&arnumber=6333881

[Nikaein-2014]   N. Nikaein, R. Knopp, F. Kaltenberger, L. Gauthier, C. Bonnet, D. Nussbaum, R. Ghaddab, "Demo: OpenAirInterface 4G: an open LTE network in a PC", In Proc. 20th annual international conference on Mobile computing and networking (MobiCom '14), pp. 305-308, 2014.
DOI: 10.1145/2639108.2641745

[Landre-2013]   J.B. Landre, Z.E. Rawas, R. Visoz, "LTE performance assessment Prediction versus field measurements", In: Proc. 2013 IEEE 24th International Symposium on Personal Indoor and Mobile Radio Communications (PIMRC), pp. 2866-2870, 2013.
DOI: 10.1109/PIMRC.2013.6666636

[Laner-2012]   M. Laner, P. Svoboda, P. Romirer-Maierhofer, N. Nikaein, F. Ricciato, M. Rupp, "A comparison between one-way delays in operating HSPA and LTE networks", In Proc. 2012 10th International Symposium on Modeling and Optimization in Mobile, Ad Hoc and Wireless Networks (WiOpt), pp. 286 – 292, 2012.
URL: http://ieeexplore.ieee.org/xpl/articleDetails.jsp?arnumber=6260469

[Mehlfuhrer-2011] C. Mehlfuhrer, J. Colom-Ikuno, M. Simko, S. Schwarz, M. Wrulich, M. Rupp, "The Vienna LTE simulators-Enabling reproducibility in wireless communications research", EURASIP Journal on Advances in Signal Processing, vol. 2011, no.29, 2011.
DOI: 10.1186/1687-6180-2011-29

[Merz-2014]   R. Merz, D. Wenger, D. Scanferla, S. Mauron, "Performance of LTE in a High-velocity Environment: A Measurement Study", In Proc. 4th workshop on All things cellular: operations, applications, & challenges (AllThingsCellular'14), pp. 47-52, 2014.
DOI: 10.1145/2627585.2627589

[Piro-2011_a]   G. Piro, L.A. Grieco, G. Boggia, F. Capozzi, P. Camarda, "Simulating LTE Cellular Systems: an Open Source Framework", IEEE Transactions on Vehicular Technology, vol. 60, no. 2, pp. 498-513, 2011.
DOI: 10.1109/TVT.2010.2091660

[Piro-2011_b]   G. Piro, N. Baldo, M. Miozzo, "An LTE module for the ns-3 network simulator", In Proc. 4th International ICST Conference on Simulation Tools and Techniques (SIMUTools '11), pp 415-422, 2011.
URL: http://dl.acm.org/citation.cfm?id=2151129

[Rivas-2013]   F.J. Rivas, A. Diaz, P. Merino, "Obtaining More Realistic Cross-Layer QoS Measurements: A VoIP over LTE Use Case", Journal of Computer Networks and Communications, vol. 2013, no. 2013, Article ID 405858, 2013.
DOI: 10.1155/2013/405858

[Rost-2014]   P. Rost, C.J. Bernardos, A.D. Domenico, M.D. Girolamo, M. Lalam, A. Maeder, D. Sabella, D. Wübben, "Cloud technologies for flexible 5G radio access networks", IEEE Communications Magazine, vol. 52, no. 5, pp. 68-76, 2014.
DOI: 10.1109/MCOM.2014.6898939

[Sanchez-2011]   Y. Sanchez, T. Schierl, C. Hellge, T. Wiegand, D. Vleeschauwer, W. van Leekwijck, "iDASH: Improved Dynamic Adaptive Streaming over HTTP using Scalable Video Coding", In Proc. Second annual ACM conference on Multimedia systems, pp. 257–264, 2011.
DOI: 10.1145/1943552.1943586

[Seufert-2015]   M. Seufert, S. Egger, M. Slanina, T.; Zinner, T. Hobfeld, P. Tran-Gia, "A Survey on Quality of Experience of HTTP Adaptive Streaming", IEEE Commun Surv Tut, vol. 17, no. 1, pp. 469–492, 2015.
DOI: 10.1109/COMST.2014.2360940

[Sevindik-2012] V. Sevindik, J. Wang, O. Bayat, V. Sevindik, J. Weitzen, "Performance evaluation of a real long term evolution (LTE) network", In Proc. 2012 IEEE 37th Conference on Local Computer Networks Workshops (LCN Workshops), pp. 679 – 685, 2012.
DOI: 10.1109/LCNW.2012.6424050

[Sieber-2013]   C. Sieber, T. Hossfeld, T. Zinner, P. Tran-Gia, C. Timmerer, "Implementation and User-centric Comparison of a Novel Adaptation Logic for DASH with SVC", In Proc. IFIP/IEEE International Symposium on Integrated Network Management, pp. 1318–1323, 2013.
URL: http://ieeexplore.ieee.org/xpls/abs_all.jsp?arnumber=6573184

[Slanina-2014]   M. Slanina, L. Klozar, S. Hanus, "Practical measurement of data throughput in LTE network depending on physical layer parameters", In Proc. 2014 24th International Conference Radioelektronika (RADIOELEKTRONIKA), pp. 1-4, 2014.
DOI: 10.1109/Radioelek.2014.6828484

[Soldani-2015]   D. Soldani, A. Manzalini, "Horizon 2020 and Beyond: On the 5G Operating System for a True Digital Society", IEEE Veh Technol Mag, vol. 10, no. 1, pp. 32-42, 2015..
DOI: 10.1109/MVT.2014.2380581

[Sommers-2012]   J. Sommers, P. Barford, "Cell vs. WiFi: on the performance of metro area mobile connections", In Proc. 2012 ACM conference on Internet measurement conference, pp. 301-314, 2012.
DOI: 10.1145/2398776.2398808

[Taboada-2012_a] I. Taboada, J.O. Fajardo, F. Liberal, B. Blanco, "Size-based and channel-aware scheduling algorithm proposal for mean delay optimization in wireless networks", In Proc. 2012 IEEE International Conference on Communications (ICC), pp. 6596–6600, 2012.
DOI: 10.1109/ICC.2012.6364896

[Taboada-2012_b]   I. Taboada, J.O. Fajardo, F. Liberal, "Performance Analysis of Scheduling Algorithms for Web QoE Optimization in Wireless Networks", Network Protocols and Algorithms, vol. 4, no. 4, pp. 27–43, 2012.
DOI: 10.5296/npa.v4i4.2101

[Taboada-2014_a]   I. Taboada, F. Liberal, J.O. Fajardo, U. Ayesta, "QoE–aware optimization of multimedia flow scheduling", Computer Communications, vol. 36, no.15, pp. 1629-1638, 2013.
DOI: 10.1016/j.comcom.2013.06.007

[Taboada-2014_b]   I. Taboada, P. Jacko, U. Ayesta, F. Liberal, "Opportunistic scheduling of ows with general size distribution in wireless time-varying channels", In Proc. 26th IEEE International Teletraffic Congress (ITC), pp. 1-9, 2014.
DOI: 10.1109/ITC.2014.6932952

[Thompson-1997]   K. Thompson, G.J. Miller, R. Wilder, "Wide-area Internet traffic patterns and characteristics", IEEE Network, vol. 11, no. 6, pp. 10-23, 1997.
DOI: 10.1109/65.642356

[Tran-2012]   T.T. Tran, Y. Shin, O.S. Shin, "Overview of enabling technologies for 3GPP LTE-advanced", EURASIP Journal on Wireless Communications and Networking vol. 2012, no. 54, pp. 1-12, 2012.
DOI: 10.1186/1687-1499-2012-54

[Xu-2014]   Y. Xu, Z. Wang, W.K. Leong, B. Leong, "An End-to-End Measurement Study of Modern Cellular Data Networks", In Proc. 15th International Conference (PAM 2014), pp. 34-45, 2014.
DOI: 10.1007/978-3-319-04918-2_4

[Wu-2015]   J. Wu, Z. Zhang, Y. Hong, Y. Wen, "Cloud Radio Access Network (C-RAN): A Primer", IEEE Network, vol. 29, no. 1, pp. 35-41, 2015.
DOI: 10.1109/MNET.2015.7018201

[Zinner-2010]   T. Zinner, O. Abboud, O. Hohlfeld, T. Hossfeld, P. Tran-Gia, "Towards QoE management for scalable video streaming", In Proc. the 21st ITC Specialist Seminar on Multimedia Applications—Traffic, Performance and QoE Program, pp. 64–69, 2010.
URL: https://www.net.t-labs.tu-berlin.de/papers/ZAHHT-TQMSVS-10.pdf